Infection phenotypes and host specialization of closely related *Zymoseptoria* pathogens

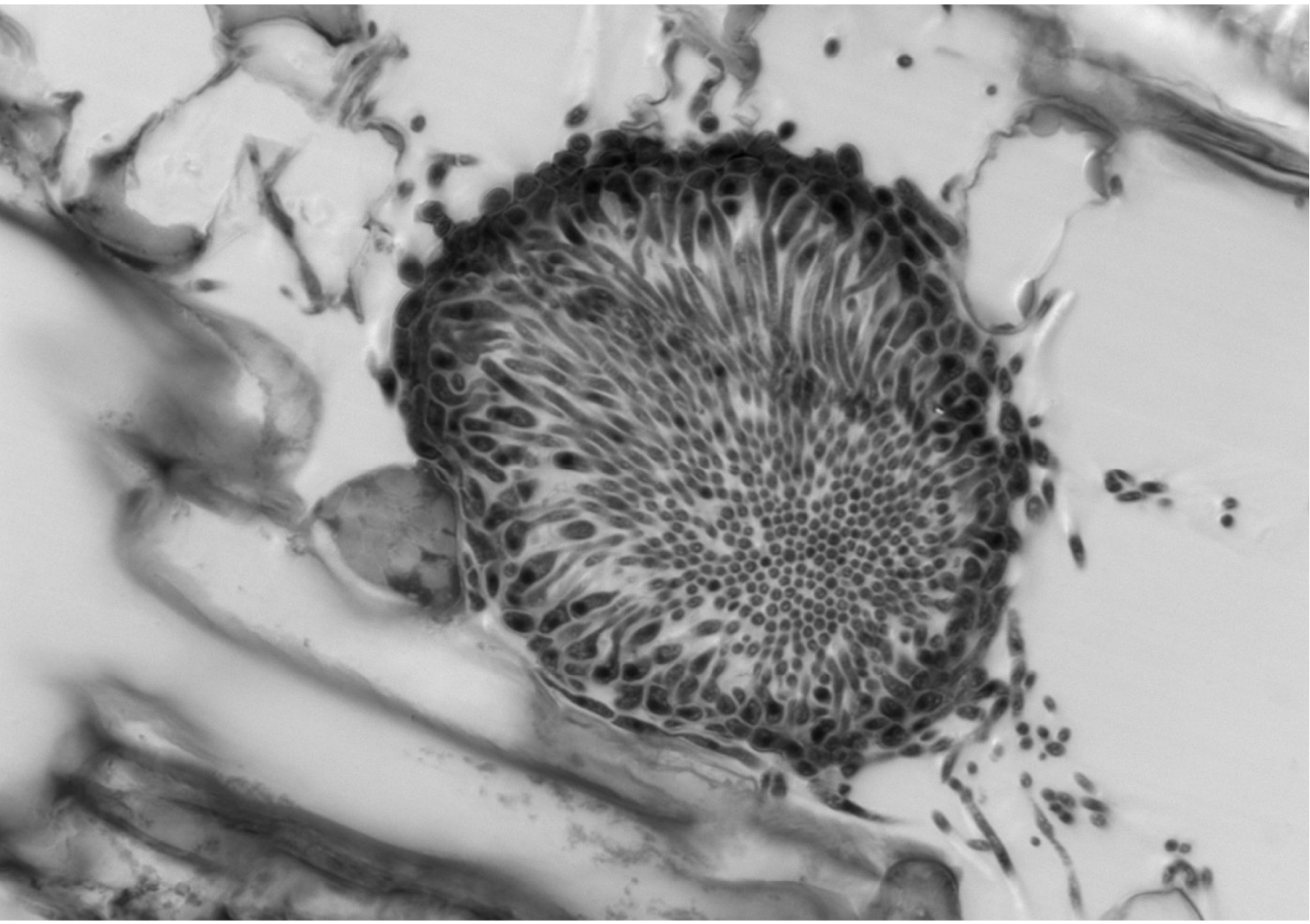

Dissertation

in fulfilment of the requirements for the degree “Dr. rer. nat.” of the Faculty of Mathematics and Natural Sciences at the Christian Albrechts University of Kiel

submitted by
Janine Haueisen
Kiel, December 2017

First referee:	**Prof. Dr. Eva Holtgrewe Stukenbrock**
Second referee:	**Prof. Dr. Alga Zuccaro**
Date of the oral examination:	**09.03.2018**

Title picture: Micrograph of a cross section through a *Zymoseptoria tritici* pycnidium located in necrotic leaf tissue of wheat.

Contents

Summary

Plant pathogens depend on their hosts to complete their lifecycles. Host specialization allows pathogens to exploit host tissues as ecological niche for growth and reproduction. Adapted pathogens are able to successfully infect their hosts while non-adapted pathogens are blocked and host-pathogen interactions are incompatible. Secreted pathogen effectors are prime candidates for factors conferring host specialization as they interfere with host plant immunity. Furthermore, host specialization involves a diversity of lifecycle traits that are directly and indirectly related to pathogenicity and virulence. **Chapter 1** reviews strategies and structures filamentous pathogens use to colonize and exploit their hosts and emphasizes the importance of plant-associated microbiota.

Rapid adaptation of filamentous plant pathogens is proposed to be facilitated by high levels of genomic variability. Field populations of the wheat pathogen *Zymoseptoria tritici* exhibit high levels of genetic diversity. In **Chapter 2**, we address the impact of high genomic variation on host infection phenotypes of *Z. tritici* by studying three genetically differentiated isolates that cause similar quantitative disease. By combining disease monitoring, reactive oxygen staining, confocal laser-scanning microscopy, and infection stage-specific RNA-seq, we show an unexpectedly high extent of plasticity in the *Z. tritici* infection program. The three isolates showed highly differentiated spatial and temporal infection development whereby more than 20% of the genes were differentially expressed between the isolates. Our finding demonstrate an extremely flexible infection program in a highly host-specialized fungal pathogen that may be a consequence of high genetic diversity and distinct epigenetic landscapes.

As discussed in Chapter 1, factors that confer host specialization and determine host specificity are diverse and involve molecular and morphological strategies as well as metabolic and reproductive adaptations. In **Chapter 3**, we address host specialization in closely related fungal plant pathogens by comparative analyses of compatible and incompatible host-pathogen interactions of *Z. tritici*, *Zymoseptoria pseudotritici*, and *Zymoseptoria ardabiliae*. The early infection program of the three species is conserved to a large extent. We found conserved initial infection development and similar gene expression profiles in the adapted and non-adapted *Zymoseptoria* species on the same host. We identified a small number of differentially expressed orthologous genes that contain candidates for ten host-specific effectors and five avirulence genes in *Z. tritici*. Our comparative analyses strongly suggest that only few key traits are involved in facilitating host specialization in the three recently diverged *Zymoseptoria* species.

Little is known about the biology and host-pathogen interactions of the *Z. tritici* sister species *Z. pseudotritici* and *Z. ardabiliae* that were isolated from uncultivated grasses in the Middle East. **Chapter 4** describes the experiments we performed to establish host species and study virulence and infection development of both fungi. We conducted plant infection experiments on 20 host species and genotypes *in vivo* and *in vitro* to study the host range of both species. Further, we tested the influence of leaf age and light stress on *Zymoseptoria* infections. *In vivo*, host infections were blocked early after infection. *In vitro*, and rarely on light-stressed, senescent, or otherwise compromised leaves, asexual pycnidia were formed by *Z. pseudotritici* and *Z. ardabiliae*. We propose that both species can infect a range of grass hosts but grow as opportunistic pathogens that are weak and less aggressive than *Z. tritici*. For future infection experiments and advanced *in planta* microscopy, we have engineered fluorescent strains of *Z. tritici*, *Z. pseudotritici*, and *Z. ardabiliae*.

Zusammenfassung

Um sich erfolgreich zu vermehren und ihren Lebenszyklus zu vollenden sind Pflanzenpathogene auf ihre Wirte angewiesen. Spezialisierungen und Anpassungen ermöglichen es ihnen dabei, den Wirt und das besiedelte Gewebe als ihre ökologische Nische für Wachstum und Fortpflanzung zu nutzen. Angepasste Pathogene sind in der Lage ihre Wirtspflanzen erfolgreich zu infizieren, während Infektionen von nicht angepassten Pathogenen abgewehrt werden und die Interaktionen zwischen Pflanze und Pathogen inkompatibel sind. Pathogene sekretieren sogenannte Effektoren, die eine große Rolle für die Wirtsspezialisierung von Pathogenen spielen, da sie die Immunität der Wirtspflanze beeinträchtigen können. Für die Anpassung an die Wirtspflanze ist jedoch eine Vielzahl zusätzlicher Faktoren, die sowohl direkt als auch indirekt mit Pathogenität und Virulenz zusammenhängen, wichtig. **Kapitel 1** befasst sich mit Strategien und Strukturen, die filamentöse Pflanzenpathogene zur Besiedlung und Ausbeutung ihrer Wirte nutzen, und hebt die Bedeutung der Gesamtheit der pflanzenassoziierten Mikroorganismen für Wirtsspezialisierung von Pathogenen hervor.

Genomische Vielfalt und Variabilität spielen eine große Rolle dabei, filamentösen Pflanzenpathogenen eine schnelle Anpassung an sich verändernde Bedingungen zu ermöglichen. Populationen des Weizenpathogens *Zymoseptoria tritici* weisen eine hohe genomische Diversität auf. **Kapitel 2** befasst sich mit den Auswirkungen, die diese Diversität auf die Infektions-Phänotypen von drei ähnlich virulenten *Z. tritici* Isolaten hat. Wir haben Virulenz-Analysen, Färbung von reaktiven Sauerstoffspezies, konfokale Laser-Scanning-Mikroskopie und die Analyse von RNA-Sequenzierungsdaten kombiniert und beobachteten dabei ein unerwartet hohes Maß an Plastizität im Infektionsprogramm von *Z. tritici*. Die Infektionsentwicklung der drei Isolate war räumlich und zeitlich sehr differenziert und mehr als 20% der Gene wurden unterschiedlich exprimiert. Unsere Ergebnisse zeigen ein äußerst flexibles Infektionsprogramm in einem hochspezialisierten pilzlichen Pflanzenpathogen, das wahrscheinlich mit der hohen genetischen Vielfalt und epigenetischen Unterschieden in Individuen von *Z. tritici* zusammen hängt.

Wie in Kapitel 1 dargestellt, sind die Faktoren, die Anpassungen an Wirtspflanzen vermitteln und damit determinieren, welche Wirtspflanzen infiziert werden können, sehr vielfältig. Sie beinhalten sowohl molekulare und morphologische Strategien als auch spezifische Anpassungen des Metabolismus und der sexuellen und asexuellen Vermehrung der Pathogene. **Kapitel 3** befasst sich mit Wirtsspezialisierung und –anpassung bei nah verwandten Pflanzenpathogenen. Dazu haben wir vergleichende Analysen anhand von kompatiblen und inkompatiblen Weizen-Infektionen von *Z. tritici*, *Z. pseudotritici* und *Z. ardabiliae* durchgeführt. Dabei war das frühe Infektionsprogramm der drei Arten weitgehend konserviert. Die initiale Infektionsentwicklung und die Genexpressionsprofile unterscheiden sich nur wenig zwischen kompatiblen und inkompatiblen *Zymoseptoria*-Arten auf demselben Wirt. Dennoch konnten wir eine geringe

Anzahl an orthologen Genen identifizieren, die differentiell exprimiert wurden. Darin sind zehn Kandidaten für wirtsspezifische Effektoren von *Z. tritici* und fünf Kandidaten für Avirulenzgene enthalten. Unsere vergleichenden Analysen legen den Schluss nahe, dass für die drei *Zymoseptoria*-Arten, die sich erst vor zwanzigtausend Jahren aus einem gemeinsamen Vorfahren entwickelt haben, wenige Merkmale eine Schlüsselrolle bei der Wirtsspezialisierung spielen.

Vergleichsweise wenig ist über die Biologie und die Wirts-Interaktionen der *Z. tritici*-Schwesterarten *Z. pseudotritici* und *Z. ardabiliae* bekannt. Beide Arten wurden im Nahen Osten von den Blättern wilder Gräser isoliert. **Kapitel 4** umfasst die Experimente, die wir durchgeführt haben, um für diese beiden *Zymoseptoria*-Arten Wirtspflanzen zu etablieren und ihre Virulenz und Infektionsentwicklung zu untersuchen. Wir haben Infektionsexperimente an 20 Pflanzenarten und Genotypen *in vivo* und *in vitro* durchgeführt, um das Wirtsspektrum beider Arten zu untersuchen. Darüber hinaus haben wir den Einfluss von Blattalter und Licht-Stress auf *Zymoseptoria*-Infektionen getestet. Wirtsinfektionen *in vivo* wurden frühzeitig von der Pflanze abgewehrt. Asexuelle Fruchtkörper von *Z. pseudotritici* und *Z. ardabiliae* wurden hingegen *in vitro* und selten auch auf gestressten, seneszenten oder anderweitig geschwächten Blättern gebildet. Diese Beobachtungen legen nahe, dass beide Arten verschiedene Gräser infizieren können, aber opportunistische Pathogene und damit deutlich schwächer und weniger aggressiv als *Z. tritici* sind. Für zukünftige Infektionsexperimente und mikroskopische Untersuchungen der Pilzstrukturen in lebendem Pflanzengewebe haben wir fluoreszierende Stämme von *Z. tritici*, *Z. pseudotritici* und *Z. ardabiliae* generiert.

General Introduction

General Introduction

Fungal pathogens cause virulent infectious diseases to animals and plants in all ecosystems and pose a serious threat to biodiversity, human health and food security (Fisher *et al.*, 2012). New pathogens can emerge through host jumps or by host range expansions (Restrepo *et al.*, 2014) and species divergence can be accompanied by the acquisition of new virulence traits and lifecycle specializations. Transposable elements and extraordinarily high genome plasticity enable fast-paced evolution of fungi facilitating lifestyle transitions and rapid adaptation to new host environments (Möller & Stukenbrock, 2017).

Crop plants in agro-ecosystems are in particular vulnerable to fungal diseases. Domestication of wild ancestors by selective breeding and the development of farming practices including monocultures and fertilization, have selected for fungal pathogens (McDonald & Stukenbrock, 2016). New pathogens can diverge from populations that grow and reproduce in non-domesticated relatives of crops or in other crop species (Menardo *et al.*, 2016; Farman *et al.*, 2017). However, specific adaptations ranging from host colonization strategies over metabolic adaptation to propagation and dispersal are required to exploit the tissues of a new host as ecological niche for growth and reproduction (Haueisen & Stukenbrock, 2016; van der Does & Rep, 2017).

A key to improve our understanding of the evolution and emergence of new fungal crop-pathogens is to increase our knowledge about the biology of closely related fungal species that are associated with "wild" non-domesticated host species. These fungi likely represent the ancestral state as also found in the most recent common ancestors of the diverged populations and provide a comparative framework to study how pathogens adapt to new host environments.

Closely related *Zymoseptoria* species – A model system for the evolution of plant pathogens

Grass-associated species belonging to the genus *Zymoseptoria* (Ascomycota, Dothideomycetes, Capnodiales, Mycosphaerellaceae) provide a powerful model system to study pathogen speciation and host specialization in closely related fungi. These include closely related *Zymoseptoria* plant pathogens that are adapted to grow and reproduce in the leaf tissue of different graminicolous hosts in different ecosystems.

In addition to this scientific relevance and potential, the model system is also of economic importance as the most prominent species is the highly specialized wheat pathogen *Zymoseptoria tritici* (syn. *Mycosphaerella graminicola*) that causes septoria leaf blotch pandemics (Fig 1) in wheat growing agro-ecosystems worldwide (O'Driscoll *et al.*, 2014). Only within the last 10,000 to 20,000 years, *Z. tritici* diverged from an ancestral lineage shared with its sister species *Zymoseptoria pseudotritici* and *Zymoseptoria ardabiliae* (Stukenbrock *et al.*, 2007, 2011). Phylo-geographic studies demonstrated that speciation occurred in the region of the Fertile Crescent,

thereby temporally and spatially coinciding with the origin of wheat domestication (Banke & McDonald, 2005). Rapidly evolving genes (Poppe *et al.*, 2015), recombination (Stukenbrock & Dutheil, *in press*; Croll *et al.*, 2015), and extraordinary genome plasticity (Stukenbrock *et al.*, 2010; Grandaubert *et al.*, 2017; Hartmann *et al.*, 2017) play important roles for adaptation of *Z. tritici* to wheat.

The two sister species have been isolated in natural grasslands in Iran from leaves of several wild Poaceae species that showed typical symptoms of septoria leaf blotch (Stukenbrock *et al.*, 2007, 2012b). Population genomics studies revealed that *Z. pseudotritici* is a hybrid species that very recently emerged through the fusion of two diverged haploid individuals (Stukenbrock *et al.*, 2012a). Like *Z. tritici*, isolates of both species can be cultivated under laboratory conditions and genetically modified by *Agrobacterium*-mediated transformations (Zwiers & De Waard, 2001). Although the evolutionary history of the closely related *Zymoseptoria* species is well studied, we know surprisingly little about the biology and pathogenesis of *Z. pseudotritici* and *Z. ardabiliae*.

Figure 1. Septoria leaf blotch on leaves of *Triticum aestivum*. Typical disease symptoms on wheat leaves infected with *Z. tritici*. Necrotic lesions contain small dark fruiting bodies, the asexual pycnidia. Picture was taken in a wheat field near Marburg Wehrda, Germany in June 2013.

Confocal laser scanning microscopy to study host-pathogen interactions

Since its commercial introduction around the early 1990s, the potentials and applications of confocal laser-scanning microscopy (CLSM) have excited biologists and medical researchers. CLSM is an optical imaging technique that allows specific detection of fluorescence signals from very thin layers within thick specimens with extraordinary sensitivity, high optical resolution and at a great speed (Inoué, 2006). Early, the new technique has proven its advantages and universal applicability (White *et al.*, 1987) and has since become an indispensable tool used across all fields of the life sciences.

In the study of plant-microbe interactions, CLSM enables investigation and visualization of the interacting structures of plants and microbes in space and time, e.g. morphology of root colonization by arbuscular mycorrhizal fungi (Rath *et al.*, 2014), haustoria formation of the wheat pathogen *Puccinia striiformis* (Sørensen *et al.*, 2012), or development of expressoria by the endophyte *Epichloë festuca* (Becker *et al.*, 2016). Due to further advantages in signal detection, weak fluorescence signals from deep tissue layers can be captured non-invasively. It is possible to scan whole plant organs and collect large stacks of serial optical sections. In combination with specific fluorescent labeling and staining, these image z-stacks allow the three-dimensional reconstructions of microbial host colonization at different times. By these means, CLSM analyses are applied to study phenotypic variation in pathogenesis and infection development of fungal plant pathogens and endophytes (Marcel *et al.*, 2010; Zuccaro *et al.*, 2011; O'Connell *et al.*, 2012; Bradshaw *et al.*, 2015; Minker *et al.*, 2016). Moreover, CLSM is used to infer the localization and action of pathogenicity-related molecules, e.g. pathogen effectors that are secreted and function in the host-microbe interaction zones (Manning & Ciuffetti, 2005; Khang *et al.*, 2010; Hemetsberger *et al.*, 2012; Dagdas *et al.*, 2016; Wawra *et al.*, 2016).

Hence, CLSM can, as demonstrated in this thesis, be an essential tool to provide detailed information about the infection biology, adaptive differences and phenotypic variation of *Zymoseptoria* species. It enables us to link conclusions we draw based on genomics and transcriptomics approaches to phenotypic observations of the different *Zymoseptoria* species e.g. during interaction with the host plant. Thereby, we investigate how their different genetic and evolutionary backgrounds translate into host-associated phenotypes.

Scope of this Thesis

The overall aim of this thesis has been to gain insight into the infection biology and host specialization of closely related fungal plant pathogens that are adapted to different hosts and different ecosystems. To this end, the four chapters of this thesis focus on the following research questions:

- How do plant pathogens adapt to host environments?

In **Chapter 1**, we review host specialization of filamentous plant pathogens in an ecological context. Most research on host specialization of pathogens focuses on molecular host-pathogen interactions, in particular on the dynamics of pathogen effectors as they interfere with host plant immunity. We propose that, in addition to traits that are directly related to virulence, host specialization involves a broad range of pathogen lifecycle traits related to growth, metabolism, reproduction and dispersal. We present and discuss strategies and structures, which filamentous pathogens use to colonize and exploit their hosts and emphasize the importance of the plant-associated microbiota.

- Is the infection program of a highly host-specialized plant pathogen conserved or does high genetic diversity between individuals translate into variable infection programs?

In **Chapter 2**, we address the impact of high genomic variation on host infection phenotypes of *Z. tritici* by studying three genetically differentiated field isolates that cause similar quantitative disease. Our aim was to characterize infection development and gene expression profiles of these three distinct isolates in detail to elucidate to what extent genomic variation translates into phenotypic variation during host infection. Our analyses reveal an extremely flexible infection program in a highly host-specialized fungal pathogen demonstrating that genetically distinct individuals of pathogen populations can infect one host with differentiated infection programs.

- Which traits confer host specialization in recently diverged plant pathogens adapted to different grass hosts and different ecosystems?

In **Chapter 3**, we address host specialization in closely related fungal plant pathogens by comparative analyses of compatible and incompatible host-pathogen interactions of *Z. tritici*, *Z. pseudotritici*, and *Z. ardabiliae*. Our aim was to shed light on the factors that facilitate successful infections of the adapted *Z. tritici* and determine the outcome of *Zymoseptoria*-wheat interactions. We identified surprisingly little differences between the compatible and incompatible species on

the same host and propose that a few key traits facilitate specialization to different grass host environments in the three recently diverged *Zymoseptoria* species.

- Which host plants can be infected by *Z. pseudotritici* and *Z. ardabiliae* and how does host physiology influence host-pathogen interactions?

The aim of the experiments described in **Chapter 4** was to establish host species for the *Z. tritici* sister species *Z. pseudotritici* and *Z. ardabiliae* and to study virulence and infection development of both fungi. *In vivo*, isolates of both fungi were avirulent on 20 plant species and species accessions. The two fungal species reproduced only *in vitro* or episodically on compromised leaves. We propose that both species can grow and reproduce on leaves of a range of grass hosts but infect as opportunistic pathogens that are weak and less aggressive than *Z. tritici*.

Chapter 1

Life cycle specialization of filamentous pathogens – colonization and reproduction in plant tissues

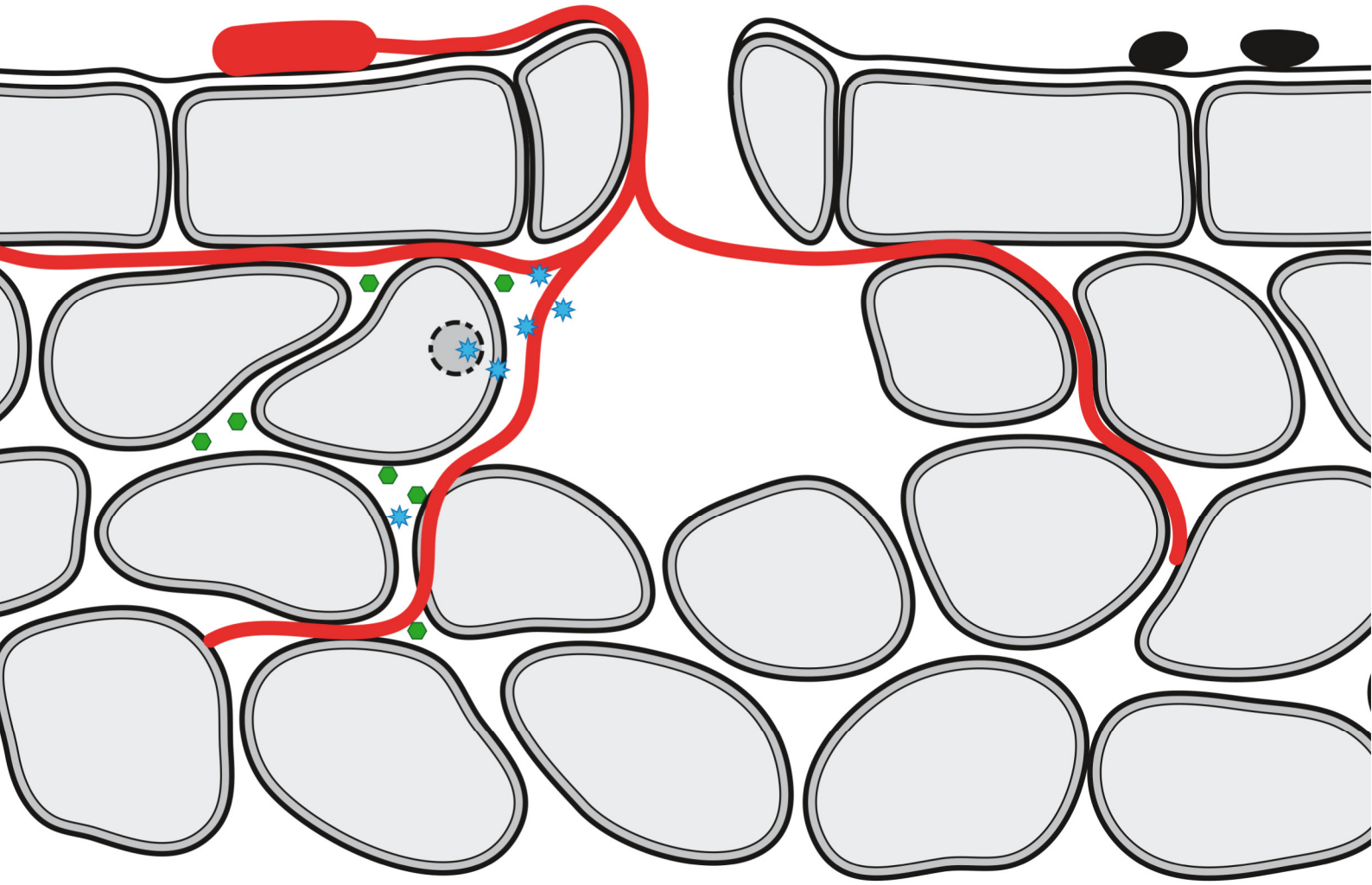

Chapter 1

Life cycle specialization of filamentous pathogens – colonization and reproduction in plant tissues

Published review

Haueisen J, Stukenbrock EH. **2016**. Life cycle specialization of filamentous pathogens - colonization and reproduction in plant tissues. *Current Opinion in Microbiology* **32**: 31–37.

Highlights

- Plant pathogens specialize to plant tissue as their niche for growth and reproduction.
- Pathogens sense plant-derived signals to recognize and localize their hosts.
- Different strategies allow filamentous pathogens to enter and colonize plant tissues.
- Pathogens kill plant cells or develop feeding structures to take up nutrients.
- Specialized fruiting bodies facilitate spore dispersal to new host plants.

Abstract

Filamentous plant pathogens explore host tissues to obtain nutrients for growth and reproduction. Diverse strategies for tissue invasion, defense manipulation, and colonization of inter and intra-cellular spaces have evolved. Most research has focused on effector molecules, which are secreted to manipulate plant immunity and facilitate infection. Effector genes are often found to evolve rapidly in response to the antagonistic host-pathogen co-evolution but other traits are also subject to adaptive evolution during specialization to the anatomy, biochemistry and ecology of different plant hosts. Although not directly related to virulence, these traits are important components of specialization but little is known about them. We present and discuss specific life cycle traits that facilitate exploration of plant tissues and underline the importance of increasing our insight into the biology of plant pathogens.

Introduction

Plants are habitats for a large diversity of microbial species colonizing the outside and inside of roots and all aerial tissues. Many microbes are harmless to plants and some even beneficial. Mycorrhizal symbionts are known to be strong enhancers of plant growth and health and are found in all plant-inhabited environments [1,2]. So are filamentous plant pathogens, which exploit plants as substrate for their growth and reproduction by inducing disease and thereby compromise host viability and reproduction. These fungal and oomycete species have evolved diverse strategies to infect and loot nutrients from the plant for their own growth and reproduction.

Theoretical and experimental approaches have shed light on the origin, diversity, and biology of a small number of well-studied pathogen species [3–5]. Most studies addressing host specialization have focused on recent micro-evolutionary changes related to host jumps or breakdowns of plant resistances [6,7]. A particular focus has been the fast evolutionary dynamic of genes encoding 'effectors' in many plant pathogens. Effectors are secreted molecules that interfere with plant defenses and in some cases act as determinants of host range [8–10]. A general finding from a diverse range of pathogen species is that rapid evolution of many effector genes is enabled by compartmentalized genomes with particular repeat-rich regions where genes undergo an increased accumulation of mutational changes [3,11–13]. A number of reviews summarize and discuss studies focusing on such rapid adaptive changes in pathogens and the role of these in determining host specificities [14–17]. However, not only effectors with a direct role in the manipulation of host defenses are subject to adaptive evolution in plant pathogens [4,18]. In the wheat pathogen *Zymoseptoria tritici* genes encoding plant cell wall degrading enzymes and genes with functional relevance during late infection and asexual reproduction also show signatures of positive selection and species-specific adaptation [7,19]. Likewise several genes involved in metabolism and signal transduction have evolved under positive selection during divergence of plant pathogenic species in the genus *Botrytis* [18]. These findings underline that host specialization of plant pathogens not only comprises pathogenicity related traits but also affects a range of life cycle developmental stages and processes not directly related to virulence.

Our goal in this review is to address a broader perspective of host specialization of filamentous pathogens, considering, in addition to the molecular battlefield of host-pathogen interactions, also specialization to plant tissues as an ecological niche for growth and reproduction (Figure 1). We suggest that host specialization involves, across diverse lifestyles of plant pathogens: 1) the evolution of particular infection strategies to invade the inter- or intra-cellular spaces of plant hosts, 2) the production of an appropriate repertoire of effectors to suppress host defenses, 3) the expression of genes encoding an arsenal of enzymes and transporters for the uptake of available nutrients within or between plant cells, 4) the ability to co-exist or compete with other microbes

inhabiting plant surfaces, and 5) an efficient reproduction program evolved to facilitate dispersal of spores to new uninfected hosts.

We still know surprisingly little about the ecology of plant pathogens including their interaction with other plant-associated microbes as well as the saprotrophic stage of many species outside their host. Here, we summarize and discuss studies that present examples how filamentous pathogens specialize to the infection of plant tissues, and we highlight the importance of additional research to better understand the origin and biology of plant pathogens. We focus on studies covering fungi and oomycetes that comprise some of the most important crop pathogens and model pathogens of wild plants.

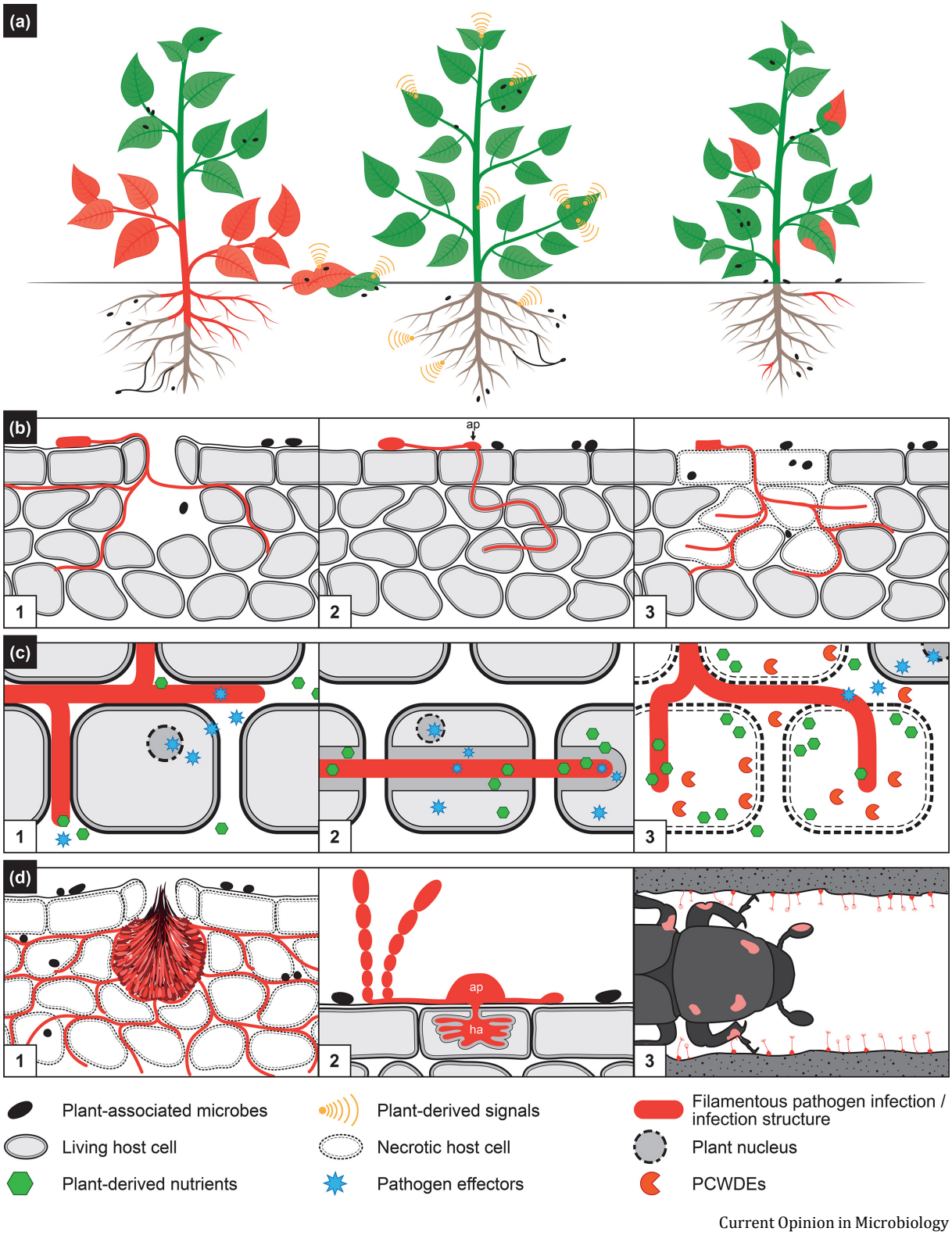

Current Opinion in Microbiology

Figure 1. The host plant as an ecological niche of filamentous pathogens. (a) Plant rhizo-, phyllo- and endosphere are inhabited by different microbes (black ovals) ranging from beneficial to pathogenic. Specific plant signals (signal symbols) serve to recruit beneficial species but likewise attract pathogens [28]. Infection by filamentous pathogens (red areas) can be local or systemic and affect several organs up to whole plants. **(b)** Pathogens invade plant tissue by natural openings e.g. stomata **(b.1)** or form appressoria (ap) **(b.2)(d.2)** to break down plant cell walls. Many necrotrophic pathogens use toxins and enzymes to kill epidermal cells and enter by direct penetration **(b.3)**. Colonization of host tissues occurs by inter- (**b.1**) or intra-cellular growth **(b.2)**. **(c)** Pathogens take up host-derived nutrients and secrete effectors that are delivered to host apoplast, cytoplasma or nuclei to silence host defense and manipulate plant physiology [9]. Biotrophic pathogens establish intimate host-pathogen interaction zones e.g. invaginations of host cell membrane **(c.2)** or haustoria (ha) **(d.2)**. Intercellular biotrophs have limited amounts of nutrients available in the apoplast **(c.1)** whereas necrotrophs kill plant cells and mobilize large quantities of carbohydrates by degradation of cell wall components with PCWDEs **(c.3)**. **(d)** Shape and position of fruiting bodies of plant pathogens facilitate spore dispersal by biotic or abiotic vectors. Foliar pathogens produce fructifications below stomata **(d.1)** or directly on the leaf surface **(d.2)** to expose their spores to be carried to new hosts e.g. by water droplets or wind. Pathogens that rely on plant-associated or -visiting animals for spore dispersal reproduce in plant organs that are attractive for their vectors e.g. flowers or fruits and have developed mechanisms to load them with their propagules e.g. by producing fruiting bodies in bark beetle galleries that "paint" passing beetles with spores **(d.3)**.

Host invasion

Plant pathogens have evolved distinct strategies to sense both biotic and abiotic plant-derived signals that enable them to orient growth towards their host (Figure 1a). Root exudates are known to act as strong enhancers of microbial proliferation and as signal molecules for beneficial as well as antagonistic fungi and oomycetes [20]. A recent study demonstrated the capacity of the soil-inhabiting plant pathogen *Fusarium oxysporum* to sense plant-produced peroxidases in root exudates [21]. The peroxidases induce chemotrophic growth of hyphae towards roots. Interestingly, the pathogen uses the same signaling pathway for chemotrophic sensing of mating factors as for host stimuli, involving a homolog of the transmembrane protein Ste2 known to function as an α pheromone receptor in yeast [21]. Given that chemotrophic sensing in *F. oxysporum* depends on highly conserved elements of the fungal cell wall integrity MAPK cascade [21], it is possible that the peroxidase-dependent host-sensing in *F. oxysporum* reflects a general chemotrophic interaction between soil-borne plant pathogens and plant roots.

Leaf pathogens can adhere to the highly hydrophobic cuticle of their hosts and find their way to natural openings or penetrate directly through plant cell walls (Figure 1b). Many leaf pathogens invade their host through open stomata and show polarized growth towards stomata based on sensing of the particular topology of leaf surfaces [22]. Experimental studies with the rust fungus *Uromyces viciae-fabae* showed that the extent of stomatal opening affected the growth direction of hyphae on leaves and open stomata induced stronger polarized growth [23]. Open and closed stomata create different gradients of pH on leaf surfaces and this is likely perceived by pathogens allowing them to orient hyphal growth towards the openings [23]. In *Zymoseptoria tritici* directed growth towards open stomata was observed on different Poaceae species but not on the leaf surface of the dicot *Arabidopsis thaliana* (J. Haueisen, unpubl.). This observation suggests that also the sensing of more specific host signals allows leaf pathogens to find their way to entry points on plant surfaces.

Host invasion can also take place by direct penetration of hyphae. Some pathogens make use of an arsenal of toxins, plant cell wall degrading enzymes (PCWDEs), and reactive oxygen species to kill plant cells [24]. This type of infection is associated with many necrotrophic pathogens such as species of *Botrytis, Sclerotinia* and *Parastagonospora* [25,26]. Other pathogens, including both biotrophs and necrotrophs, form specialized appressoria (Figure 1b.2, 1d.2) in which high turgor pressure builds up to eventually destroy rigid plant cell walls. Appressoria are not only developed by pathogens. Arbuscular mycorrhizal symbionts also use appressorial structures, called hyphopodia to colonize roots cells [1]. Appressoria formation involves the regulation of complex developmental processes to generate structures ranging from simple swellings such as in *Ustilago maydis* to highly differentiated multicellular structures such as in *Magnaporthe oryzae* [27]. Wang and colleagues showed that development of *Phytophthora infestans* appressoria as well as of

hyphopodia and arbuscules of mycorrhizal fungi are triggered by the same plant signal, cutin monomers on the surface of root cells [28]. These similar strategies and structures of filamentous pathogens and beneficial endophytes likely reflect a parallel adaptation to the penetration of rigid plant surfaces.

Host manipulation

Filamentous pathogens as well as all other plant-associated microbes are immediately recognized by the plant upon contact with its surfaces through pathogen- and microbial-associated molecular patterns (PAMPs and MAMPs) or damage-associated molecular patterns (DAMPs). MAMPs, PAMPs and DAMPs trigger immune responses that block the propagation of most invading microbes except for those species that have evolved particular strategies to counteract the immune responses of their hosts [29]. Plant pathogens as well as beneficial symbionts such as mycorrhizal fungi secrete effectors (Figure 1c) that act to silence host defenses or promote infection by altering plant metabolism [6,30–34]. These interactions are often very specific and can define the host range of distinct pathogens.

Several described effectors are small proteins with no homologs in non-pathogenic relatives, but also non-proteinaceous molecules such as secondary metabolites or small RNAs can act as effectors. During infection *Botrytis cinerea* produces small RNAs that are transported across the host plasma membrane by unknown mechanisms [35]. Inside the host cell they bind to the host protein AGO1, a key component of the RNA interference machinery and induce selective silencing of defense-related genes [35].

Like *B. cinerea*, *Sclerotinia sclerotiorum* has a broad host range [36]. Comparative secretome analysis of *S. sclerotiorum* suggests that the ability to infect many different host species may be conferred by a diverse effector repertoire and host-specific effector gene expression patterns [37]. Different host species possibly induce expression of different effector genes thereby allowing the pathogen to overcome immune defenses in a diversity of hosts.

Lastly, many necrotrophic pathogens produce host-specific toxins (HSTs). HSTs are effectors that induce toxicity and promote disease only in hosts that express a specific and often dominant susceptibility gene [38,39]. One of the best characterized HSTs is ToxA in the wheat pathogens *Pyrenophora tritici-repentis* and *Parastagonospora nodorum* [40,41]. ToxA induces a hypersensitive response and thereby host cell death in wheat lines carrying the resistance gene *Tsn1* that otherwise confers resistance against certain biotrophic pathogens [42]. This fascinating example illustrates how some virulence determinants of necrotrophs have evolved as a by-product of host resistance responses towards biotrophic pathogens.

In summary, studies of pathogen effectors demonstrate that plant pathogens employ diverse strategies to manipulate host defenses. Some interactions are very specific while other effectors interact with highly conserved plant targets and thereby might cause similar effects in a broad range of different host species [43]. An intriguing question is how effector genes arise and evolve and how the often complex host manipulating functions have been acquired. Indeed, we still know very little about the origin and acquisition of effectors, although some studies indicate that horizontal gene transfer among pathogens and between pathogens and their hosts contributes to the evolution of novel effectors [41,44,45]. Also gene duplication followed by rapid sequence evolution has been shown to play a role in effector emergence and diversification [46].

Colonizing and feeding from the plant

Upon successful suppression of host immune responses, pathogens further invade and exploit host tissues. Some filamentous pathogens are specialized to locally colonize particular host tissues or organs. *Zymoseptoria tritici* for example, maintains all stages of infection in the leaves [47]. Other species colonize several different plant parts or cause systemic infections of their host (Figure 1a). Species such as *Magnaporthe oryzae* and *Ustilago maydis* have adapted to the colonization of different tissues [48] involving the secretion of organ-specific effectors [49] what suggests that pathogens can perceive tissue-specific signals during host infection.

The nutrient sources of filamentous pathogens during infection are host-derived compounds. Pathogens apply different strategies to mobilize and take up nutrients from their hosts depending on their lifestyle (Figure 1c). Necrotrophic pathogens feed from dead plant cells and secrete enzymes specialized to degrade polysaccharide cell wall components such as hemicellulose and pectin [25]. Similar hydrolytic enzymes are present in fungi that decompose dead plant material. However, comparative genome analyses of 94 distantly related fungi showed that plant pathogenic species in general possess more genes encoding enzymes for the breakdown of complex carbohydrates (CAZymes) than saprotrophic or mutualistic species underlining the importance of such enzymes in plant pathogen lifestyles [50]. Moreover, host range (e.g. monocots or dicots), lifestyle and infection mode of plant pathogenic fungi have been found to be reflected in the specific composition of their PCWDE arsenals, a subgroup of CAZymes [25,50,51]. Biotrophic fungi have limited repertoires of enzymes for plant polysaccharide degradation [9,50] and depend on sugars taken up from living plant cells. Many biotrophic species establish intimate interaction zones, e.g. intracellular hyphae that invaginate host plasma membranes. Some biotrophic pathogens, such as the powdery mildew *Blumeria graminis*, have evolved highly specialized feeding structures called haustoria that resemble arbuscules of mycorrhizal fungi and provide very large intracellular surfaces for nutrient uptake [52].

Reproduction and dispersal

Pathogens explore their hosts to obtain nutrients for their reproduction and propagation. Fruiting bodies of leaf pathogens are often exposed on leaf surfaces facilitating dispersal of asexual spores (e.g. pycnidiospores from pycnidia in *Z. tritici*) or sexual spores (e.g. ascospores from sexual cleistothecia in *B. graminis*). The production and deposition of spores on leaf surfaces or in litter allows pathogens to disperse their propagules (Figure 1d) either by rain droplets to neighboring plants or by wind over longer distances [53].

Some plant pathogens have evolved sophisticated strategies to change the physiology and development of their hosts in a manner that favors pathogen reproduction and spread. The smut fungus *Microbotryum lychnidis-dioicae* produces teliospores exclusively inside the anthers of its host, *Silene latifolia*, from where the spores are transmitted to new hosts by pollinators [54]. While *S. latifolia* is a dioecious plant (only male individuals develop flowers with stamina), *M. lychnidis-dioicae* counteracts the potential for sex-biased dispersal by inducing major transcriptional changes in female and to a lesser extent in male host plants. Thereby, female host plants become masculinized and develop rudimentary stamina that facilitate spore production and dispersal of *M. lychnidis-dioicae* [54]. The underlying molecular mechanisms whereby this host manipulation takes place as well as its origin are so far unknown.

Other pathogens rely on plant-associated vectors for the dispersal of spores. *Ophiostoma novo-ulmi*, the causal agent of Dutch elm disease, forms specialized asexual synnemata as well as sexual perithecia in the galleries of elm bark beetles. The fungal spores are deposited on insects passing through the galleries. Bark beetles, loaded with spores, feed on healthy elms, thereby enable the fungus to enter into the host xylem and facilitate infections of new hosts [55]. *Ophiostoma* is even able to induce an elevated production of particular volatiles in elms that function as a signal to attract insect vectors and thereby increase the probability of pathogen spore dispersal [56].

Plant-associated microbiota

Above, we summarize elements of plant-pathogen interactions and specialization of filamentous fungi to growth and reproduction in plant tissues. Plant surfaces and tissues are, however, also occupied by other microorganisms, which in different ways may interact with co-existing pathogens. A number of new studies highlight a functional importance of microorganisms in the rhizo- and phyllosphere of different plant species and also suggest an effect on plant defenses against pathogens [57–59]. Hence, plant pathogens do not only co-evolve with their hosts but also evolve strategies to co-exist with plant-associated microbiota. This can for example involve the secretion of special effectors that target microbes inhabiting the same niche for self-defense and competition [60]. Recent studies of rhizo- and phyllosphere-associated bacteria suggest that the

surrounding soil is the main reservoir for bacterial plant colonizers [57,61] and show a similar composition of root and leaf communities in terms of taxonomy and function [62]. Highly interconnected taxa have been identified and are called "hub" species, acting as mediators and stabilizers of biotic and abiotic factors that influence plant-microbial community assembly [63]. These hubs may also shape the molecular and co-evolutionary interactions of plants and pathogens, though mechanistic work is still lacking.

Direct pathogen-microbiota interactions can involve secretion of antimicrobial compounds [64] that have an impact on pathogen fitness. Endophytic strains of the bacterium *Burkholderia gladioli* isolated from wild and domesticated maize have been found to exhibit an antifungal effect on *Sclerotinia homoeocarpa*, presumably by production and secretion of antifungal compounds [65]. Hence, the presence or absence of particular "key" microbes may influence niche availability and determine overall pathogenicity or virulence of pathogens on host individuals. Studies of *Agave* species demonstrate that the composition of plant-associated fungal communities is mainly shaped by the geographic location of the host plants [66]. In contrast, bacterial communities were shown to be stable and reproducible and are mainly shaped by their plant-associated microhabitats e.g. rhizosphere or endosphere of roots and leaves [62,66]. Still, very little is known about the strategies filamentous pathogens employ to adapt to co-existing microbial communities of plants.

Conclusive remarks

Plant pathogens have evolved a broad diversity of strategies to infect their hosts. Some traits are generally found among species sharing the same lifestyle such as PCWDEs of necrotrophic pathogens and intracellular hyphal structures of many biotrophs for nutrient uptake. Others are more specific such as particular effector proteins that determine host ranges of distinct pathogens. Many pathogenicity-related traits are well characterized in model species, however less is known about traits that do not relate directly to pathogenicity. As summarized above, these include traits involved in host sensing, the exploration of host compounds, reproduction, and interactions with other microbial species. Future research will aim at improving our knowledge of pathogen ecology and evolution. A broader understanding of these is not only biologically relevant, but may also support the development of improved strategies to control pathogens in agricultural ecosystems.

Acknowledgements

We are grateful to Holger Adamiak for realization of artwork. We thank Mareike Möller for fruitful discussions and Michael Freitag for insightful comments to a previous version of this manuscript. This work was supported by intramural funding of the Max Planck Society to Eva H. Stukenbrock.

References

1. Parniske M: **Arbuscular mycorrhiza: the mother of plant root endosymbioses.** *Nat. Rev. Microbiol.* 2008, **6**:763–775.
2. Jung SC, Martinez-Medina A, Lopez-Raez JA, Pozo MJ: **Mycorrhiza-Induced Resistance and Priming of Plant Defenses**. *J. Chem. Ecol.* 2012, **38**:651–664.
3. Raffaele S, Farrer RA, Cano LM, Studholme DJ, MacLean D, Thines M, Jiang RHY, Zody MC, Kunjeti SG, Donofrio NM, et al.: **Genome Evolution Following Host Jumps in the Irish Potato Famine Pathogen Lineage**. *Science* 2010, **330**:1540–1543.
4. Stukenbrock EH, Bataillon T, Dutheil JY, Hansen TT, Li R, Zala M, McDonald BA, Wang J, Schierup MH: **The making of a new pathogen: insights from comparative population genomics of the domesticated wheat pathogen Mycosphaerella graminicola and its wild sister species.** *Genome Res.* 2011, **21**:2157–66.
5. Wicker T, Oberhaensli S, Parlange F, Buchmann JP, Shatalina M, Roffler S, Ben-David R, Doležel J, Simková H, Schulze-Lefert P, et al.: **The wheat powdery mildew genome shows the unique evolution of an obligate biotroph.** *Nat. Genet.* 2013, doi:10.1038/ng.2704.
6. Dong S, Stam R, Cano LM, Song J, Sklenar J, Yoshida K, Bozkurt TO, Oliva R, Liu Z, Tian M, et al.: **Effector Specialization in a Lineage of the Irish Potato Famine Pathogen**. *Science* 2014, **343**:552–555.
7. Poppe S, Dorsheimer L, Happel P, Stukenbrock EH: **Rapidly Evolving Genes Are Key Players in Host Specialization and Virulence of the Fungal Wheat Pathogen Zymoseptoria tritici (Mycosphaerella graminicola)**. *PLOS Pathog.* 2015, **11**:e1005055.
8. Giraldo MC, Valent B: **Filamentous plant pathogen effectors in action.** *Nat. Rev. Microbiol.* 2013, **11**:800–14.
9. Lo Presti L, Lanver D, Schweizer G, Tanaka S, Liang L, Tollot M, Zuccaro A, Reissmann S, Kahmann R: **Fungal Effectors and Plant Susceptibility.** *Annu. Rev. Plant Biol.* 2015, **66**:513–545.
10. Asai S, Shirasu K: **Plant cells under siege: Plant immune system versus pathogen effectors**. *Curr. Opin. Plant Biol.* 2015, **28**:1–8.
11. Stukenbrock EH, Jørgensen FG, Zala M, Hansen TT, McDonald BA, Schierup MH: **Whole-genome and chromosome evolution associated with host adaptation and speciation of the wheat pathogen Mycosphaerella graminicola.** *PLoS Genet.* 2010, **6**:e1001189.
12. de Jonge R, Bolton MD, Kombrink A, van den Berg GCM, Yadeta KA, Thomma BPHJ: **Extensive chromosomal reshuffling drives evolution of virulence in an asexual pathogen**. *Genome Res.* 2013, **23**:1271–1282.
13. Grandaubert J, Lowe RGT, Soyer JL, Schoch CL, Van de Wouw AP, Fudal I, Robbertse B, Lapalu N, Links MG, Ollivier B, et al.: **Transposable element-assisted evolution and adaptation to host plant within the Leptosphaeria maculans-Leptosphaeria biglobosa species complex of fungal pathogens.** *BMC Genomics* 2014, **15**:891.
14. Croll D, McDonald BA: **The accessory genome as a cradle for adaptive evolution in pathogens**. *PLoS Pathog.* 2012, **8**:8–10.
15. Stukenbrock EH, Croll D: **The evolving fungal genome**. *Fungal Biol. Rev.* 2014, **28**:1–12.
16. Seidl MF, Thomma BPHJ: **Sex or no sex: Evolutionary adaptation occurs regardless**. *BioEssays* 2014, **36**:335–345.
17. Dong S, Raffaele S, Kamoun S: **The two-speed genomes of filamentous pathogens: Waltz with plants**. *Curr. Opin. Genet. Dev.* 2015, **35**:57–65.
18. Aguileta G, Lengelle J, Chiapello H, Giraud T, Viaud M, Fournier E, Rodolphe F, Marthey S, Ducasse A, Gendrault A, et al.: **Genes under positive selection in a model plant pathogenic fungus, Botrytis**. *Infect. Genet. Evol.* 2012, **12**:987–996.
19. Brunner PC, Torriani SFF, Croll D, Stukenbrock EH, McDonald BA: **Coevolution and life cycle specialization of plant cell wall degrading enzymes in a hemibiotrophic pathogen.** *Mol. Biol. Evol.* 2013, **30**:1337–47.
20. Venturi V, Keel C: **Signaling in the Rhizosphere**. *Trends Plant Sci.* 2016, **21**:187–198.

21. Turrà D, El Ghalid M, Rossi F, Di Pietro A: **Fungal pathogen uses sex pheromone receptor for chemotropic sensing of host plant signals.** *Nature* 2015, **527**:521–524.
22. Tucker SL, Talbot NJ: **Surface attachment and pre-penetration stage development by plant pathogenic fungi**. *Annu. Rev. Phytopathol.* 2001, **39**:385–417.
23. Edwards MC, Bowling DJF: **The growth of rust germ tubes towards stomata in relation to pH gradients**. *Physiol. Mol. Plant Pathol.* 1986, **29**:185–196.
24. Horbach R, Navarro-Quesada AR, Knogge W, Deising HB: **When and how to kill a plant cell: infection strategies of plant pathogenic fungi.** *J. Plant Physiol.* 2011, **168**:51–62.
25. Kubicek CP, Starr TL, Glass NL: **Plant Cell Wall-Degrading Enzymes and Their Secretion in Plant-Pathogenic Fungi.** *Annu. Rev. Phytopathol.* 2014, doi:10.1146/annurev-phyto-102313-045831.
26. Zeilinger S, Gupta VK, Dahms TES, Silva RN, Singh HB, Upadhyay RS, Gomes EV, Tsui CK-M, Nayak S C: **Friends or foes? Emerging insights from fungal interactions with plants.** *FEMS Microbiol. Rev.* 2015, doi:10.1093/femsre/fuv045.
27. Ryder LS, Talbot NJ: **Regulation of appressorium development in pathogenic fungi.** *Curr. Opin. Plant Biol.* 2015, **26**:8–13.
28. Wang E, Schornack S, Marsh JF, Gobbato E, Schwessinger B, Eastmond P, Schultze M, Kamoun S, Oldroyd GED: **A common signaling process that promotes mycorrhizal and oomycete colonization of plants**. *Curr. Biol.* 2012, **22**:2242–2246.
29. Jones JDG, Dangl JL: **The plant immune system.** *Nature* 2006, **444**:323–9.
30. Djamei A, Schipper K, Rabe F, Ghosh A, Vincon V, Kahnt J, Osorio S, Tohge T, Fernie AR, Feussner I, et al.: **Metabolic priming by a secreted fungal effector**. *Nature* 2011, **478**:395–398.
31. Plett JM, Kemppainen M, Kale SD, Kohler A, Legué V, Brun A, Tyler BM, Pardo AG, Martin F: **A secreted effector protein of Laccaria bicolor is required for symbiosis development**. *Curr. Biol.* 2011, **21**:1197–1203.
32. Kloppholz S, Kuhn H, Requena N: **A secreted fungal effector of glomus intraradices promotes symbiotic biotrophy**. *Curr. Biol.* 2011, **21**:1204–1209.
33. Tanaka S, Brefort T, Neidig N, Djamei A, Kahnt J, Vermerris W, Koenig S, Feussner K, Feussner I, Kahmann R: **A secreted *Ustilago maydis* effector promotes virulence by targeting anthocyanin biosynthesis in maize**. *Elife* 2014, **3**:1–27.
34. Dagdas YF, Belhaj K, Maqbool A, Chaparro-Garcia A, Pandey P, Petre B, Tabassum N, Cruz-Mireles N, Hughes RK, Sklenar J, et al.: **An effector of the Irish potato famine pathogen antagonizes a host autophagy cargo receptor**. *Elife* 2016, doi:10.7554/eLife.10856.
35. Weiberg A, Wang M, Lin F-M, Zhao H, Zhang Z, Kaloshian I, Huang H-D, Jin H: **Fungal small RNAs suppress plant immunity by hijacking host RNA interference pathways.** *Science* 2013, **342**:118–23.
36. Bolton MD, Thomma BPHJ, Nelson BD: **Sclerotinia sclerotiorum (Lib.) de Bary: Biology and molecular traits of a cosmopolitan pathogen**. *Mol. Plant Pathol.* 2006, **7**:1–16.
37. Guyon K, Balagué C, Roby D, Raffaele S: **Secretome analysis reveals effector candidates associated with broad host range necrotrophy in the fungal plant pathogen Sclerotinia sclerotiorum**. *BMC Genomics* 2014, **15**:336.
38. Friesen TL, Faris JD, Solomon PS, Oliver RP: **Host-specific toxins: effectors of necrotrophic pathogenicity.** *Cell. Microbiol.* 2008, **10**:1421–1428.
39. Oliver RP, Friesen TL, Faris JD, Solomon PS: **Stagonospora nodorum: From Pathology to Genomics and Host Resistance**. *Annu. Rev. Phytopathol.* 2012, **50**:23–43.
40. Manning VA, Ciuffetti LM: **Localization of Ptr ToxA Produced by Pyrenophora tritici-repentis Reveals Protein Import into Wheat Mesophyll Cells.** *Plant Cell* 2005, **17**:3203–3212.
41. Friesen T, Stukenbrock E, Liu Z, Meinhardt S, Ling H, Faris J, Rasmussen J, Solomon P, McDonald B, Oliver R: **Emergence of a new disease as a result of interspecific virulence gene transfer.** *Nat. Genet.* 2006, **38**:953–956.

42. Faris JD, Zhang Z, Lu H, Lu S, Reddy L, Cloutier S, Fellers JP, Meinhardt SW, Rasmussen JB, Xu SS, et al.: **A unique wheat disease resistance-like gene governs effector-triggered susceptibility to necrotrophic pathogens**. *Proc. Natl. Acad. Sci.* 2010, **107**:13544–13549.
43. Lyu X, Shen C, Fu Y, Xie J, Jiang D, Li G, Cheng J: **A Small Secreted Virulence-Related Protein Is Essential for the Necrotrophic Interactions of Sclerotinia sclerotiorum with Its Host Plants**. *PLOS Pathog.* 2016, **12**:e1005435.
44. Ma L-J, van der Does HC, Borkovich KA, Coleman JJ, Daboussi M-J, Di Pietro A, Dufresne M, Freitag M, Grabherr M, Henrissat B, et al.: **Comparative genomics reveals mobile pathogenicity chromosomes in Fusarium.** *Nature* 2010, **464**:367–373.
45. de Jonge R, van Esse HP, Maruthachalam K, Bolton MD, Santhanam P, Saber MK, Zhang Z, Usami T, Lievens B, Subbarao K V, et al.: **Tomato immune receptor Ve1 recognizes effector of multiple fungal pathogens uncovered by genome and RNA sequencing.** *Proc. Natl. Acad. Sci. U. S. A.* 2012, **109**:5110–5.
46. Dutheil JY, Mannhaupt G, Schweizer G, Sieber CM, Münsterkötter M, Güldener U, Schirawski J, Kahmann R: **A tale of genome compartmentalization: the evolution of virulence clusters in smut fungi**. *Genome Biol. Evol.* 2016, **8**:681–704.
47. Ponomarenko A, Goodwin SB, Kema GHJ: **Septoria tritici blotch (STB) of wheat**. *Plant Heal. Instr.* 2011, doi:10.1094/PHI-I-2011-0407-01.
48. Marcel S, Sawers R, Oakeley E, Angliker H, Paszkowski U: **Tissue-adapted invasion strategies of the rice blast fungus Magnaporthe oryzae.** *Plant Cell* 2010, **22**:3177–87.
49. Schilling L, Matei A, Redkar A, Walbot V, Doehlemann G: **Virulence of the maize smut Ustilago maydis is shaped by organ-specific effectors**. *Mol. Plant Pathol.* 2014, **15**:780–789.
50. Zhao Z, Liu H, Wang C, Xu J: **Comparative analysis of fungal genomes reveals different plant cell wall degrading capacity in fungi**. *BMC Genomics* 2013, **14**:274.
51. Ohm RA, Feau N, Henrissat B, Schoch CL, Horwitz BA, Barry KW, Condon BJ, Copeland AC, Dhillon B, Glaser F, et al.: **Diverse lifestyles and strategies of plant pathogenesis encoded in the genomes of eighteen Dothideomycetes fungi.** *PLoS Pathog.* 2012, **8**:e1003037.
52. Hückelhoven R, Panstruga R: **Cell biology of the plant-powdery mildew interaction**. *Curr. Opin. Plant Biol.* 2011, **14**:738–746.
53. Brown JKM, Hovmøller MS: **Aerial dispersal of pathogens on the global and continental scales and its impact on plant disease.** *Science* 2002, **297**:537–541.
54. Zemp N, Tavares R, Widmer A: **Fungal Infection Induces Sex-Specific Transcriptional Changes and Alters Sexual Dimorphism in the Dioecious Plant Silene latifolia**. *PLOS Genet.* 2015, **11**:e1005536.
55. Comeau AM, Dufour J, Bouvet GF, Jacobi V, Nigg M, Henrissat B, Laroche J, Levesque RC, Bernier L: **Functional annotation of the Ophiostoma novo-ulmi genome: Insights into the phytopathogenicity of the fungal agent of Dutch elm disease**. *Genome Biol. Evol.* 2015, **7**:410–430.
56. McLeod G, Gries R, von Reuss SH, Rahe JE, McIntosh R, König WA, Gries G: **The pathogen causing Dutch elm disease makes host trees attract insect vectors.** *Proc. Biol. Sci.* 2005, **272**:2499–503.
57. Bulgarelli D, Rott M, Schlaeppi K, Ver Loren van Themaat E, Ahmadinejad N, Assenza F, Rauf P, Huettel B, Reinhardt R, Schmelzer E, et al.: **Revealing structure and assembly cues for Arabidopsis root-inhabiting bacterial microbiota.** *Nature* 2012, **488**:91–95.
58. Pieterse CMJ, Zamioudis C, Berendsen RL, Weller DM, Van Wees SCM, Bakker PAHM: **Induced systemic resistance by beneficial microbes.** *Annu. Rev. Phytopathol.* 2014, **52**:347–75.
59. Vandenkoornhuyse P, Quaiser A, Duhamel M, Le Van A, Dufresne A: **The importance of the microbiome of the plant holobiont**. *New Phytol.* 2015, **206**:1196–1206.
60. Rovenich H, Boshoven JC, Thomma BPHJ: **Filamentous pathogen effector functions: Of pathogens, hosts and microbiomes**. *Curr. Opin. Plant Biol.* 2014, **20**:96–103.

61. Zarraonaindia I, Owens SM, Weisenhorn P, West K, Hampton-Marcell J, Lax S, Bokulich NA, Mills DA, Martin G, Taghavi S, et al.: **The Soil Microbiome Influences Grapevine-Associated Microbiota**. *MBio* 2015, **6**:1–10.
62. Bai Y, Müller DB, Srinivas G, Garrido-Oter R, Potthoff E, Rott M, Dombrowski N, Münch PC, Spaepen S, Remus-Emsermann M, et al.: **Functional overlap of the Arabidopsis leaf and root microbiota**. *Nature* 2015, **528**:364–369.
63. Agler MT, Ruhe J, Kroll S, Morhenn C, Kim S-T, Weigel D, Kemen EM: **Microbial Hub Taxa Link Host and Abiotic Factors to Plant Microbiome Variation**. *PLOS Biol.* 2016, **14**:e1002352.
64. Hernández-León R, Rojas-Solís D, Contreras-Pérez M, Orozco-Mosqueda M del C, Macías-Rodríguez LI, Reyes-de la Cruz H, Valencia-Cantero E, Santoyo G: **Characterization of the antifungal and plant growth-promoting effects of diffusible and volatile organic compounds produced by Pseudomonas fluorescens strains**. *Biol. Control* 2015, **81**:83–92.
65. Shehata HR, Lyons E, Jordan K, Raizada MN: **Bacterial endophytes from wild and ancient maize suppress the fungal pathogen Sclerotinia homoeocarpa**. *J. Appl. Microbiol.* 2015, doi:10.1111/jam.13050.
66. Coleman-Derr D, Desgarennes D, Fonseca-Garcia C, Gross S, Clingenpeel S, Woyke T, North G, Visel A, Partida-Martinez LP, Tringe S: **Biogeography and cultivation affect microbiome composition in the drought-adapted plant Subgenus Agave**. *New Phytol.* 2016, **209**:798–811.

Recommended references

* of special interest

** of outstanding interest

****Dong S, Stam R, Cano LM, Song J, Sklenar J, Yoshida K, Bozkurt TO, Oliva R, Liu Z, Tian M, et al.: Effector Specialization in a Lineage of the Irish Potato Famine Pathogen. Science 2014, 343:552–555.**

First study that provides functional evidence how accelerated gene evolution contributes to host adaptation. Plant pathogens of the oomycete genus *Phytophthora* secrete the effector EPIC1, a cystatin-like protease inhibitor that targets host defense proteases in the apoplast. *epiC1* has been under strong positive selection since the divergence of *Phytophthora infestans* and *P. mirabilis* and their specialization to distantly related hosts *Solanum* sp. and *Mirabilis jalapa*. EPIC1 of *P. mirabilis* inhibits the *M. jalapa* protease target more efficiently than *Solanum* proteases and vice versa. Dong and colleagues demonstrate that this particular host adaptation is conferred by a single amino acid change in the pathogen effector reciprocal to a single amino acid polymorphism in the host protease.

****Poppe S, Dorsheimer L, Happel P, Stukenbrock EH: Rapidly Evolving Genes Are Key Players in Host Specialization and Virulence of the Fungal Wheat Pathogen Zymoseptoria tritici (Mycosphaerella graminicola). *PLOS Pathog.* 2015, 11:e1005055.**

Based on genome-wide evolutionary predictions in the wheat pathogen *Zymoseptoria tritici* and two close relatives *Z. pseudotritici* and *Z. ardabiliae* genes that evolved under positive selection during speciation were identified. Functional analysis showed that one of these genes, *Zt80707* has a putative role in asexual reproduction of *Z. tritici* on wheat. The respective mutant was strongly impaired in pycnidia development what could not be restored by insertion of the homologs from the sister species. The study demonstrates how certain species-specific nucleotide substitutions are essential for asexual reproduction of *Z. tritici* in wheat.

***Lo Presti L, Lanver D, Schweizer G, Tanaka S, Liang L, Tollot M, Zuccaro A, Reissmann S, Kahmann R: Fungal Effectors and Plant Susceptibility. *A. Rev. Plant Biol.* 2015, 66:513–545.**

This review article presents an excellent overview about effectors in plant-colonizing fungi with different lifestyles.

****Lyu X, Shen C, Fu Y, Xie J, Jiang D, Li G, Cheng J: A Small Secreted Virulence-Related Protein Is Essential for the Necrotrophic Interactions of Sclerotinia sclerotiorum with Its Host Plants. *PLOS Pathog.* 2016, 12:e1005435.**

This study provides insight into the molecular interactions between a non-specific effector and a conserved component of plant metabolism. Lyu and colleagues functionally characterized the small secreted protein SsSSVP1 of the necrotrophic fungus *Sclerotinia sclerotiorum* that is strongly induced during plant infection and required for full virulence. SsSSVP1 interacts with QCR8, a component of the cytochrome b-c_1 complex of mitochondrial respiratory chain and thereby induces cell death. The *QCR8* gene is highly conserved in plants and interaction of SsSSVP1 and QCR8 might be instrumental for *S. sclerotiorum* to infect a broad diversity of hosts.

****Zemp N, Tavares R, Widmer A: Fungal Infection Induces Sex-Specific Transcriptional Changes and Alters Sexual Dimorphism in the Dioecious Plant Silene latifolia. *PLOS Genet.* 2015, 11:e1005536.**

This paper shows that the smut fungus *Microbotryum lychnidis-dioicae* induces strong transcriptional reprogramming in infected *Silene latifolia* plants. Changes in host transcriptomes were found to be highly sex-specific and cause a reduced sexual dimorphism in the dioecious host plant. Changes mainly impact floral traits and lead to a partial sex reversal in female plants. Infected females also develop rudimentary stamina that are required for production and dispersal of fungal teliospores.

****Turrà D, El Ghalid M, Rossi F, Di Pietro A: Fungal pathogen uses sex pheromone receptor for chemotropic sensing of host plant signals. *Nature* 2015, 527:521–524.**

The soil-borne pathogen *Fusarium oxysporum* exhibits chemotrophic growth towards nutrients and host plants roots. Turrà and colleagues show that plant peroxidases in roots and root exudate induce chemotropic response towards host tissue. Peroxidases are sensed by activation of a seven-pass transmembrane receptor that is a functional homolog of yeast α pheromone receptor Ste2 and chemotrophic growth of *F. oxysporum* hyphae involves subsequent intracellular signaling.

****Agler MT, Ruhe J, Kroll S, Morhenn C, Kim S-T, Weigel D, Kemen EM: Microbial Hub Taxa Link Host and Abiotic Factors to Plant Microbiome Variation. *PLOS Biol.* 2016, 14:e1002352.**

This is the first study on phyllosphere microbial communities in *Arabidopsis* that covers fungi, oomycetes, and bacteria. The authors identify strongly interconnected "hub" taxa that occupy central positions in the plant-associated microbial networks.

***Bai Y, Müller DB, Srinivas G, Garrido-Oter R, Potthoff E, Rott M, Dombrowski N, Münch PC, Spaepen S, Remus-Emsermann M, et al.: Functional overlap of the Arabidopsis leaf and root microbiota. *Nature* 2015, 528:364–369.**

The paper demonstrates that many bacterial taxa that are associated with *Arabidopsis* roots are also present on *Arabidopsis* leaves. Based on genome sequencing of around 400 root- and leaf-associated taxa the authors show that bacterial species on roots and on leaves possess genes with similar functional capabilities.

***Zeilinger S, Gupta VK, Dahms TES, Silva RN, Singh HB, Upadhyay RS, Gomes EV, Tsui CK-M, Nayak S C: Friends or foes? Emerging insights from fungal interactions with plants. *FEMS Microbiol. Rev.* 2015, doi:10.1093/femsre/fuv045.**

This article presents a comprehensive and broad review of plant-fungal interactions.

Chapter 2

Extremely flexible infection programs in a fungal plant pathogen

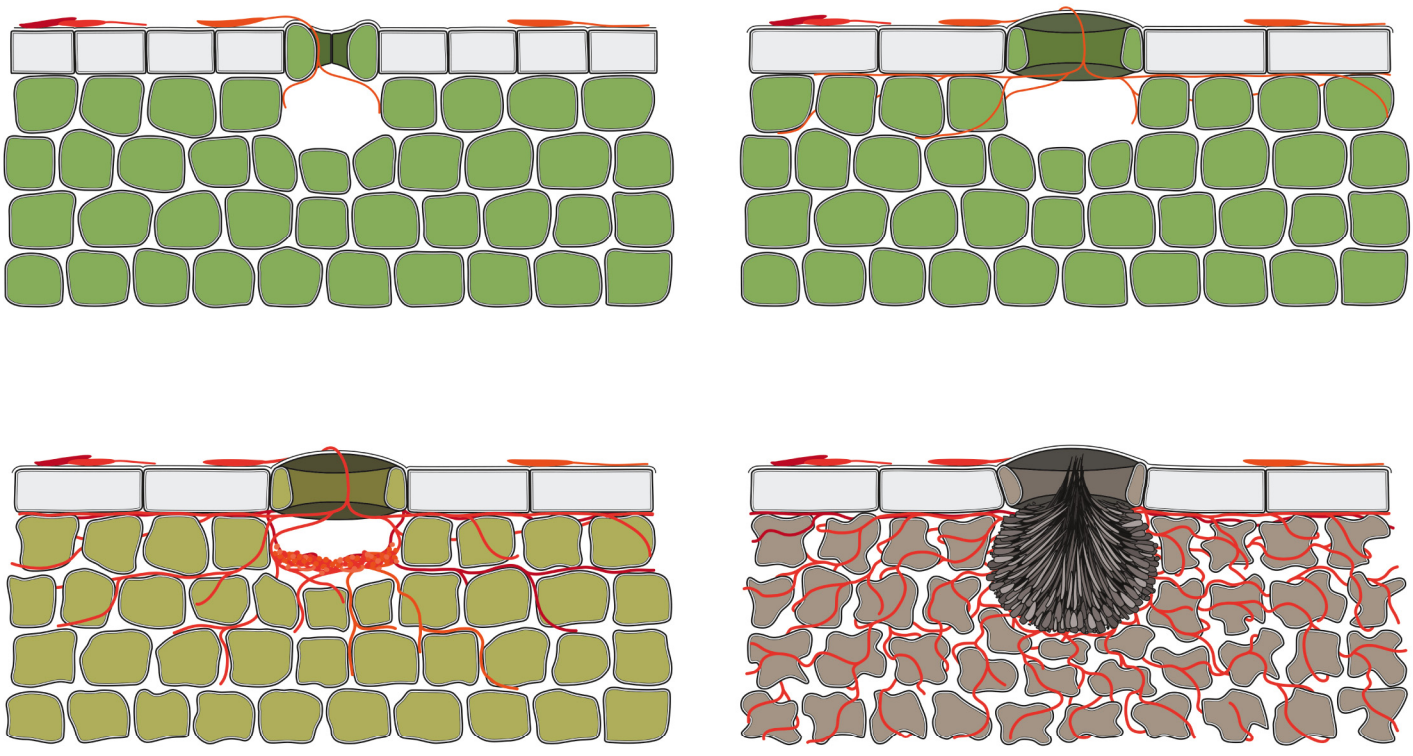

Chapter 2

Extremely flexible infection programs in a fungal plant pathogen

Research paper, published as preprint on bioRxiv (doi: 10.1101/229997). Currently, submitted and under peer review.

Authors: Janine Haueisen, Mareike Möller, Christoph J. Eschenbrenner, Jonathan Grandaubert, Heike Seybold, Holger Adamiak and Eva H. Stukenbrock

Abstract

Filamentous plant pathogens exhibit extraordinary levels of genomic variability that is proposed to facilitate rapid adaptation to changing host environments. However, the impact of genomic variation on phenotypic differentiation in pathogen populations is largely unknown. Here, we address the extent of variability in infection phenotypes of the hemibiotrophic wheat pathogen *Zymoseptoria tritici* by studying three field isolates collected in Denmark, Iran, and the Netherlands. These three isolates differ extensively in genome structure and gene content, but produce similar disease symptoms in the same susceptible wheat cultivar. Using advanced confocal microscopy, staining of reactive oxygen species, and comparative analyses of infection stage-specific RNA-seq data, we demonstrate considerable variation in the temporal and spatial course of infection of the three isolates. Based on microscopic observation, we determined four core infection stages: establishment, biotrophic growth, lifestyle transition, and necrotrophic growth and asexual reproduction. Comparative analyses of the fungal transcriptomes, sequenced for every infection stage, revealed that the gene expression profiles of the isolates differed significantly, and 20% of the genes are differentially expressed between the three isolates during infection. The genes exhibiting isolate-specific expression patterns are enriched in genes encoding effector candidates that are small, secreted, cysteine-rich proteins and putative virulence determinants. Moreover, the differentially expressed genes were located significantly closer to transposable elements, which are enriched for the heterochromatin-associated histone marks H3K9me3 and H3K27me3 on the accessory chromosomes. This observation indicates that transposable elements and epigenetic regulation contribute to the infection-associated transcriptional variation between the isolates. Our findings illustrate how high genetic diversity in a pathogen population can result in highly differentiated infection and expression phenotypes that can support rapid adaptation in changing environments. Furthermore, our study reveals an

exceptionally high extent of plasticity in the infection program of an important wheat pathogen and shows a substantial redundancy in infection-related gene expression.

Author summary

Zymoseptoria tritici is a pathogen that infects wheat and induces necrosis in leaf tissue. *Z. tritici* field populations exhibit high levels of genetic diversity, and here we addressed the consequences of this diversity on infection phenotypes. We conducted a detailed comparison of the infection processes of three *Z. tritici* isolates collected in Denmark, the Netherlands, and Iran. We inoculated leaves of a susceptible wheat cultivar and monitored development of disease symptoms and infection structures in leaf tissue by confocal microscopy. The three isolates exhibited highly differentiated spatial and temporal patterns of infection, although quantitative disease was similar. Furthermore, more than 20% of the genes were differentially expressed in the three isolates during wheat infection. Variation in gene expression is particularly associated with transposable elements, suggesting a role of epigenetic regulation in transcriptional variation among the three isolates. Finally, we find that genes encoding putative virulence determinants were enriched among the differentially expressed genes, suggesting that each of the three *Z. tritici* isolates utilizes different strategies to manipulate host defenses. Our results emphasize that phenotypic diversity plays an important role in pathogen populations and should be considered when developing crop protection strategies.

Introduction

Population genomics and comparative genome analyses have been applied to characterize genetic variation within and between species of pathogens [1]. Studies of eukaryotic pathogens have demonstrated high levels of intraspecies genetic variability, even in species that predominantly propagate by clonal reproduction [2–5]. In sexual species, frequent recombination contributes to the formation of new genotypes, while transposable elements and repeat-rich genome compartments facilitate the generation of novel genetic variants, most notably in asexual species [6–8]. In addition, many fungal plant pathogens–both sexual and asexual species–carry exceptionally high levels of karyotypic variability that originates from structural chromosome rearrangements and the presence of accessory chromosomes or genome compartments composed of transposable elements [4,5,9–11].

Genetic variation can translate into phenotypic variation that is important for populations to persist in changing environments. High levels of phenotypic variation can provide an adaptive advantage to pathogens exposed to new host resistances or, in agricultural systems, drug treatments. However, while theoretical and empirical data support the importance of genetic variation in rapid adaptation, we still know little about the overall extent and consequences of phenotypic variation in populations of pathogens.

Phenotypic variation in pathogen populations has been studied mainly in the context of virulence and drug resistance. Disease phenotypes have been correlated with genetic maps or genome-wide single nucleotide polymorphism (SNP) data to identify variable sites responsible for distinct virulence phenotypes [12–15]. While virulence and drug resistance traits are main determinants of the overall fitness of a pathogen, other traits also influence infection development. For example, individual strains of pathogens may exhibit variation in the spatial, temporal, and physiological exploration of host tissues, as well in reproductive success. While these traits are not directly linked to virulence, they may greatly impact the fitness of individual isolates and evolution at the population scale [16].

In this study, we addressed the extent of variation in infection phenotypes of a fungal plant pathogen characterized by a high level of genomic variability. We used the wheat pathogen *Zymoseptoria tritici* (syn. *Mycosphaerella graminicola*) as a model to investigate how the development of disease symptoms and the transcriptional program induced during infection varies among three field isolates from geographically distinct locations. *Z. tritici* has a hemibiotrophic lifestyle characterized by an initial biotrophic phase, where the fungus feeds on living host cells, followed by necrotrophic growth where the fungus degrades and takes up nutrients from dead host cells. Genomics, transcriptomics, and proteomics studies have been applied to identify virulence determinants of *Z. tritici*. The haploid genome of *Z. tritici* comprises a high number of accessory chromosomes ranging from 400 kb to 1 Mb in size in the reference

isolate IPO323 [17,18]. Recent studies provide evidence for the presence of virulence determinants on the accessory chromosomes, however the genes responsible for these effects have so far not been identified [19]. Furthermore, several genome-wide association (GWAS) and quantitative trait loci (QTL) mapping studies have linked a variety of phenotypic traits to genetic variants and candidate genes [20–24], including the avirulence gene *AvrStb6,* which interacts with the wheat resistance gene *Stb6* [25]. *Z. tritici* has served as a prominent model in population genetic studies of crop pathogens, and genetic variation has been assessed on a local (individual lesions) up to a continental scale. The amount of genetic variation in a *Z. tritici* field population is comparable to the variation found on a continental scale, including multiple regional populations [26–28]. Thus, the plants in a single wheat field are infected by *Z. tritici* isolates with wide genotypic diversity.

Here, we investigated how infection of a susceptible host by genetically and morphologically distinct isolates results in similar levels of quantitative virulence. By combining confocal microscopy, disease monitoring, reactive oxygen species (ROS) localization, and transcriptome analyses, we compiled a detailed characterization of infection phenotypes of the three isolates. We hypothesized that high genetic diversity not only increases the evolutionary potential of the pathogen but also results in a variety of host-pathogen interactions that cause a range of different infection phenotypes. Our combined comparative analyses enabled us to characterize infection morphology and gene expression of the three *Z. tritici* isolates, including a core infection program and isolate-specific infection phenotypes. We conclude that variation in infection and expression phenotypes is important for adaptive evolution of pathogens and needs to be considered in the development of disease control strategies.

Results and Discussion

The *Z. tritici* isolates Zt05, Zt09, and Zt10 are equally virulent, but disease symptoms develop at different speeds

We compared virulence phenotypes of three *Z. tritici* isolates Zt05 [29], Zt09 (≙ IPO323ΔChr18, a derivate of the reference strain IPO323 [18] that lost chromosome 18 [30]), and Zt10 [31], previously collected in Denmark, the Netherlands, and Iran, respectively (S1 Table), on leaves of the highly susceptible winter wheat cultivar Obelisk. We evaluated infections 28 days post inoculation (dpi) by estimating the percentage of leaf area affected by necrosis (Fig 1A) and covered with pycnidia, the asexual fruiting bodies (Fig 1B). The production of pycnidia is an essential measure for pathogen fitness and virulence [32]. Although we observed different levels of necrosis (two-sided Mann-Whitney *U* tests, $P \leq 0.0048$) we found no significant differences in the amount of pycnidia produced by the three isolates (two-sided Mann-Whitney *U* tests, $P \geq 0.034$) (S1 Fig).

Because the three *Z. tritici* isolates are equally fit and virulent on the wheat cultivar Obelisk, we next investigated whether disease symptoms and pathogen infection develop at a similar pace. We monitored temporal disease progress by screening the leaves every other day for visible necrotic spots and pycnidia. Leaves inoculated with Zt05 and Zt09 showed necrosis and pycnidia significantly earlier than leaves inoculated with Zt10 (one-sided Mann-Whitney *U* tests, $P \leq 7.73*10^{-8}$) (Fig 2A). The median onset of necrosis caused by Zt09 occurred one day after that caused by Zt05 and is significantly later (one-sided Mann-Whitney *U* test, $P = 0.0089$), although the first pycnidia of both isolates developed at the same time (two-sided Mann-Whitney *U* test, $P = 0.9455$). Thus, although the three *Z. tritici* isolates produced the same pycnidia density in the cultivar Obelisk, disease develops at different paces.

ROS play a central role in plant pathogen defense by acting as signalling molecules after pathogen recognition and activating defense responses [33]. We visualized the accumulation of the ROS H_2O_2 in infected leaves by diaminobenzidine (DAB) staining to determine whether the observed differences in temporal disease development of *Z. tritici* isolates reflect a temporal variation in host response. Ten to 14 days after inoculation, we observed no ROS (Fig 2B) indicating that *Z. tritici* suppresses the activation of wheat immune responses during this phase. ROS accumulation coincided with the onset of necrosis (Fig 2B, S2 Fig) and, consistent with the faster disease progress, ROS accumulates earlier in leaves infected with Zt05 than Zt09 or Zt10. For Zt09 and Zt10, high ROS concentrations appear at only 18 dpi when Zt05 infected leaves are already largely necrotic and the DAB staining indicates further increased ROS concentrations (Fig 2B, S2 Fig). Thereby, the timing of ROS accumulation in response to the three *Z. tritici* isolates is consistent with the observed differences in the temporal development of disease symptoms in infected wheat tissue.

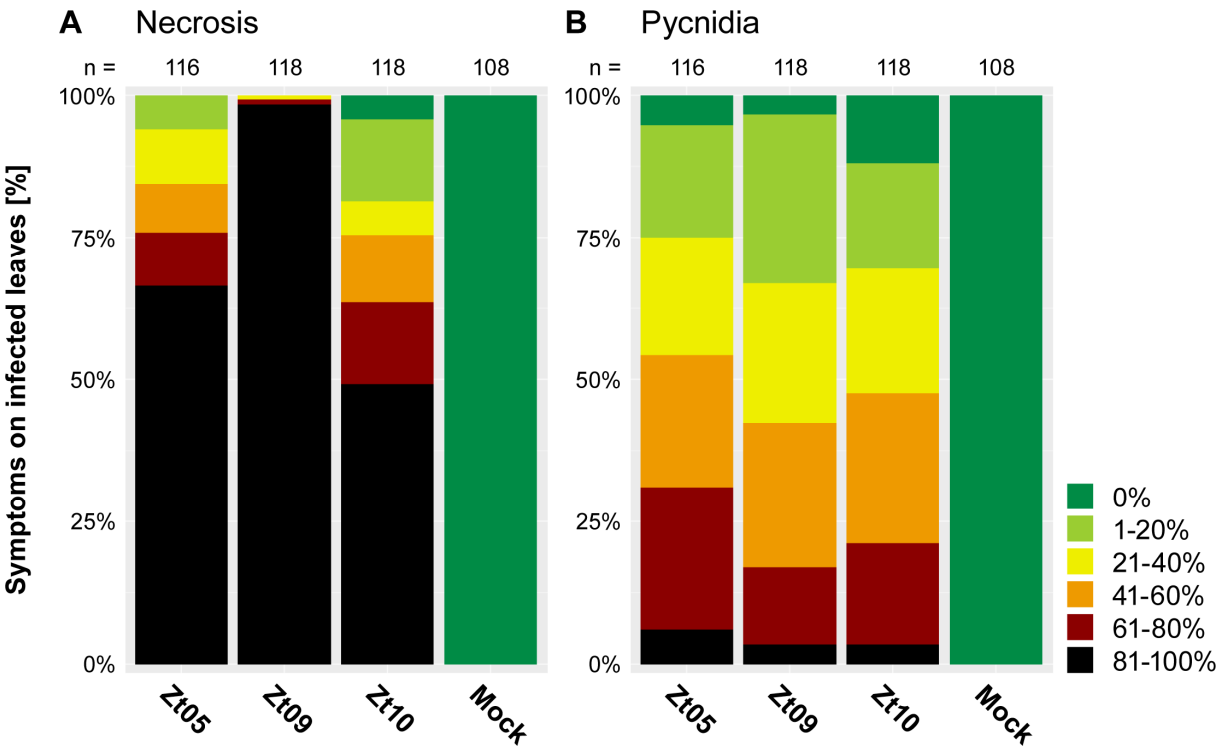

Figure 1. ***In-planta*** **phenotypic assay demonstrates similar pycnidia levels of** ***Z. tritici*** **isolates on the susceptible wheat cultivar Obelisk.** Quantitative differences in **(A)** necrosis and **(B)** pycnidia coverage of inoculated leaf areas were manually assessed at 28 days post inoculation based on six categories: 0 (without visible symptoms), 1 (1% to 20%), 2 (21% to 40%), 3 (41% to 60%), 4 (61% to 80%), and 5 (81% to 100%). The three isolates caused different levels of necrosis (two-sided Mann-Whitney *U* tests, $P \leq 0.0048$) but pycnidia levels were not different (two-sided Mann-Whitney *U* tests, $P \geq 0.034$).

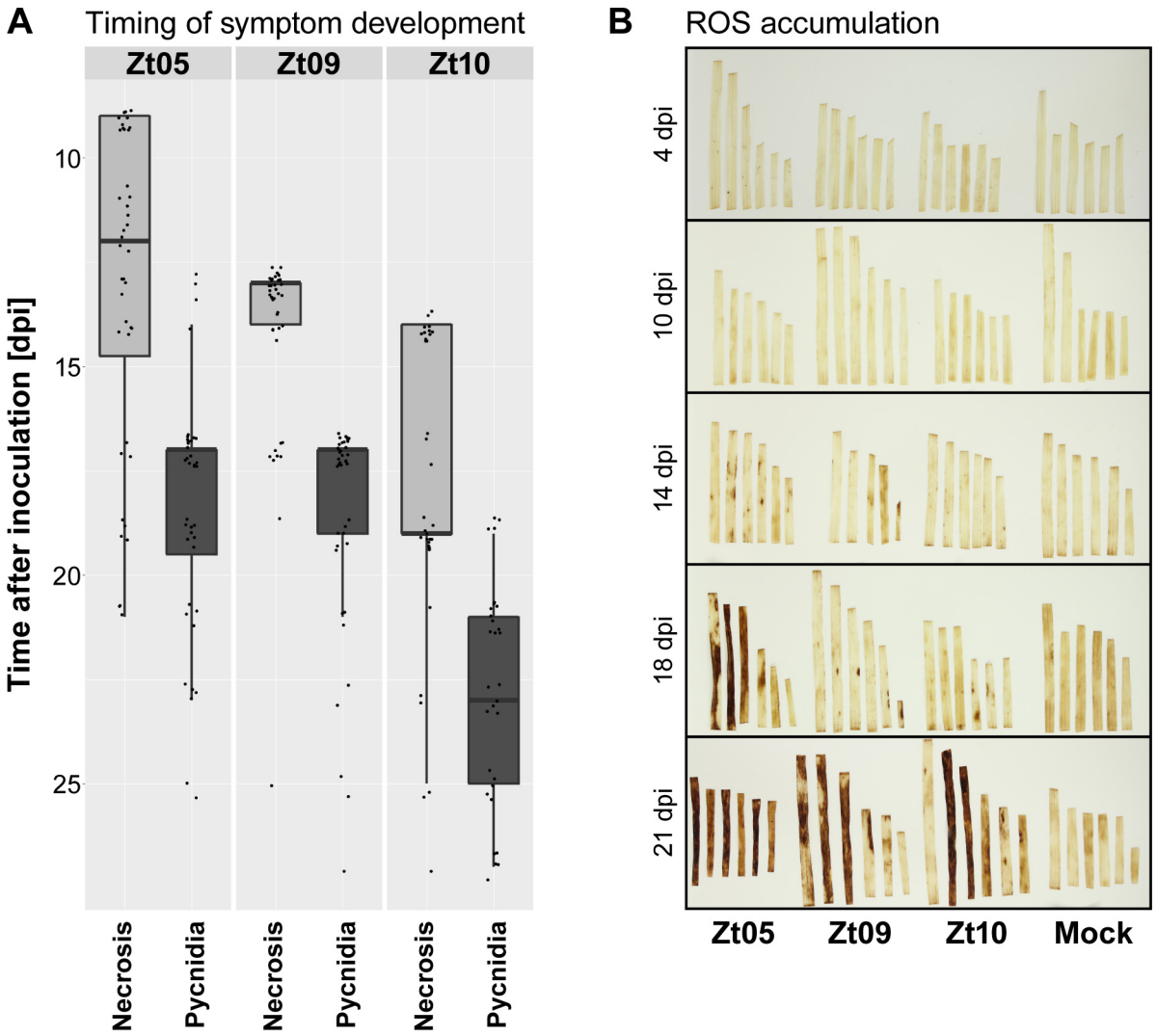

Figure 2. Timing of disease symptom development and H_2O_2 accumulation varies between wheat leaves infected with different *Z. tritici* isolates. (A) Temporal disease progression for infections with Zt05, Zt09, and Zt10 was measured by daily manual screening for the first occurrence of necrotic spots and pycnidia. For each isolate, 40 leaves of the wheat cultivar Obelisk were inoculated and tested. No disease developed on seven of the leaves inoculated with Zt10. **(B)** Infected leaves were stained for accumulation of the reactive oxygen species H_2O_2 at 4, 10, 14, 18, and 21 dpi by 3,3'-diaminobenzidine. Dark red-brown precipitate indicates H_2O_2 accumulation and appeared first in leaves infected with Zt05 in leaf areas beginning to undergo necrosis.

Z. tritici isolates tolerate different levels of abiotic stress

Z. tritici is characterized by a dimorphic lifestyle with hyphal growth during host infection and predominantly yeast-like growth in culture [34]. The yeast/hyphae dimorphism is likely inherited as a multigenic quantitative trait [35] and is essential for pathogenicity [36]. The fungus is exposed to a multitude of environmental influences during infection, dispersal, and other less well

characterized stages of the life cycle such as saprotrophic growth and spore dormancy. We compared tolerance of the three *Z. tritici* isolates to several abiotic *in vitro* stressors (temperature, oxidative, osmotic, and cell wall stresses) to assess the variability in growth phenotypes. Colonies of the three isolates exhibited different morphologies and tolerated different levels of abiotic stress (Table 1, S3 Fig). Only osmotic stress led to the same level of reduced growth in all strains. Under all tested conditions, colonies of Zt09 and Zt10 were mainly composed of yeast-like cells, whereas Zt05 predominantly grew as hyphae. On plates with Congo red or calcofluor white, Zt05 formed hyphal colonies, similar to those formed on yeast-malt-sucrose (YMS) control plates, whereas Zt09 and Zt10 were growth-impaired. These results indicate differences in the cell wall composition of yeast-like and hyphal cells, and that yeast-like cells are more susceptible to cell wall-interfering agents.

Elevated temperatures greatly impact development of Zt10 that formed strongly melanized colonies at 20/22°C and 28°C. Melanin pigments have several important functions in fungal pathogens, including protection against harsh environmental conditions [37]. Zt10 was collected in the Ilam Province, one of the hottest and driest regions in Iran [38], and the increased melanization could reflect local adaptation to extreme temperatures and temperature fluctuations [39], desiccation, and increased UV radiation.

Oxidative stress eventually diminishes growth of all isolates, although Zt09 tolerated exposure to H_2O_2 more than Zt05 and Zt10. *Z. tritici* experiences oxidative stress *in planta* from ROS produced as a host defense response or released from dead tissue. In general, higher tolerance to ROS is advantageous [40], for example during necrotrophic growth and pycnidia formation in dead mesophyll tissue [41]. However, mechanisms to detoxify extracellular ROS must be tightly regulated to avoid ROS levels that are toxic to the hosts [33], and we speculate that the observed differences in H_2O_2 tolerance reflect divergent adaptation of the *Z. tritici* isolates to host populations with different defense responses to pathogen invasion. Together, the *in vitro* stress assay revealed unanticipated intraspecies variation in tolerance to abiotic stresses among the *Z. tritici* isolates, especially considering that all were isolated in agro-ecosystems from the same host species, *Triticum aestivum*. The variation in colony morphology and stress responses may reflect different adaptations of the *Z. tritici* isolates to their local environments, and our observations suggest that ecological adaptation of fungal plant pathogens can be a strong driver of phenotypic divergence.

Table 1. The three *Z. tritici* isolates vary in tolerance to abiotic stressors.

	20/22C° at 16-h day / 8-h night	28C°	2 mM H_2O_2	3 mM H_2O_2	1 M sorbitol	1 M NaCl	500 µg/mL Congo red	200 µg/mL calcofluor white
Zt05	-	+	++	+++	+	++	-	-
Zt09	-	-	-	+	+	++	++	++
Zt10	++	+++	+	++	+	++	++	+

Summary of the *in vitro* stress assay comparing tolerance of the *Z. tritici* isolates Zt05, Zt09, and Zt10 to abiotic stressors. Symbols indicate tolerance levels in comparison to growth on YMS control plates at 18°C: - isolate was not affected, + isolate was mildly sensitive, ++ isolate was moderately sensitive, +++ isolate was highly sensitive.

Z. tritici infection is characterized by four core developmental stages

Next, we aimed to morphologically characterize host colonization of the three *Z. tritici* isolates. We conducted detailed confocal microscopy analyses in which we scanned 101 leaves harvested at 16 time points after inoculation. Analyses of large z-stacks of longitudinal optical sections allowed us to infer the spatial and temporal fungal colonization on and in infected leaves. First, we focused on the commonalities in host colonization between the different isolates and identified a sequence of four stages that we define as the core infection program of *Z. tritici* (Fig 3).

Stage A, or infection establishment, involves the penetration of wheat leaf tissue by fungal hyphae. Fungal cells germinate after inoculation on the leaf surface, indicating that germination is triggered extrinsically after the fungus senses particular plant-derived cues, as has been previously shown for *Fusarium oxysporum* [42]. Germ tubes develop into infection hyphae, some of which grow in the direction of stomata (Fig 3A stage A, S1 and S2 Animation). During stomatal penetration and in the sub-stomatal cavities, infection hyphae grow in tight contact with the guard cells. We occasionally noticed slight swelling of hyphae on top of stomatal openings resembling primitive appressoria [43,44]. However, we never observed penetration of epidermal cells.

Stage B refers to the symptomless, biotrophic intercellular colonization of the wheat mesophyll (Fig 3A stage B, S3 and S4 Animation). During this stage, the pathogen explores host tissue while avoiding recognition by the host immune system, which otherwise would have resulted in a resistance response in the infected leaf tissue (Fig 2B). Interestingly, hyphae first grow in the interspace of epidermis and mesophyll, where they spread via the grooves between adjacent epidermal cells before deeper mesophyll cell layers are colonized.

Infection stage C comprises the transition from biotrophic to necrotrophic growth when the first disease symptoms develop (Fig 3A, stage C). For asexual reproduction, *Z. tritici* requires large amounts of nutrients that are released from dead host cells. Fungal hyphae branch extensively

and colonize all mesophyll layers, with hyphae growing around individual plant cells as they die. Primal structures of pycnidia start to develop (S5-S7 Animation), and ring-like scaffolds form in sub-stomatal cavities where hyphae align and build stromata that give rise to conidiogenous cells. Finally, infection stage D is characterized by necrotrophic colonization and asexual reproduction (Fig 3A, stage D). Hyphae colonize an environment that is nutrient-rich but also hostile due to the high abundance of ROS, as demonstrated by DAB staining (Fig 2B). Within necrotic lesions, mesophyll tissue is heavily colonized, plant cells are dead, and mature pycnidia are visible (S8 and S9 Animation). Hyphae wrap around collapsed host cells, possibly to improve the acquisition of nutrients and protect resources from competing saprotrophs. Sub-stomatal cavities are occupied by sub-globose pycnidia which harbour hyaline, oblong asexual pycnidiospores that extrude through stomatal openings.

While the four infection stages of *Z. tritici* can be clearly distinguished, infections by different cells of one isolate are not completely synchronized; different infection stages can be present simultaneously on the same inoculated leaf.

During biotrophic colonization of wheat tissue, fluorescence emitted from fluorescein isothiocyanate conjugated to wheat germ agglutinin (WGA-FITC) primarily came from septa and was weak compared to that during necrotrophic colonization, during which fluorescence was also emitted from interseptal regions. Previously, similar observations were reported in endophytic and epiphyllous [45] and biotrophic and necrotrophic hyphae [46]. WGA binds to N-acetylglucosamine residues that build chitin, an elicitor of plant immunity [47]. Fungal plant pathogens can prevent recognition, e.g. through chitin-binding LysM effectors [48–50] like the extracellular LysM protein ChELP2, that was also shown to limit accessibility of chitin to WGA in biotrophic hyphae of *C. higginsianum* [46]. In *Z. tritici*, two LysM effectors protect hyphae from plant chitinases [51], and Mg3LysM shields chitin from recognition by wheat receptors [52]. Hence, it is possible that Mg3LysM also limits binding of WGA to chitin during biotrophic, but not necrotrophic, colonization of *Z. tritici* leading to the differences in fluorescence signals from biotrophic and necrotrophic hyphae.

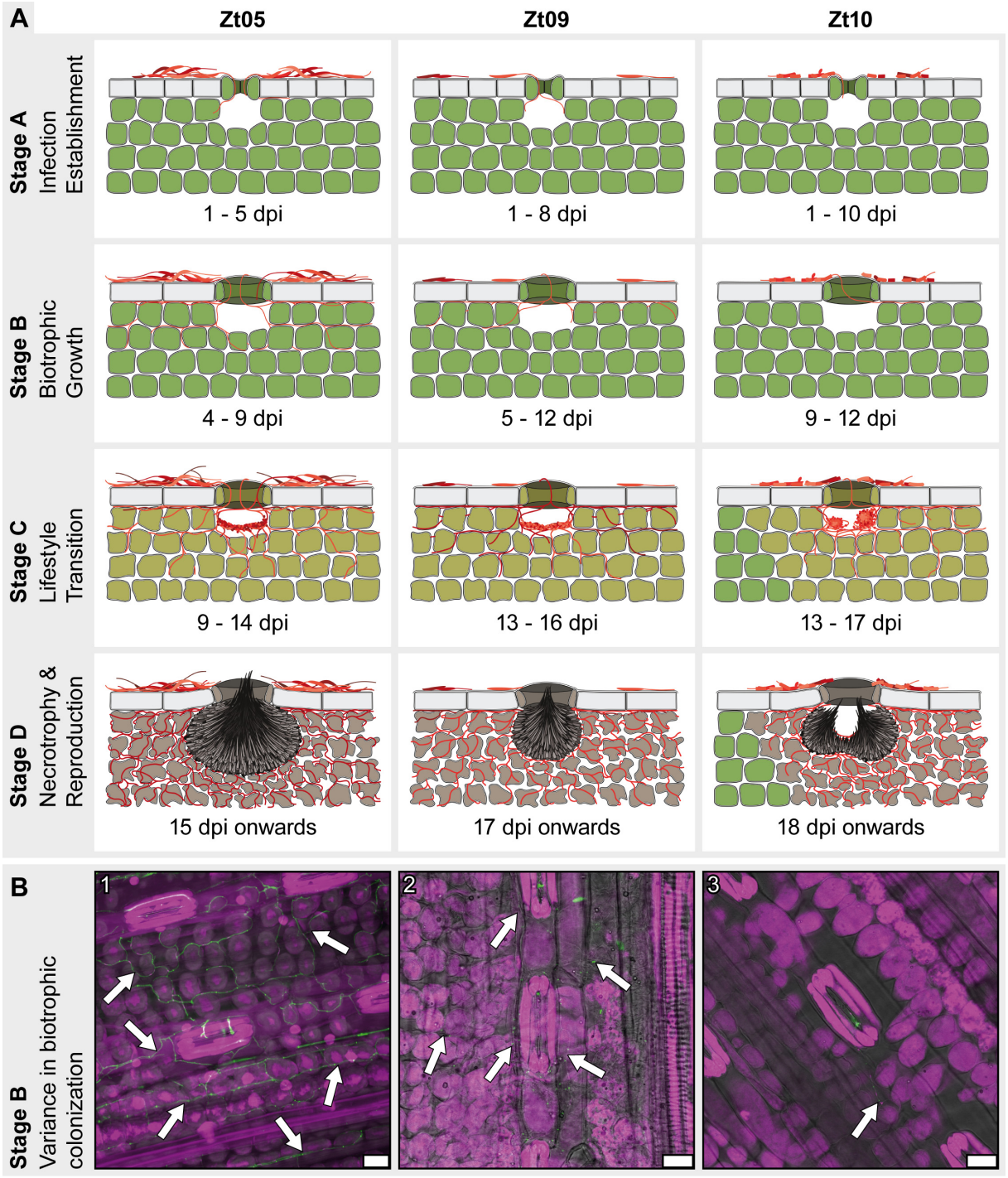

Figure 3. *Z. tritici* wheat infections are characterized by four distinct infection stages and isolate-specific infection development. (A) Schematic drawings of the key features that characterize the four infection stages of *Z. tritici* and illustrate the infection phenotypes of isolates Zt05, Zt09, and Zt10 on the wheat cultivar Obelisk. **(B)** Micrographs showing *Z. tritici* hyphae (arrows) during biotrophic growth inside wheat leaves. Maximum projections of confocal image z-stacks. Nuclei and wheat cells are displayed in *purple* and fungal hyphae or septa in *green*. The panel shows biotrophic colonization of **(1)** isolate Zt05 at 7 dpi, **(2)** Zt09 at 11 dpi, and **(3)** Zt10 at 9 dpi. Scale bars = 25 µm.

Highly distinct development of host infection by the three *Z. tritici* isolates

While we clearly recognized the four core infection stages for the isolates Zt05, Zt09, and Zt10, we also observed differences. In stage A, a main difference was the time between inoculation and first stomatal penetration. Infection hyphae of Zt05 enter stomata at 1 to 5 dpi, whereas germ tube formation and stomatal penetration for Zt09 and Zt10 occur later (Fig 3A, stage A). For Zt05, we observed strong epiphyllous proliferation and, in contrast to the two other isolates, frequently the occurrence of several hyphae entering a single stoma (Fig 3A, stage A: Zt05). Stomatal penetrations were evenly distributed for Zt05 and Zt09 within inoculated leaf areas, while Zt10 penetrations were more clustered, leading to patchy infections (Fig 3A, stage C and D: Zt10).

The most striking difference between the isolates was the extent of biotrophic colonization during stage B (Fig 3B). Zt05 develops expanded biotrophic hyphal networks with long "runner" hyphae growing longitudinally between epidermis and mesophyll (Fig 3A, stage B: Zt05, Fig 3B.1, S3 Animation). Zt09 produces fewer hyphae that are located mainly between epidermis and mesophyll and in the first mesophyll cell layer (Fig 3A, stage B: Zt09, Fig 3B.2). Biotrophic growth of Zt10 is limited to the mesophyll cells adjacent to sub-stomatal cavities (Fig 3A, stage B: Zt10, Fig 3B.3). Because biotrophic colonization depends on successful evasion of host immunity [53], the different extent of colonization could reflect different strategies to bypass recognition in a given host genotype.

During stages C and D, the differences in infection development primarily relate to temporal variances. First, Zt05 switches to necrotrophic growth (9 to 14 dpi), followed by Zt09 (13 to 16 dpi) and Zt10 (13 and 17 dpi) (Fig 3A, stage C). The isolates enter stage D in the same order. Furthermore, Zt10 forms two pycnidia in one sub-stomatal cavity (Fig 3A, stages C and D: Zt10, S7 Animation) more often than Zt05 and Zt09. Taken together, the infection development of the studied *Z. tritici* isolates is highly divergent, although the final production of asexual pycnidia does not differ significantly (Fig 1), suggesting that the isolate-specific characteristics in host-pathogen interactions add up to equally successful strategies for colonization and reproduction in a susceptible wheat cultivar. We conclude that infection development of *Z. tritici* can be highly flexible with respect to the timing of the lifestyle transition and the spatial distribution of infecting hyphae inside host tissue.

Genomes of the three *Z. tritici* isolates exhibit high variation and different chromosome composition

Next, we investigated the genomes of the three isolates. High levels of genomic variability have previously been described within and between species in the genus *Zymoseptoria* to which, in particular, the content and composition of the accessory chromosomes contribute [18,28,54–56]. A previously conducted whole genome comparison using the isolate IPO323 (39.7 Mb) [18] as

reference, identified 500,177 single nucleotide polymorphisms (SNPs) in Zt05 and 617,431 SNPs in Zt10, indicating a considerable genetic distance between the three isolates [57]. In order to further quantify genomic variation between the three isolates in our study, we performed electrophoretic karyotyping and whole genome long read-sequencing (S1 Text).

We visualized and compared small chromosomes in the range of 225 to 1,125 kb that are known to exhibit size variation and presence-absence polymorphisms by pulsed-field gel electrophoresis (PFGE). We observed very different karyotypes with no small chromosomes of the same size (S4 Fig). Further, the PFGE results suggest that Zt05 and Zt10 possess at least seven and four putative accessory chromosomes, respectively and show length polymorphisms of the smallest core chromosomes 12 (~1.463 kb) and 13 (~1,186 kb) compared to Zt09, consistent with a previous study [58]. However, the loss of chromosome 18 (~574 kb) in Zt09 in comparison to IPO323 could not be visualized by PFGE as the applied conditions allow no separation from chromosomes 17 (~584 kb) and 16 (~607 kb).

To further assess variation in genomic content and structure, we compared the synteny of Zt05 and Zt10 contigs to the chromosomes of the *Z. tritici* reference IPO323 [18]. To this end, we assembled long-read SMRT Sequencing data for Zt05 and Zt10 and obtained high-quality *de novo* genome assemblies with contig N50 values of 2.45 Mb and 2.93 Mb and assembly sizes of 41.95 Mb and 39.33 Mb, respectively (S2 Table). In total, we obtained 62 unique contigs (unitigs) for Zt05 and 22 for Zt10. We identified telomeric repeats at both ends of 15 unitigs in Zt05 and 17 unitigs in Zt10 and consider these to be completely assembled chromosomes (S2 Table). By whole-chromosome synteny analyses using SyMAP, we identified large syntenic DNA blocks for all 21 chromosomes of IPO323 in the Zt05 assembly, while Zt10 lacked homologs of chromosomes 18, 20 and 21 (S5 and S6 Figs, S2 Table). Although karyotypes and chromosome structure are very different in Zt05 and Zt10 in comparison to the reference IPO323 and hence the derived Zt09 (≙IPO323ΔChr18), we find homologous regions from all chromosomes and only ~ 2.58 Mb (Zt05) and ~ 2.75 Mb (Zt10) of unique DNA.

To identify the genes that are shared between the three *Z. tritici* isolates, we performed nucleotide BLAST analyses using the coding sequences of the 11,839 annotated genes of the reference IPO323 as input [59]. We identified 11,138 IPO323 genes (94.08%) in Zt05 and 10,745 (90.76%) in Zt10 (e-value cut-off $1e^{-3}$, identity ≥90%, query coverage between 90% and 110%). The gene presence/absence patterns correlate with the absence of large syntenic DNA blocks of chromosomes 18, 20, and 21 in Zt10 (S6 Fig, S2 Table). 91% of genes on core chromosomes are shared, while only 49% (313 of 643) of the genes located on accessory chromosomes are present in Zt05, Zt09, and Zt10 (S2 Table). Similarly, only 85% (370 of 434) of the previously identified genes encoding candidate secreted effector proteins (CSEPs) [6] were found in all isolates, pointing to high levels of plasticity in the effector repertoire of the three isolates Zt05, Zt09, and Zt10. In total, 10,426 genes were present in Zt05, Zt09, and Zt10 and were considered to be

Z. tritici core genes for further analyses (S3 Table). In summary, the genome comparison of Zt05, Zt09, and Zt10 shows a high extent of variation at single nucleotide positions as well as structural variation including differences in the total gene content.

Generation of isolate- and stage-specific transcriptomes based on confocal microscopy analyses

Given the morphological and temporal differences in infection development, we next asked how gene expression profiles differ between the *Z. tritici* isolates Zt05, Zt09, and Zt10 during wheat infection. Previous studies have demonstrated transcriptional re-programming in *Z. tritici* during infection [30,60–64] and shown different transcriptional programs of strains that differ in extent of virulence [65]. Those studies focused primarily on the reference isolate IPO323, and the sequenced material was sampled at defined time points of infection that were not coordinated to distinct infection stages as described above.

We collected leaf material at up to nine time points per isolate and conducted confocal microscopy analyses to select samples for RNA extraction and transcriptome sequencing based on the morphological infection stage (S7 Fig, S4 Table). We generated stage-specific RNA-seq datasets corresponding to the four core infection stages, allowing us to compare the isolate-specific expression profiles at the same developmental stage of infection. Our final dataset comprises four stage-specific transcriptomes per isolate with two biological replicates per sample (Table 2).

We obtained 89.2 to 147.5 million single-end, strand-specific reads per replicate (in total >2.7 billion reads) that were quality trimmed and filtered. Between 4.54% (early infection) and 76.4% (late infection) of the reads could be mapped to the genome of the respective isolate, reflecting the infection stage-specific amount of fungal biomass (Table 2, S5 Table, S1 Text). Across all isolates, transcriptomes of stages A and B, representing biotrophic growth, cluster together and are clearly different from transcriptomes of stages C and D that likewise cluster and represent necrotrophic growth of *Z. tritici* (S8 and S9 Figs). Exploring the transcriptome datasets based on gene read counts shows the greatest variation of biological replicates for Zt10 at stage C (S10 Fig), possibly reflecting variability in the infection development of the two biological replicates.

Table 2. Summary of the stage-specific transcriptomes (A-D) of the three *Z. tritici* isolates.

Isolate	Infection stage	Sample	Time point (dpi)	No. of filtered reads	No. of reads mapped to genome	% reads mapped to genome	No. of genes FPKM ≥2*	No. of genes FPKM ≥10*
Zt05[1]	A	Zt05_Ta_A_01	3	107,507,137	15,213,307	14.15	9,302	7,455
		Zt05_Ta_A_02		81,479,903	10,509,515	12.90		
	B	Zt05_Ta_B_01	8	113,732,295	15,057,425	13.24	9,404	7,623
		Zt05_Ta_B_02		128,271,704	14,856,314	11.58		
	C	Zt05_Ta_C_01	13	91,298,814	26,756,807	29.31	9,538	7,982
		Zt05_Ta_C_02		135,198,719	34,329,884	25.39		
	D	Zt05_Ta_D_01	20	86,100,462	41,871,582	48.63	9,585	7,914
		Zt05_Ta_D_02		119,101,106	76,123,086	63.91		
Zt09[2]	A	Zt09_Ta_A_01	4	129,342,007	5,868,572	4.54	9,435	7,482
		Zt09_Ta_A_02		92,711,865	5,582,561	6.02		
	B	Zt09_Ta_B_01	11	96,767,482	5,034,677	5.20	9,718	7,910
		Zt09_Ta_B_02		103,428,015	5,964,566	5.77		
	C	Zt09_Ta_C_01	13	121,529,652	31,264,373	25.73	9,892	8,220
		Zt09_Ta_C_02		93,253,633	27,790,773	29.80		
	D	Zt09_Ta_D_01	20	110,296,264	84,263,562	76.40	9,867	7,949
		Zt09_Ta_D_02		101,757,635	75,044,880	73.75		
Zt10[3]	A	Zt10_Ta_A_01	6	93,557,587	4,895,650	5.23	8,814	7,219
		Zt10_Ta_A_02		91,111,840	4,836,535	5.31		
	B	Zt10_Ta_B_01	11	94,828,793	5,951,869	6.28	9,068	7,407
		Zt10_Ta_B_02		110,255,245	7,896,227	7.16		
	C	Zt10_Ta_C_01	13	86,652,710	20,804,110	24.01	9,241	7,742
		Zt10_Ta_C_02		91,070,127	8,620,099	9.47		
	D	Zt10_Ta_D_01	24	98,493,807	29,939,216	30.40	9,062	7,308
		Zt10_Ta_D_02		93,690,628	34,607,371	36.94		

Overview of RNA-seq datasets including time point of sampling, number of sequenced reads post filtering, number of mapped reads, percentage of mapped reads, and numbers of transcribed genes. * FPKM values were calculated using Cuffdiff2 and are normalized over all infection stages within the respective isolate (normalization method: geometric, dispersion method: per-condition). [1] 11,138 genes of IPO323 (94.08%) found by nucleotide blast for Zt05. [2] 11,754 of the 11,839 genes predicted and annotated for IPO323 [59]; 85 genes located on chromosome 18 were not considered. [3] 10,745 genes of IPO323 (90.76%) found by nucleotide blast for Zt10.

Core *Zymoseptoria tritici* transcriptional program during wheat infection

The mean expression of genes located on accessory chromosomes was between 6-fold and 20-fold lower than the expression levels of genes located on core chromosomes (S6 Table). We performed differential gene expression analyses to compare expression of the 10,426 *Z. tritici* core genes. We identified 597 genes that were differentially expressed between the infection stages (DESeq2, $P_{adj} \leq 0.01$, $|\log_2 \text{fold change}| \geq 2$) and show the same expression kinetics in all three isolates (Fig 4A). Interestingly, 79 of these genes were differentially expressed between several infection stages, suggesting dynamic, wave-like expression kinetics (S11 Fig). A total of 246 genes were differentially expressed (S7 Table) between stage A and stage B; the vast majority of these (242) were up-regulated in stage B. In stage A, three of the four genes that were up-regulated encode candidate secreted effector proteins (CSEPs), and the fourth encodes a carbohydrate active enzyme (CAZyme) similar to an extracellular chitosanase (*Zt09_chr_11_00040*). This gene is significantly down-regulated or not expressed during later infection (stages B to D), suggesting a role of the enzyme during early establishment in the leaf, similar to the role of a homolog described in *Fusarium solani* [66]. Another gene (*Zt09_chr_6_00402*) that was strongly up-regulated in all isolates during early infection encodes a putative hsp30-like small heat shock protein, possibly reflecting a response to stressful environmental conditions on the wheat leaf surface [67].

The 242 genes up-regulated during biotrophic colonization are enriched with Gene Ontology (GO) groups involved in proteolysis (GO:0006508; 27 genes) and amino acid transmembrane transport (GO:0003333; 5 genes) ($P < 0.01$, Fischer's exact test). Furthermore, three previously characterized LysM homologs [51] and two homologs (*Zt09_chr_11_00358*, *Zt09_chr_13_00167*) of *Ecp2*, an effector gene of the tomato-infecting fungus *Cladosporium fulvum* [68], are also strongly up-regulated during early infection, emphasizing the importance of these genes for biotrophic colonization. PFAM domain analysis further shows enrichment of genes encoding cytochrome P450- and polyketide synthase-like proteins that possibly play a role in the production of secondary metabolites ($P < 0.001$, χ^2 test).

In stage B, 22 genes are up-regulated compared to stage C (S8 Table), including four genes encoding CSEPs of unknown function and a gene encoding the putative non-secreted catalase *Zt09_chr_6_00289*. Metabolite profiling showed that oxidative catabolism of lipids plays an important role for *Z. tritici* during biotrophic colonization [63]. High catabolic activity in the peroxisome entails accumulation of H_2O_2, which likely requires high abundance of catalase to maintain cellular redox homeostasis. *Zt09_chr_10_00421* is also highly expressed during biotrophic growth and down-regulated at later infection stages. It encodes a protein similar to siderophore iron transporter 1, previously described to be involved in the uptake of iron [69] which is essential for fungal growth and pathogenesis [70].

In stage C, 334 genes are significantly up-regulated compared to stage B (S8 Table) and 58 genes in comparison to stage D (S9 Table). Genes up-regulated from B to C are enriched with GO groups involved in metabolic processes (GO:0008152; 97 genes), in particular L-arabinose metabolic processes (GO:0046373; 4 genes), and transmembrane transport (GO:0055085; 25 genes). Similarly, a PFAM analysis shows an enrichment of genes encoding transporters; CAZymes including different groups of glycosyl hydrolases, serine hydrolases, alpha-L-arabinofuranosidases and cutinases that play important roles as plant tissue and cell wall degrading enzymes [71]; polyketide synthases; and cytochrome P450s. This transcriptional reprogramming reflects the physiological changes that *Z. tritici* undergoes during the transition from biotrophic to necrotrophic growth and is consistent with our microscopic observations. Among the 58 genes down-regulated from C to D (S9 Table) we identified GO groups involved in arabinan metabolic processes (GO:0031221; one gene) and an enrichment of PFAM domains related to beta-ketoacyl-ACP synthases, which are known to be involved in fatty acid production and important for the generation of new cell membrane, as well as cytochrome P450s, polyketide synthases, hydrophobic surface binding protein A [72], and tyrosinases.

Only 16 genes were significantly up-regulated from stage C to D, which is when the pycnidia mature (S9 Table), indicating overall similar transcription profiles during the two necrotrophic stages. Genes that are up-regulated during necrotrophic growth and reproduction are predicted to encode proteins similar to CAZymes, transporters, and proteins containing RNA-binding domains. Up-regulation of the secreted catalase-like protein-encoding gene *Zt09_chr_5_00821* shows the importance of detoxification of the ROS H_2O_2, which is highly abundant in necrotic leaf tissue as shown by DAB staining (Fig 2B).

In summary, we identified a core set of genes that show the same expression pattern in the three isolates during infection development. This core set includes genes encoding putative effectors as well as enzymes predicted to play a role in the breakdown and metabolism of plant cell components.

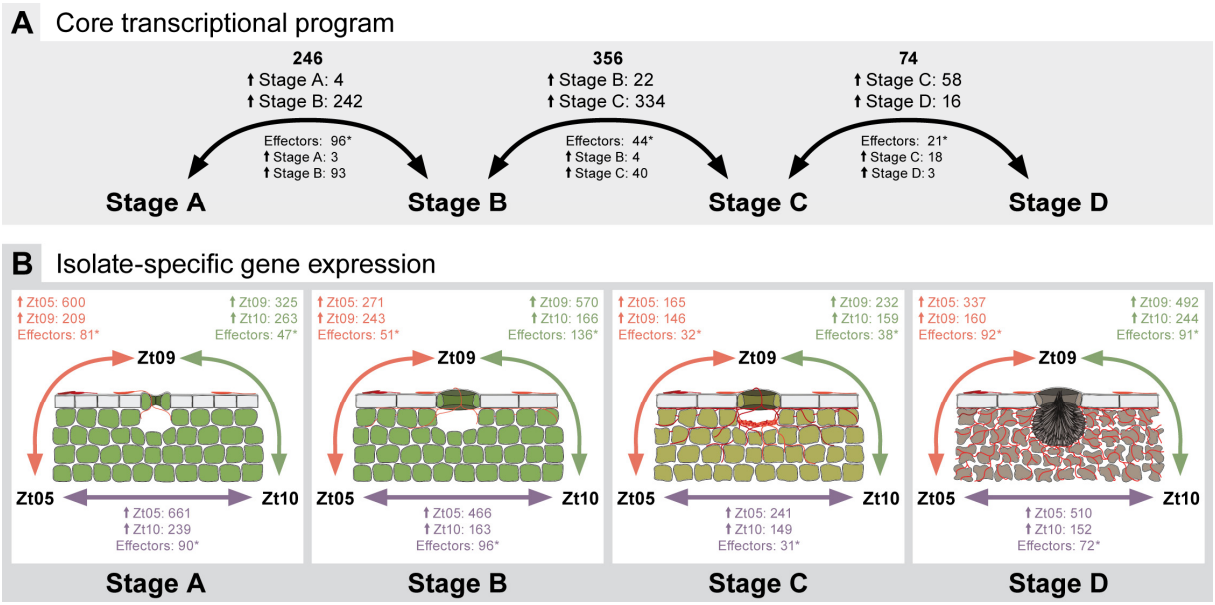

Figure 4. *Z. tritici* core transcriptional program during wheat infection and isolate-specific expression during the four infection stages. Numbers of significantly differentially expressed genes across all isolates **(A)** between the four core *Z. tritici* infection stages and **(B)** between the isolates within the infection stages (between Zt05 and Zt09: orange arrows, between Zt05 and Zt10: purple arrows, between Zt09 and Zt10: green arrows). Small arrows (↑) with stage or isolate names indicate the number of genes specifically up-regulated during that stage or in that isolate for the respective comparison. Differential gene expression analyses performed with DESeq2. Genes were considered to be significantly differentially expressed if $P_{adj} \leq 0.01$ and $|\log_2$ fold change$| \geq 2$. *Indicates significant enrichment of effector candidates among differentially expressed genes (Fischer's exact tests, $P < 0.001$). Effector candidates encode secreted proteins putatively involved in modulating molecular host-pathogen interactions [73].

Core biotrophic and necrotrophic effector candidates with shared expression profiles in *Z. tritici* isolates

Given their importance in plant-pathogen interactions, we particularly focused our analyses on genes encoding candidate secreted effector proteins (CSEPs) [73]. CSEP genes are significantly enriched among the core differentially expressed genes ($P \leq 2.7*10^{-13}$, Fischer's exact tests) (Fig 4A), indicating highly dynamic expression profiles of many core effectors during all stages of wheat infection. We filtered the differentially expressed CSEP genes according to their expression profiles (S12 Fig, S13 Fig) to identify putative key genes for biotrophic and necrotrophic growth inside the host (Table 3 and 4).

During symptomless stage B, 78 CSEP genes are specifically up-regulated, highlighting that a large suite of *Z. tritici* effectors is induced after stomatal penetration and is required for biotrophic colonization of the mesophyll. We narrowed down these genes to 25 core biotrophic CSEP genes (Table 3, S12 Fig, S10 Table) that mostly encode hypothetical proteins and may have a role in bypassing host recognition. In comparison to Zt05 and Zt09, expression of the biotrophic effectors in Zt10 is lower during stage B, and expression profiles often greatly deviated during the other infection stages. This diverging expression phenotype likely reflects the strongly limited biotrophic colonization that we observed for Zt10 (Fig 3B).

Among the biotrophic CSEP genes is *MgNLP* (*Zt09_chr_13_00229*) that encodes the necrosis and ethylene-inducing peptide 1-like protein MgNLP in *Z. tritici* [74]. *MgNLP* is strongly expressed before the transition to necrotrophy in wheat; however it only induces necrosis in dicots and its role in *Z. tritici* is still unknown [74,75].

A set of 35 CSEP genes are specifically up-regulated at stage C (S13 Fig) and represent candidates for necrotrophic core effectors (Table 4, S11 Table). These genes may be involved in the transition from biotrophic to necrotrophic growth and the induction of necrosis. 9 CSEP genes encode putative plant cell wall degrading enzymes and cutinase-like proteins, demonstrating that the lifestyle switch to necrotrophy involves intensified degradation of plant tissue and cell wall components. The gene *Zt09_chr_9_00038* encodes a putative hydrophobin; hydrophobins are small fungal-specific proteins with various functions [76], such as formation of a protective surface layer on hyphae and conidia [77] or as toxins in plant-pathogen interactions [78]. Further, *Zt09_chr_7_00263* encodes a putative secreted metalloprotease, which are known fungal virulence factors in animal pathogens [79] and are significantly induced during the transition to necrotrophy in the hemibiotrophic anthracnose-causing *Colletotrichum higginsianum* [80]. In *Fusarium verticillioides* and *F. oxysporum* f. sp. *lycopersici,* the secreted metalloproteases Fv-cmp and FoMep1 cleave antifungal extracellular host chitinases [81,82].

Table 3. *Z. tritici* core biotrophic effector candidate genes.

Criteria	• Significantly up-regulated at stage B • Lower/No expression during stage C and D • FPKM stage B > FPKM stage C in Zt05 and Zt09			
Expression profiles	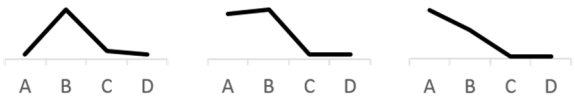			
Putative functions	• Bypass host recognition during biotrophic colonization			
Candidate genes	25 (S12 Fig)			
Candidates encoding hypothetical proteins	23 (S10 Table)			
Candidates with predicted function	Gene	Function/Functional prediction	PFAM domains	GO terms associated
	MgNLP [74] *Zt09_chr_13_00229*	necrosis and ethylene-inducing peptide 1-like protein MgNLP [74,75]	PF05630	GO:0008150; GO:0003674; GO:0005575
	Zt09_chr_2_00129	hypothetical protein, secreted phospholipase A2 precursor	PF06951	GO:0004623; GO:0005509; GO:0005576; GO:0016042

Summary of core *Z. tritici* biotrophic effector candidate genes that were identified based on their specific expression profiles within the *Z. tritici* core transcriptional program during wheat infection. Functional annotation, PFAM, and GO term information from [59].

Table 4. *Z. tritici* core necrotrophic effector candidate genes.

Criteria	• Significantly up-regulated at stage C • Lower/No expression during stage A and B			
Expression profiles	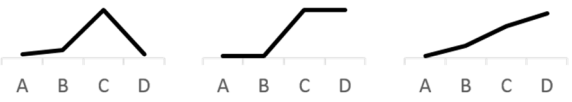			
Putative functions	• Facilitate transition from biotrophy to necrotrophy • Induction of necrosis			
Candidate genes	35 (S13 Fig)			
Candidates encoding hypothetical proteins	24 (S11 Table)			
Candidates with predicted function	Gene	Functional prediction	PFAM domains	GO terms associated
	Zt09_chr_3_00584	PCWDE, similar to alpha-1, Glycosyl transferases group 1	PF00128; PF00534; PF08323	GO:0003824; GO:0043169; GO:0005975; GO:0009058
	Zt09_chr_9_00308	PCWDE, similar to carbohydrate-binding		GO:0008150; GO:0003674; GO:0005575

		module family 63 protein, expansin-like		
	Zt09_chr_3_01063	PCWDE, similar to pectate lyase	PF00544	GO:0008150; GO:0003674; GO:0005575
	Zt09_chr_12_00112	cutinase-like protein	PF01083	GO:0050525; GO:0016787; GO:0005576; GO:0008152
	Zt09_chr_2_00663	similar to Chain A, cutinase-like protein	PF01083	GO:0050525; GO:0016787; GO:0005576; GO:0008152
	Zt09_chr_2_01151	PCWDE, similar to acetyl xylan esterase,	PF01083	GO:0016787; GO:0008152
	Zt09_chr_6_00446	PCWDE , similar to acetyl xylan esterase,	PF01083	GO:0016787; GO:0008152
	Zt09_chr_10_00107	PCWDE, similar to glycoside hydrolase family 12 protein	PF01670	GO:0008810; GO:0004553; GO:0000272
	Zt09_chr_2_01205	PCWDE, similar to putative extracellular cellulase CelA/allergen Asp F7-like protein	PF03330	GO:0008150; GO:0003674; GO:0005575
	Zt09_chr_6_00626	similar to metalloprotease	PF05572	GO:0008237
	Zt09_chr_9_00038	similar to hydrophobin	PF06766	GO:0005576

Summary of core *Z. tritici* necrotrophic effector candidate genes that were identified based on their specific expression profiles within the *Z. tritici* core transcriptional program during wheat infection. PCWDE = putative plant cell wall degrading enzyme. Functional annotation, PFAM, and GO term information from [59].

Isolate-specific transcriptional changes during wheat infection

The 597 genes that we identified as differentially expressed between the stages show the same regulatory profile in each of the three isolates and we consider them as part of the core *Z. tritici* transcriptional infection program. However, we observed that transcript levels of many genes strongly deviate between the isolates within an infection stage.

To further study how the infection phenotypes of the *Z. tritici* isolates relate to differences in gene expression, we compared expression profiles during the infection stages (Fig 4B). In total, 2,377 (~22.8%) of the 10,426 shared genes are differentially expressed between the *Z. tritici* isolates during wheat infection (Table 5, S12 and S13 Tables), suggesting a high extent of redundancy and flexibility in the transcriptional program of *Z. tritici* during infection.

For all isolate comparisons, the identified differentially expressed genes are significantly enriched in CSEP genes ($P \leq 1.18*10^{-7}$, Fischer's exact tests) (Fig 4B) indicating isolate-specific effector

transcriptional profiles (S14 Table). Figure 5 summarizes the expression kinetics of five CSEP genes in the three isolates during the four infection stages. These examples illustrate the differentiated expression profiles of CSEP genes in *Z. tritici* isolates during wheat infection (Fig 5) They encode one hypothetical effector (*Zt09_chr_12_00427*) and secreted proteins with various functions, including a hydrophobin (*Zt09_chr_9_00020*), a DNase (*Zt09_chr_2_01162*), and the ribonuclease Zt6 (*Zt09_chr_3_00610*), which possesses ribotoxin-like activity and is cytotoxic against plants and various microbes [83]. Among them, there is also a gene (*Zt09_chr_4_00039*) encoding a protein with homology to the phytotoxin cerato-platanin that was shown to induce necrosis and defense responses in the plant pathogen *Ceratocystis fimbriata* [84]. During all infection stages, *Zt09_chr_4_00039* is significantly higher expressed in Zt09 than in Zt10, as well as during stages B and D in comparison to Zt05 and might contribute to the higher necrosis levels caused by Zt09 (Fig 1A).

In addition to the differences in the expression of CSEP genes, we also noted isolate-specific expression patterns for genes located on accessory chromosomes. For example, three neighboring genes located on chromosome 19 in Zt09 (*Zt09_chr_19_00071*, *Zt09_chr_19_00072*, and *Zt09_chr_19_00073*) are significantly higher expressed in Zt10 during all four infection stages (S14 Fig, S13 Table), and other genes located ~70 kb downstream are likewise specifically up-regulated in Zt10 compared to one or both of the other isolates. In Zt10, these genes are located on unitig 16, which is syntenic to the accessory chromosome 19 of Zt09. However, transposable elements (RLG elements) are located downstream of *Zt09_chr_19_00072* and upstream of *Zt09_chr_19_00073* in Zt09, and these are not present within the vicinity of these genes on unitig 16 in Zt10. Instead, the right arm of unitig 16 of Zt10 (~100 MB) is inverted compared to Zt09 and Zt05, and the inversion starts up-stream of the gene *Zt09_chr_19_00073,* reflecting a significant sequence variation in the accessory chromosomes.

Table 5. Genes with isolate-specific expression profiles during wheat infection

Genes differentially expressed between isolates*	• 2,377 genes in total • 22.8% of all 10,426 core genes		
	Comparison (all four stages)	DE genes**	Regulation
	Zt05 - Zt09	1,311	↑Zt05: 917 ↑Zt09: 436
	Zt05 - Zt10	1,482	↑Zt05: 1086 ↑Zt10: 412
	Zt09 - Zt10	1,514	↑Zt09: 1062 ↑Zt10: 541
GO groups enriched***	GO term	DE genes in GO group	GO ID
	transmembrane transport	159 (of 491)	GO:0055085
	carbohydrate metabolic process	82 (of 242)	GO:0005975
	proteolysis	64 (of 237)	GO:0006508
	amino acid transmembrane transport	17 (of 36)	GO:0003333
	oxidation-reduction process	159 (of 627)	GO:0055114

	lipid catabolic process	6 (of 15)	GO:0016042
Candidate secreted effector genes	• 245 of 370 effector candidate genes		
	Comparison (all four stages)	DE effector genes****	Regulation
	Zt05 - Zt09	161	↑Zt05: 120 ↑Zt09: 50
	Zt05 - Zt10	167	↑Zt05: 141 ↑Zt10: 31
	Zt09 - Zt10	193	↑Zt09: 167 ↑Zt10: 60

Summary of genes that are differentially expressed between the three *Z. tritici* isolates Zt05, Zt09, and Zt10 during the four infection stages. *Differentially expressed genes identified by DESeq2, $P_{adj} \leq 0.01$, $|\log_2$ fold change$| \geq 2$. **774 genes are differentially expressed in at least two isolate comparisons. ***Gene Ontology (GO) group enrichment analyses by topGO for ontology "Biological Process", $P \leq 0.01$. ****198 effector candidate genes are differentially expressed in at least two isolate comparisons. DE = differentially expressed. ↑ = significantly up-regulated in the isolate.

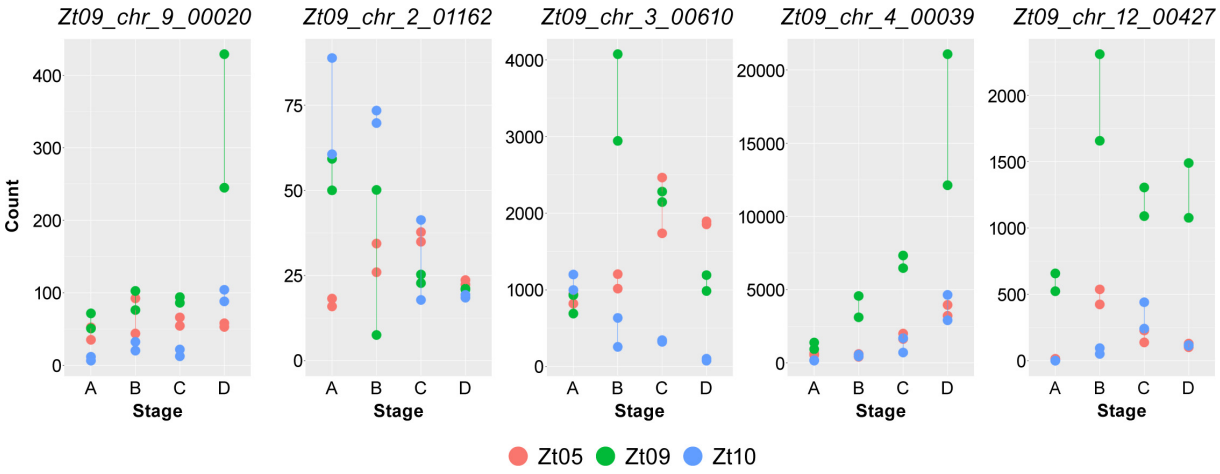

Figure 5. Five effector candidates with highly different expression profiles during wheat infection in the three isolates. The plots display normalized read counts for five effector candidate genes calculated by DESeq2 [95] for the twelve RNA-seq datasets. Read counts were normalized across the four core infection stages (A to D) and the three *Z. tritici* isolates Zt05, Zt09, and Zt10 and represent a measure of relative gene expression between the infection stages and between the isolates.

Transposable elements are associated with the differentially expressed genes

Detailed analyses of the *Z. tritici* transcriptomes revealed considerable variation in the transcriptional landscapes among isolates. The extent of genetic differentiation between Zt05, Zt09, and Zt10 likely accounts for much of the transcriptional variation in the form of SNPs in regulatory sequences. However, other layers of gene regulation may also contribute to the heterogeneous transcriptional landscapes. We hypothesized that epigenetic transcriptional regulation, such as co-regulation of sequences associated with transposable elements, could impact gene expression variation. In a previous study, we showed that transposable elements and the accessory chromosomes of *Z. tritici* are enriched with the histone modifications H3K9me3 and H3K27me3, which are associated with repressive regions of chromatin [85]. In *Fusarium graminearum*, the histone modification H3K27me3 is associated with gene clusters encoding secondary metabolites and pathogenicity-related traits [86]. It is possible that variation in the distribution of histone modifications like H3K27me3 across the genome sequences of Zt05, Zt09, and Zt10 contributes to the dramatic variation in expression phenotypes.

To test this, we assessed the distances of all genes to the closest annotated transposable element. In the genomes of all three isolates, we found that isolate-specific differentially expressed genes are located significantly closer to transposable elements than genes that were not differentially expressed (Mann-Whitney U tests, $P < 2.2*10^{-16}$). Within the differentially expressed genes, isolate-specific up-regulated genes (genes that are significantly up-regulated in one isolate in contrast to the others) are significantly enriched within a distance of 2 kb to transposable elements in Zt05 and Zt09 (Fisher's exact tests, $p \leq 0.0094$), but not in Zt10. We note however, that the transposable element annotation in Zt10 is not as complete as in Zt05 and Zt09 as it was based on the Illumina short read assembly which is 6.7 Mb smaller than the *de novo* genome assembly of SMRT Sequencing reads. We also analyzed the *in vitro* histone 3 methylation data for Zt09 [85] and found that differentially expressed genes are indeed significantly closer to H3K9me3 and H3K27me3 peaks (Mann-Whitney U tests, $P < 2.2*10^{-16}$). Further, we observed significant enrichment of genes significantly up-regulated in Zt09 in comparison to Zt05 and Zt10 within a distance of 2 kb to H3K9me3 and H3K27me3 peaks (Fisher's exact tests, $P \leq 1.55*10^{-15}$), but down-regulated genes were only enriched in the vicinity of H3K27me3 peaks (distance ≤2 kb, Fisher's exact test, $P = 1.35*10^{-15}$). Poor transcription of genes located on the accessory chromosomes was explained by enrichment of H3K27me3 covering the entire chromosomes and H3K9me3, which is mostly associated with repetitive DNA [85]. Our findings indicate that during host infection chromatin state of repeat-rich genome compartments is highly dynamic and changes between "active" euchromatin and "repressive" heterochromatin, as suggested in *Leptosphaeria maculans* [87]. Further, our observation suggests that the fine-scale distribution of epigenetic marks likely differs between the genomes of *Z. tritici* isolates and contributes to the isolate-specific gene expression phenotypes that we observed. To further visualize the

transcriptional landscape across the three *Z. tritici* genomes, we calculated expression values (FPKM) of 1 kb windows (S6 Table) and plotted them in heatmaps along the chromosomes and unitigs (S15-S17 Figs). This approach allows visualization of the transcriptional landscapes at a high resolution and resulted in the identification of heterogeneous gene expression patterns across chromosomes, such as chromosome 19 in Zt10 (S17 Fig), and suggests conservation of previously identified patterns. Almost no loci on the right arm of chromosome 7 were transcribed in Zt05, Zt09, and Zt10 (S16 Fig), as was previously found in Zt09 and IPO323 [30,63]. This chromosomal segment has characteristics of an accessory chromosome, as it is significantly enriched with H3K27me3 that mediates transcriptional silencing [85]. While syntenic chromosomal regions generally have a similar composition of transcribed and silenced loci, the fine-scale distribution of transcriptional cold- and hot-spots is clearly different between the genomes of the three isolates studied.

Conclusions

We conducted a detailed comparison of infection phenotypes of three pathogenic *Z. tritici* isolates that are equally virulent in a susceptible host genotype and show an unexpectedly high extent of plasticity in the infection program of a fungal plant pathogen. The three isolates differ significantly in their genomic composition, and we show that the genetic variation of the three isolates translates into highly distinct infection phenotypes that deviate temporally and spatially. The transcriptional programs associated with host colonization show a high degree of variability between the three isolates: more than 20% of the core genes are differentially expressed between the three *Z. tritici* isolates during the four infection stages. This suggests strong redundancy in the *Z. tritici* "infection program" between isolates. Effector candidates are enriched among the differentially expressed genes, suggesting that the three isolates employ different molecular strategies to manipulate host defenses. Strikingly, highly variable infection programs result in the same level of virulence, showing that "host specialization" in *Z. tritici* involves a very flexible strategy to exploit wheat tissue for growth and reproduction. As necrotic lesions are usually composed of several distinct *Z. tritici* genotypes, it is highly relevant to investigate whether strains in one lesion have similar or different infection phenotypes. Various infection strategies within a lesion could complement each other or, in contrast, have antagonistic effects and facilitate competition.

An intriguing question that emerges from our analyses is which factors cause deviation in gene expression phenotypes in *Z. tritici*. Genetic variants associated with transcriptional regulation likely contribute to differences in gene regulation. However, we hypothesize that variation in epigenetic traits promotes different transcriptional programs. Genome-wide patterns of

transcriptional activity (S15-S17 Figs) indeed suggest some variation in the physical distribution of transcriptionally active and silent regions, which may result from distinct epigenetic landscapes related to histone modifications or DNA methylation.

We hypothesize that highly diverging infection phenotypes are not exclusive among isolates of *Z. tritici* and are likely found in populations of other pathogens that retain high levels of genetic diversity. Variation in infection and expression profiles contributes another layer of polymorphism to pathogen populations and may be important for the pathogen to rapidly adjust to environmental changes. Hence, the resulting diversity of infection phenotypes needs to be acknowledged to understand pathogen evolution and develop sustainable crop protection strategies.

Materials and Methods

Isolates and growth conditions

Cells of *Zymoseptoria tritici* isolates (S1 Table) were inoculated from glycerol stocks onto YMS agar (0.4% [w/v] yeast extract, 0.4% [w/v] malt extract, 0.4% [w/v] sucrose, 2% [w/v] bacto agar) and grown at 18°C for 5 days. Single cells were grown in liquid YMS (200 rpm, 18°C) for 2 days and harvested by centrifugation (3500 rpm for 10 min).

Plant infection experiments

For all plant infection experiments, we used 14-day-old seedlings of the winter wheat (*Triticum aestivum*) cultivar Obelisk (Wiersum Plantbreeding, Winschoten, Netherlands). The fungal inoculum was adjusted to 1 x 10^8 cells/mL in 0.1% [v/v] Tween 20 (Roth, Karlsruhe, Germany) and brushed onto labeled areas (8 to 12 cm) of the second leaf of each plant. The same treatment without fungal cells was conducted for mock controls. After inoculation, plants were incubated at 22°C [day]/20°C [night] and 100% humidity with a 16-h light period for 48 h. Then, humidity was reduced to 70%. Plants were grown for 3 or 4 weeks after inoculation, depending on the experiment.

In planta phenotypic assays

To compare quantitative virulence of Zt05, Zt09, and Zt10 on wheat, we performed three independent, randomized infection experiments with blinded inoculation and evaluation. Inoculated leaf areas of 460 leaves were evaluated at 28 days post infection (dpi) by scoring the observed disease symptoms based on the percentage of leaf area covered by necrosis and pycnidia as previously described [88]. We differentiated six categories: 0 (no visible symptoms), 1 (1-20%), 2 (21-40%), 3 (41-60%), 4 (61-80%), and 5 (81-100%). Statistical differences were evaluated by Mann-Whitney *U* test considering differences significant if $P \leq 0.01$.

To compare the temporal development of disease, we manually inspected 40 inoculated leaves between 9 and 27 dpi and registered the occurrence of first visible symptoms every two days. Individual leaves were visualized using a Leica S8APO equipped with a Leica DFC450 camera.

To localize accumulation of the reactive oxygen species H_2O_2 within infected leaf tissue, we conducted 3,3'-diaminobenzidine (DAB) staining [89] at 4, 10, 14, 18, and 21 dpi (S2 Text). The presence of H_2O_2 is indicated by reddish-brown precipitate in cleared leaves. Samples were documented before (iPhone 7 camera) and after (Canon EOS 600D) staining.

Phenotypic assays *in vitro*

To compare tolerance towards stress conditions and assess the *in vitro* phenotypes of the *Z. tritici* isolates, we conducted a stress assay as previously described [88]. After five days, we compared

growth on solid YMS medium at 18°C to growth on YMS medium exposed to stress conditions: temperature (20/22°C with 16-h day/8-h night rhythm, 28°C in darkness), oxidative stress (2 and 3 mM H_2O_2), osmotic stress (1 M NaCl, 1 M sorbitol), and cell wall stress (500 µg/mL Congo red, 200 µg/mL calcofluor white). Colony development was documented using a Canon EOS 600D. Each stress treatment was replicated three times.

Analysis of *Z. tritici* wheat infection by confocal microscopy

Structures of *Z. tritici* isolates inside and on the surface of wheat leaves were analyzed by confocal laser scanning microscopy. We harvested infected wheat leaves at 3-5, 7, 8, 10-14, 17, 19-21, 25, and 28 dpi and analyzed the interactions between fungal hyphae and wheat tissue. Likewise, we analyzed infected leaves to determine the infection stage of leaf samples used for RNA extraction (see below). In total, we studied 37 infected wheat leaves for Zt05, 34 for Zt09, and 30 for Zt10, analyzed at least 15 infection events per leaf sample by confocal microscopy, and created a total of 113 confocal image z-stacks. Cleared leaf material was stained with wheat germ agglutinin conjugated to fluorescein isothiocyanate (WGA-FITC) in combination with propidium iodide (PI) (S2 Text for staining protocol). Microscopy was conducted using a Leica TCS SP5 (Leica Microsystems, Germany) and a Zeiss LSM880 (Carl Zeiss Microscopy, Germany). FITC was excited at 488 nm (argon laser) and detected between 500-540 nm. PI was excited at 561 nm (diode-pumped solid-state laser) and detected between 600-670 nm. Image stacks were obtained with a *x/y* scanning resolution of 1024 x 1024 (Leica) or 1500 x 1500 pixels (Zeiss) and a step size of 0.5 - 1 µm in *z*. Analyses, visualization, and processing of image z-stacks were performed using Leica Application Suite Advanced Fluorescence (Leica Microsystems, Germany), ZEN black and Zen blue (Carl Zeiss Microscopy, Germany), and AMIRA® (FEI™ Visualization Science Group, Germany). Animations of image z-stacks are .avi format and can be played in VLC media player (available at http://www.videolan.org/vlc/).

Transcriptome analyses of *Z. tritici* isolates during wheat infection

High-quality total RNA from *Z. tritici*-infected wheat material was isolated using the TRIzol™ reagent (Invitrogen, Karlsruhe, Germany) according to the manufacturer's instructions. Material of three wheat leaves was harvested synchronously, pooled, and immediately homogenized in liquid nitrogen. The resulting leaf powder (100 mg) was used for RNA extraction. Because our analyses revealed differences in the temporal development of infection between the isolates, we set up independent sampling schedules for each isolate to compare transcriptomes of the same infection stage (S4 Table). We collected infected leaf material at one to three determined time points and assigned infection stage based on examination of central sections (1 - 2 cm) of each leaf by confocal microscopy (S7 Fig). We determined the best representatives of each infection stage and chose two samples per isolate at each stage as biological replicates for transcriptome

sequencing (Table 2). Preparation of strand-specific RNA-seq libraries including polyA enrichment was performed at the Max Planck Genome Center, Cologne, Germany (http://mpgc.mpipz.mpg.de) using the NEBNext Ultra™ Directional RNA Library Prep Kit for Illumina according to the manufacturer's protocol (New England BioLabs, Frankfurt/Main, Germany) with an input of 1 μg total RNA. Sequencing, performed using an Illumina HiSeq 2500 platform, generated strand-specific, 100-base, single-end reads with an average yield of 112 million reads per sample (S5 Table). We assessed the quality of sequencing data with *FastQC* v0.11.2 (http://www.bioinformatics.babraham.ac.uk/projects/fastqc/), removed residual TruSeq adapter sequences, and applied a stringent read trimming and quality filtering protocol using *FASTX-toolkit* v0.0.14 (http://hannonlab.cshl.edu/fastx_toolkit/) and *Trimmomatic* [90] v0.33 (S3 Text for details). The resulting 88-bp reads were mapped against the genome of the respective *Z. tritici* isolate with *TopHat2* v2.0.9 [91]. Read alignments were stored in SAM format, and indexing, sorting, and conversion to BAM format was performed using *SAMtools* v0.1.19 [92]. The relative abundance of transcripts for predicted genes was calculated in FPKM by *Cuffdiff2* v2.2.1 [93]. Total raw read counts per gene were estimated with *HTSeq* v0.6.1p1 using union mode [94]. Gene coordinates in the Zt05 (S15 Table) and Zt10 (S16 Table) genomes were obtained by mapping the predicted genes of IPO323 using nucleotide BLAST alignments (e-value cutoff $1e^{-3}$, identity ≥90%, query coverage between 90% and 110%). Differential gene expression analyses between *Z. tritici* infection stages and isolates were performed in R using the Bioconductor package *DESeq2* v1.10.1 [95]. Significantly differentially expressed genes were determined with $P_{adj} \leq 0.01$ and $|\log_2 \text{fold-change} \geq 2|$. The R package topGO [96] was used to perform Gene Ontology (GO) term enrichment analyses within the differentially expressed genes. *P* values for each GO term [59] were calculated using Fischer's exact test applying the topGO algorithm "weight01" that takes into account GO term hierarchy. We reported categories significant with $P \leq 0.01$ for the ontology "Biological Process". PFAM domain enrichment analyses were performed using a custom Python script, and *P* values were calculated using χ^2 tests. To analyze genomic distances between differentially expressed genes and transposable elements (TEs), we annotated TEs as described in [59] for Zt05 (S17 Table) and Zt10 (S18 Table) and used the published TE annotation of IPO323 for Zt09 [59]. Distances between the genes of interest and the closest annotated TEs were calculated with *bedtools* v2.26 [97]. Likewise, we used ChIP-seq peak data [85] to calculate distances between genes and the closest H3K9me3 and H3K27me3 peaks. Statistical analyses were performed in R. For an overview of all programs and codes used to process and analyze transcriptome data, including the applied settings and parameters, see S3 Text.

Pulsed-field gel electrophoresis

A non-protoplast protocol (S2 Text) was used to produce DNA plugs for separation of small chromosomes (~0.2 to 1.6 Mb) by pulsed-field gel electrophoresis (PFGE) [98]. Chromosomal DNA of *Saccharomyces cerevisiae* (Bio-Rad) was used as standard size marker. Gels were stained for 30 min in 1 µg/mL ethidium bromide solution, and chromosome bands were detected with Thyphoon Trio™ (GE).

De novo genome assemblies of *Z. tritici* isolates Zt05 and Zt10 and synteny analyses

High molecular weight DNA of Zt05 and Zt10 was extracted from single cells grown in liquid YMS, using a modified version of the cetyltrimethylammonium bromide (CTAB) extraction protocol [99], and used as input to prepare Pacific Biosciences (PacBio) SMRTbell libraries that were size-selected with a 10- to 15-kb cut-off. Single-molecule real-time (SMRT) sequencing was performed on four SMRT cells and run on a PacBio RS II instrument at the Max Planck Genome Center in Cologne, Germany (http://mpgc.mpipz.mpg.de). Genome assemblies of Zt05 and Zt10 based on the generated PacBio long reads were done as previously described [56] using *HGAP* [100] v3.0 included in the *SMRTanalysis suite* v2.3.0. Briefly, we applied default settings for *HGAP* runs and tested the influence of different minimum seed read lengths (13 kb, 15 kb, 19 kb, and 21 kb) used for initiation of self-correction. A 19-kb minimum seed read length cut-off generated the most favorable results in terms of pre-assembly yield, assembly N50, and length of total assembly. Assembled unitigs were polished by applying default settings of *Quiver,* which is part of the *SMRTanalysis suite*. Unitigs in which median PacBio read coverage deviated more than a factor of 1.5X from all contigs were removed from the final assemblies. Synteny of *Z. tritici* reference strain IPO323 and the Zt05 and Zt10 unitigs was compared using SyMAP [101] v4.2 applying default settings and considering all unitigs ≥1,000 kb (Zt05) and ≥10,000 kb (Zt10). To estimate the amount of unique DNA in Zt05 and Zt10 in comparison to IPO323 and Zt09 respectively, we generated pairwise genome alignments with *Mugsy* v1.r2.2 [102] applying default settings. Alignments were analyzed using a custom Python script to extract unique DNA blocks with a minimum length of 1 bp.

Data availability

All generated RNA-seq datasets have been deposited at the NCBI Gene Expression Omnibus and are accessible with the accession number GSE106136. *De novo* genome assemblies of isolates Zt05 and Zt10 are available under accession numbers PEBP00000000 and PEBO00000000. The genome sequence of the reference isolate IPO323 used for transcriptome analysis of Zt09 is available at: http://genome.jgi.doe.gov/Mycgr3/Mycgr3.home.html. Genome assemblies based on whole genome shotgun sequencing (Illumina) were also used; the assembly for Zt10 is

available at GenBank (Zt10 = STIR04_A26b) GCA_000223645.2. Sequencing data and assembly for Zt05 (Zt05 = MgDk09_U34) are available through NCBI BioProject PRJNA312067 [57].

Acknowledgements

We thank Ronny Kellner for insightful comments to a previous version of this manuscript, Julien Y. Dutheil for support with comparative transcriptome analyses and Petra Happel for help with the *in vitro* stress assays.

Funding statement

This work was supported by intramural funding of the Max Planck Society and a personal grant from the State of Schleswig-Holstein to Eva H. Stukenbrock. The funders had no role in study design, data collection and analyses, decision to publish, or preparation of the manuscript.

References

1. Möller M, Stukenbrock EH (2017) Evolution and genome architecture in fungal plant pathogens. Nat Rev Microbiol 15: 756–771.
2. Spanu PD, Abbott JC, Amselem J, Burgis TA, Soanes DM, et al. (2010) Genome Expansion and Gene Loss in Powdery Mildew Fungi Reveal Tradeoffs in Extreme Parasitism. Science 330: 1543–1546.
3. Raffaele S, Farrer RA, Cano LM, Studholme DJ, MacLean D, et al. (2010) Genome Evolution Following Host Jumps in the Irish Potato Famine Pathogen Lineage. Science 330: 1540–1543.
4. Ma L-J, van der Does HC, Borkovich KA, Coleman JJ, Daboussi M-J, et al. (2010) Comparative genomics reveals mobile pathogenicity chromosomes in Fusarium. Nature 464: 367–373. doi:10.1038/nature08850.
5. Rouxel T, Grandaubert J, Hane JK, Hoede C, van de Wouw AP, et al. (2011) Effector diversification within compartments of the Leptosphaeria maculans genome affected by Repeat-Induced Point mutations. Nat Commun 2: 202.
6. Stukenbrock E, Dutheil JY (2017) Comparison of fine-scale recombination maps in fungal plant pathogens reveals dynamic recombination landscapes and intragenic hotspots. bioRxiv.
7. Xue M, Yang J, Li Z, Hu S, Yao N, et al. (2012) Comparative Analysis of the Genomes of Two Field Isolates of the Rice Blast Fungus Magnaporthe oryzae. PLoS Genet 8. doi:10.1371/journal.pgen.1002869.
8. Faino L, Seidl MF, Shi-Kunne X, Pauper M, Van Den Berg GCM, et al. (2016) Transposons passively and actively contribute to evolution of the two-speed genome of a fungal pathogen. Genome Res 26: 1091–1100. doi:10.1101/gr.204974.116.
9. Miao VP, Covert SF, VanEtten HD (1991) A fungal gene for antibiotic resistance on a dispensable ("B") chromosome. Science 254: 1773–1776. doi:10.1126/science.1763326.
10. Balesdent M-H, Fudal I, Ollivier B, Bally P, Grandaubert J, et al. (2013) The dispensable chromosome of *Leptosphaeria maculans* shelters an effector gene conferring avirulence towards *Brassica rapa*. New Phytol 198: 887–898.
11. Raffaele S, Kamoun S (2012) Genome evolution in filamentous plant pathogens: why bigger can be better. Nat Rev Microbiol 10: 417–430.
12. Dalman K, Himmelstrand K, Olson Å, Lind M, Brandström-Durling M, et al. (2013) A genome-wide association study identifies genomic regions for virulence in the non-model organism Heterobasidion annosum s.s. PLoS One 8: e53525.

13. Cumagun CJR, Bowden RL, Jurgenson JE, Leslie JF, Miedaner T (2004) Genetic Mapping of Pathogenicity and Aggressiveness of *Gibberella zeae* (*Fusarium graminearum*) Toward Wheat. Phytopathology 94: 520–526. doi:10.1094/PHYTO.2004.94.5.520.
14. Lind M, Dalman K, Stenlid J, Karlsson B, Olson Å (2007) Identification of quantitative trait loci affecting virulence in the basidiomycete Heterobasidion annosum s.l. Curr Genet 52: 35–44. doi:10.1007/s00294-007-0137-y.
15. Talas F, Kalih R, Miedaner T, McDonald BA (2016) Genome-Wide Association Study Identifies Novel Candidate Genes for Aggressiveness, Deoxynivalenol Production, and Azole Sensitivity in Natural Field Populations of Fusarium graminearum. Mol Plant-Microbe Interact 29: MPMI-09-15-0218.
16. Haueisen J, Stukenbrock EH (2016) Life cycle specialization of filamentous pathogens - colonization and reproduction in plant tissues. Curr Opin Microbiol 32: 31–37.
17. Wittenberg AHJ, van der Lee T a J, Ben M'barek S, Ware SB, Goodwin SB, et al. (2009) Meiosis drives extraordinary genome plasticity in the haploid fungal plant pathogen Mycosphaerella graminicola. PLoS One 4: e5863.
18. Goodwin SB, M'barek S Ben, Dhillon B, Wittenberg AHJ, Crane CF, et al. (2011) Finished genome of the fungal wheat pathogen Mycosphaerella graminicola reveals dispensome structure, chromosome plasticity, and stealth pathogenesis. PLoS Genet 7: e1002070.
19. Habig M, Quade J, Stukenbrock EH (2017) Forward genetics approach reveals host-genotype dependent importance of accessory chromosomes in the fungal wheat pathogen Zymoseptoria tritici. MBio: Forthcoming.
20. Lendenmann MH, Croll D, Stewart EL, McDonald B a (2014) Quantitative Trait Locus Mapping of Melanization in the Plant Pathogenic Fungus Zymoseptoria tritici. G3 (Bethesda).
21. Lendenmann MH, Croll D, McDonald B a. (2015) QTL mapping of fungicide sensitivity reveals novel genes and pleiotropy with melanization in the pathogen Zymoseptoria tritici. Fungal Genet Biol 80: 53–67
22. Mirzadi Gohari A, Ware SB, Wittenberg AHJ, Mehrabi R, Ben M'Barek S, et al. (2015) Effector discovery in the fungal wheat pathogen Zymoseptoria tritici. Mol Plant Pathol 16: 931–945.
23. Stewart EL, Croll D, Lendenmann MH, Sanchez-Vallet A, Hartmann FE, et al. (2017) QTL mapping reveals complex genetic architecture of quantitative virulence in the wheat pathogen Zymoseptoria tritici. Mol Plant Pathol: 1–16. doi:10.1111/mpp.12515.
24. Hartmann FE, Sánchez-Vallet A, McDonald BA, Croll D (2017) A fungal wheat pathogen evolved host specialization by extensive chromosomal rearrangements. ISME J: 1189–1204.

25. Zhong Z, Marcel TC, Hartmann FE, Ma X, Plissonneau C, et al. (2017) A small secreted protein in Zymoseptoria tritici is responsible for avirulence on wheat cultivars carrying the Stb6 resistance gene. New Phytol 214: 619–631.
26. Linde CC, Zhan J, McDonald B a (2002) Population Structure of Mycosphaerella graminicola: From Lesions to Continents. Phytopathology 92: 946–955.
27. Zhan J, Pettway RE, McDonald BA (2003) The global genetic structure of the wheat pathogen Mycosphaerella graminicola is characterized by high nuclear diversity, low mitochondrial diversity, regular recombination, and gene flow. Fungal Genet Biol 38: 286–297. doi:10.1016/S1087-1845(02)00538-8.
28. McDonald MC, McGinness L, Hane JK, Williams AH, Milgate A, et al. (2016) Utilizing Gene Tree Variation to Identify Candidate Effector Genes in Zymoseptoria tritici. G3 (Bethesda) 6: 779–791.
29. Thygesen K, Jørgensen LN, Jensen KS, Munk L (2008) Spatial and temporal impact of fungicide spray strategies on fungicide sensitivity of Mycosphaerella graminicola in winter wheat. Eur J Plant Pathol 123: 435–447.
30. Kellner R, Bhattacharyya A, Poppe S, Hsu TY, Brem RB, et al. (2014) Expression Profiling of the Wheat Pathogen Zymoseptoria tritici Reveals Genomic Patterns of Transcription and Host-Specific Regulatory Programs. Genome Biol Evol 6: 1353–1365.
31. Stukenbrock EH, Banke S, Javan-Nikkhah M, McDonald B a (2007) Origin and domestication of the fungal wheat pathogen Mycosphaerella graminicola via sympatric speciation. Mol Biol Evol 24: 398–411.
32. Stewart EL, McDonald BA (2014) Measuring quantitative virulence in the wheat pathogen Zymoseptoria tritici using high-throughput automated image analysis. Phytopathology 104: 985–992.
33. Heller J, Tudzynski P (2011) Reactive Oxygen Species in Phytopathogenic Fungi: Signaling, Development, and Disease. Annu Rev Phytopathol Vol 49 49: 369–390. doi:10.1146/annurev-phyto-072910-095355.
34. Quaedvlieg W, Kema GHJ, Groenewald JZ, Verkley GJM, Seifbarghi S, et al. (2011) Zymoseptoria gen. nov.: a new genus to accommodate Septoria-like species occurring on graminicolous hosts. Persoonia 26: 57–69.
35. Lendenmann MH, Croll D, Palma-Guerrero J, Stewart EL, McDonald BA (2016) QTL mapping of temperature sensitivity reveals candidate genes for thermal adaptation and growth morphology in the plant pathogenic fungus Zymoseptoria tritici. Heredity (Edinb) 116: 384–394.

36. Mehrabi R, Zwiers L-H, de Waard M a, Kema GHJ (2006) MgHog1 regulates dimorphism and pathogenicity in the fungal wheat pathogen Mycosphaerella graminicola. Mol Plant Microbe Interact 19: 1262–1269.
37. Butler MJ, Day AW (1998) Fungal melanins : a review. Can J Microbiol 44: 1115–1136.
38. National Centers for Environmental Information: Climate Data Online Asia. Available: https://www1.ncdc.noaa.gov/pub/data/wwr/documents/Asia/WWR_1991-2000_tables.txt.
39. Zhan J, McDonald BA (2011) Thermal adaptation in the fungal pathogen Mycosphaerella graminicola. Mol Ecol 20: 1689–1701. doi:10.1111/j.1365-294X.2011.05023.x.
40. Shetty NP, Mehrabi R, Lütken H, Haldrup A, Kema GHJ, et al. (2007) Role of hydrogen peroxide during the interaction between the hemibiotrophic fungal pathogen Septoria tritici and wheat. New Phytol 174: 637–647. doi:10.1111/j.1469-8137.2007.02026.x.
41. Shetty NP, Kristensen BK, Newmana MA, Møller K, Gregersen PL, et al. (2003) Association of hydrogen peroxide with restriction of Septoria tritici in resistant wheat. Physiol Mol Plant Pathol 62: 333–346. doi:10.1016/S0885-5765(03)00079-1.
42. Turrà D, El Ghalid M, Rossi F, Di Pietro A (2015) Fungal pathogen uses sex pheromone receptor for chemotropic sensing of host plant signals. Nature 527: 521–524.
43. Cohen L, Eyal Z, Aviv T (1993) The histology of processes associated with the infection of resistant and susceptible wheat cultivars with Septoria tritici. Plant Pathol 42: 737–743. doi:10.1111/j.1365-3059.1993.tb01560.x.
44. Kema GHJ, Yu D, Rijkenberg FHJ, Shaw MW, Baayen RP (1996) Histology of pathogenesis of Mycosphaerella graminicola in wheat. Phytopathology 7: 777–786. doi:10.1094/Phyto-86-777.
45. Becker M, Becker Y, Green K, Scott B (2016) The endophytic symbiont Epichloe festucae establishes an epiphyllous net on the surface of Lolium perenne leaves by development of an expressorium, an appressorium-like leaf exit structure. New Phytol 211: 240–254. doi:10.1111/nph.13931.
46. Takahara H, Hacquard S, Kombrink A, Hughes HB, Halder V, et al. (2016) Colletotrichum higginsianum extracellular LysM proteins play dual roles in appressorial function and suppression of chitin-triggered plant immunity. New Phytol 211: 1323–1337. doi:10.1111/nph.13994.
47. Sánchez-Vallet A, Mesters JR, Thomma BPHJ (2015) The battle for chitin recognition in plant-microbe interactions. FEMS Microbiol Rev 39: 171–183. doi:10.1093/femsre/fuu003.

48. van den Burg H a, Harrison SJ, Joosten MHAJ, Vervoort J, de Wit PJGM (2006) Cladosporium fulvum Avr4 protects fungal cell walls against hydrolysis by plant chitinases accumulating during infection. Mol Plant Microbe Interact 19: 1420–1430.
49. de Jonge R, Peter van Esse H, Kombrink A, Shinya T, Desaki Y, et al. (2010) Conserved Fungal LysM Effector Ecp6 Prevents Chitin-Triggered Immunity in Plants. Science 329: 953–955.
50. Sánchez-Vallet A, Saleem-Batcha R, Kombrink A, Hansen G, Valkenburg DJ, et al. (2013) Fungal effector Ecp6 outcompetes host immune receptor for chitin binding through intrachain LysM dimerization. Elife 2013: 1–16. doi:10.7554/eLife.00790.
51. Marshall R, Kombrink A, Motteram J, Loza-Reyes E, Lucas J, et al. (2011) Analysis of two in planta expressed LysM effector homologs from the fungus Mycosphaerella graminicola reveals novel functional properties and varying contributions to virulence on wheat. Plant Physiol 156: 756–769.
52. Lee W, Rudd JJ, Hammond-kosack KE, Kanyuka KK (2013) Mycosphaerella graminicola LysM effector-mediated stealth pathogenesis subverts recognition through both CERK1 and CEBiP homologues in wheat. Mol Plant Microbe Interact 27: 236–243.
53. Jones JDG, Dangl JL (2006) The plant immune system. Nature 444: 323–329.
54. Stukenbrock EH, Bataillon T, Dutheil JY, Hansen TT, Li R, et al. (2011) The making of a new pathogen: insights from comparative population genomics of the domesticated wheat pathogen Mycosphaerella graminicola and its wild sister species. Genome Res 21: 2157–2166.
55. Croll D, Zala M, McDonald BA (2013) Breakage-fusion-bridge Cycles and Large Insertions Contribute to the Rapid Evolution of Accessory Chromosomes in a Fungal Pathogen. PLoS Genet 9. doi:10.1371/journal.pgen.1003567.
56. Plissonneau C, Stürchler A, Croll D (2016) The evolution of orphan regions in genomes of a fungal pathogen of wheat. MBio 7. doi:10.1128/mBio.01231-16.
57. Grandaubert J, Dutheil JY, Stukenbrock EH (2017) The genomic rate of adaptation in the fungal wheat pathogen Zymoseptoria tritici. bioRxiv: 1–33.
58. Mehrabi R, Taga M, Kema GHJ (2007) Electrophoretic and cytological karyotyping of the foliar wheat pathogen Mycosphaerella graminicola reveals many chromosomes with a large size range. Mycologia 99: 868–876.
59. Grandaubert J, Bhattacharyya A, Stukenbrock EH (2015) RNA-seq Based Gene Annotation and Comparative Genomics of Four Fungal Grass Pathogens in the Genus Zymoseptoria Identify Novel Orphan Genes and Species-Specific Invasions of Transposable Elements. G3 (Bethesda) 5: g3.115.017731-.

60. Keon J, Antoniw J, Carzaniga R, Deller S, Ward JL, et al. (2007) Transcriptional adaptation of Mycosphaerella graminicola to programmed cell death (PCD) of its susceptible wheat host. Mol Plant Microbe Interact 20: 178–193.
61. Brunner PC, Torriani SFF, Croll D, Stukenbrock EH, McDonald B a (2013) Coevolution and life cycle specialization of plant cell wall degrading enzymes in a hemibiotrophic pathogen. Mol Biol Evol 30: 1337–1347.
62. Yang F, Li W, Jørgensen HJL (2013) Transcriptional Reprogramming of Wheat and the Hemibiotrophic Pathogen Septoria tritici during Two Phases of the Compatible Interaction. PLoS One 8: e81606.
63. Rudd JJ, Kanyuka K, Hassani-Pak K, Derbyshire M, Andongabo A, et al. (2015) Transcriptome and Metabolite Profiling of the Infection Cycle of Zymoseptoria tritici on Wheat Reveals a Biphasic Interaction with Plant Immunity Involving Differential Pathogen Chromosomal Contributions and a Variation on the Hemibiotrophic Lifestyle Def. Plant Physiol 167: 1158–1185.
64. Palma-Guerrero J, Torriani SFF, Zala M, Carter D, Courbot M, et al. (2016) Comparative transcriptomic analyses of Zymoseptoria tritici strains show complex lifestyle transitions and intraspecific variability in transcription profiles. Mol Plant Pathol 17: 845–859.
65. Palma-Guerrero J, Ma X, Torriani SFF, Zala M, Francisco CS, et al. (2017) Comparative Transcriptome Analyses in Zymoseptoria tritici Reveal Significant Differences in Gene Expression Among Strains During Plant Infection. Mol Plant-Microbe Interact 30: 231–244.
66. Liu H, Zhang B, Li C, Bao X (2010) Knock down of chitosanase expression in phytopathogenic fungus Fusarium solani and its effect on pathogenicity. Curr Genet 56: 275–281. doi:10.1007/s00294-010-0299-x.
67. Haslbeck M, Vierling E (2015) A first line of stress defense: Small heat shock proteins and their function in protein homeostasis. J Mol Biol 427: 1537–1548.
68. Laugé R (1997) The in planta-produced extracellular proteins ECP1 and ECP2 of Cladosporium fulvum are virulence factors. Mol Plant Microbe Interact 10: 725–734. doi:10.1094/MPMI.1997.10.6.725.
69. Yun CW, Tiedeman JS, Moore RE, Philpott CC (2000) Siderophore-iron uptake in Saccharomyces cerevisiae: Identification of ferrichrome and fusarinine transporters. J Biol Chem 275: 16354–16359. doi:10.1074/jbc.M001456200.
70. Haas H, Eisendle M, Turgeon BG (2008) Siderophores in Fungal Physiology and Virulence. Annu Rev Phytopathol 46: 149–187.
71. Kubicek CP, Starr TL, Glass NL (2014) Plant Cell Wall-Degrading Enzymes and Their Secretion in Plant-Pathogenic Fungi. Annu Rev Phytopathol: 1–25.

72. Ohtaki S, Maeda H, Takahashi T, Hasegawa F, Gomi K, et al. (2006) Novel Hydrophobic Surface Binding Protein , HsbA , Produced by Aspergillus oryzae Novel Hydrophobic Surface Binding Protein , HsbA , Produced by Aspergillus oryzae. Appl Environ Microbiol 72: 2407–2413.
73. Lo Presti L, Lanver D, Schweizer G, Tanaka S, Liang L, et al. (2015) Fungal Effectors and Plant Susceptibility. Annu Rev Plant Biol 66: 513–545.
74. Motteram J, Küfner I, Deller S, Brunner F, Hammond-Kosack KE, et al. (2009) Molecular Characterization and Functional Analysis of *MgNLP* , the Sole NPP1 Domain–Containing Protein, from the Fungal Wheat Leaf Pathogen *Mycosphaerella graminicola*. Mol Plant-Microbe Interact 22: 790–799.
75. Kettles GJ, Bayon C, Canning G, Rudd JJ, Kanyuka K (2017) Apoplastic recognition of multiple candidate effectors from the wheat pathogen Zymoseptoria tritici in the nonhost plant Nicotiana benthamiana. New Phytol 213: 338–350. doi:10.1111/nph.14215.
76. Wösten H a (2001) Hydrophobins: multipurpose proteins. Annu Rev Microbiol 55: 625–646. doi:10.1146/annurev.micro.55.1.625.
77. Aimanianda V, Bayry J, Bozza S, Kniemeyer O, Perruccio K, et al. (2009) Surface hydrophobin prevents immune recognition of airborne fungal spores. Nature 460: 1117–1121.
78. Takai S (1974) Pathogenicity and cerato-ulmin production in Ceratocystis ulmi. Nature 252: 124–126.
79. Vu K, Tham R, Uhrig JP, Thompson GR, Pombejra SN, et al. (2014) Invasion of the central nervous system by Cryptococcus neoformans requires a secreted fungal metalloprotease. MBio 5: 1–13. doi:10.1128/mBio.01101-14.
80. O'Connell RJ, Thon MR, Hacquard S, Amyotte SG, Kleemann J, et al. (2012) Lifestyle transitions in plant pathogenic Colletotrichum fungi deciphered by genome and transcriptome analyses. Nat Genet 44: 1060–1065.
81. Naumann TA, Wicklow DT, Price NPJ (2011) Identification of a chitinase-modifying protein from Fusarium verticillioides: Truncation of a host resistance protein by a fungalysin metalloprotease. J Biol Chem 286: 35358–35366. doi:10.1074/jbc.M111.279646.
82. Karimi Jashni M, Dols IHM, Iida Y, Boeren S, Beenen HG, et al. (2015) Synergistic action of serine- and metallo-proteases from *Fusarium oxysporum* f. sp. lycopersici cleaves chitin-binding tomato chitinases, reduces their antifungal activity and enhances fungal virulence. Mol Plant-Microbe Interact 28: 150427105219007.
83. Kettles G, Bayon C, Sparks CA, Canning G, Kanyuka K, et al. (2017) Characterisation of an antimicrobial and phytotoxic ribonuclease secreted by the fungal wheat pathogen Zymoseptoria tritici. New Phytol 44: 1–25. doi:10.1101/130393.

84. Pazzagli L, Cappugi G, Manao G, Camici G, Santini A, et al. (1999) Purification, characterization, and amino acid sequence of cerato- platanin, a new phytotoxic protein from Ceratocystis fimbriata f. sp. platani. J Biol Chem 274: 24959–24964.
85. Schotanus K, Soyer JL, Connolly LR, Grandaubert J, Happel P, et al. (2015) Histone modifications rather than the novel regional centromeres of Zymoseptoria tritici distinguish core and accessory chromosomes. Epigenetics Chromatin 8: 41.
86. Connolly LR, Smith KM, Freitag M (2013) The Fusarium graminearum Histone H3 K27 Methyltransferase KMT6 Regulates Development and Expression of Secondary Metabolite Gene Clusters. PLoS Genet 9. doi:10.1371/journal.pgen.1003916.
87. Soyer JL, El Ghalid M, Glaser N, Ollivier B, Linglin J, et al. (2014) Epigenetic Control of Effector Gene Expression in the Plant Pathogenic Fungus Leptosphaeria maculans. PLoS Genet 10: e1004227. Available: http://dx.plos.org/10.1371/journal.pgen.1004227.
88. Poppe S, Dorsheimer L, Happel P, Stukenbrock EH (2015) Rapidly Evolving Genes Are Key Players in Host Specialization and Virulence of the Fungal Wheat Pathogen Zymoseptoria tritici (Mycosphaerella graminicola). PLOS Pathog 11: e1005055.
89. Thordal-Christensen H, Zhang Z, Wei Y, Collinge DB (1997) Subcellular localization of H2O2 in plants. H2O2 accumulation in papillae and hypersensitive response during the barley-powdery mildew interaction. Plant J 11: 1187–1194. doi:10.1046/j.1365-313X.1997.11061187.x.
90. Bolger AM, Lohse M, Usadel B (2014) Trimmomatic: A flexible trimmer for Illumina sequence data. Bioinformatics 30: 2114–2120. doi:10.1093/bioinformatics/btu170.
91. Kim D, Pertea G, Trapnell C, Pimentel H, Kelley R, et al. (2013) TopHat2: accurate alignment of transcriptomes in the presence of insertions, deletions and gene fusions. Genome Biol 14: R36.
92. Li H, Handsaker B, Wysoker A, Fennell T, Ruan J, et al. (2009) The Sequence Alignment/Map format and SAMtools. Bioinformatics 25: 2078–2079. doi:10.1093/bioinformatics/btp352.
93. Trapnell C, Hendrickson DG, Sauvageau M, Goff L, Rinn JL, et al. (2013) Differential analysis of gene regulation at transcript resolution with RNA-seq. Nat Biotechnol 31: 46–53.
94. Anders S, Pyl PT, Huber W (2015) HTSeq—a Python framework to work with high-throughput sequencing data. Bioinformatics 31: 166–169.
95. Love MI, Huber W, Anders S (2014) Moderated estimation of fold change and dispersion for RNA-seq data with DESeq2. Genome Biol 15: 550.
96. Alexa A, Rahnenführer J, Lengauer T (2006) Improved scoring of functional groups from gene expression data by decorrelating GO graph structure. Bioinformatics 22: 1600–1607. doi:10.1093/bioinformatics/btl140.

97. Quinlan AR, Hall IM (2010) BEDTools: A flexible suite of utilities for comparing genomic features. Bioinformatics 26: 841–842. doi:10.1093/bioinformatics/btq033.

98. Stukenbrock EH, Jørgensen FG, Zala M, Hansen TT, McDonald BA, et al. (2010) Whole-genome and chromosome evolution associated with host adaptation and speciation of the wheat pathogen Mycosphaerella graminicola. PLoS Genet 6: e1001189.

99. Allen GC, Flores-Vergara M a, Krasynanski S, Kumar S, Thompson WF (2006) A modified protocol for rapid DNA isolation from plant tissues using cetyltrimethylammonium bromide. Nat Protoc 1: 2320–2325. doi:10.1038/nprot.2006.384.

100. Chin C-S, Alexander DH, Marks P, Klammer AA, Drake J, et al. (2013) Nonhybrid, finished microbial genome assemblies from long-read SMRT sequencing data. Nat Methods 10: 563–569.

101. Soderlund C, Bomhoff M, Nelson WM (2011) SyMAP v3.4: A turnkey synteny system with application to plant genomes. Nucleic Acids Res 39. doi:10.1093/nar/gkr123.

102. Angiuoli S V., Salzberg SL (2011) Mugsy: Fast multiple alignment of closely related whole genomes. Bioinformatics 27: 334–342. doi:10.1093/bioinformatics/btq665.

Supporting Information

Supplementary Tables

All supplementary tables are in .xlsx or .gff file format and are deposited on the supplementary USB key.

S1 Table. *Zymoseptoria tritici* isolates used in this study.

S2 Table. SMRT Sequencing-based *de novo* genome assemblies, synteny analyses, and conserved genes.
The table summarizes basic statistics of *de novo* genome assemblies generated for isolates Zt05 and Zt10 based on SMRT Sequencing long-read data, results of synteny analyses between IPO323/Zt09 chromosomes and Zt05 and Zt10 unitigs, and the presence/absence of IPO323/Zt09 genes and effector candidates in the genomes of Zt05 and Zt10.

S3 Table. *Z. tritici* core genes and effector candidates.
List of 10,426 genes and 370 effector candidate genes that are present in the genomes of the *Z. tritici* isolates Zt05, Zt09, and Zt10 based on nBLAST analyses. Genes are based on the *Z. tritici* genome annotation [59] and effector gene candidates were predicted by [6].

S4 Table. Isolate-specific sampling schedules for transcriptome sequencing of infection stages.
Post-inoculation time points were scheduled based on previous plant infection experiments to cover each of the four *Z. tritici* infection stages. Samples for transcriptome sequencing and analyses were collected at one to three different times points and eventually selected based on the results of microscopic analyses of central leaf sections. Selected samples are marked by *.
S5 Table. Detailed overview of stage-specific transcriptomes of *Z. tritici* isolates during wheat infection generated in this study.

S6 Table. Comparison of expression on core and accessory chromosomes of *Z. tritici* during wheat infection.
FPKM expression values calculated with Cuffdiff2 [93] for genes and 1-kb windows located on the core (CC) and accessory (AC) chromosomes.

S7 Table. Genes that are significantly differentially expressed between infection stage A and B across all *Z. tritici* isolates.

S8 Table. Genes that are significantly differentially expressed between infection stage B and C across all *Z. tritici* isolates.

S9 Table. Genes that are significantly differentially expressed between infection stage C and D across all *Z. tritici* isolates.

S10 Table. *Z. tritici* biotrophic core effector candidates.

S11 Table. *Z. tritici* necrotrophic core effector candidates.

S12 Table. Core *Z. tritici* genes that are differentially expressed between the three isolates during wheat infection.

S13 Table. Core *Z. tritici* genes that are differentially expressed between the three isolates during wheat infection, sorted by up-regulation per isolate.

S14 Table. *Z. tritici* effector candidate genes that are differentially expressed between the three isolates during wheat infection.

S15 Table. Gene annotation for the *Z. tritici* isolate Zt05.
Gene annotation in .gff file format for the Zt05 genome assembly based on Illumina short reads (NCBI BioSample: SAMN04494882).

S16 Table. Gene annotation for the *Z. tritici* isolate Zt10.
Gene annotation in .gff file format for the Zt10 genome assembly based on Illumina short reads (NCBI accession number: GCA_000223645.2).

S17 Table. Transposable element annotation for the *Z. tritici* isolate Zt05.
Transposable element annotation in .gff file format for the Zt05 genome assembly based on Illumina short reads (NCBI BioSample: SAMN04494882).

S18 Table. Transposable element annotation for the *Z. tritici* isolate Zt10.
Transposable element annotation in .gff file format for the Zt10 genome assembly based on Illumina short reads (NCBI accession number: GCA_000223645.2).

Supplementary Figures

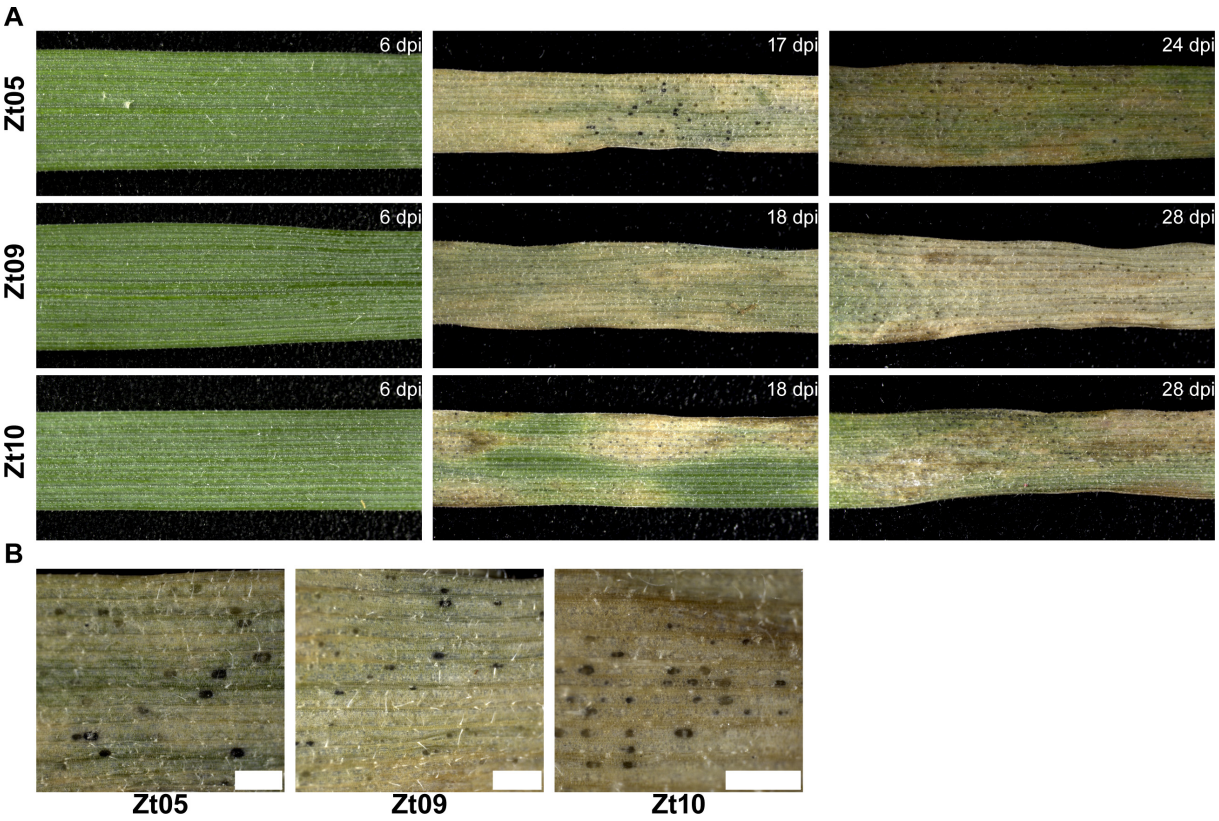

S1 Figure. Disease development on wheat leaves infected with *Z. tritici* isolates Zt05, Zt09, and Zt10. (A) Photographs of wheat leaves taken at different time points after inoculation with *Z. tritici* isolates Zt05, Zt09, and Zt10. **(B)** Infected wheat leaves contained similar numbers of pycnidia. Scale bars = 500 µm.

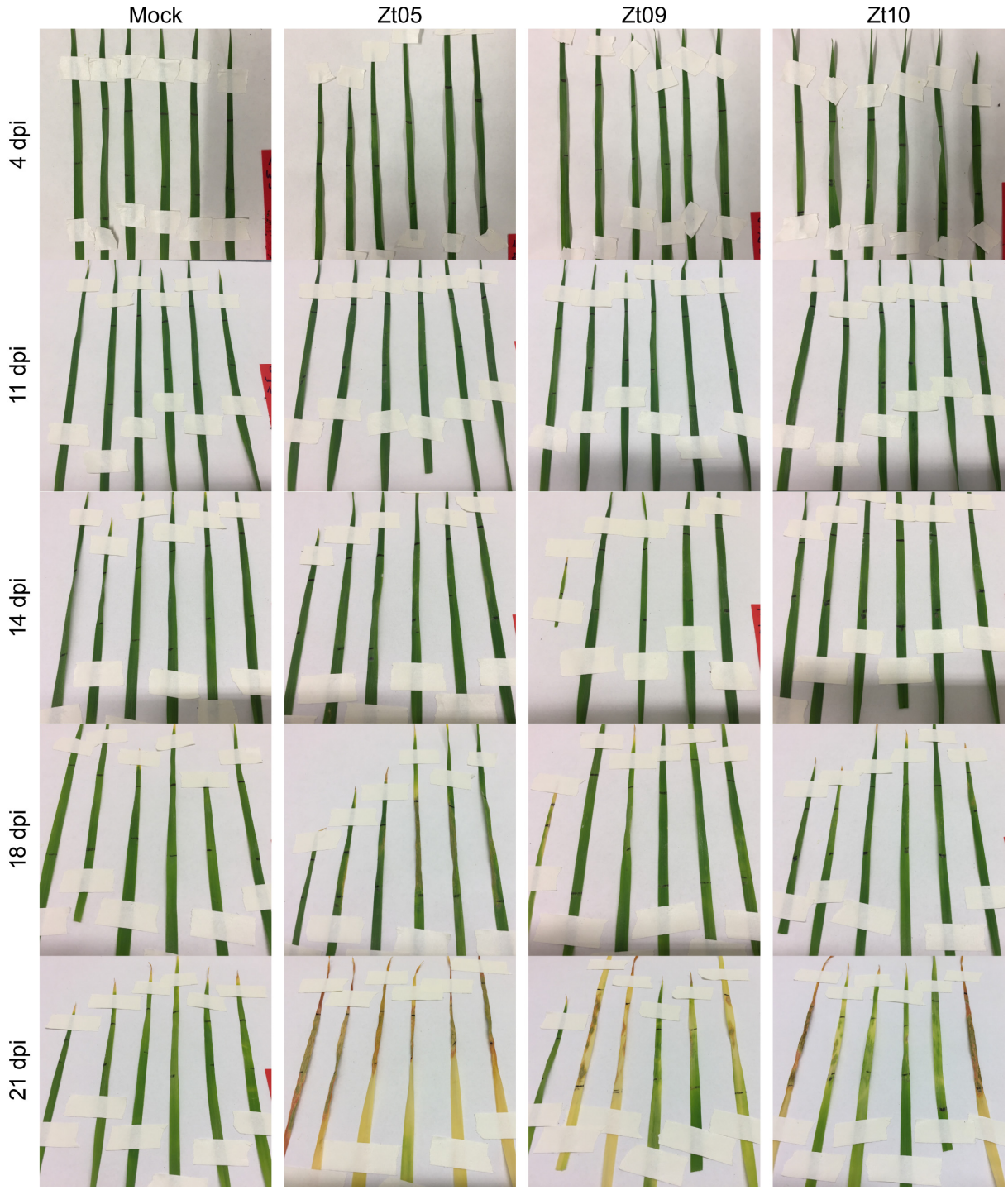

S2 Figure. Symptom development on wheat leaves used for the ROS staining assay. Photographs of *Triticum aestivum* cv. Obelisk leaves taken at 4, 11, 14, 18, and 21 days post inoculation with *Z. tritici* isolates Zt05, Zt09, and Zt10 and mock treatment. Leaves were subsequently subjected to ROS detection staining.

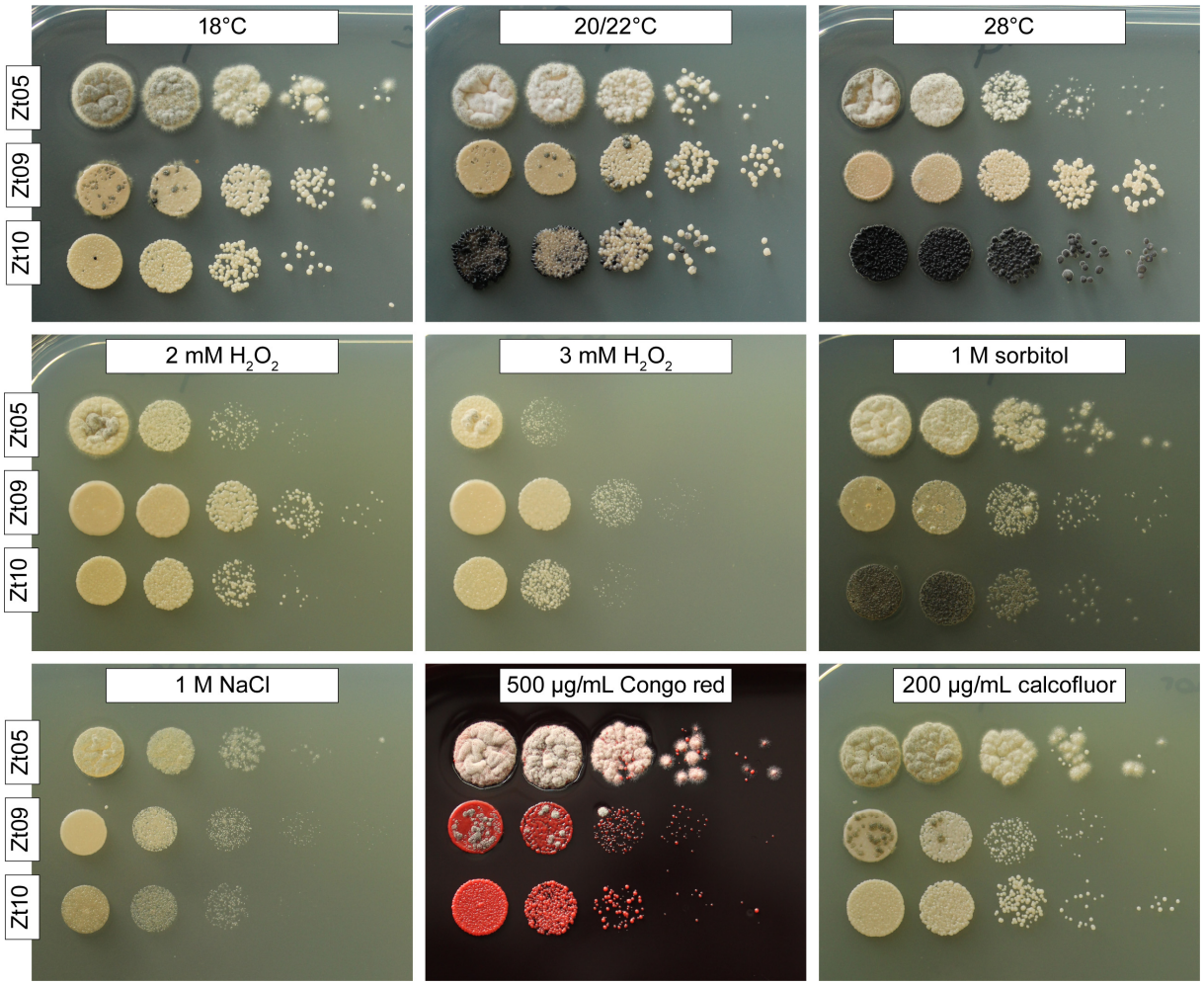

S3 Figure. Differences in colony morphology and abiotic stress tolerance between *Z. tritici* isolates. Growth of the isolates Zt05, Zt09, and Zt10 was tested under multiple stress conditions in comparison to the standard cultivation condition *in vitro* (solid YMS medium at 18°C, no light): growing conditions of wheat (20/22°C at 16-h day/8-h night rhythm), heat stress (28°C), oxidative stress (2 and 3 mM H_2O_2), osmotic stress (1 M sorbitol, 1 M NaCl), and cell wall stress (500 µg/mL Congo red, 200 µg/mL calcofluor white).

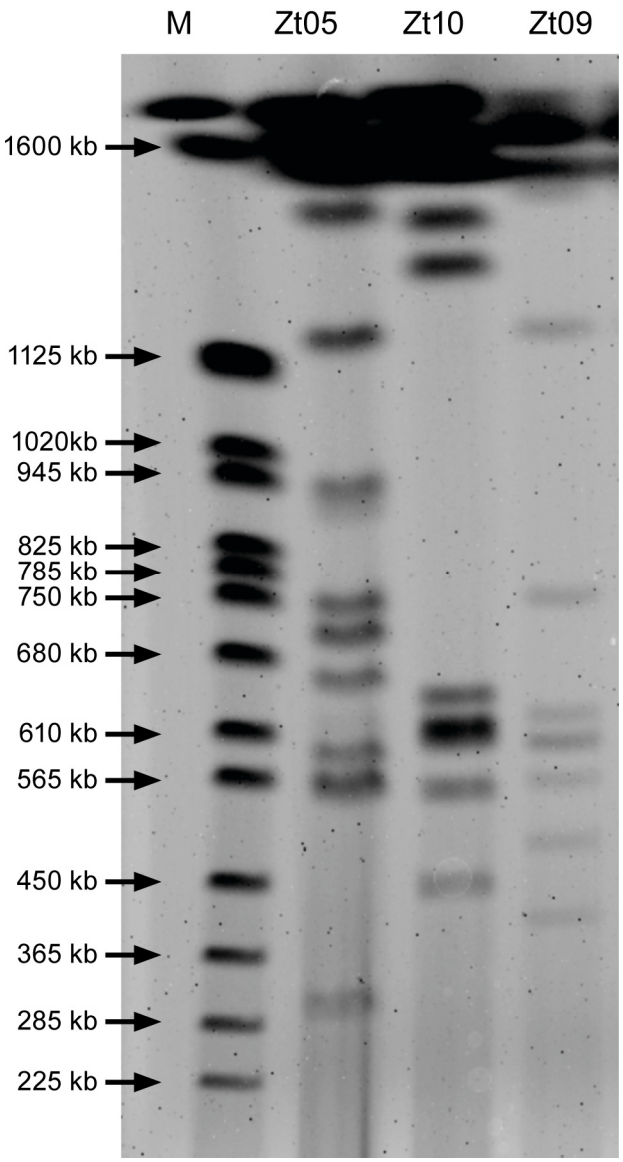

S4 Figure. Karyotype variation of *Z. tritici* field isolates. Pulsed-field gel electrophoresis shows number and size variations for small chromosomes (~225 to 1,460 kb) of *Z. tritici* isolates Zt05, Zt10, and Zt09. Standard chromosome size marker (M): *Saccharomyces cerevisiae*.

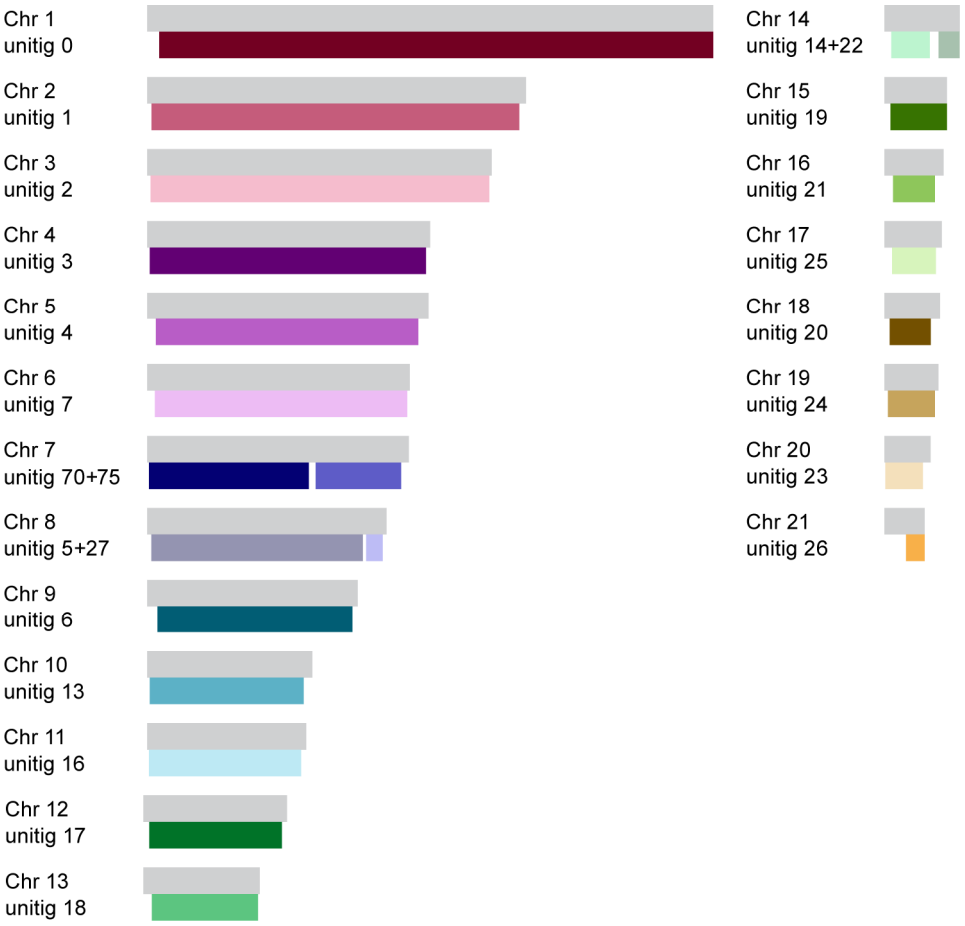

S5 Figure. Synteny between Zt05 *de novo* assembled unitigs and IPO323 chromosomes.

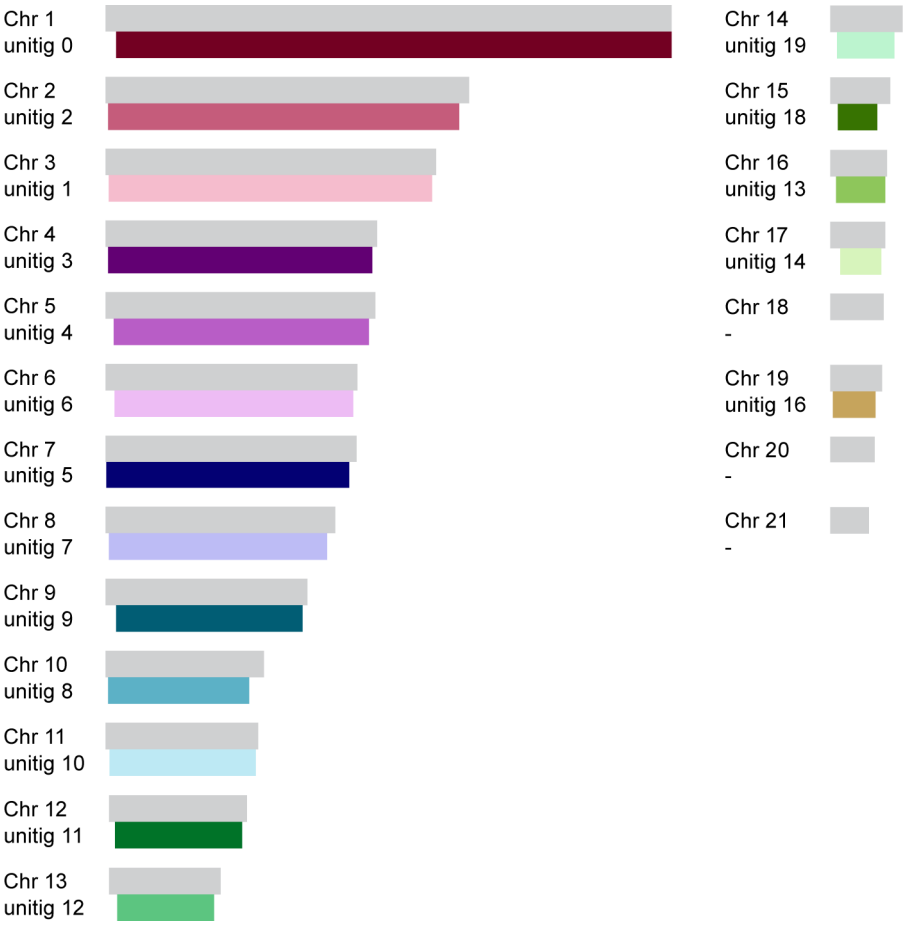

S6 Figure. Synteny between Zt10 *de novo* assembled unitigs and IPO323 chromosomes.

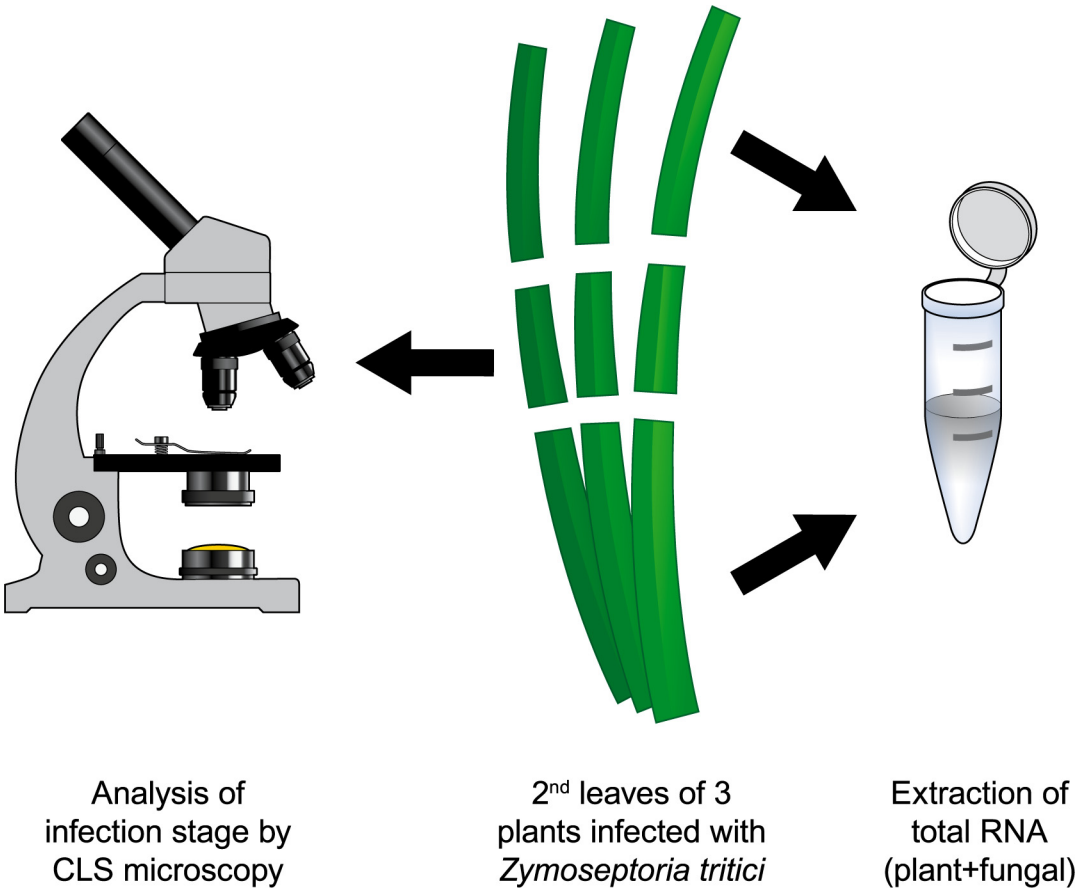

S7 Figure. Generation of isolate- and stage-specific transcriptomes was enabled by confocal microscopy analyses. The schematic drawing illustrates how we selected samples for RNA-seq. Central sections of *Z. tritici*-infected wheat leaves from three independent plants (second leaf of each plant) were stained and analyzed by confocal laser-scanning microscopy while the remaining infected leaf material was pooled and ground in liquid nitrogen for total RNA extraction. RNA samples subjected to sequencing were chosen based on the morphological infection stage that we observed in the central leaf section by microscopy.

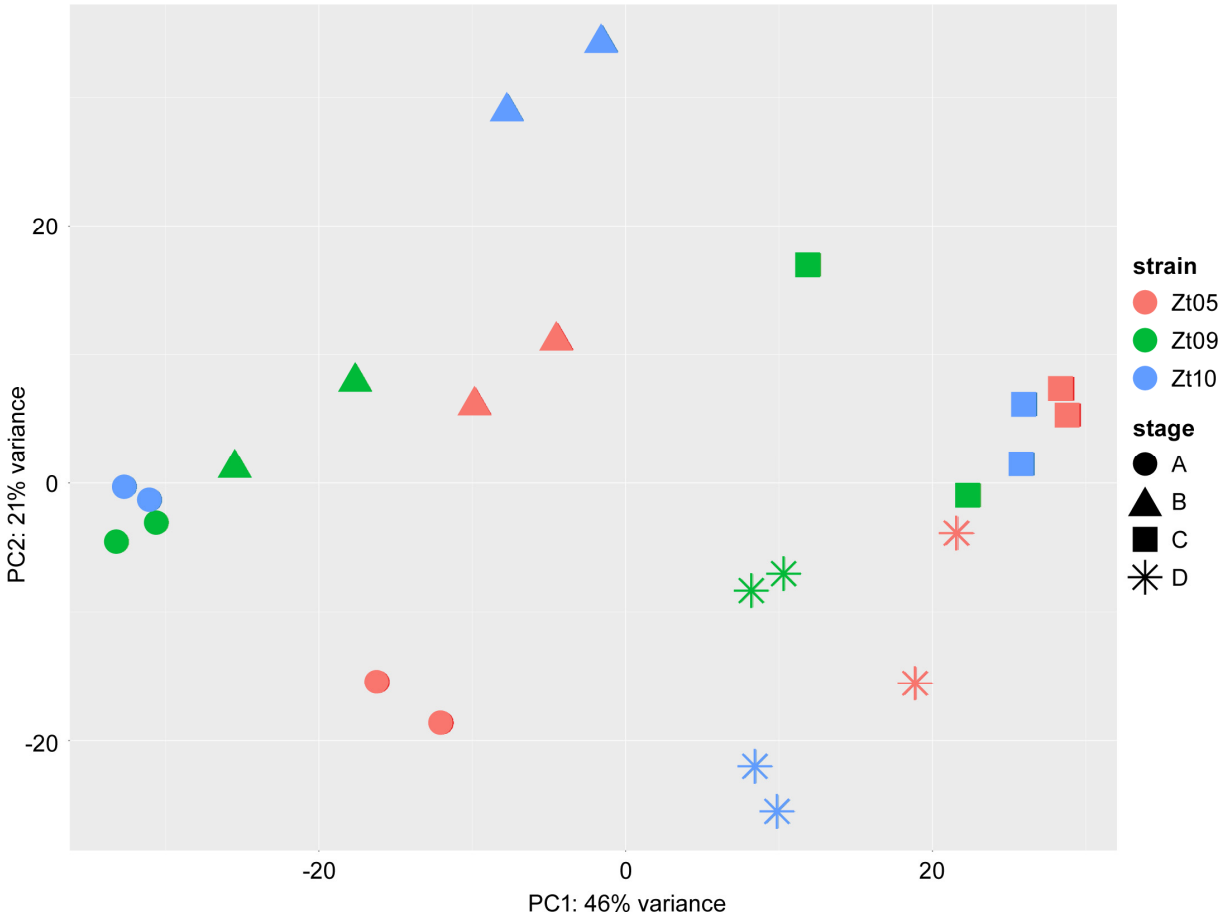

S8 Figure. RNA-seq data principal component analysis plot based on rlog-transformed read counts for *Z. tritici* core genes. PC1 separates datasets from infections stages A and B from stages C and D. Stage-specific datasets from all isolates cluster together.

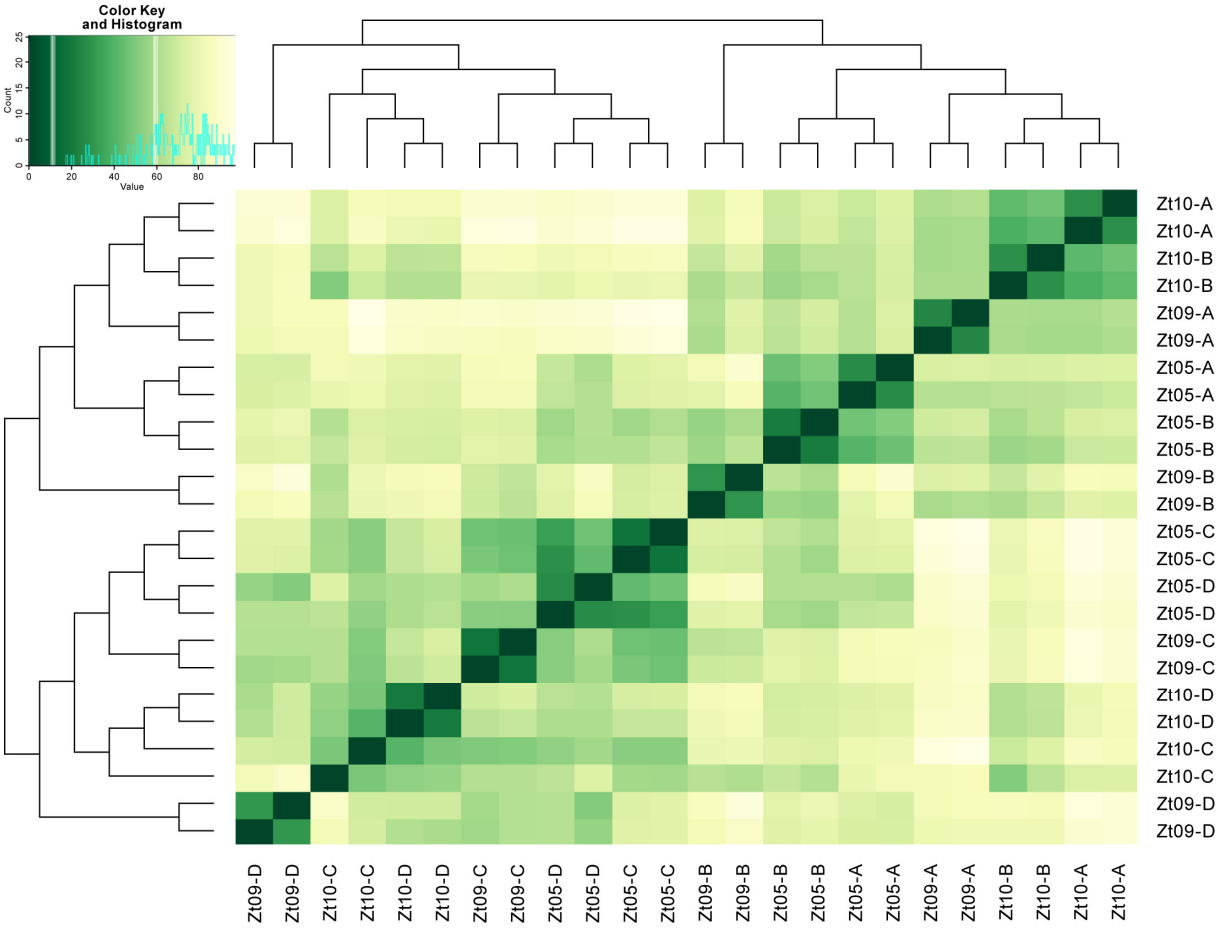

S9 Figure. Transcriptome data distance matrix based on rlog-transformed read counts for *Z. tritici* core genes. Datasets from stages A and B representing biotrophic growth form one cluster as do datasets of stages C and D representing necrotrophic growth.

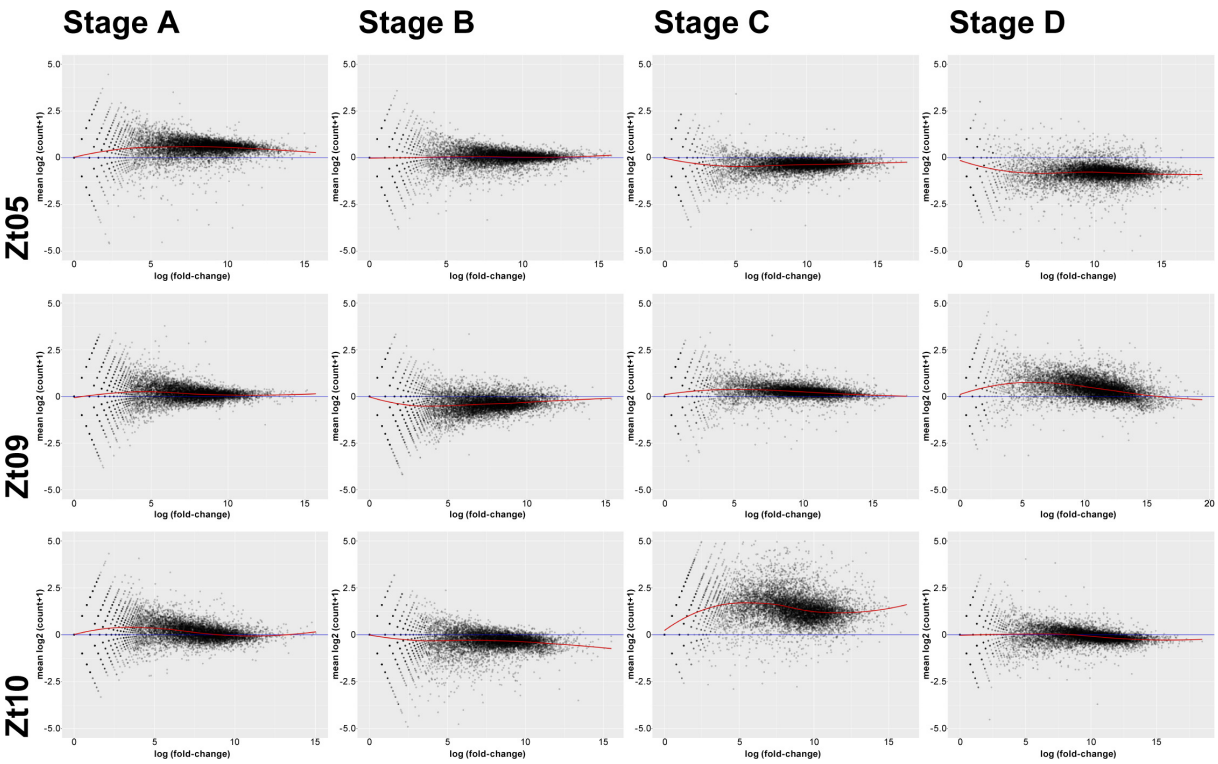

S10 Figure. MA plots comparing replicates for each RNA-seq dataset. Pairwise comparisons of replicates for each wheat infection stage of each *Z. tritici* isolate without normalization. x-axis: mean $\log_2$ (read count per gene+1), y-axis: log (fold-change). The greatest variation among replicates was between the Zt10 stage C datasets.

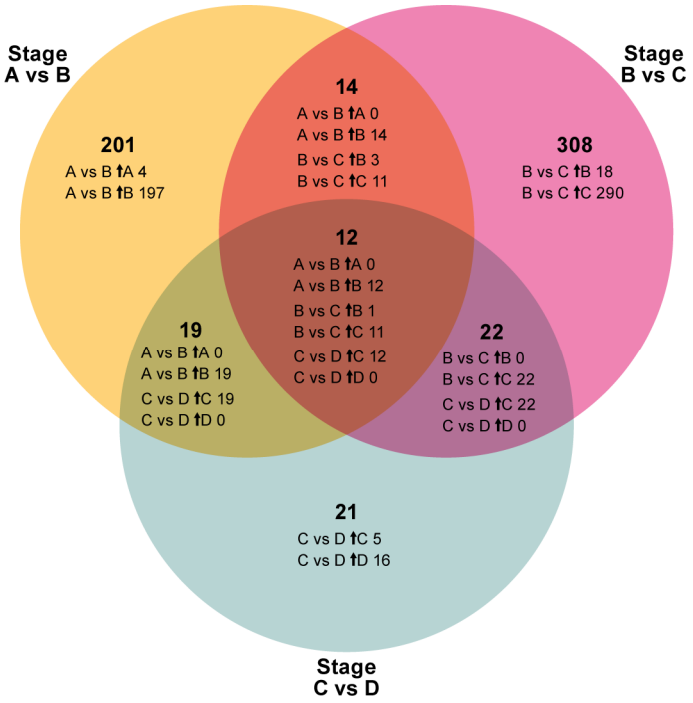

S11 Figure. 597 genes are differentially expressed between the infection stages in all three isolates, and 79 genes are differentially expressed between more than two stages. The Venn diagram illustrates how genes that are differentially expressed between *Z. tritici* infection stages are shared between stage comparisons. Differential expression analyses were performed with DESeq2. Differentially expressed genes have $P_{adj} \leq 0.01$ and an absolute $\log_2$ fold change between infection stages of ≥2. Small arrows (↑) indicate the stage in which genes are significantly up-regulated.

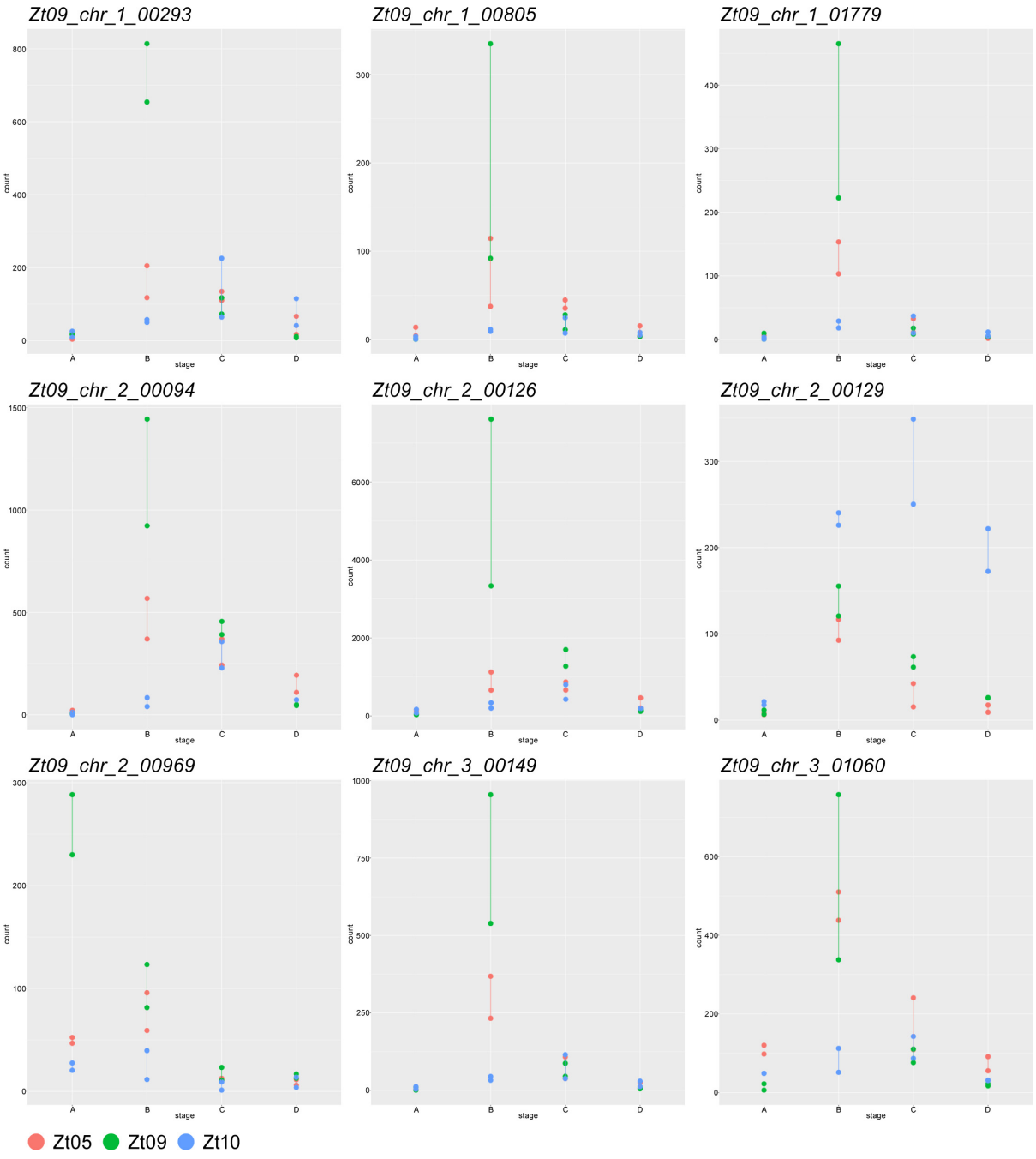
Zt09_chr_1_00293
Zt09_chr_1_00805
Zt09_chr_1_01779
Zt09_chr_2_00094
Zt09_chr_2_00126
Zt09_chr_2_00129
Zt09_chr_2_00969
Zt09_chr_3_00149
Zt09_chr_3_01060
count
stage
A
B
C
D
Zt05
Zt09
Zt10

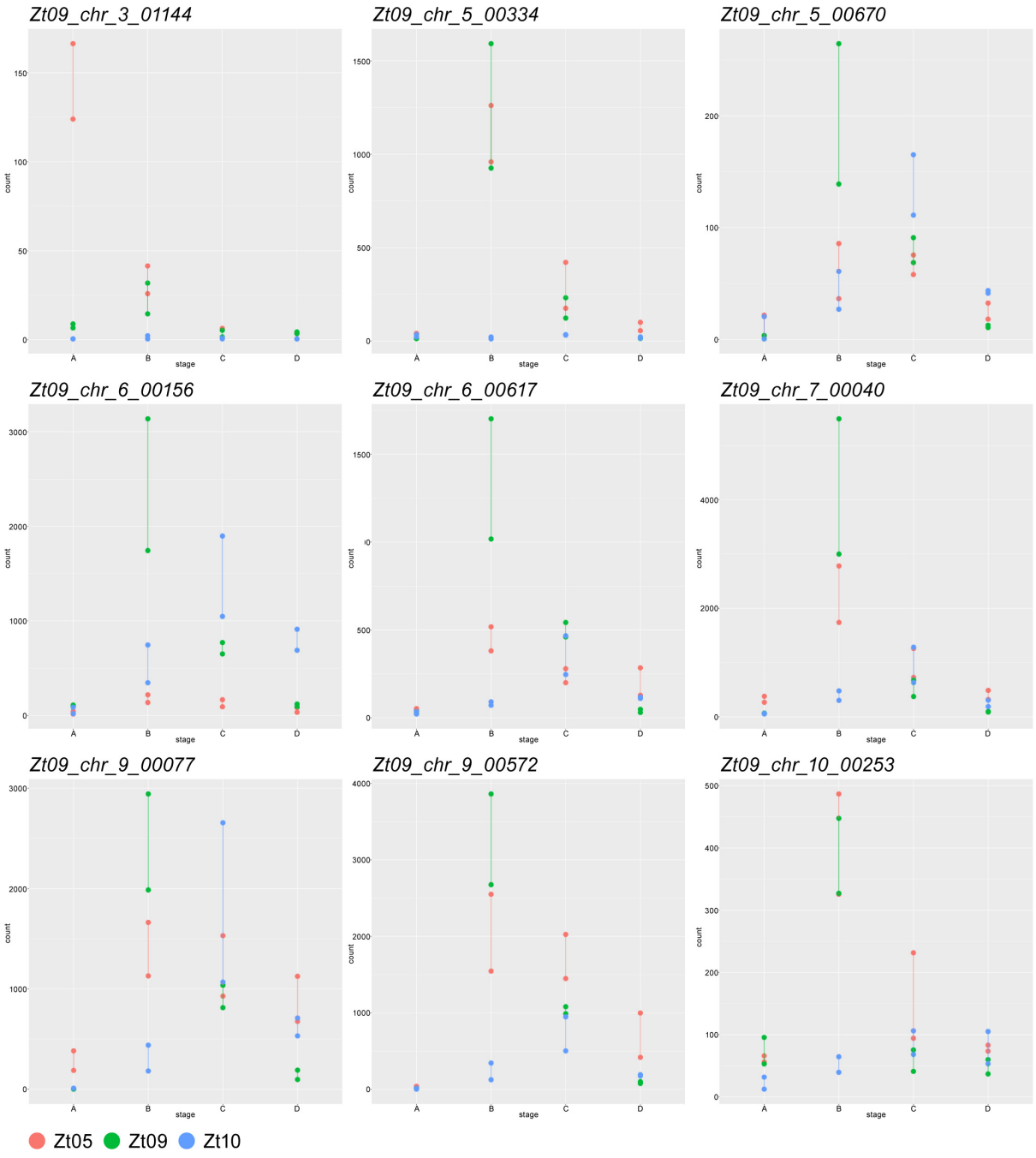
Zt09_chr_3_01144
Zt09_chr_5_00334
Zt09_chr_5_00670
Zt09_chr_6_00156
Zt09_chr_6_00617
Zt09_chr_7_00040
Zt09_chr_9_00077
Zt09_chr_9_00572
Zt09_chr_10_00253
count
stage
A
B
C
D
Zt05
Zt09
Zt10

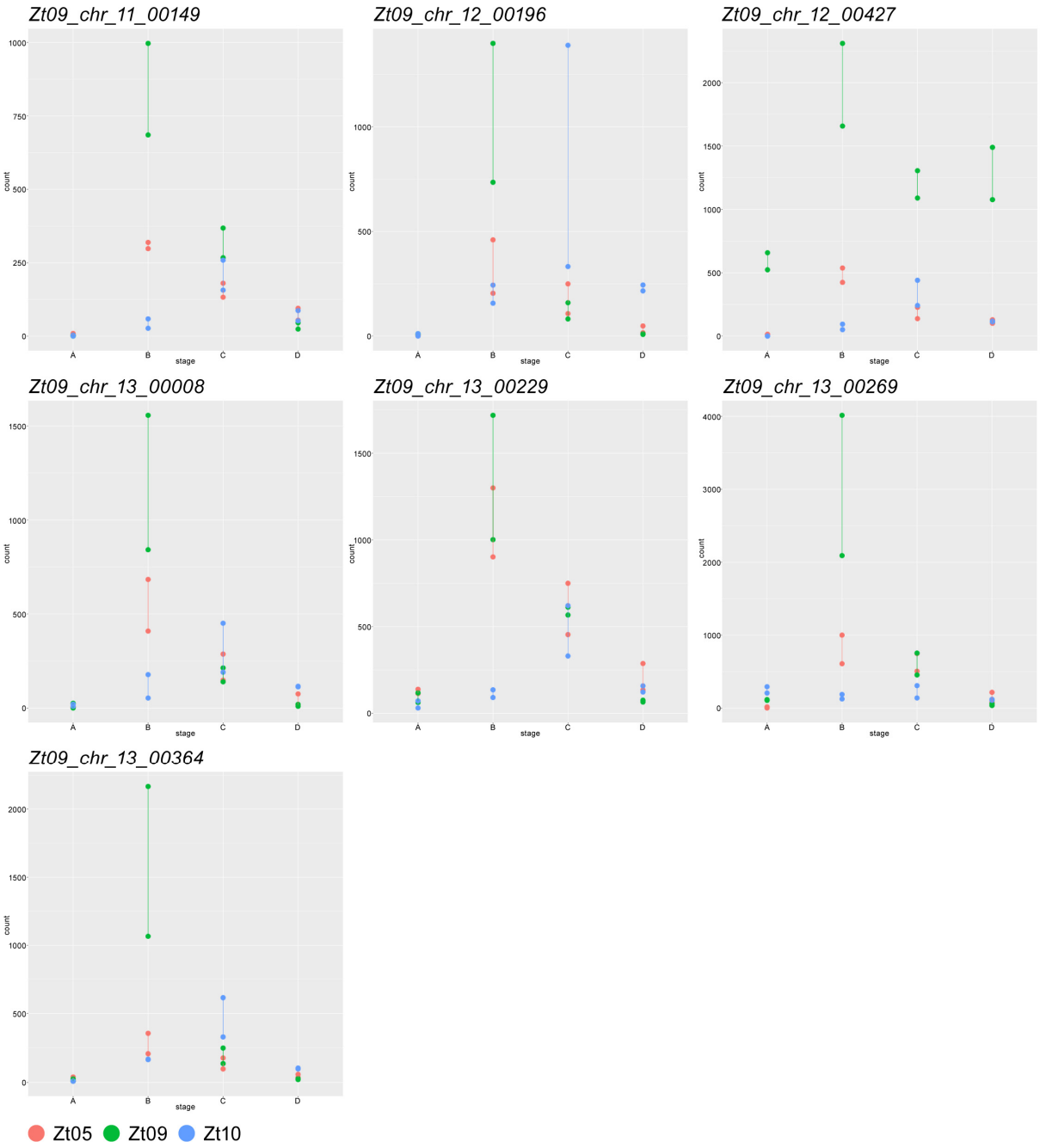

S12 Figure 1-3. Expression profiles of core *Z. tritici* biotrophic effector candidates based on normalized read counts per gene. Read counts were normalized across the four core infection stages (A to D) and the three *Z. tritici* isolates Zt05, Zt09, and Zt10 and represent a measure of relative gene expression between infection stages and between isolates.

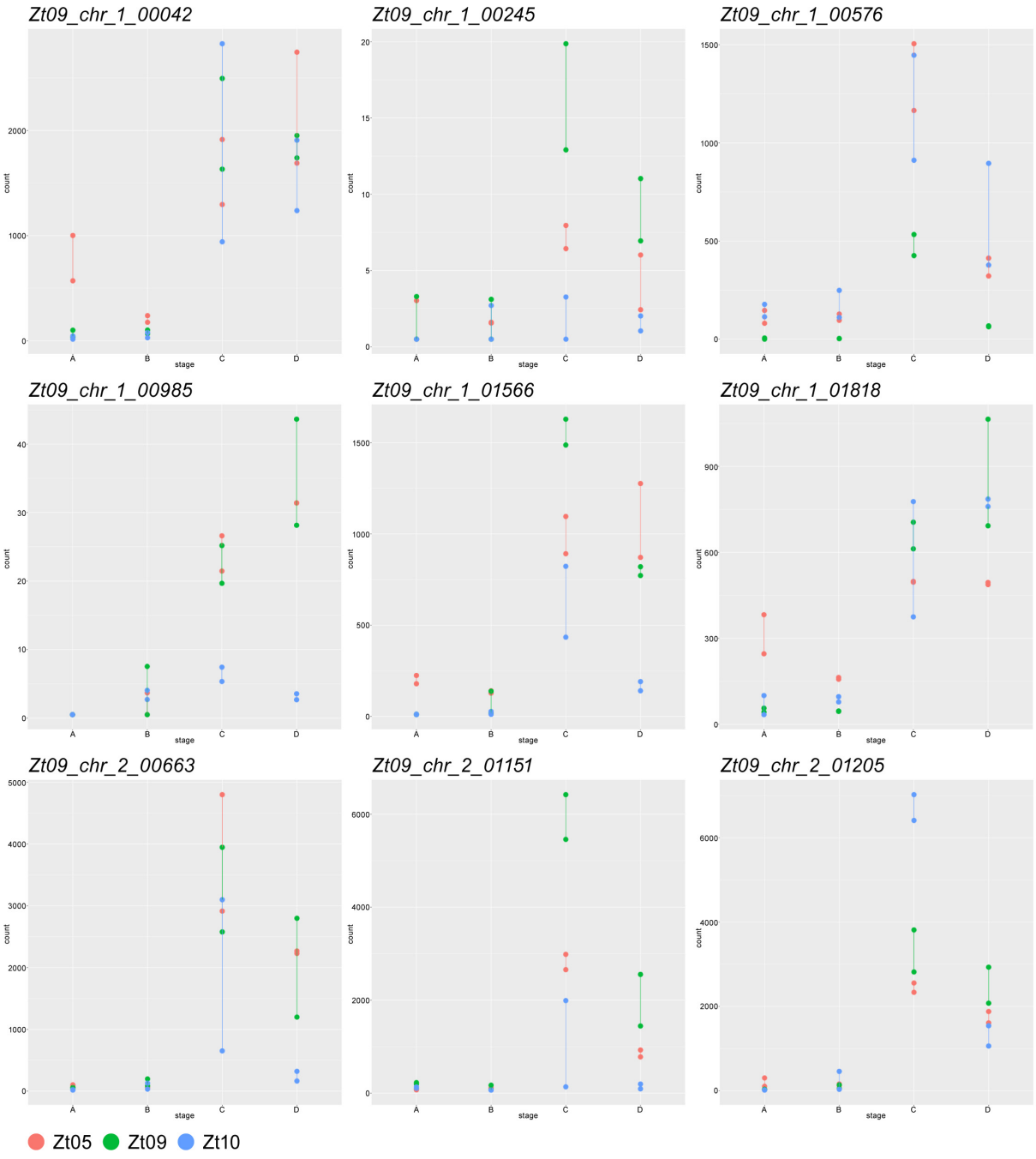
Zt09_chr_1_00042
Zt09_chr_1_00245
Zt09_chr_1_00576
Zt09_chr_1_00985
Zt09_chr_1_01566
Zt09_chr_1_01818
Zt09_chr_2_00663
Zt09_chr_2_01151
Zt09_chr_2_01205
count
stage
A
B
C
D
Zt05
Zt09
Zt10

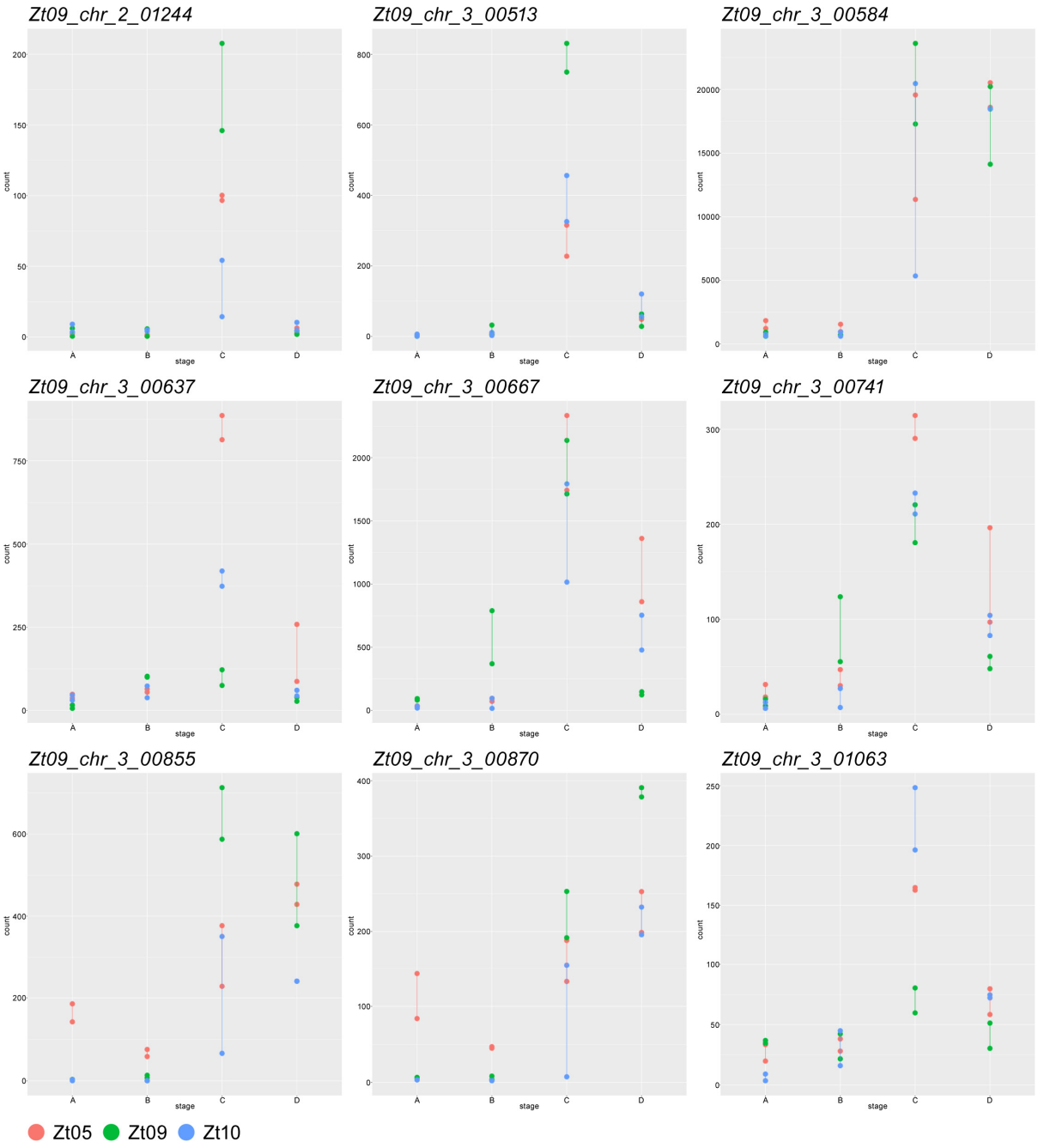
Zt09_chr_2_01244
Zt09_chr_3_00513
Zt09_chr_3_00584
Zt09_chr_3_00637
Zt09_chr_3_00667
Zt09_chr_3_00741
Zt09_chr_3_00855
Zt09_chr_3_00870
Zt09_chr_3_01063
count
stage
A
B
C
D
Zt05
Zt09
Zt10

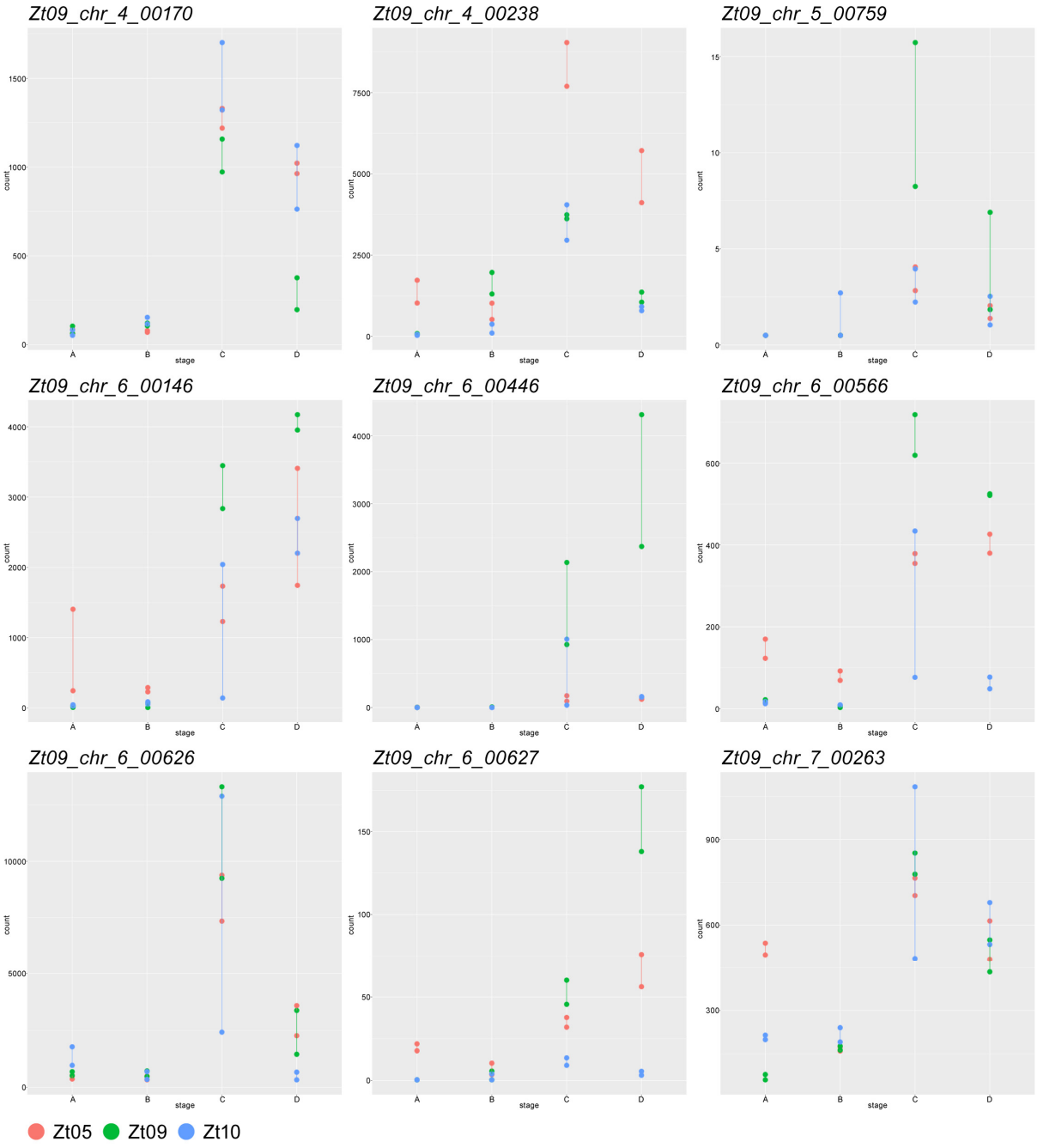
Zt09_chr_4_00170
Zt09_chr_4_00238
Zt09_chr_5_00759
Zt09_chr_6_00146
Zt09_chr_6_00446
Zt09_chr_6_00566
Zt09_chr_6_00626
Zt09_chr_6_00627
Zt09_chr_7_00263
count
stage
A
B
C
D
Zt05
Zt09
Zt10

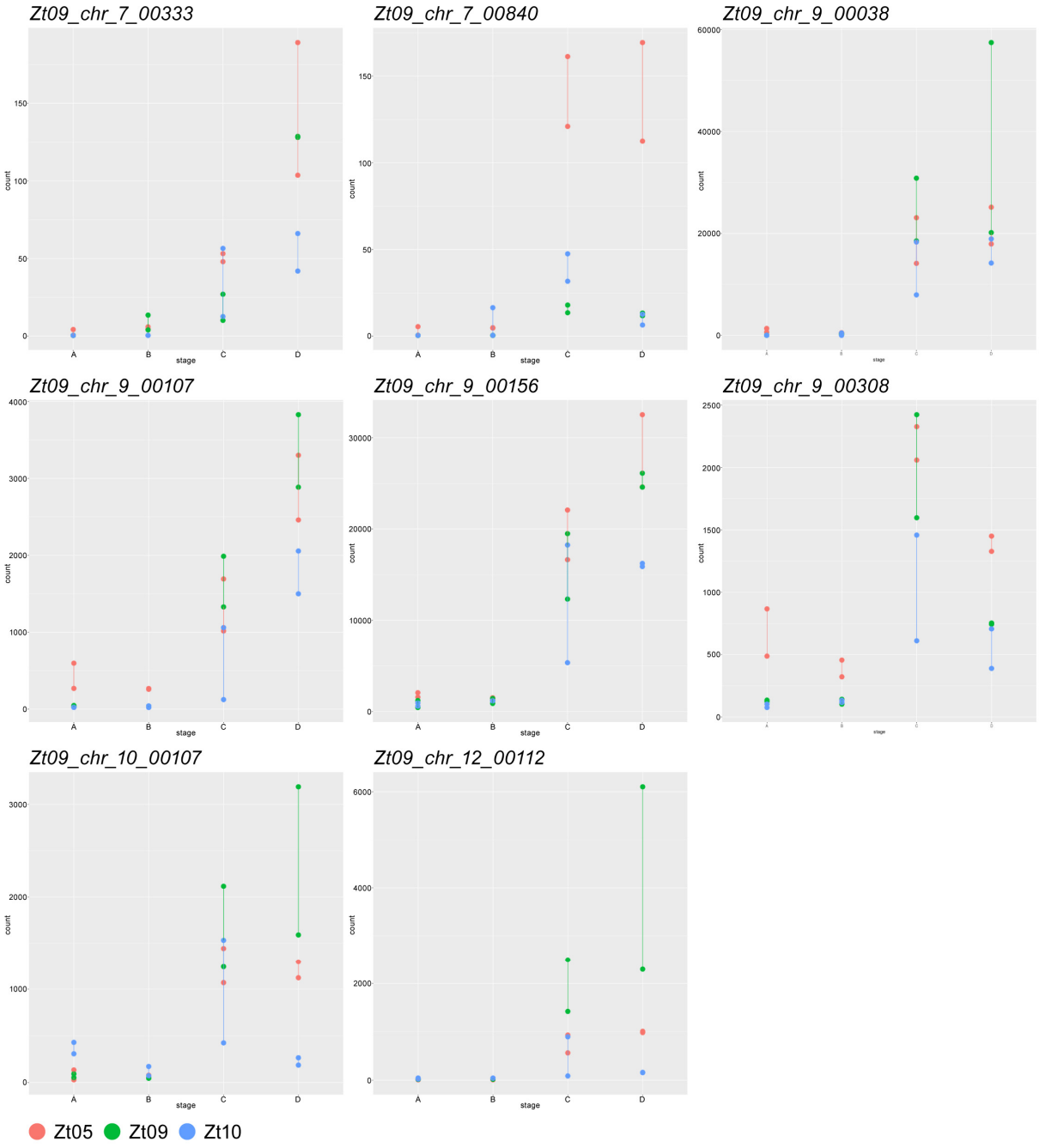

S13 Figure 1-4. Expression profiles of *Z. tritici* core necrotrophic effector candidates based on normalized read counts per gene. Read counts were normalized across the four core infection stages (A to D) and the three *Z. tritici* isolates Zt05, Zt09, and Zt10 and represent a measure of relative gene expression between infection stages and between isolates.

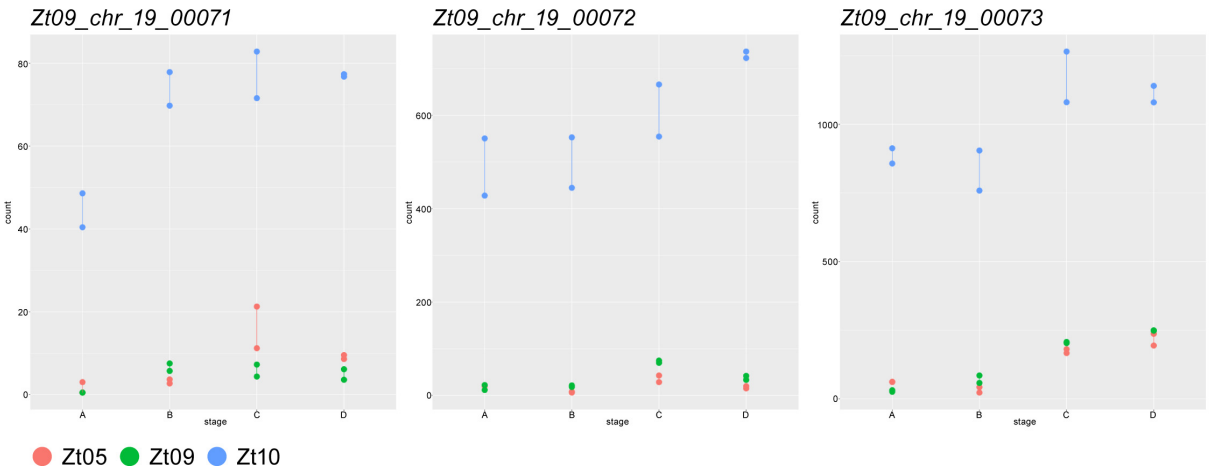

S14 Figure. Expression profiles of three *Z. tritici* genes located on accessory chromosome 19 in Zt09. The neighboring genes *Zt09_chr_19_00071*, *Zt09_chr_19_00072,* and *Zt09_chr_19_00073* are significantly higher expressed in Zt10 during all four infection stages. Read counts were normalized across the four core infection stages (A to D) and the three *Z. tritici* isolates (Zt05, Zt09, and Zt10) and represent a measure of relative gene expression between infection stages and between isolates.

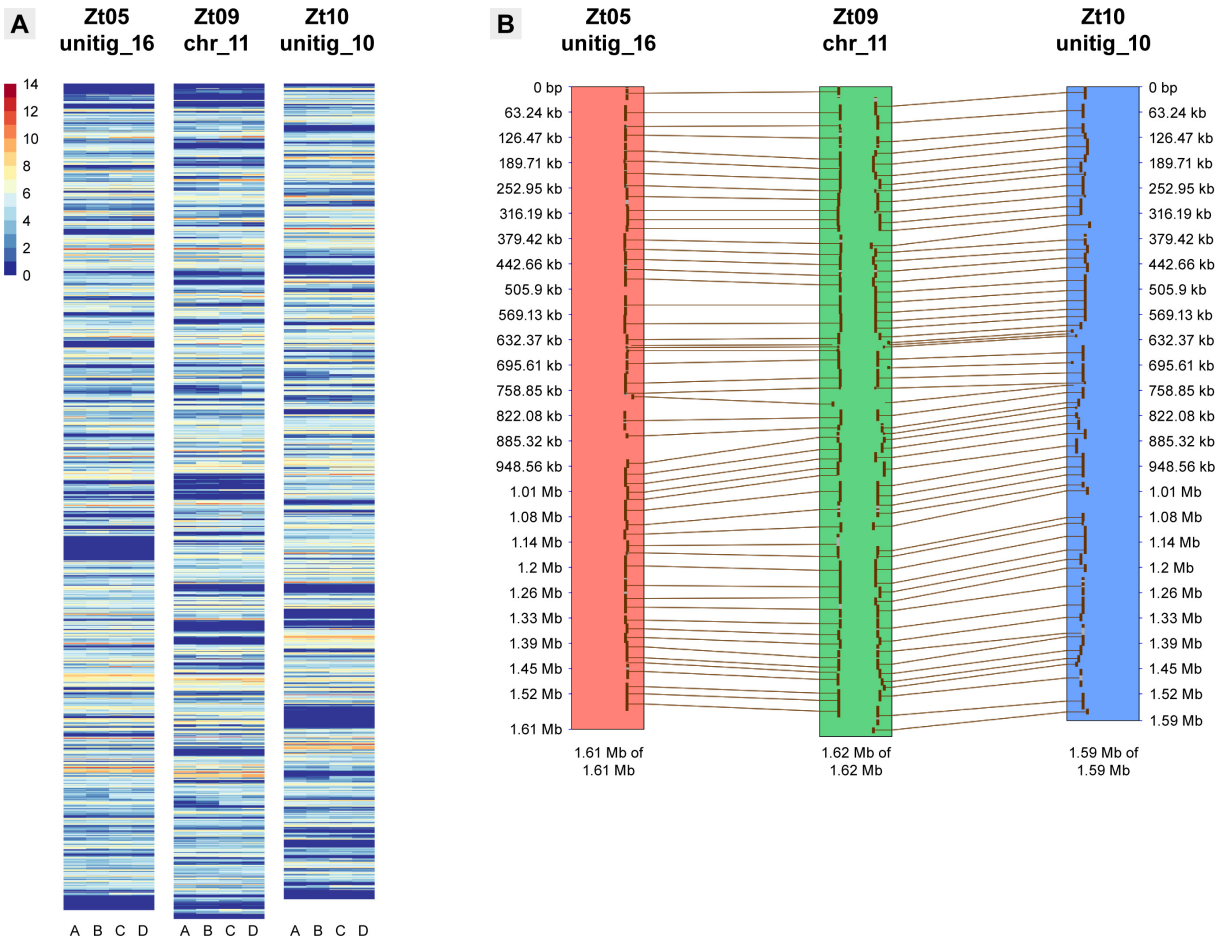

S15 Figure. Distribution of transcriptionally active loci on core chromosome 11. (A) Heatmaps of log_2-transformed FPKM expression values for 1-kb windows along IPO323/Zt09 core chromosome 11 and unitigs 16 and 10 in Zt05 and Zt10 for the four wheat infection stages. **(B)** Synteny plot comparing IPO323/Zt09 chromosome 11 and unitigs 16 and 10 in Zt05 and Zt10.

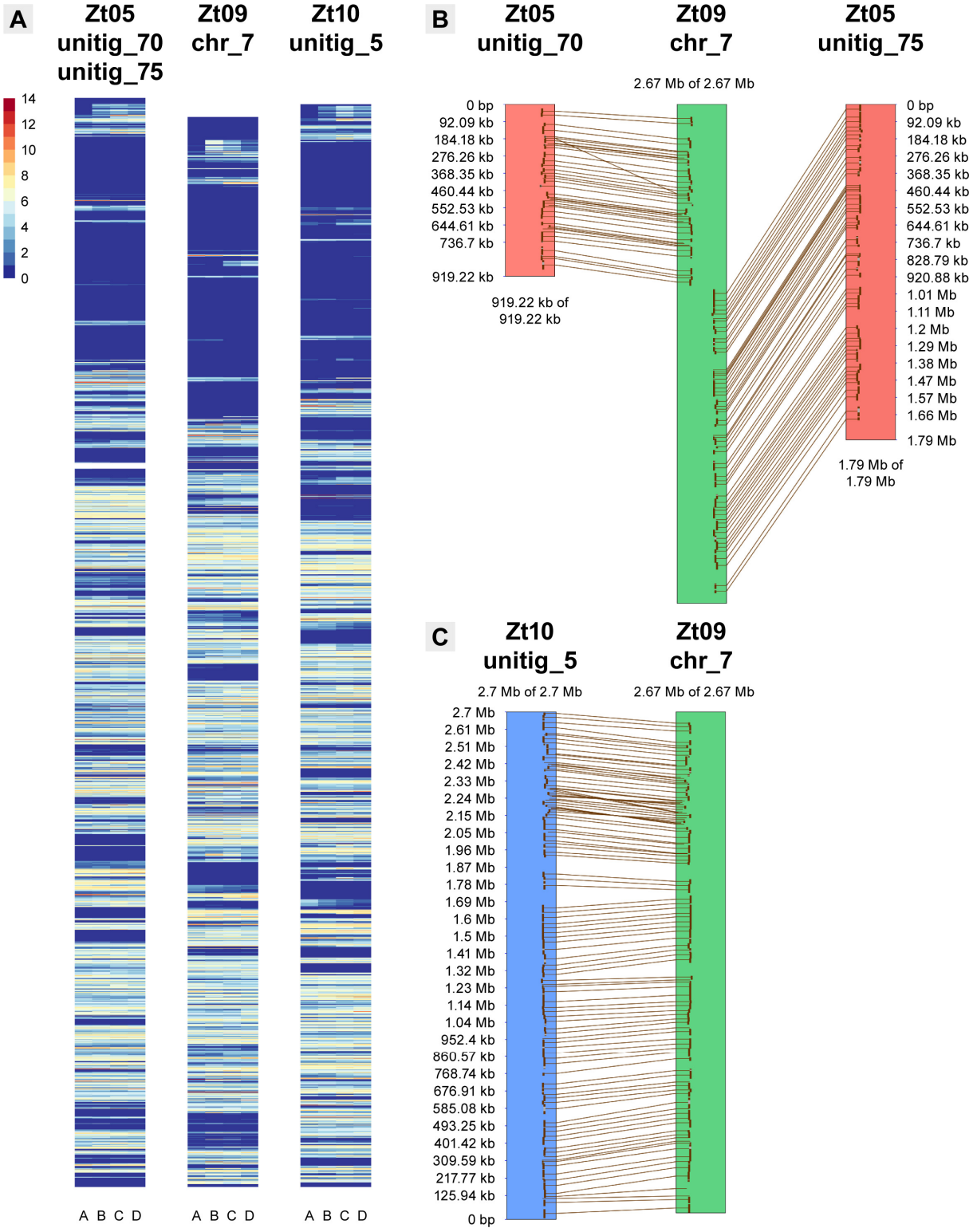

S16 Figure. Distribution of transcriptionally active loci on core chromosome 7. (A) Heatmaps of log_2-transformed FPKM expression values for 1-kb windows along IPO323/Zt09 core chromosome 7 and unitig 5 in Zt10 and unitigs 70 and 75 in Zt05 for the four wheat infection stages. **(B)** Synteny plots comparing IPO323/Zt09 chromosome 7 and unitigs 70 and 75 of Zt05 and **(C)** unitig 5 of Zt10.

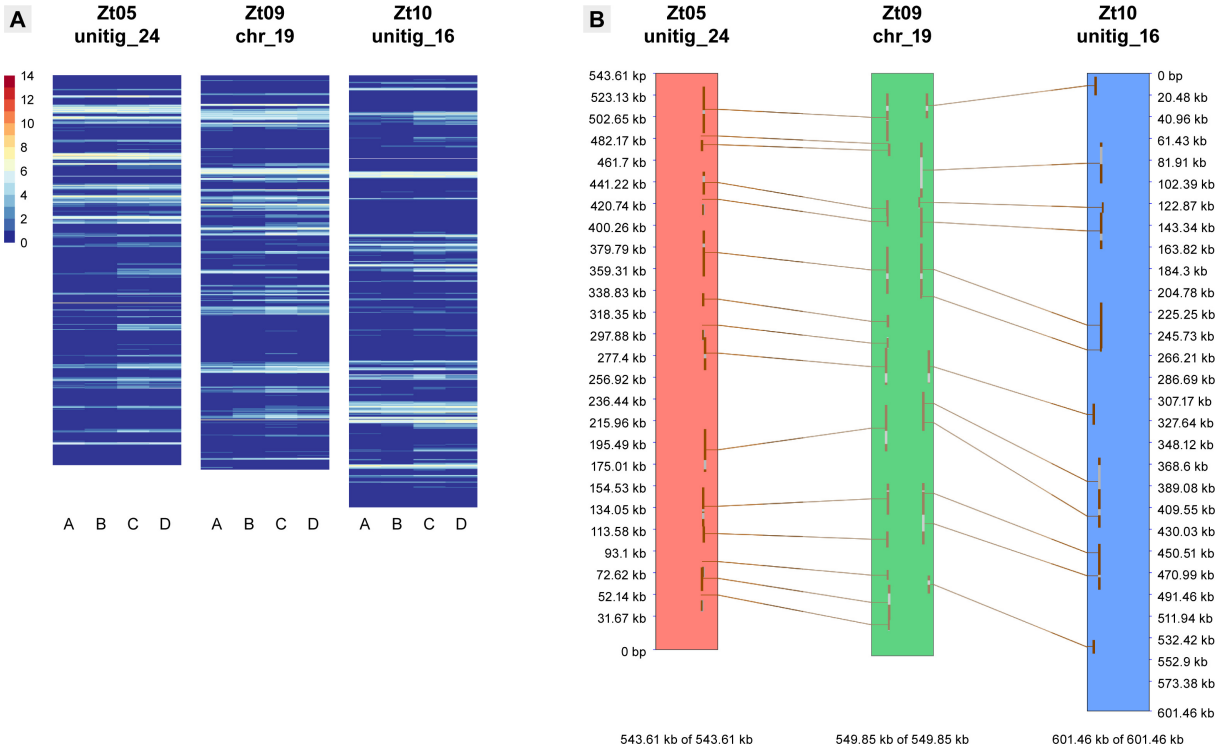

S17 Figure. Distribution of transcriptionally active loci on accessory chromosome 19. (A) Heatmaps of log_2-transformed FPKM expression values for 1-kb windows along IPO323/Zt09 accessory chromosome 19 and the syntenic unitigs 24 and 16 in Zt05 and Zt10 for the four wheat infection stages. **(B)** Synteny plot comparing IPO323/Zt09 chromosome 19 and unitigs 24 and 16 of Zt05 and Zt10, respectively.

Supplementary Animations

All supplementary animations are in .avi file format and are deposited on the supplementary USB key. Animations can be played with standard media players e.g. VLC media player available at http://www.videolan.org/vlc/.

S1 Animation. *Z. tritici* initial wheat infection stage.

Tomographic animation of confocal image z-stack showing infection hypha of *Z. tritici* isolate Zt09 entering wheat leaf tissue by open stoma at 4 dpi. The hypha grows closely attached to stomatal guard cell. Nuclei and wheat cells are displayed in *purple* and fungal structures in *green*. Reference transmitted images are in *grey*. Scale bar = 25 µm.

S2 Animation. *Z. tritici* initial wheat infection stage.

Tomographic animation of confocal image z-stack showing epiphyllous proliferation, infecting hyphae, and hyphal growth inside wheat sub-stomatal cavity and mesophyll of *Z. tritici* isolate Zt05 at 3 dpi. Nuclei and wheat cells are displayed in *purple* and fungal structures in *green*. Reference transmitted images are in *grey*. Scale bar = 25 µm.

S3 Animation. Biotrophic colonization of wheat mesophyll by *Z. tritici* Zt05.

Tomographic animation of confocal image z-stack showing epiphyllous hyphae as well as the dense biotrophic intercellular hyphal network of *Z. tritici* isolate Zt05 inside wheat mesophyll at 7 dpi. Long, straight hyphae grow in the interspace of wheat epidermis and mesophyll cells. Hyphae grow in close contact to plant cells. Nuclei and wheat cells are displayed in *purple* and fungal structures in *green*. Scale bar = 50 µm.

S4 Animation. Biotrophic colonization of wheat mesophyll by *Z. tritici* Zt09.

Tomographic animation of confocal image z-stack showing biotrophic intercellular hyphae of *Z. tritici* isolate Zt09 inside wheat leaf tissue at 11 dpi. Nuclei and wheat cells are displayed in *purple* and fungal structures in *green*. Reference transmitted images are in *grey*. Scale bar = 25 µm.

S5 Animation. *Z. tritici* Zt05 pycnidium development.

Tomographic animation of confocal image z-stack showing the development of primal structures of *Z. tritici* Zt05 pycnidium in the wheat sub-stomatal cavity during the early lifestyle transition stage at 11 dpi. Nuclei and wheat cells are displayed in *purple* and fungal structures in *green*. Reference transmitted images are in *grey*. Scale bar = 25 µm.

S6 Animation. *Z. tritici* Zt09 pycnidium development.

Tomographic animation of confocal image z-stack showing the development of primal structures of *Z. tritici* Zt09 pycnidium in the wheat sub-stomatal cavity during the lifestyle transition stage at 13 dpi. Nuclei and wheat cells are displayed in *purple* and fungal structures in *green*. Reference transmitted images are in *grey*. Scale bar = 25 µm.

S7 Animation. Development of two pycnidium initials of *Z. tritici* Zt10.

Tomographic animation of confocal image z-stack showing *Z. tritici* Zt10 pycnidium in the wheat sub-stomatal cavity developing from two initial stromata during the early lifestyle transition stage at 13 dpi. Nuclei and wheat cells are displayed in *purple* and fungal structures in *green*. The fluorescence of *Z. tritici* hyphae inside plant tissue is very weak. *Purple* fungal nuclei are mainly visible. Reference transmitted images are in *grey*. Scale bar = 25 µm.

S8 Animation. Mature pycnidia of *Z. tritici* Zt05.

Tomographic animation of confocal image z-stack showing asexual pycnidia of *Z. tritici* isolate Zt05 with pycnidiospores during necrotrophic infection stage at 21 dpi. The intercellular space of wheat mesophyll is densely colonized by *Z. tritici* hyphae. Nuclei and wheat cells are displayed in *purple* and fungal structures in *green*. The fluorescence of *Z. tritici* hyphae inside the plant tissue is weak. *Purple* fungal nuclei are mainly visible. Reference transmitted images are in *grey*. Scale bar = 50 µm.

S9 Animation. Pycnidium of *Z. tritici* Zt09.

Tomographic animation of confocal image z-stack showing asexual pycnidium of *Z. tritici* isolate Zt09 at 20 dpi. Hyphae grow in close contact to collapsing wheat mesophyll cells. Nuclei and wheat cells are in *purple* and fungal structures in *green*. Reference transmitted images are in *grey*. Scale bar = 25 µm.

Supplementary Text

All supplementary text files are in .docx file format and are deposited on the supplementary USB key.

S1 Text. Supplementary Results.

S2 Text. Supplementary Material and Methods.

S3 Text. Supplementary Information. Tools and commands used for genome analyses and for processing and analyses of *Z. tritici* transcriptome data.

Chapter 3

Few key factors determine incompatible and compatible host-pathogen interactions in closely related grass infecting fungi

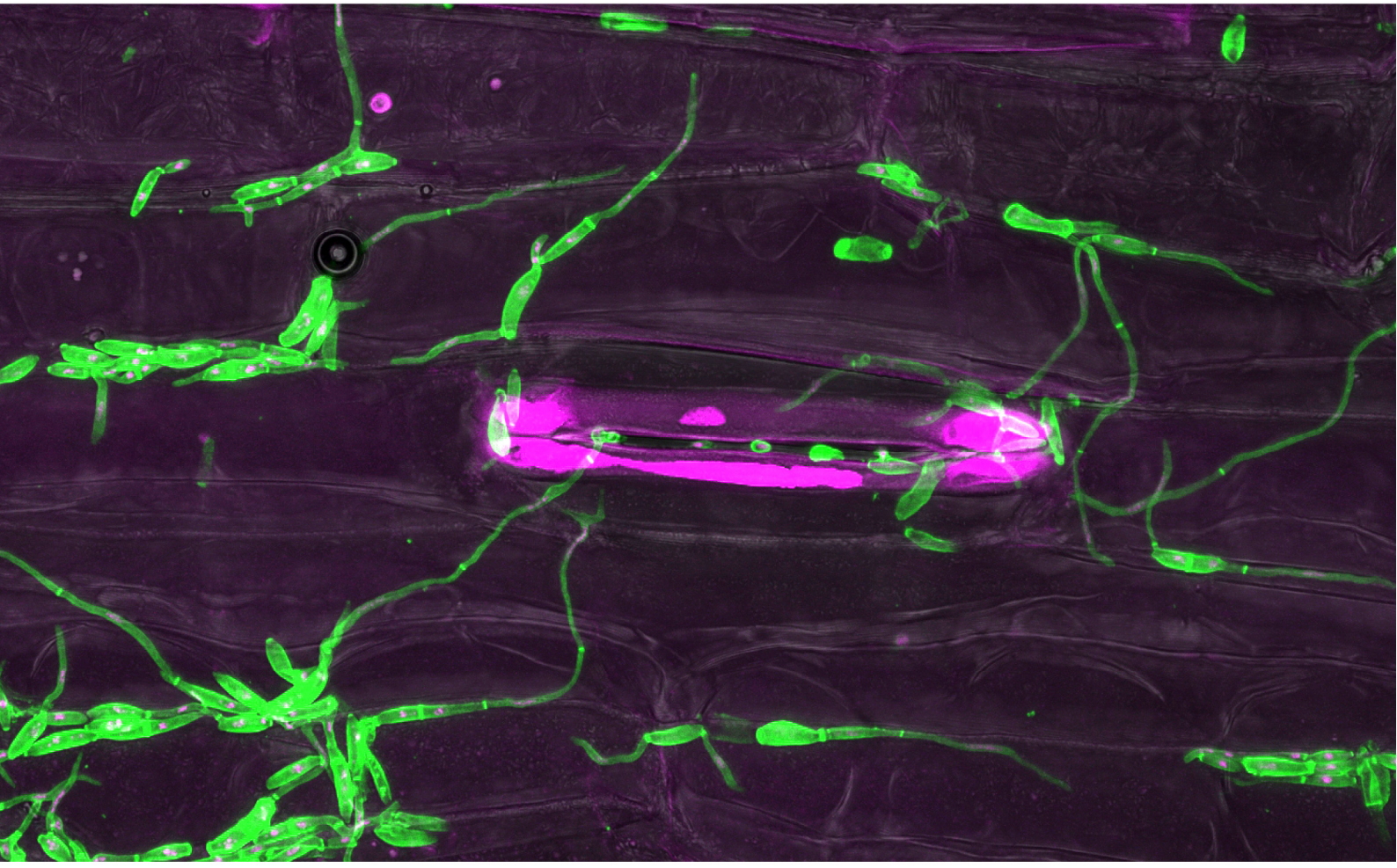

Chapter 3

Few key factors determine incompatible and compatible host-pathogen interactions in closely related grass infecting fungi

Research paper manuscript

Authors: Janine Haueisen, Mareike Möller, Heike Seybold and Eva H. Stukenbrock

Abstract

Host-pathogen co-evolutionary dynamics force microbial plant pathogens to constantly develop and adjust specific adaptations to thrive in their plant host, and likewise act as a strong driver of divergence and speciation in pathogens. Factors that confer host specialization and determine host specificity are very diverse and range from molecular and morphological strategies to metabolic and reproductive adaptations. Identification of these key factors is a major goal in the study of pathogen evolution and may aid the development of sustainable crops and crop protection. We took a novel experimental approach and conducted comparative microscopy and transcriptome analyses of the closely related, recently diverged fungal pathogens *Zymoseptoria tritici*, *Z. pseudotritici*, and *Z. ardabiliae* that establish compatible and incompatible interactions with wheat. Although infections of the incompatible species are blocked involving a plant defense response, we found highly conserved early infection development in all three species. Likewise, transcriptional programs in the closely related fungi are conserved to a large extent, as only 6.5% of the 7,309 orthologous genes are significantly differentially expressed during initial infection of wheat. The genes up-regulated in the compatible pathogen reflect metabolic re-programming and adaptation to growth in wheat tissue. In contrast, genes primarily involved in counteracting cell stress and damage are significantly higher expressed in the incompatible species. Based on the species-specific gene expression profiles, we further identified 15 candidates for host-specific effectors and avirulence genes in the compatible pathogen. Host-specific effectors are significantly induced in the compatible species and might contribute to host adaptation e.g. by interfering with host recognition, while avirulence genes are silenced, possibly to avoid effector-triggered immunity in the host. Together, the results presented here indicate that only few key factors confer host specialization in recently diverged fungal pathogens and determine the outcome of plant infections. Our findings demonstrate that comparative analyses of compatible and incompatible infections of closely related pathogens are a powerful experimental strategy to identify traits putatively involved in pathogen evolution and host specialization.

Introduction

Most plant pathogens depend on the host to complete their life-cycle. Some pathogens, mostly necrotrophic species that kill and feed on dead host tissue, are able to infect a broad range of plant hosts. Biotrophic and hemibiotrophic pathogens which, at least initially, depend on living host tissue, establish intimate host interactions and are often specialized to few host species or even host genotypes (Eyal *et al.*, 1985; McMullan *et al.*, 2015; Menardo *et al.*, 2016; Inoue *et al.*, 2017). The ability of plant pathogens to exploit the tissues of their hosts as ecological niche for growth and reproduction requires a multitude of specializations ranging from molecular and morphological host invasion strategies, over metabolic adaptation to efficient propagation and dispersal (Haueisen & Stukenbrock, 2016; van der Does & Rep, 2017). Prime candidates for molecular pathogen factors conferring specialization to the host environment are effectors. Effectors are small secreted molecules that modulate host plant physiology to achieve plant susceptibility and facilitate pathogen growth and reproduction (Lo Presti *et al.*, 2015).

Pathogen effector genes evolve rapidly as their evolution is driven by a molecular arms-race with the host targets (Jones & Dangl, 2006). Functional characterization of effector genes accumulating non-synonymous mutations demonstrated that genes evolving under positive selection indeed play key roles in host specialization of filamentous pathogens (Dong *et al.*, 2014; Poppe *et al.*, 2015). However, studies comparing genome-wide rates of molecular evolution in related pathogens adapted to different hosts have shown that rapid evolution is certainly not limited to typical effectors. Also genes involved in metabolism, chromosome condensation, and signal transduction were shown to exhibit strong signatures of diversifying selection e.g. in the fungal pathogens *Botrytis* (Aguileta *et al.*, 2012) and *Zymoseptoria* (Grandaubert *et al.*, 2017). For nutrient acquisition and self-protection, pathogens moreover need to be equipped with host-specific repertoires of enzymes and secondary metabolites that are adapted to kill and break down host cell and tissue components, and degrade putatively toxic host compounds (Amselem *et al.*, 2011; Brunner *et al.*, 2013).

In this study, we define infections of adapted pathogens that result in disease and pathogen reproduction as compatible host-pathogen interactions. Fungal pathogens, which are not adapted to a host, show incompatible host interactions characterized by arrested development of infectious hyphae during early infection. Consequently, tissue colonization as well as the production of sexual or asexual spores is blocked. As experimental strategy, comparing incompatible and compatible host infections of pathogens is a powerful tool and has shed light on factors determining pathogenicity and host specialization (Kawahara *et al.*, 2012; Hacquard *et al.*, 2013; Kellner *et al.*, 2014; Thatcher *et al.*, 2016). Besides adaptive mutations and gene presence-absence polymorphisms (van Dam *et al.*, 2016; Inoue *et al.*, 2017), host specialization can be facilitated by transcriptional adaptations as gene silencing or induction, e.g. by mutations in

regulatory sequences or changes in epigenetic landscapes. For the barley pathogen *Blumeria graminis*, comparative transcriptomics showed that gene expression programs during host infections are very robust and only little influenced by different host environments. Expression of effector genes however, differed significantly in compatible and incompatible hosts (Hacquard *et al.*, 2013). Candidate genes with host-specific expression profiles were also identified by comparing the transcriptome of *Z. tritici* on wheat and on the incompatible host grass *Brachypodium distachyon* (Kellner *et al.*, 2014). The transcription factor Zt107320 is strongly up-regulated on the compatible host and functional studies indeed indicate a specific role in fungal development and virulence in wheat (Habig *et al., in prep*).

In this study, we set out to identify traits that confer host specialization and thereby determine host specificity in fungal plant pathogens. We hypothesized that host-specific virulence and non-virulence related traits can be identified by comparative analyses of compatible and incompatible host-pathogen interactions of closely related pathogen species. To this end, we conducted a novel experimental approach by exposing isolates of an adapted pathogen, *Z. tritici*, and isolates of two non-adapted pathogens, *Z. pseudotritici* and *Z. ardabiliae*, to the same host plant species wheat (*Triticum aestivum*). The three *Zymoseptoria* species (Ascomycota, Dothideomycetes) are closely related, however, specialized to colonize and reproduce inside the leaf tissue of Poaceae species growing in different ecosystems. *Z. tritici* is a specialized pathogen of wheat causing pandemics in all wheat-growing areas worldwide (Ponomarenko *et al.*, 2011; O'Driscoll *et al.*, 2014). The sister species *Z. pseudotritici* and *Z. ardabiliae* have been isolated from leaves of a range of uncultivated grass species in natural grasslands in North Iran and are endemic to the Middle East (Stukenbrock *et al.*, 2007, 2012b). Phylo-geographic and coalescence analyses suggest that divergence of *Z. tritici* from a wild-grass associated ancestor occurred only ~11,000 years ago in the Fertile crescent, temporally and spatially coinciding with the domestication of wheat in the Middle East (Banke & McDonald, 2005; Stukenbrock *et al.*, 2007, 2011). Given their recent divergence, close relatedness, and association to different host environments, *Z. tritici*, *Z. pseudotritici*, and *Z. ardabiliae* provide an excellent model system to study host specialization.

Here, we conducted comparative analyses of the three *Zymoseptoria* species including *in vitro* and *in planta* assays, staining of reactive oxygen species (ROS), detailed confocal microscopy of inoculated wheat leaves, and gene expression analyses during early wheat infections. Thereby, the previously characterized *Z. tritici* core infection program (Haueisen *et al.*, 2017) served as reference for compatible *Zymoseptoria*-wheat infections. Isolates of the incompatible *Z. pseudotritici* and *Z. ardabiliae* developed very similar to *Z. tritici* upon inoculation on wheat leaves, suggesting conserved infection developmental stages, but infections were blocked when hyphae penetrated wheat stomata. Consequently, *Z. pseudotritici* and *Z. ardabiliae* isolates did not cause disease on wheat and blocked infections are accompanied by a host defense response

indicated by the accumulation of ROS. Similarly as for early infection morphology, comparative transcriptome analyses demonstrated conserved infection programs in the adapted and non-adapted *Zymoseptoria* species as less than 7% of the orthologous genes are significantly differentially expressed. However, among the genes specifically up-regulated in the wheat infecting *Z. tritici* are genes involved in lipid metabolism and the production of enzymes catalyzing degradation of ROS and halogenation of organic compounds. Certainly, reprogramming of pathogen metabolism upon host infection and detoxification of putatively toxic host compounds are crucial adaptations for successful host infection. Further, we identified candidate genes for host-specific effectors putatively involved in the evasion of wheat immunity as well as putative avirulence genes that were significantly up-regulated in the blocked *Z. pseudotritici* and *Z. ardabiliae* and might have caused effector-triggered immunity.

Materials and Methods

Zymoseptoria spp. isolates and growth conditions

Cells of *Zymoseptoria tritici*, *Z. pseudotritici*, and *Z. ardabiliae* isolates (Table 1) were inoculated from glycerol stocks onto YMS agar (0.4% [w/v] yeast extract, 0.4% [w/v] malt extract, 0.4% [w/v] sucrose, 2% [w/v] bacto agar) and grown at 18°C for 5 days. Single cells were grown in liquid YMS (200 rpm, 18°C) and harvested by centrifugation (3500 rpm for 10 min).

Table 1. *Zymoseptoria* species isolates used in this study.

Species	Isolate	Original ID	Origin	Host	Year	Description	References
Zymoseptoria tritici	Zt05	MgDk09_U34	Denmark	*Triticum aestivum*	2004	Field isolate	Thygesen *et al*., 2008
	Zt09	IPO323ΔChr18	Nether-lands	*Triticum aestivum*	1981	Derivate of reference strain IPO323, without chromosome 18	Kema and Silfhout, 1997; Goodwin *et al*., 2011; Kellner *et al*., 2014
	Zt10	STIR04_A26b	Iran, Ilam province, Mehran	*Triticum aestivum*	2001	Field isolate	Stukenbrock *et al*., 2007
Zymoseptoria pseudotritici	Zp13	S1_STIR04_2.2.1	Iran, Ardabil province	*Dactylis glomerata*	2004	Natural isolates	Stukenbrock *et al*., 2007; 2011; 2012
	Zp72	S1_STIR04_4.8.1		*Elymus repens*			
	Zp75	S1_STIR04_5.6		*Dactylis glomerata*			
Zymoseptoria ardabiliae	Za17	S2_STIR04_1.1.1	Iran, Ardabil province	*Lolium perenne*	2004	Natural isolates	Stukenbrock *et al*., 2007; 2011; 2012
	Za48	S2_STIR04_3.4.2		*Elymus repens*	2004		
	Za94	STIR11_1.15.1		Unknown grass	2011		

Plant infection experiments

We used 14-day-old seedlings of the winter wheat (*Triticum aestivum*) cultivar Obelisk (Wiersum Plantbreeding, Winschoten, Netherlands) for all plant infection experiments. The fungal inoculum was adjusted to 1 x 10^8 cells/mL in 0.1% [v/v] Tween 20 (Roth, Karlsruhe, Germany) and marked leaf areas (8 to 12 cm) of the second leaf of each plant were brush-inoculated. For mock controls, we conducted the same treatment without fungal cells. Plants were incubated at 22°C [day]/20°C [night] and 100% humidity with a 16-h light period for the first 48 h after inoculation. Subsequently, humidity was reduced to 70% and plants were grown for 3 or 4 weeks after inoculation, depending on the experiment.

In planta phenotypic assays

To compare quantitative virulence of the *Z. tritici* isolates Zt05, Zt09, and Zt10, the *Z. pseudotritici* isolates Zp13, Zp72, and Zp75, and the *Z. ardabiliae* isolates Za17, Za48, and Za94 on wheat, we conducted randomized infection experiments with blinded inoculation and evaluation. Virulence of the isolates Zp72, Zp75, Za48, and Za94 was assessed in one experiment on 40 Obelisk leaves for each isolate. For the *Z. tritici* isolates, Zp13, and Za17, we performed three independent experiments and tested virulence on 116 to 118 leaves per isolate. Inoculated leaf areas of 854 leaves in total were evaluated at 28 days post infection (dpi) by scoring the observed disease symptoms based on the percentage of leaf area covered by necrosis and pycnidia as previously described (Poppe *et al.*, 2015). We differentiated six categories: 0 (no visible symptoms), 1 (1-20%), 2 (21-40%), 3 (41-60%), 4 (61-80%), and 5 (81-100%).

To visualize and localize the accumulation of the reactive oxygen species H_2O_2 in *Zymoseptoria* spp. infected leaf tissue, we conducted 3,3'-diaminobenzidine (DAB) staining (Thordal-Christensen *et al.*, 1997) at 4, 10, 14, 18, and 21 dpi for Zt05, Zt09, Zt10, Zp13, and Za17. Inoculated leaf parts were excised with a razorblade and immersed in DAB solution (1 mg/mL 3,3'-diaminobenzidine tetrahydrochloride (Thermo Fisher Scientific, Rockford, USA) in 0.05% [v/v] Tween 20 (Roth, Karlsruhe, Germany). Samples were protected from light and DAB solution was infiltrated in two steps: 1st at low pressure (600 mbar) for two times 15 min and 2nd at gentle shaking (22 rpm) for 90 min. Subsequently, leaf samples were incubated overnight in de-staining solution (96% ethanol: acetic acid = 3:1 [v/v]) at gentle shaking (25 rpm). Cleared samples were stored in 96% ethanol and examined in 40% glycerol. The presence of H_2O_2 is indicated by reddish-brown precipitate in cleared leaves. Samples were documented before (iPhone 7 camera) and after (Canon EOS 600D) staining.

Phenotypic assays *in vitro*

To compare tolerance towards abiotic stressor and to assess the *in vitro* phenotypes of the nine *Zymoseptoria* spp. isolates, we conducted an *in vitro* stress assay as described in (Poppe *et al.*, 2015). After five days, we compared growth on solid YMS medium at 18°C to growth on YMS medium exposed to stress conditions: temperature (20/22°C with 16-h day/8-h night rhythm, 28°C in darkness), oxidative stress (2 and 3 mM H_2O_2), osmotic stress (1 M NaCl, 1 M sorbitol), and cell wall stress (500 µg/mL Congo red, 200 µg/mL calcofluor white). Each treatment was replicated three times and development of *Zymoseptoria* ssp. isolates was documented using a Canon EOS 600D.

Single cells of Zt09, Zp13, and Za17 grown in liquid YMS were examined by light microscopy using a Zeiss Axioplan 2 (Carl Zeiss, Jena, Germany).

To compare the *in vitro* growth rates of the isolates Zt05, Zt09, Zt10, Zp13, and Za17, we grew single cells for 165 h in liquid YMS medium (18°C, 200 rpm) with a starting concentration of 100,000 cells/mL and assessed cell concentrations on average every 24 h using a Neubauer-improved counting chamber. The growth assay was replicated three times for each strain. Growth curve data for each isolate was fitted in R (R Core Team, 2017) using the package Growthcurver (Sprouffske & Wagner, 2016).

Analysis of *Zymoseptoria* spp. wheat infections by confocal microscopy

We conducted comparative analyses of the structures produced by nine *Zymoseptoria* spp. isolates (Table 1) within and on the surface of wheat leaves by confocal laser scanning microscopy. Infected wheat leaves were harvested at 3, 5, 8, 10, 12, 14, 17, and 21 days post inoculation (dpi) and host-pathogen interactions were analyzed. Following the same protocol, we determined the infection stage of leaf samples used for RNA extraction and transcriptome sequencing (see below). In total, we studied 72 *Zymoseptoria*-inoculated leaves of the wheat cultivar Obelisk, analyzed at least 15 infection events per leaf sample by confocal microscopy, and created a total of 164 confocal image z-stacks. Cleared leaf material was stained with wheat germ agglutinin conjugated to fluorescein isothiocyanate (WGA-FITC) combined with propidium iodide (PI) as described by (Haueisen *et al.*, 2017). Microscopy was conducted using a Leica TCS SP5 (Leica Microsystems, Germany) and a Zeiss LSM880 (Carl Zeiss Microscopy, Germany). FITC was excited at 488 nm (argon laser) and detected between 500-540 nm. PI was excited at 561 nm (diode-pumped solid-state laser) and detected between 600-670 nm. Image stacks were obtained with a *x/y* scanning resolution of 1024 x 1024 (Leica) or 1500 x 1500 pixels (Zeiss) and a step size of 0.5 - 1 µm in *z*. Analyses, visualization, and processing of image z-stacks were performed using Leica Application Suite Advanced Fluorescence (Leica Microsystems, Germany), ZEN black and Zen blue (Carl Zeiss Microscopy, Germany), and AMIRA® (FEI™ Visualization Science Group, Germany). Animations of image z-stacks are .avi format and can be played e.g. in VLC media player (available at http://www.videolan.org/vlc/).

Comparative transcriptome analyses of *Zymoseptoria* spp. during early wheat infection

High-quality total RNA from wheat leaves inoculated with *Z. tritici* isolates Zt05, Zt09, Zt10, *Z. pseudotritici* Zp13, and *Z. ardabiliae* Za17 was isolated using the TRIzol™ reagent (Invitrogen, Karlsruhe, Germany) according to the manufacturer's instructions. Material of three wheat leaves was harvested at the same time, pooled, and immediately homogenized in liquid nitrogen. The resulting leaf powder (100 mg) was used for RNA extraction. We collected inoculated leaf material at 10 and 21 dpi and conducted confocal microscopy analyses of central leaf sections (1 - 2 cm) in

order to select samples for RNA-seq. We chose 10 dpi samples as they showed high rates of stomatal penetrations and vital fungal cells.

Preparation of strand-specific RNA-seq libraries including polyA enrichment was performed at the Max Planck Genome Center, Cologne, Germany (http://mpgc.mpipz.mpg.de) using the NEBNext Ultra™ Directional RNA Library Prep Kit for Illumina according to the manufacturer's protocol (New England BioLabs, Frankfurt/Main, Germany) with an input of 1 µg total RNA. Sequencing, performed using an Illumina HiSeq 2500 platform, generated strand-specific, 100-base pair, single-end reads with an average yield of 110 million reads per sample (S1 Table).

Quality of sequencing data was assessed using *FastQC* v0.11.2 (www.bioinformatics.babraham .ac.uk/projects/fastqc/). Residual TruSeq adapter sequences were removed and a stringent read trimming and quality filtering protocol was applied using *FASTX-toolkit* v0.0.14 (http://hannonlab.cshl.edu/fastx_toolkit/) and *Trimmomatic* (Bolger *et al.*, 2014) v0.33 as described in (Haueisen *et al.*, 2017). Trimmed 88-bp reads were mapped against the *de novo* genome assemblies of Zp13 and Za17 with *TopHat2* v2.0.9 (Kim *et al.*, 2013). Read alignments were stored in SAM format, and indexing, sorting, and conversion to BAM format was performed using SAMtools v0.1.19 (Li *et al.*, 2009). Relative abundance of transcripts for predicted genes was calculated in FPKM by *Cuffdiff2* v2.2.1 (Trapnell *et al.*, 2013). Total raw read counts per gene were counted with *HTSeq* v0.6.1p1 using union mode (Anders *et al.*, 2015). Gene coordinates in the Zp13 and Za17 *de novo* genome assemblies were obtained by mapping the previously annotated genes (Grandaubert *et al.*, 2015) using nucleotide BLAST alignments (e-value cutoff $1e^{-5}$). Differential gene expression analyses for 7,309 orthologous genes between *Z. tritici* Zt05, Zt09, Zt10, *Z. pseudotritici* Zp13, and *Z. ardabiliae* Za17 were performed in R (R Core Team, 2017) using the Bioconductor package *DESeq2* v1.10.1 (Love *et al.*, 2014). Differences in gene length between species were taken into account for count data normalization and genes with $P_{adj} \leq 0.01$ and $|\log_2$ fold-change $\geq 2|$ were considered as significantly differentially expressed.

Heatmaps were created using the R package pheatmap (Kolde, 2015). The R package topGO (Alexa *et al.*, 2006) was used to perform Gene Ontology (GO) term enrichment analyses within the differentially expressed genes. *P* values for each GO term (Grandaubert *et al.*, 2015) were calculated using Fischer's exact test applying the topGO algorithm "weight01" that takes into account GO term hierarchy. We reported categories significant with $P \leq 0.01$ for the ontology "Biological Process". PFAM domain enrichment analyses were performed using a custom Python script, and *P* values were calculated using χ^2 tests. We conducted homology analyses for 15 effector candidates by BLASTp searches using protein sequences of the *Z. tritici* reference IPO323 (Goodwin *et al.*, 2011) as input. We reported one hit outside the genus *Zymoseptoria* with an e value < 0.01. A detailed overview of all programs and code used to process and analyze transcriptome data was previously published (Haueisen *et al.*, 2017).

Results and Discussion

Zymoseptoria spp. isolates tolerate different levels of abiotic stressors and show different growth *in vitro*

During host colonization and dispersal, pathogens are exposed to a variety of influences such as temperature dynamics (Bernard *et al.*, 2013), light changes (Yu *et al.*, 2013), or osmotic (Mehrabi *et al.*, 2006) and oxidative stress (O'Brien *et al.*, 2012) and have to adapt to thrive in the environmental conditions of their host niche (Haueisen & Stukenbrock, 2016; van der Does & Rep, 2017). We conducted an *in vitro* stress assay to assess and compare the tolerance towards abiotic stressors (temperature, oxidative, osmotic, and cell wall stress) of *Z. pseudotritici* and *Z. ardabiliae* to *Z. tritici* isolates. Previously, we have shown that *Z. tritici* isolates grow differently *in vitro* and vary in tolerance towards elevated temperatures, oxidative stress, and cell wall-interfering agents (Table 2) (Haueisen *et al.*, 2017). Interestingly, we did not find a similarly high level of intraspecific variation among the tested *Z. pseudotritici* and *Z. ardabiliae* isolates likely reflecting the lower intraspecific genetic variation in both species (Stukenbrock & Dutheil, *in press*; Stukenbrock *et al.*, 2011, 2012a) as compared to the genetically highly diverse *Z. tritici* (Linde *et al.*, 2002; Zhan *et al.*, 2003; McDonald *et al.*, 2016). Isolates *Z. pseudotritici* and *Z. ardabiliae* grew in colonies of yeast-like cells (S1 Figure) and tolerated identical (*Z. pseudotritici*) or similar levels (*Z. ardabiliae*) of abiotic stress (Table 2). However, tolerance levels differed between the three *Zymoseptoria* species; most strikingly in their tolerance towards oxidative and cell wall stress. Only osmotic stress had similar effects on the tested *Zymoseptoria* species. Isolates were mildly to moderately sensitive indicating adaptation to similar solute concentrations in their host environments. While *Z. pseudotritici* isolates were not (2 mM H_2O_2) or only mildly affected (3 mM H_2O_2) by the reactive oxygen species (ROS) H_2O_2, we observed moderate and high sensitivity for *Z. tritici* isolates and drastic reduction of growth for *Z. ardabiliae* isolates (S1 Figure). Plant pathogens are exposed to ROS inside host tissues where it is produced by the plant upon pathogen recognition as an integral part of defense against biotrophic pathogens (Heller & Tudzynski, 2011) and during growth in necrotic plant tissue. As ROS can induce programmed cell death (Zurbriggen *et al.*, 2009) plants depend on strict regulation and containment of ROS to prevent damage of non-infected tissue (Overmyer *et al.*, 2003). Hence, variation in tolerance to oxidative stress in plant pathogens can reflect adaptation to different ROS sources and control in their host plants. Cell wall stress induced by the dyes Congo red and calcoflour white led to strong growth reduction in the *Z. pseudotritici* isolates while the inhibiting effect on *Z. tritici* and *Z. ardabiliae* isolates was weaker. Both dyes interfere with fungal cell wall assembly by inhibiting the connection of chitin to β-glucans, and variation in susceptibility can indicate quantitative differences in cell wall composition (Ram & Klis, 2006). Also, cell shape and size could influence susceptibility to cell wall stress. Microscopy of Zt09, Zp13, and Za17 grown in liquid YMS demonstrated that *in vitro* single cells of the three

Zymoseptoria spp. differ in size and shape. Cells of *Z. pseudotritici* Zp13 are oval and smaller as the cylindrical, multi-septate cells of *Z. tritici* Zt09 and *Z. ardabiliae* Za17 (S2 Fig), as previously shown (Stukenbrock *et al.*, 2012b). Heat stress (28°C) evoked only slightly reduced growth in *Z. pseudotritici* and *Z. ardabiliae*, except for isolate Za48 that was severely impaired at 28°C. However, *Z. pseudotritici* and *Z. ardabiliae* colonies melanized in response to elevated temperatures and heat stress but to a lower degree than *Z. tritici* Zt10. Among several virulence-related functions (Perez-Nadales *et al.*, 2014), melanins associated with the fungal cell wall can facilitate resistance to environmental influences (Butler & Day, 1998). Zt10 was collected in a semi-arid, hot region in Iran (Ilam province, Mehran) while *Z. pseudotritici* and *Z. ardabiliae* isolates originate from the mountainous Ardabil province in North West Iran characterized by cool summers and cold winters (Pauw *et al.*, 2014). Possibly, increased melanization in the Iranian isolates is an adaption to protect against temperature extremes, drought, and intense UV light.

We conducted an *in vitro* growth assay where we measured the cell concentration of liquid cultures by cell counting every ~24 h to compare growth rates of the three species (S3 Fig). Fastest growth was observed for the *Z. tritici* isolates Zt09 ($\bar{r}$ = 0.091) and Zt05 ($\bar{r}$ = 0.069), followed by *Z. pseudotritici* Zp13 ($\bar{r}$ = 0.058) and *Z. ardabiliae* Za17 ($\bar{r}$ = 0.049). The *Z. tritici* isolate Zt10 grew slower ($\bar{r}$ = 0.056) than Zt05 and Zt09 with an average rate similar to Zp13 and Za17. Variation in growth rates could reflect a co-adaptation to different host growth rates and nutrient availability in the host tissue. *Triticum aestivum* is an annual plant and was bred for rapid development and high grain yield (Austin *et al.*, 1980) while the un-cultivated Poaceae species *Dactylis glomerata*, *Lolium perenne*, and *Elymus repens* are perennials that show slower growth and biomass increase (Garnier, 1992). It is possible that overall faster growth rates in *Z. tritici* reflect an adaptation to the relatively rapid growth rate and development of an agricultural host.

Our *in vitro* comparisons revealed phenotypic variation among the three *Zymoseptoria* species but less intraspecies phenotypic variation in *Z. pseudotritici* and *Z. ardabiliae* compared to *Z. tritici*. Together, our findings indicate adaptation to different abiotic influences and host environments and likely reflect the different degrees of intraspecies genetic variation within *Zymoseptoria* spp. populations.

Table 2. Isolates of the three *Zymoseptoria* species vary in tolerance to abiotic stressors.

Species	Isolate	20/22C° at 16-h day/8-h night	28C°	2 mM H_2O_2	3 mM H_2O_2	1 M sorbitol	1 M NaCl	500 µg/mL Congo red	200 µg/mL calcofluor white
Z. tritici	Zt05	-	+	++	+++	+	++	-	-
	Zt09	-	-	-	+	+	++	++	++
	Zt10	++	+++	+	++	+	++	++	+
Z. pseudo-tritici	Zp13	-	+	-	+	+	+	+++	+++
	Zp72	-	+	-	+	+	+	+++	+++
	Zp75	-	+	-	+	+	+	+++	+++
Z. ardabiliae	Za17	-	+	+++	++++	++	++	++	++
	Za48	++	+++	+++	++++	++	++	+++	+++
	Za94	+	++	++	+++	++	++	++	++

Summary of *in vitro* stress assay comparing the tolerance of nine *Zymoseptoria* species isolates to abiotic stressors. Symbols indicate tolerance levels: - isolate was not affected, + isolate was mildly sensitive, ++ isolate was moderately sensitive, +++ isolate was highly sensitive, ++++ isolate did not grow. Results for the three *Z. tritici* isolates have been previously published in (Haueisen *et al.*, 2017).

Z. pseudotritici and *Z. ardabiliae* isolates cannot infect wheat and induce a defense response

We compared virulence of six *Zymoseptoria* spp. isolates (Table 1), including Zp13, Zp72, and Zp75 of *Z. pseudotritici* and Za17, Za48, and Za94 of *Z. ardabiliae*, to virulence levels of previously described *Z. tritici* isolates Zt05, Zt09, and Zt10 (Haueisen *et al.*, 2017) using the highly susceptible winter wheat cultivar Obelisk. To evaluate infections, we estimated the percentage of leaf area affected by necrosis (Fig 1A) and covered with pycnidia (Fig 1B) 28 days post inoculation (dpi). Pycnidia are the asexual fruiting bodies of *Zymoseptoria* species and pycnidia coverage serves as the primal quantitative measure for pathogen fitness and virulence (Stewart & McDonald, 2014). In previously conducted detached leaf assays on wheat, *Z. pseudotritici* and *Z. ardabiliae* produced pycnidia (Stukenbrock *et al.*, 2011), however, in our *in vivo* infection experiments none of the *Z. pseudotritici* and *Z. ardabiliae* isolates caused disease symptoms like necrosis or developed pycnidia on wheat leaves within 28 dpi. The *Z. tritici* isolates were virulent and caused necrosis and developed similar levels of pycnidia as previously described (Fig 1) (Haueisen *et al.*, 2017). On some inoculated and mock-treated leaves, we observed symptoms of senescence like chlorosis and red coloration of the leaf tip. However, we could clearly distinguish senescence from infection-induced necrosis, as observed on the leaves infected with *Z. tritici* isolates (S4 Figure), and conclude that they are not associated with the inoculation of fungal cells.

To compare wheat responses to *Z. pseudotritici* and *Z. ardabiliae* with *Z. tritici* infections, we stained leaves with diaminobenzidine (DAB) at 4, 10, 14, 18, and 21 dpi to visualize the reactive oxygen species (ROS) H_2O_2. ROS is produced during the oxidative burst, a very rapid host response upon pathogen recognition (Wojtaszek, 1997), and plays a central role as signaling molecule in the hypersensitive response, the primal plant defense reaction against incompatible pathogens (Mur *et al.*, 2008; Zurbriggen *et al.*, 2010). As we have previously shown, H_2O_2 accumulated only during late infection of *Z. tritici* following the switch to necrosis (Fig 2, S5 Figure) indicating that activation of wheat immunity is suppressed during biotrophic infection (Haueisen *et al.*, 2017). Inoculation with *Z. pseudotritici* Zp13 and *Z. ardabiliae* Za17 also resulted in the accumulation of ROS (Fig 2). However, compared to *Z. tritici*, ROS was not associated with the appearance of necrosis (S5 Figure) and the staining indicated lower ROS levels that were localized in small speckles, possibly co-localizing with the wheat stomata within green leaf areas (Fig 2B). This indicates that *Z. pseudotritici* and *Z. ardabiliae* isolates are recognized by the wheat immune system (Jones & Dangl, 2006) and ROS is formed as a component of plant defense.

We conclude that wheat is a non-host of *Z. pseudotritici* and *Z. ardabiliae* as both were avirulent (Fig 1) and induced a defense response on wheat leaves (Fig 2). Our findings illustrate that *Z. pseudotritici* and *Z. ardabiliae* species lack the specializations required to suppress immune responses and successfully infect wheat (Haueisen & Stukenbrock, 2016).

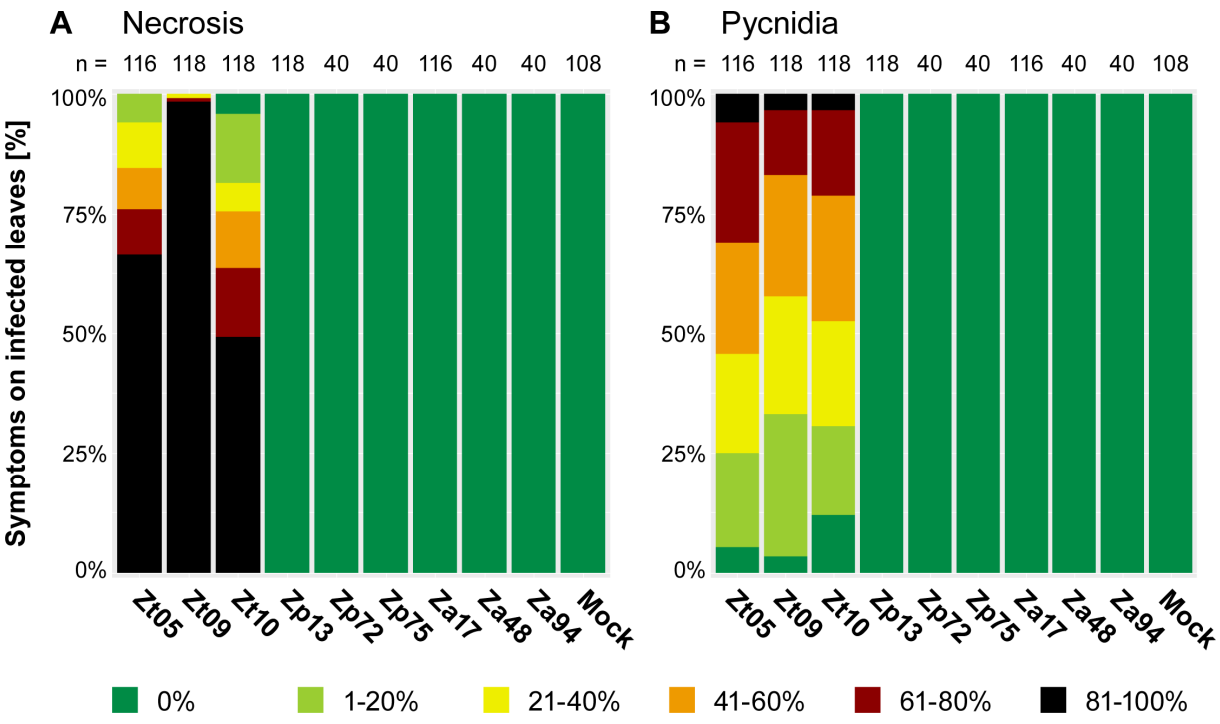

Figure 1. *In planta* phenotypic assay demonstrates similar pycnidia levels of *Z. tritici* isolates and avirulence of the sister species *Z. pseudotritici* and *Z. ardabiliae* on the susceptible wheat cultivar Obelisk. Quantitative differences in necrosis **(A)** and pycnidia

coverage **(B)** of inoculated leaf areas were manually assessed at 28 days post inoculation based on six categories: 0 (without visible symptoms), 1 (1-20 %), 2 (21-40 %), 3 (41-60 %), 4 (61-80 %), 5 (81-100 %). All isolates of *Z. pseudotritici* (Zp13, Zp72, Zp75) and *Z. ardabiliae* (Za17, Za48, Za94) cause no disease symptoms. Results for the three *Z. tritici* isolates have been previously published in (Haueisen *et al.*, 2017).

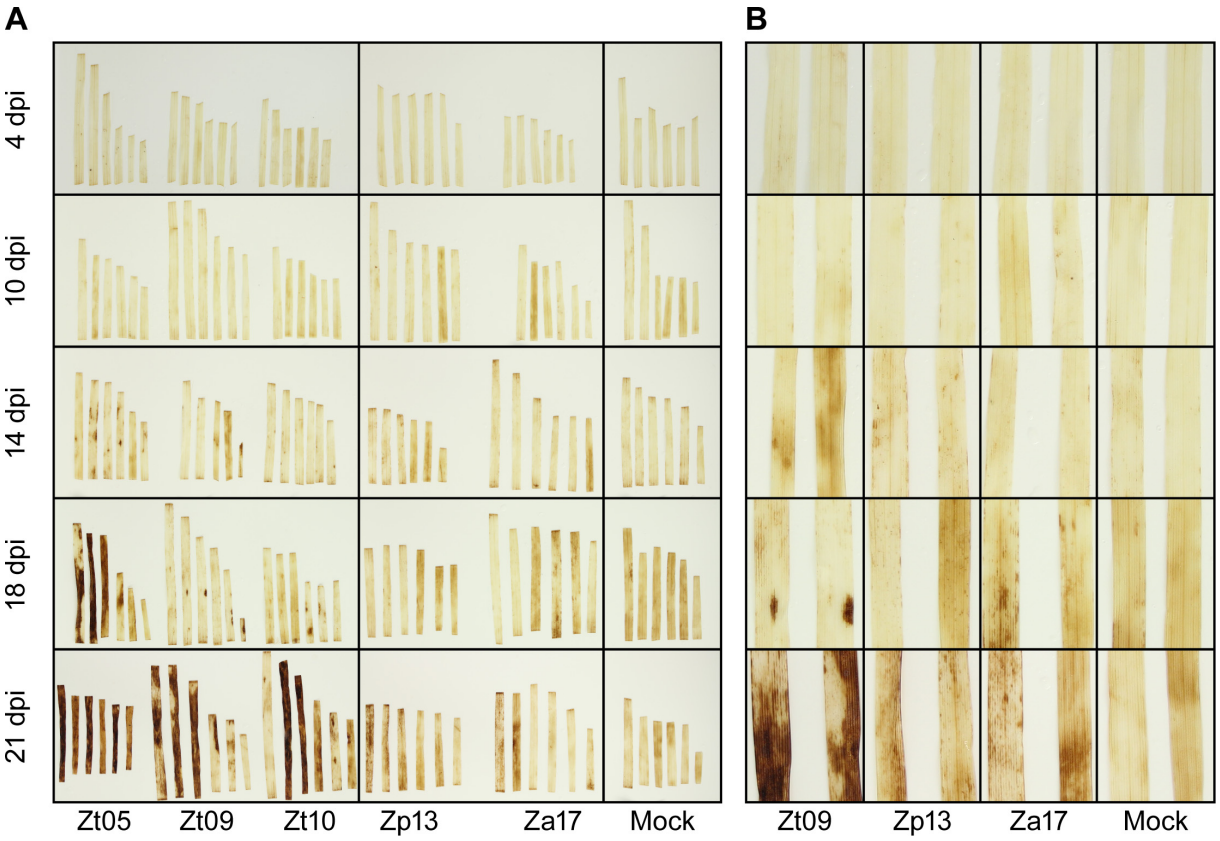

Figure 2. Different host responses in wheat leaves upon infection with *Zymoseptoria* spp. isolates. (A) *Zymoseptoria*-inoculated wheat leaves were stained for accumulation of the reactive oxygen species H_2O_2 at 4, 10, 14, 18 and 21 days post inoculation (dpi) by 3,3'-diaminobenzidine to visualize a putative host response. Dark red-brown precipitate indicates H_2O_2 accumulation and can be indicative of an oxidative burst. **(B)** In leaves infected with *Z. tritici* isolates, ROS appeared first in leaf areas with beginning necrosis and strongly accumulated in fully necrotic parts (Haueisen *et al.*, 2017). ROS staining in leaves inoculated with Zp13 and Za17 was weaker and limited to small, homogeneously distributed spots. Results for the three *Z. tritici* isolates have been previously published in (Haueisen *et al.*, 2017).

Wheat infections of the wild-grass associated *Zymoseptoria* species are blocked early

We next compared incompatible infections of *Z. pseudotritici* and *Z. ardabiliae* to successful *Z. tritici* infections by detailed confocal microscopy analyses of inoculated wheat leaves. Our aim was 1) to investigate how far *Z. pseudotritici* and *Z. ardabiliae* isolates can infect wheat leaves, 2) to assess to what extent plant infection programs of the closely related *Zymoseptoria* species are conserved, and 3) to identify the checkpoint of wheat immunity where avirulent isolates are recognized and blocked. Previously, we have described the core infection program of *Z. tritici* on wheat that consists of four developmental stages (Haueisen *et al.*, 2017). These infection stages served as basis for our comparative analyses of compatible and incompatible *Zymoseptoria* infection development on wheat. To this end, we conducted confocal microscopy analyses and scanned a total of 72 leaves that were harvested at 3, 5, 8, 10, 12, 14, 17, and 21 days after inoculation (dpi) with cells of *Z. tritici* isolates Zt05, Zt09, Zt10; *Z. pseudotritici* isolates Zp13, Zp72, Zp75; and *Z. ardabiliae* isolates Za17, Za48, Za94. We evaluated large z-stacks of longitudinal optical sections to reconstruct spatial and temporal fungal colonization on the leaf surface and in infected tissue.

As previously demonstrated, the three *Z. tritici* isolates exhibit large phenotypic variation in infection development (Haueisen *et al.*, 2017). However, during three weeks (21 dpi) we observed the characteristics of all four core infection stages for the three isolates. During stage A, cells of *Z. tritici* germinated and developed infection hyphae on the wheat leaf surface that penetrated stomata and entered the sub-stomatal cavities (Fig 3A: 5 dpi Zt10). Wheat mesophyll was colonized by *Z. tritici* hyphae (stage B, Fig 3B) and, during stage C, primal structures of the asexual pycnidia developed below stomata simultaneously with the formation of necrotic lesions (Fig 3A: 14 dpi Zt09). Three weeks after inoculation during stage D, mesophyll tissue of *Z. tritici* infected leaves was highly necrotic and fully maturated pycnidia contained pycnidiospores (Fig 3A: 21 dpi Zt05).

As during *Z. tritici* infection stage A, cells of *Z. pseudotritici* and *Z. ardabiliae* isolates germinated on the wheat phylloplane (Fig 3A: 5 dpi Zp72, 3 dpi Za94) and developed infection hyphae that showed directed growth towards stomata (Fig 3A: 5 dpi Zp72, 3 dpi Za94, 21 dpi Zp13; S1 and S2 Animation). As observed for *Z. tritici*, *Z. pseudotritici* and *Z. ardabiliae* infection hyphae penetrated open wheat stomata and grew in close contact to the stomatal guard cells (Fig 3A: 8 dpi Zp75, 10 dpi Za17; S3 and S4 Animation). Infection initiation in many plant pathogens is triggered by host-derived cues like host cell topology (Tucker & Talbot, 2001) or particular chemical signals (Turrà *et al.*, 2015). Previous work reports directed growth of *Z. tritici* germ tubes towards stomata (Duncan & Howard, 2000), the particular signals however, are yet unknown. We reason that these signals are conserved between the host grasses of *Z. pseudotritici* and *Z. ardabiliae* and wheat and induce their infection development on leaves of the incompatible host. Following the stomatal

invasion, further infection of *Z. pseudotritici* and *Z. ardabiliae* isolates were however blocked. Samples collected at 21 dpi showed no additional infection development (Fig 3A: 21 dpi Zp13, 21 dpi Za48). Infection hyphae were either stopped between the guard cells (S5-S7 Animation) or in the sub-stomatal cavities (S8-S10 Animation). Rarely, we observed some growth but hyphae were blocked close to mesophyll cells (S11 and S12 Animation). Hyphae in the sub-stomatal cavities appeared thick and hyphal tips were bulging (S13-S16 Animation), possibly in response to the accumulation of ROS (Fig 2). This shows that recognition and blocking of incompatible *Z. pseudotritici* and *Z. ardabiliae* hyphae takes place at wheat stomata or little further in sub-stomatal cavities.

Detailed studies of incompatible *Z. tritici* infections on *Brachypodium distachyon* (Habig *et al., in prep*; O'Driscoll *et al.*, 2015) and einkorn wheat (Jing *et al.*, 2008) demonstrate that *Zymoseptoria* infection hyphae were blocked at stomatal pores suggesting that stomata and sub-stomatal cavities in general serve as main checkpoints of immunity of grasses towards *Zymoseptoria* species. Pathogen associated molecular pattern (PAMP) triggered stomatal closure plays a pivotal role in plant defense against microbes depending on openings to penetrate host tissue (Grimmer *et al.*, 2012) and associated activation of signaling cascades involved in plant immunity has been demonstrated (Melotto *et al.*, 2006; Desclos-Theveniau *et al.*, 2012). *Z. pseudotritici* and *Z. ardabiliae* possibly lack required host specializations e.g. adapted effectors to counteract recognition and evade wheat PAMP-triggered immunity, as shown in *Phytophthora* species infecting different host plants (Dong *et al.*, 2014).

Although isolates of *Z. pseudotritici* and *Z. ardabiliae* are avirulent on wheat (Fig 1) and induce plant defenses (Fig 2), we observed the same initial infection development as for the virulent *Z. tritici* isolates that is likely triggered by conserved grass-specific signals and corresponds to infection stage A (Fig 3B). However, *Z. pseudotritici* and *Z. ardabiliae* are arrested after stomatal infection in wheat (Fig 3A) indicating the absence of particular host adaptations required to colonize and reproduce in healthy wheat tissue.

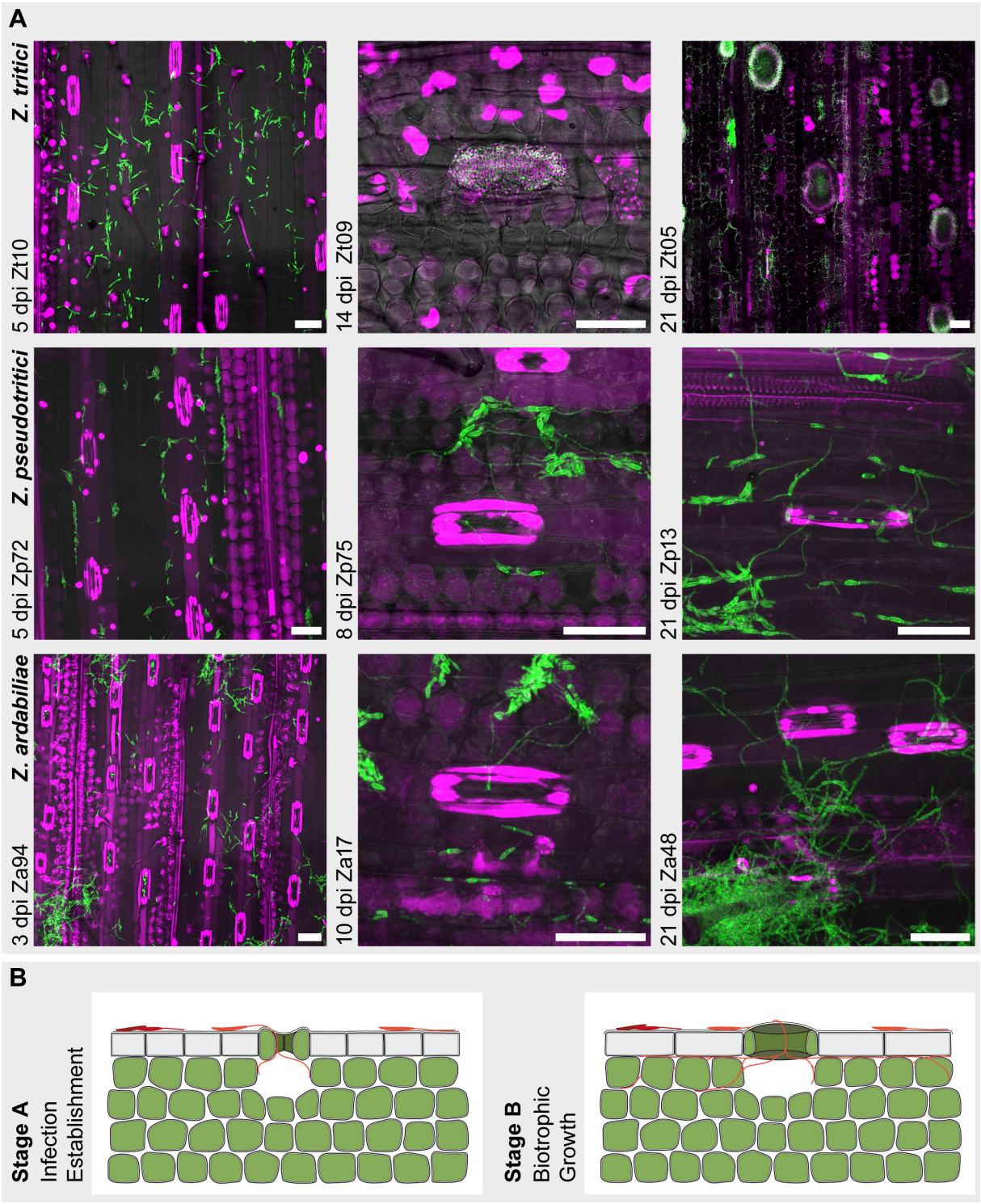

Figure 3. Conserved early infection development of *Zymoseptoria* spp. on wheat but *Z. pseudotritici* and *Z. ardabiliae* infections are blocked at wheat stomata. (A) Micrographs showing infection structures of three *Zymoseptoria* species on wheat. ***Z. tritici*** isolates successfully infect wheat leaves and complete their infection cycle by producing asexual pycnidia. ***Z. pseudotritici*** and ***Z. ardabiliae*** isolates show the same initial infection development as *Z. tritici* but development of infection hyphae is arrested between the wheat guard cells or in sub-stomatal cavities and infections are blocked. Single confocal images (Zt09, Zt05) or maximum projections

of confocal image z-stacks (all others). Nuclei and wheat cells are displayed in *purple*, fungal hyphae and septa in *green*, transmitted image information in *grey*. Scale bars = 50 µm. **(B)** Initial infection stage (Stage A) is conserved but avirulent *Z. pseudotritici* and *Z. ardabiliae* isolates cannot enter biotrophic colonization stage (Stage B) on the wheat host. *Z. tritici* core infection stages have been previously published in (Haueisen *et al.*, 2017).

Zymoseptoria spp. transcriptomes during early wheat infection

We next set out to identify how gene expression profiles in the blocked *Z. pseudotritici* and *Z. ardabiliae* differ from the successfully infecting *Z. tritici*. To this end, we collected leaf material at 10 and 21 days post inoculation with cells of the *Z. pseudotritici* reference Zp13 and the *Z. ardabiliae* reference Za17 (Grandaubert *et al.*, 2015) and applied confocal microscopy to select samples for RNA extraction and transcriptome sequencing as described in (Haueisen *et al.*, 2017). We chose the 10 dpi samples as they showed high rates of Zp13 and Za17 stomatal penetrations (S6 Fig) and generated RNA-seq datasets with two biological replicates per sample. These transcriptomes were compared to the RNA-seq datasets of the *Z. tritici* isolates Zt05, Zt09, and Zt10 corresponding to the core infection stage A (Haueisen *et al.*, 2017) (Table 3, S1 Table). We obtained in total >439 million single-end, strand-specific 100bp reads (between 96.6 and 135.3 million reads per replicate). Reads were quality trimmed and filtered and aligned to the *de novo* genome assemblies of Zp13 (40.2 Mb) (Eschenbrenner et al., *in prep*) and Za17 (39 Mb) (Möller *et al., in prep*) that are based on long-read SMRT Sequencing data. Coordinates for the previously annotated genes in Zp13 and Za17 (Grandaubert *et al.*, 2015) were transposed to the *de novo* genome reference assemblies using nucleotide BLAST (S2 and S3 Table). Between 4% and 6.7% of the reads mapped to the respective genome indicating a similar amount of fungal biomass as for the *Z. tritici* isolates during the infection establishment stage (Table 3). PCA analyses based on the rlog-transformed read counts for the 7,309 genes that are orthologous in the five *Zymoseptoria* spp. isolates (Grandaubert *et al.*, 2015) (S4 Table) positions Zp13 and Za17 close to *Z. tritici* stage A transcriptomes within datasets of all four *Z. tritici* infection stages (S7A Fig). However, Zp13 and Za17 transcriptomes are clearly separate from the *Z. tritici* RNA-seq datasets representing early wheat infection (S7B Fig).

Table 3. Summary of the *Zymoseptoria* spp. transcriptomes representing infection stage A on wheat.

Isolate	Sample	Time point (dpi)	No. of filtered reads	No. of reads mapped to genome	% reads mapped to genome	No. of genes FPKM ≥2*	No. of genes FPKM ≥10*
Zt05	Zt05_Ta_A_01	3	107,507,137	15,213,307	14.15	9,302[1]	7,455[1]
	Zt05_Ta_A_02		81,479,903	10,509,515	12.90		
Zt09	Zt09_Ta_A_01	4	129,342,007	5,868,572	4.54	9,435[2]	7,482[2]
	Zt09_Ta_A_02		92,711,865	5,582,561	6.02		
Zt10	Zt10_Ta_A_01	6	93,557,587	4,895,650	5.23	8,814[3]	7,219[3]
	Zt10_Ta_A_02		91,111,840	4,836,535	5.31		
Zp13	Zp13_Ta_A_01	10	97,337,296	6,563,229	6.74	10,009[4]	8,148[4]
	Zp13_Ta_A_02		91,338,935	5,292,833	5.79		
Za17	Za17_Ta_A_01	10	85,076,032	3,397,144	3.99	9,777[5]	8,128[5]
	Za17_Ta_A_02		114,095,186	6,601,920	5.79		

Overview of RNA-seq datasets including time point of sampling, number of sequenced reads post filtering, number reads mapping to genomes of the isolates, percentage of mapped reads, and numbers of transcribed genes. * FPKM values were calculated using Cuffdiff2 (normalization method: geometric, dispersion method: per-condition). [1] 11,138 genes of IPO323 (94.08%) found by nucleotide blast for Zt05. [2] 11,754 of the 11,839 genes predicted and annotated for IPO323 (Grandaubert *et al.*, 2015); 85 genes located on chromosome 18 were not considered. [3] 10,745 genes of IPO323 (90.76%) found by nucleotide blast for Zt10. [4] 11,040 of the 11,044 genes (99.96%) predicted for Zp13 (Grandaubert *et al.*, 2015) annotated for the *de novo* reference genome assembly. [5] 10,785 of the 10,787 genes (99.98%) predicted for Za17 (Grandaubert *et al.*, 2015) annotated for the *de novo* reference genome assembly. Transcriptomes for the three *Z. tritici* isolates have been previously published in (Haueisen *et al.*, 2017).

Few genes are differentially expressed between compatible and incompatible *Zymoseptoria* spp. wheat interactions

Overall, we found similar expression profiles for orthologous genes during early wheat colonization in the three *Zymoseptoria* species, irrespective of the outcome of the interaction (Fig 4). We identified in total 561 genes to be significantly differentially expressed among all three *Zymoseptoria* species (S8A Fig), and only 476 genes (6.5 % of 7,309 orthologous genes) that are differentially expressed in compatible (*Z. tritici*) versus incompatible (*Z. pseudotritici* and *Z. ardabiliae*) host-pathogen interactions (DESeq2, $P_{adj} \leq 0.01$, $|\log_2$ fold change$| \geq 2$). 86 of the 476 differentially expressed genes (18%) are shared between both *Z. tritici* – incompatible *Zymoseptoria* species comparisons; 62 are specifically up-regulated in *Z. tritici* (S5 Table, S8B Fig) and may play a crucial role in the establishment of the compatible host-pathogen interaction.

We conducted Gene Ontology (GO) group enrichment analyses for the species-specific up-regulated genes (Table 4) and found that genes involved in metabolic processes (GO:0008152), in particular in carbohydrate-reduction (GO:0005975), glycerol (GO:0006071), and L-arabinose (GO:0046373) metabolic processes, are enriched among the genes that are up-regulated in *Z. tritici* compared to the incompatible *Z. pseudotritici* and *Z. ardabiliae* during early host infection. PFAM enrichment analyses indicate that the genes up-regulated during early wheat infection encode proteins with very different functions in the three *Zymoseptoria* species (S6 Table). Up-regulated genes in *Z. tritici* encode proteins e.g. similar to carbohydrate-active enzymes (PF03443; PF05592; PF05637; PF00331), transporters (PF07690; PF02705), chloroperoxidases (PF01328), and proteins involved in lipid metabolism (PF03009; PF00755); while in *Z. pseudotritici* and *Z. ardabiliae* genes encoding ribosomal proteins (PF00253), proteins involved in DNA repair (PF02735; PF03731;PF00505), chromosome condensation (PF00415), and cytoskeleton remodeling (PF06371) were significantly higher expressed. Functional enrichment analyses of the up-regulated genes in *Z. pseudotritici* and *Z. ardabiliae* indicates responses to cell stress and damage e.g. by up-regulating the *KU80* homolog (*Zt09_chr_4_00618*) to repair double-strand DNA breaks or by producing increased amounts of ribosomal proteins (*Zt09_chr_1_01884*), possibly to enhance translation or compensate protein degradation (S7 and S8 Table). In contrast, functional composition of up-regulated genes in *Z. tritici* reflects the fungal metabolism during early wheat infection (S9 Table) that was shown to involve β-oxidation of lipids and the glycoxylate pathway (Rudd *et al.*, 2015). Also, up-regulation of chloroperoxidase-encoding genes was described as an important transcriptional adaptation in *Z. tritici* during stomatal penetration and in the sub-stomatal cavities (Rudd *et al.*, 2015). Hence, our results confirm that chloroperoxidases play an important role during the initial infection of wheat tissue and indicate that the specific up-regulation of four putative chloroperoxidase-encoding genes in the compatible pathogen *Z. tritici* represents a specific adaptation to the wheat host. Together, transcriptomes of the *Z. tritici* isolates show expression profiles typical for successful early wheat infections, while up-regulated genes in the incompatible *Z. pseudotritici* and *Z. ardabiliae* reflect cell stress and damage probably induced by the host defense responses.

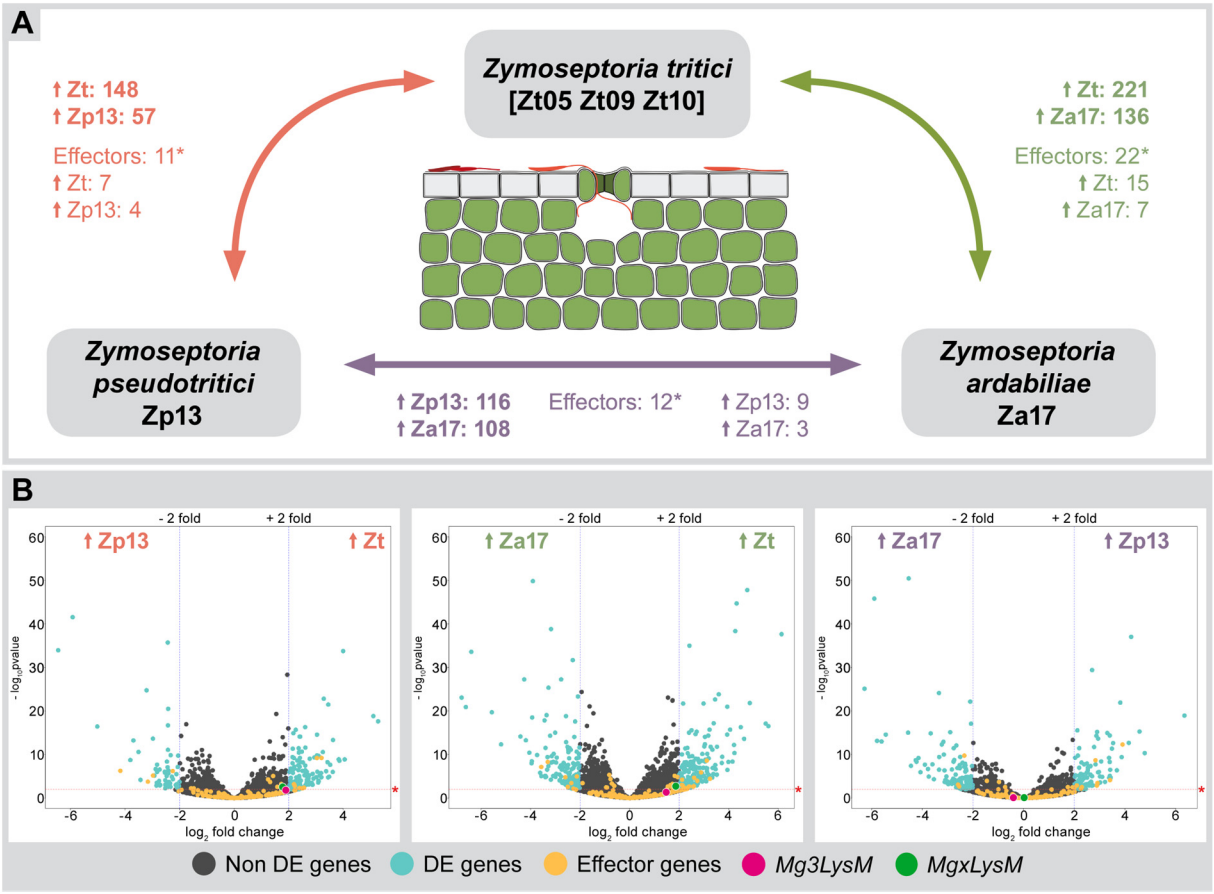

Figure 4. A low number of genes are differentially expressed between *Z. tritici* isolates and *Z. pseudotritici* and *Z. ardabiliae* during early wheat infection. (A) Numbers of significantly differentially expressed genes between the three *Zymoseptoria* species during infection stage A on wheat [orange arrow: between *Z. tritici* isolates (Zt) and *Z. pseudotritici* (Zp13), green arrow: between *Z. tritici* isolates (Zt) and *Z. ardabiliae* (Za17), purple arrow: between *Z. pseudotritici* (Zp13) and *Z. ardabiliae* (Za17)]. Small arrows (↑) with species/isolate name indicate the number of genes specifically up-regulated in this species/isolate. Differential gene expression analyses performed with DESeq2 for 7,309 orthologous genes. Genes were considered to be significantly differentially expressed if $P_{adj} \leq 0.01$ and $|\log_2$ fold change$| \geq 2$. *Indicates significant enrichment of effector candidates among differentially expressed genes (Fischer's exact tests, $P < 0.01$). **(B)** Volcano plots displaying significance ($-\log_{10}P_{adj}$) versus $\log_2$ fold change for the expression of 7,309 orthologous *Zymoseptoria* genes (indicated by dots). Arrows (↑) with species/isolate name specify the comparison and indicate the species/isolate where genes are up-regulated. Red stars (*) and red dashed lines mark threshold for significance ($P_{adj} = 0.01$). Blue dashed lines mark threshold for fold change ($|\log_2$ fold change$| \geq 2$). Non effector genes are indicated by turquois points when considered as significantly differentially expressed (DE). Genes encoding effectors are indicated by orange points and are significantly differentially expressed if $P_{adj} \leq 0.01$ and $|\log_2$ fold change$| \geq 2$. Differences for expression of *Mg3LysM* (pink points) and *MgxLysM* (green points) are shown.

Table 4. Summary of genes that are differentially expressed between the three *Zymoseptoria* species during early wheat infection.

	Genes up-regulated in *Z. pseudotritici*	Genes up-regulated in *Z. ardabiliae*		Genes up-regulated in *Z. tritici*			
Comparison	Zt - ↑ Zp13	Zt - ↑ Za17		↑ Zt - Zp13		↑ Zt - Za17	
DE genes *	57	136		148		221	
	total: 169 shared: 24			total: 307 shared: 62			
GO ** enrichment DE genes	no GO groups enriched	trans-membrane transport (15 genes)	GO:0055085	metabolic process (59 genes)	GO:0008152	trans-membrane transport (22 genes)	GO:0055085
				glycerol metabolic process (3 genes)	GO:0006071	metabolic process (74 genes)	GO:0008152
				L-arabinose metabolic process (2 genes)	GO:0046373	carbo-hydrate-reduction process (14 genes)	GO:0005975
						oxidation-reduction process (22 genes)	GO:0055114
DE candidate effector * genes**	4	7		7		15	
	total: 9 shared: 2			total: 18 shared: 4			
Candidates unknown function	4 (S6 Table)	5 (S6 Table)		5 (S6 Table)		13 (S6 Table)	
Candidates with predicted function #	–	*Zt09_chr_12_00112*	similar to cutinase	*Zt09_chr_4_00039*	similar to eliciting plant response-like protein	*Zt09_chr_6_00626*	similar to metallo-protease
		Zt09_chr_2_00914	similar to metallo-protease	*Zt09_chr_3_00584*	similar to alpha-1	*Zt09_chr_10_00107*	similar to glycoside hydrolase family 12 protein
Shared candidate effectors	*Zt09_chr_1_01386* - hypothetical protein			*Zt09_chr_4_00266* - predicted protein			
	Zt09_chr_1_01747 - hypothetical protein			*Zt09_chr_7_00180* - predicted protein			
				Zt09_chr_7_00299 - predicted protein			
				Zt09_chr_11_00287 - hypothetical protein			

*Genes identified to be differentially expressed between *Z. tritici* and *Z. pseudotritici* and *Z. ardabiliae* during early wheat infection by DESeq2, $P_{adj} \leq 0.01$, $|\log_2$ fold change$| \geq 2$. **Gene Ontology (GO) group enrichment analyses by topGO for ontology "Biological Process", $P \leq 0.01$. ***Effector gene candidates were predicted by (Stukenbrock & Dutheil, *in press*). #Functional annotation by (Grandaubert *et al.*, 2015).

Differentially expressed effector genes include candidates for host specific effectors and avirulence genes

In line with our observations, comparative transcriptomics of the barley powdery mildew pathogen *Blumeria graminis* f. sp. *hordei* during early pathogenesis identified a gene expression program that is conserved among compatible and incompatible infections (Hacquard *et al.*, 2013). However, *B. graminis* genes encoding effectors were in general down-regulated in incompatible host-pathogen interactions 24 h post infection (Hacquard *et al.*, 2013). Effector genes encode small secreted molecules that act in the host-pathogen interaction zone or inside host cells to alter plant physiology and suppress defense responses (Lo Presti *et al.*, 2015). As effectors are known to be of central importance for plant-pathogen interactions and major facilitators of pathogen host specialization (Dong *et al.*, 2014; Poppe *et al.*, 2015; van Dam *et al.*, 2016), we focused our analyses on the candidate effector genes that are differentially expressed between the compatible *Z. tritici* and the incompatible *Z. pseudotritici* and *Z. ardabiliae* (Figure 4B). We hypothesized that effectors involved in specialization to wheat show significantly different expression patterns in *Z. pseudotritici* and *Z. ardabiliae* compared to *Z. tritici*. Among the differentially expressed genes, we identified 15 candidate effectors and respective putative proteins mostly show homology to proteins of other Dothideomycete plant pathogens e.g. *Ramularia collo-cygni*, *Cercospora beticola*, and *Cladosporium fulvum* (Table 5). Next, we further categorized the effector genes based on their expression in the three *Zymoseptoria* species (S9 Fig), and based on functional predictions and expression profiles in the *Z. tritici* isolate Zt09 during the four core wheat infection stages.

The ten genes that are up-regulated in *Z. tritici* encode candidates for effectors required for successful wheat infections. Among them, we propose four as biotrophic and three as necrotrophic effector candidates (Table 5). *Z. tritici* is a hemibiotrophic pathogen and putative biotrophic effectors are higher expressed during biotrophic growth (stages A and B), while necrotrophic effectors are up-regulated during necrotrophic growth (stages C and D). Biotrophic effectors serve to bypass host recognition (van den Burg *et al.*, 2006; de Jonge *et al.*, 2010; Sánchez-Vallet *et al.*, 2013; Wawra *et al.*, 2016), interfere with host signaling (Djamei *et al.*, 2011; Plett *et al.*, 2014), and counteract host defenses (Hemetsberger *et al.*, 2012; Zhang *et al.*, 2012; Mueller *et al.*, 2013; Tanaka *et al.*, 2014). Necrotrophic effectors are involved in host cell death and necrosis, e.g. as non-proteinaceous host-specific toxins (Friesen *et al.*, 2008; Faris *et al.*, 2010) or as small secreted proteins that harm conserved host cell metabolic pathways (Lyu *et al.*, 2016). In a previous study comparing infection stage-specific transcriptomes of three *Z. tritici* isolates with highly differentiated infection phenotypes, we identified candidates for *Z. tritici* core biotrophic and necrotrophic effectors showing the same expression profile in the three isolates (Haueisen *et al.*, 2017). One of the core biotrophic and three of the core necrotrophic effector candidate genes were also identified in this study, demonstrating that comparative transcriptome analyses of compatible and incompatible infections, including multiple isolates of the same species, provide

strong candidates for effectors adapted to a particular host environment. Among the genes up-regulated in the blocked *Z. pseudotritici* and *Z. ardabiliae*, we identified five candidates for avirulence (Avr) genes (Table 5). Avr gene products are recognized by resistant hosts and induce effector-triggered immunity (Jones & Dangl, 2006); what possibly contributes to block wheat infections of *Z. pseudotritici* and Z. *ardabiliae*. Activation of wheat immunity by a compatible pathogen, in this case *Z. tritici* can be evaded e.g. by expression of other effectors and transcriptional silencing or overall low expression of Avr genes. Three of the avirulence candidate genes show strong up-regulation during the necrotrophic infection stages C and D in *Z. tritici* Zt09 (Table 5), and hence also encode putative necrotrophic effectors; possibly with a similar mode of action as ToxA effectors in the wheat pathogens *Pyrenophora tritici-repentis*, *Parastagonospora nodorum,* and *Bipolaris sorokiniana* (Friesen *et al.*, 2008; McDonald *et al.*, 2017). ToxA acts similar as avirulence proteins but "hijacks" the wheat resistance protein Tsn1. Interaction of ToxA and Tsn1 induces necrosis although Tsn1 otherwise confers resistance against biotrophic pathogens (Faris *et al.*, 2010).

The *Z. tritici* LysM effector genes *Mg3LysM* (*Zt09_chr_11_00155*) and *MgxLysM* (*Zt09_chr_8_00412*) were not identified as significantly differentially expressed between the compatible and incompatible *Zymoseptoria* species. LysM proteins are biotrophic effectors that bind chitin and can protect hyphae against host hydrolytic enzymes in order to evade pathogen-associated-molecular-pattern (PAMP) triggered immunity (Marshall *et al.*, 2011). Nevertheless, we found that *Mg3LysM* and *MgxLysM* are higher expressed in *Z. tritici* compared to *Z. pseudotritici* (*Mg3LysM*: 3.7-fold, *MgxLysM*: 3.5-fold; $P_{adj} \leq 0.02$) and *Z. ardabiliae* (*Mg3LysM*: 2.8-fold, *MgxLysM*: 3.6-fold; $P_{adj} \leq 0.055$) (Fig 4B). Between the two incompatible *Zymoseptoria* species, we can almost not detect a difference in the expression of both *LysM* genes (Fig 4B). Hence, transcriptional regulation of *Mg3LysM* and *MgxLysM* in *Z. tritici* might also facilitate adaptation to the wheat host environment.

In summary, a small number of putative effector genes is significantly differentially expressed in compatible and incompatible *Zymoseptoria* species during early wheat infection, however, we could identify ten candidates for host-specific effectors and five putative avirulence genes in the wheat pathogen *Z. tritici*. Host-specific effector candidates are up-regulated in *Z. tritici* and might play important roles for successful wheat infections, while avirulence gene candidates are up-regulated in *Z. pseudotritici* and *Z. ardabiliae* and down-regulated in *Z. tritici* as they possibly trigger wheat immunity during early infection.

Table 5. Up-regulated effector genes are candidates for host-specific effectors and avirulence genes in *Z. tritici.*

Candidate	Gene	Expression*	Functional prediction#	PFAM#	Homology to *Z. tritici* protein sequence	Expression in *Z. tritici* Zt09 (FPKM)**	Putative role in *Z. tritici*
Host-specific effector	*Zt09_chr_4_00266*	↑ Zt vs Zp13 + Za17	predicted protein	-	uncharacterized protein RCC_03304 in *Ramularia collo-cygni*	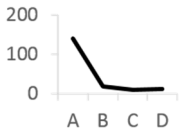	biotrophic effector
	Zt09_chr_7_00180	↑ Zt vs Zp13 + Za17	predicted protein	-	no homology	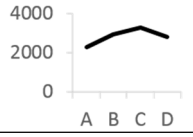	host specific effector
	Zt09_chr_7_00299	↑ Zt vs Zp13 + Za17	hypothetical protein	-	extracellular protein 20-2 in *Cladosporium fulvum*	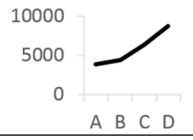	host specific effector
	Zt09_chr_11_00287	↑ Zt vs Zp13 + Za17	hypothetical protein	-	hypothetical protein CB0940_09835 in *Cercospora beticola*	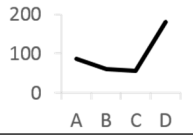	host specific effector
	Zt09_chr_3_00584	↑ Zt vs Zp13	similar to alpha-1	PF00128 PF00534 PF08323	cell wall alpha-1,3-glucan synthase ags1 in *Ramularia collo-cygni*	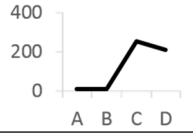	core necrotrophic effector
	Zt09_chr_10_00107	↑ Zt vs Za17	similar to glycoside hydrolase family 12	PF01670	endoglucanase I precursor in *Ramularia collo-cygni*	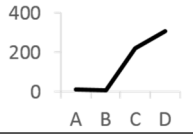	core necrotrophic effector
	Zt09_chr_6_00626	↑ Zt vs Za17	similar to metallo-protease	PF05572	extracellular metalloprotease in *Cercospora beticola*	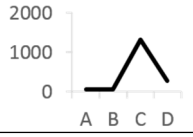	core necrotrophic effector
	Zt09_chr_2_00969	↑ Zt vs Za17	predicted protein	-	uncharacterized protein RCC_09945 in *Ramularia collo-cygni*	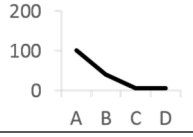	core biotrophic effector
	Zt09_chr_12_00267	↑ Zt vs Za17	predicted protein	-	hypothetical protein CB0940_06044 in *Cercospora beticola*	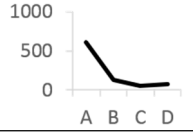	biotrophic effector
	Zt09_chr_6_00044	↑ Zt vs Za17	similar to pathogenesis-related 1 proteins	PF00188	PR-1-like protein in *Aureobasidium namibiae*	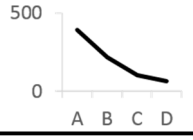	biotrophic effector
Avr gene	*Zt09_chr_7_00558*	↑ Zp13 vs Zt	predicted protein	-	Allergen Ste b 1 in *Cercospora beticola*	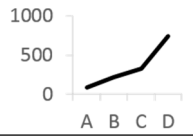	necrotrophic effector

	Zt09_chr_11_00525	↑ Zp13 vs Zt	predicted protein	-	no homology	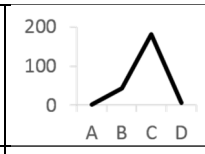	necrotrophic effector
	Zt09_chr_1_01386	↑ Zp13 + ↑ Za17 vs Zt	predicted protein	-	hypothetical protein CB0940_12042 in *Cercospora beticola*	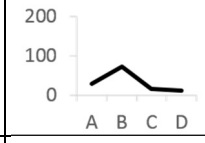	avirulence gene
	Zt09_chr_12_00112	↑ Za17 vs Zt	similar to cutinase	PF01083	cutinase 1 in *Aspergillus lentulus*	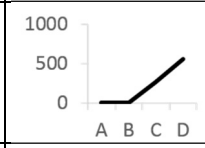	necrotrophic effector
	Zt09_chr_8_00320	↑ Za17 vs Zt	predicted protein	-	amino acid transporter in *Plasmodium ovale*		avirulence gene

Overview of 15 candidate genes for host-specific effectors and avirulence (Avr) genes in the wheat pathogen *Z. tritici*. Names for the orthologous *Zymoseptoria* spp. genes refer to the gene annotation of *Z. tritici*. Homologous proteins were identified by BLASTp; hit outside genus *Zymoseptoria* with e value < 0.01 is reported. *Genes identified to be differentially expressed between *Z. tritici* and *Z. pseudotritici* and *Z. ardabiliae* during early wheat infection by DESeq2, P_{adj} ≤ 0.01, $|\log_2$ fold change$|$ ≥2. Arrows (↑) species/isolate where gene is up-regulated. #Functional annotation and PFAM information by (Grandaubert *et al.*, 2015). **Normalized gene expression values in FPKM calculated with Cuffdiff2 across four wheat infection stages for *Z. tritici* isolate Zt09 (Haueisen *et al.*, 2017).

Conclusions

We conducted a detailed comparison of three closely related *Zymoseptoria* species adapted to different grass hosts in different ecosystems. We found that adaptation to different host niches is already reflected in the *in vitro* growth phenotypes and stress tolerance of *Z. tritici*, *Z. pseudotritici*, and *Z. ardabiliae* isolates. The wheat pathogen *Z. tritici* grows faster and isolates show large phenotypic variation, likely reflecting adaptations to the diversity of wheat growing regions and wheat cultivars. Although isolates of *Z. pseudotritici* and *Z. ardabiliae* have been collected from different wild grass species, they show less phenotypic diversity, probably because of adaptation to their shared geographical origin in North West Iran and local host genotypes.

In contrast to earlier *in vitro* studies, we showed that *Z. pseudotritici* and *Z. ardabiliae* isolates cannot infect wheat *in vivo*. Staining with DAB indicates accumulation of ROS as part of a hypersensitive response of wheat that blocks infectious hyphae between wheat guard cells or in the sub-stomatal cavities. However, initial infection program of adapted and non-adapted *Zymoseptoria* pathogens on wheat is conserved to a large extent. Development of infection

structures and host penetration is highly similar in the three fungi, suggesting that traits involved in host sensing and initial infection development have been conserved during the species divergence and specialization to distinct hosts. Similarly, only 6.5% of the 7,309 orthologous genes are differentially expressed between *Z. tritici* and the blocked *Z. pseudotritici* and *Z. ardabiliae,* indicating that the host environment during early wheat infection is similar to the native grass hosts of *Z. pseudotritici* and *Z. ardabiliae* and to the host of their shared common ancestor. However, significantly up-regulated genes in *Z. tritici* are characteristic for early wheat infection and involved in metabolic re-programming and the production of enzymes important for degradation of putatively toxic compounds (Rudd *et al.*, 2015). Moreover, host-specific effector candidate genes identified here overlap with previously described candidates for core effectors in *Z. tritici* (Haueisen *et al.*, 2017) strongly indicating an important role in facilitating adaptation to wheat. In conclusion, we demonstrate that our novel approach of comparing incompatible and compatible infections of closely related pathogens can be applied to identify conserved and species-specific traits and we further provide promising candidates for host-specific effectors and avirulence factors in the wheat pathogen *Z. tritici*. The results of our comparative analyses strongly suggest that only few key traits are involved in facilitating host specialization and in determining host specificity of the three closely related *Zymoseptoria* species.

Acknowledgement

We thank Christoph Eschenbrenner for transposing gene annotations, Jonathan Grandaubert for providing access to datasets, Julien Y. Dutheil for support with comparative transcriptome analyses and Petra Happel for help with the *in vitro* stress assays.

Funding statement

This work was supported by intramural funding of the Max Planck Society and a personal grant from the State of Schleswig-Holstein to Eva H. Stukenbrock. The funders had no role in study design, data collection and analyses, decision to publish, or preparation of the manuscript.

References

Aguileta G, Lengelle J, Chiapello H, Giraud T, Viaud M, Fournier E, Rodolphe F, Marthey S, Ducasse A, Gendrault A, *et al.* 2012. Genes under positive selection in a model plant pathogenic fungus, Botrytis. *Infection, Genetics and Evolution* **12**: 987–996.

Alexa A, Rahnenführer J, Lengauer T. **2006**. Improved scoring of functional groups from gene expression data by decorrelating GO graph structure. *Bioinformatics* **22**: 1600–1607.

Amselem J, Cuomo CA, van Kan JAL, Viaud M, Benito EP, Couloux A, Coutinho PM, de Vries RP, Dyer PS, Fillinger S, *et al.* 2011. Genomic analysis of the necrotrophic fungal pathogens sclerotinia sclerotiorum and botrytis cinerea. *PLoS Genetics* **7**.

Anders S, Pyl PT, Huber W. **2015**. HTSeq—a Python framework to work with high-throughput sequencing data. *Bioinformatics* **31**: 166–169.

Austin RB, Bingham J, Blackwell RD, Evans LT, Ford MA, Morgan CL, Taylor M. **1980**. Genetic improvements in winter wheat yields since 1900 and associated physiological changes. *The Journal of Agricultural Science* **94**: 675.

Banke S, McDonald BA. **2005**. Migration patterns among global populations of the pathogenic fungus Mycosphaerella graminicola. *Molecular ecology* **14**: 1881–96.

Bernard F, Sache I, Suffert F, Chelle M. **2013**. The development of a foliar fungal pathogen does react to leaf temperature! *The New phytologist*.

Bolger AM, Lohse M, Usadel B. **2014**. Trimmomatic: A flexible trimmer for Illumina sequence data. *Bioinformatics* **30**: 2114–2120.

Brunner PC, Torriani SFF, Croll D, Stukenbrock EH, McDonald BA. **2013**. Coevolution and life cycle specialization of plant cell wall degrading enzymes in a hemibiotrophic pathogen. *Molecular biology and evolution* **30**: 1337–47.

van den Burg H a, Harrison SJ, Joosten MHAJ, Vervoort J, de Wit PJGM. **2006**. Cladosporium fulvum Avr4 protects fungal cell walls against hydrolysis by plant chitinases accumulating during infection. *Molecular plant-microbe interactions : MPMI* **19**: 1420–1430.

Butler MJ, Day AW. **1998**. Fungal melanins: a review. *Canadian Journal of Microbiology* **44**: 1115–1136.

van Dam P, Fokkens L, Schmidt SM, Linmans JHJ, Corby Kistler H, Ma LJ, Rep M. **2016**. Effector profiles distinguish formae speciales of Fusarium oxysporum. *Environmental Microbiology* **18**: 4087–4102.

Desclos-Theveniau M, Arnaud D, Huang TY, Lin GJC, Chen WY, Lin YC, Zimmerli L. **2012**. The Arabidopsis lectin receptor kinase LecRK-V.5 represses stomatal immunity induced by Pseudomonas syringae pv. tomato DC3000. *PLoS Pathogens* **8**.

Djamei A, Schipper K, Rabe F, Ghosh A, Vincon V, Kahnt J, Osorio S, Tohge T, Fernie AR, Feussner I, *et al.* 2011. Metabolic priming by a secreted fungal effector. *Nature* **478**: 395–398.

van der Does HC, Rep M. **2017**. Adaptation to the Host Environment by Plant-Pathogenic Fungi. *Annual Review of Phytopathology* **55**: 427–450.

Dong S, Stam R, Cano LM, Song J, Sklenar J, Yoshida K, Bozkurt TO, Oliva R, Liu Z, Tian M, *et al.* 2014. Effector Specialization in a Lineage of the Irish Potato Famine Pathogen. *Science* **343**: 552–555.

Duncan KE, Howard RJ. **2000**. Cytological analysis of wheat infection by the leaf blotch pathogen Mycosphaerella graminicola. *Mycological Research* **104**: 1074–1082.

Eyal Z, Scharen A, Huffman M, Prescott J. **1985**. Global insights into virulence frequencies of Mycosphaerella graminicola. *Phytopathology* **75**: 1456–1462.

Faris JD, Zhang Z, Lu H, Lu S, Reddy L, Cloutier S, Fellers JP, Meinhardt SW, Rasmussen JB, Xu SS, *et al.* 2010. A unique wheat disease resistance-like gene governs effector-triggered susceptibility to necrotrophic pathogens. *Proceedings of the National Academy of Sciences* **107**: 13544–13549.

Friesen TL, Faris JD, Solomon PS, Oliver RP. **2008**. Host-specific toxins: effectors of necrotrophic pathogenicity. *Cellular microbiology* **10**: 1421–1428.

Garnier E. **1992**. Growth Analysis of Congeneric Annual and Perennial Grass Species. *Journal of Ecology* **80**: 665–675.

Goodwin SB, M'barek S Ben, Dhillon B, Wittenberg AHJ, Crane CF, Hane JK, Foster AJ, Van der Lee T a J, Grimwood J, Aerts A, *et al.* 2011. Finished genome of the fungal wheat pathogen Mycosphaerella graminicola reveals dispensome structure, chromosome plasticity, and stealth pathogenesis. *PLoS genetics* **7**: e1002070.

Grandaubert J, Bhattacharyya A, Stukenbrock EH. **2015**. RNA-seq Based Gene Annotation and Comparative Genomics of Four Fungal Grass Pathogens in the Genus Zymoseptoria Identify Novel Orphan Genes and Species-Specific Invasions of Transposable Elements. *G3 (Bethesda, Md.)* **5**: g3.115.017731-.

Grandaubert J, Dutheil JY, Stukenbrock EH. **2017**. The genomic rate of adaptation in the fungal wheat pathogen Zymoseptoria tritici. *bioRxiv.* doi: 10.1101/176727.

Grimmer M, John Foulkes M, Paveley N. **2012**. Foliar pathogenesis and plant water relations: a review. *Journal of Experimental Botany* **63**: 4321–4331.

Habig M, Garrido S, Haueisen J, Barkmann F, Stukenbrock EH. Transcription factor Zt107320 affects growth and virulence of the fungal wheat pathogen Zymoseptoria tritici. *in preparation*.

Hacquard S, Kracher B, Maekawa T, Vernaldi S, Schulze-Lefert P, Ver Loren van Themaat E. **2013**. Mosaic genome structure of the barley powdery mildew pathogen and conservation of transcriptional programs in divergent hosts. *Proceedings of the National Academy of Sciences of the United States of America* **110**: E2219-28.

Haueisen J, Möller M, Eschenbrenner CJ, Grandaubert J, Seybold H, Adamiak H, Stukenbrock EH. **2017**. Extremely flexible infection programs in a fungal plant pathogen. *bioRxiv*. doi: 10.1101/229997

Haueisen J, Stukenbrock EH. **2016**. Life cycle specialization of filamentous pathogens - colonization and reproduction in plant tissues. *Current Opinion in Microbiology* **32**: 31–37.

Heller J, Tudzynski P. **2011**. Reactive Oxygen Species in Phytopathogenic Fungi: Signaling, Development, and Disease. *Annual Review of Phytopathology, Vol 49* **49**: 369–390.

Hemetsberger C, Herrberger C, Zechmann B, Hillmer M, Doehlemann G. **2012**. The Ustilago maydis effector Pep1 suppresses plant immunity by inhibition of host peroxidase activity. *PLoS Pathogens* **8**.

Inoue Y, Vy TTP, Yoshida K, Asano H, Mitsuoka C, Asuke S, Anh VL, Cumagun CJR, Chuma I, Terauchi R, *et al.* 2017. Evolution of the wheat blast fungus through functional losses in a host specificity determinant. *Science* **357**: 80–83.

Jing HC, Lovell D, Gutteridge R, Jenk D, Kornyukhin D, Mitrofanova OP, Kema GHJ, Hammond-Kosack KE. **2008**. Phenotypic and genetic analysis of the Triticum monococcum-Mycosphaerella graminicola interaction. *New Phytologist* **179**: 1121–1132.

Jones JDG, Dangl JL. **2006**. The plant immune system. *Nature* **444**: 323–9.

de Jonge R, Peter van Esse H, Kombrink A, Shinya T, Desaki Y, Bours R, van der Krol S, Shibuya N, Joosten MH a J, Thomma BPHJ. **2010**. Conserved Fungal LysM Effector Ecp6 Prevents Chitin-Triggered Immunity in Plants. *Science* **329**: 953–955.

Kawahara Y, Oono Y, Kanamori H, Matsumoto T, Itoh T, Minami E. **2012**. Simultaneous RNA-Seq Analysis of a Mixed Transcriptome of Rice and Blast Fungus Interaction. *PLoS ONE* **7**: e49423.

Kellner R, Bhattacharyya A, Poppe S, Hsu TY, Brem RB, Stukenbrock EH. **2014**. Expression Profiling of the Wheat Pathogen Zymoseptoria tritici Reveals Genomic Patterns of Transcription and Host-Specific Regulatory Programs. *Genome biology and evolution* **6**: 1353–65.

Kim D, Pertea G, Trapnell C, Pimentel H, Kelley R, Salzberg SL. **2013**. TopHat2: accurate alignment of transcriptomes in the presence of insertions, deletions and gene fusions. *Genome biology* **14**: R36.

Kolde R. **2015**. Pretty heatmaps. *R Package 'pheatmap'*: 1–7.

Li H, Handsaker B, Wysoker A, Fennell T, Ruan J, Homer N, Marth G, Abecasis G, Durbin R. **2009**. The Sequence Alignment/Map format and SAMtools. *Bioinformatics* **25**: 2078–2079.

Linde CC, Zhan J, McDonald BA. **2002**. Population Structure of Mycosphaerella graminicola: From Lesions to Continents. *Phytopathology* **92**: 946–55.

Love MI, Huber W, Anders S. **2014**. Moderated estimation of fold change and dispersion for RNA-seq data with DESeq2. *Genome Biology* **15**: 550.

Lyu X, Shen C, Fu Y, Xie J, Jiang D, Li G, Cheng J. **2016**. A Small Secreted Virulence-Related Protein Is Essential for the Necrotrophic Interactions of Sclerotinia sclerotiorum with Its Host Plants. *PLOS Pathogens* **12**: e1005435.

Marshall R, Kombrink A, Motteram J, Loza-Reyes E, Lucas J, Hammond-Kosack KE, Thomma BPHJ, Rudd JJ. **2011**. Analysis of two in planta expressed LysM effector homologs from the fungus Mycosphaerella graminicola reveals novel functional properties and varying contributions to virulence on wheat. *Plant physiology* **156**: 756–69.

McDonald MC, Ahren D, Simpfendorfer S, Milgate A, Solomon PS. **2017**. The discovery of the virulence gene *ToxA* in the wheat and barley pathogen *Bipolaris sorokiniana*. *Molecular Plant Pathology*: 1–8.

McDonald MC, McGinness L, Hane JK, Williams AH, Milgate A, Solomon PS. **2016**. Utilizing Gene Tree Variation to Identify Candidate Effector Genes in Zymoseptoria tritici. *G3 (Bethesda, Md.)* **6**: 779–91.

McMullan M, Gardiner A, Bailey K, Kemen E, Ward BJ, Cevik V, Robert-Seilaniantz A, Schultz-Larsen T, Balmuth A, Holub E, *et al.* 2015. Evidence for suppression of immunity as a driver for genomic introgressions and host range expansion in races of Albugo candida, a generalist parasite. *eLife* **4**: 1–24.

Mehrabi R, Zwiers L-H, de Waard M a, Kema GHJ. **2006**. MgHog1 regulates dimorphism and pathogenicity in the fungal wheat pathogen Mycosphaerella graminicola. *Molecular plant-microbe interactions : MPMI* **19**: 1262–9.

Melotto M, Underwood W, Koczan J, Nomura K, He SY. **2006**. Plant Stomata Function in Innate Immunity against Bacterial Invasion. *Cell* **126**: 969–980.

Menardo F, Praz C, Wyder S, Bourras S. A, McNally KE, Parlange F, Riba A, Roffler S, Schaefer L, Shimizu KK, *et al.* 2016. Hybridization of powdery mildew strains gives raise to pathogens on novel agricultural crop species. *Nature genetics* **48**: 1–24.

Möller M, Habig M, Freitag M, Stukenbrock EH. Extraordinary instability of whole chromosomes and widespread genome rearrangements during vegetative growth. *in preparation*.

Mueller AN, Ziemann S, Treitschke S, Aßmann D, Doehlemann G. **2013**. Compatibility in the Ustilago maydis–Maize Interaction Requires Inhibition of Host Cysteine Proteases by the Fungal Effector Pit2. *PLoS Pathogens* **9**: e1003177.

Mur LAJ, Kenton P, Lloyd AJ, Ougham H, Prats E. **2008**. The hypersensitive response; The centenary is upon us but how much do we know? *Journal of Experimental Botany* **59**: 501–520.

O'Brien JA, Daudi A, Butt VS, Bolwell GP. **2012**. Reactive oxygen species and their role in plant defence and cell wall metabolism. *Planta* **236**: 765–779.

O'Driscoll A, Doohan F, Mullins E. **2015**. Exploring the utility of Brachypodium distachyon as a model pathosystem for the wheat pathogen Zymoseptoria tritici. *BMC research notes* **8**: 132.

O'Driscoll A, Kildea S, Doohan F, Spink J, Mullins E. **2014**. The wheat-Septoria conflict: a new front opening up? *Trends in plant science* **19**: 602–10.

Overmyer K, Brosché M, Kangasjärvi J. **2003**. Reactive oxygen species and hormonal control of cell death. *Trends in Plant Science* **8**: 335–342.

Pauw E De, Ghaffari A, Ghasemi V. **2014**. *Agroclimatic zones map of Iran*.

Perez-Nadales E, Almeida Nogueira MF, Baldin C, Castanheira S, El Ghalid M, Grund E, Lengeler K, Marchegiani E, Mehrotra PV, Moretti M, *et al.* 2014. Fungal model systems and the elucidation of pathogenicity determinants. *Fungal Genetics and Biology* **70**: 42–67.

Plett JM, Daguerre Y, Wittulsky S, Vayssieres A, Deveau A, Melton SJ, Kohler A, Morrell-Falvey JL, Brun A, Veneault-Fourrey C, *et al.* 2014. Effector MiSSP7 of the mutualistic fungus Laccaria bicolor stabilizes the Populus JAZ6 protein and represses jasmonic acid (JA) responsive genes. *Proceedings of the National Academy of Sciences* **111**: 8299–8304.

Ponomarenko A, Goodwin SB, Kema GHJ. **2011**. Septoria tritici blotch (STB) of wheat. *Plant Health Instructor*: 1–7.

Poppe S, Dorsheimer L, Happel P, Stukenbrock EH. **2015**. Rapidly Evolving Genes Are Key Players in Host Specialization and Virulence of the Fungal Wheat Pathogen Zymoseptoria tritici (Mycosphaerella graminicola). *PLOS Pathogens* **11**: e1005055.

Lo Presti L, Lanver D, Schweizer G, Tanaka S, Liang L, Tollot M, Zuccaro A, Reissmann S, Kahmann R. **2015**. Fungal Effectors and Plant Susceptibility. *Annual review of plant biology* **66**: 513–545.

R Core Team. **2017**. R: A Language and Environment for Statistical Computing.

Ram A, Klis F. **2006**. Identification of fungal cell wall mutants using susceptibility assays based on Calcofluor white and Congo red. *Nature protocols* **1**: 2253–2256.

Rudd JJ, Kanyuka K, Hassani-Pak K, Derbyshire M, Andongabo A, Devonshire J, Lysenko A, Saqi M, Desai NM, Powers SJ, *et al.* 2015. Transcriptome and Metabolite Profiling of the Infection Cycle of Zymoseptoria tritici on Wheat Reveals a Biphasic Interaction with Plant Immunity Involving Differential Pathogen Chromosomal Contributions and a Variation on the Hemibiotrophic Lifestyle Def. *Plant Physiology* **167**: 1158–1185.

Sánchez-Vallet A, Saleem-Batcha R, Kombrink A, Hansen G, Valkenburg DJ, Thomma BPHJ, Mesters JR. **2013**. Fungal effector Ecp6 outcompetes host immune receptor for chitin binding through intrachain LysM dimerization. *eLife* **2013**: 1–16.

Sprouffske K, Wagner A. **2016**. Growthcurver: an R package for obtaining interpretable metrics from microbial growth curves. *BMC Bioinformatics* **17**: 172.

Stewart EL, McDonald BA. **2014**. Measuring quantitative virulence in the wheat pathogen Zymoseptoria tritici using high-throughput automated image analysis. *Phytopathology* **104**: 985–92.

Stukenbrock EH, Banke S, Javan-Nikkhah M, McDonald BA. **2007**. Origin and domestication of the fungal wheat pathogen Mycosphaerella graminicola via sympatric speciation. *Molecular biology and evolution* **24**: 398–411.

Stukenbrock EH, Bataillon T, Dutheil JY, Hansen TT, Li R, Zala M, McDonald BA, Wang J, Schierup MH. **2011**. The making of a new pathogen: insights from comparative population genomics of the domesticated wheat pathogen Mycosphaerella graminicola and its wild sister species. *Genome research* **21**: 2157–66.

Stukenbrock EH, Christiansen FB, Hansen TT, Dutheil JY, Schierup MH. **2012a**. Fusion of two divergent fungal individuals led to the recent emergence of a unique widespread pathogen species. *Proceedings of the National Academy of Sciences of the United States of America* **109**: 1–6.

Stukenbrock E, Dutheil JY. ***In press.*** Comparison of fine-scale recombination maps in fungal plant pathogens reveals dynamic recombination landscapes and intragenic hotspots. *Genetics*.

Stukenbrock EH, Quaedvlieg W, Javan-Nikhah M, Zala M, Crous PW, McDonald BA. **2012b**. Zymoseptoria ardabiliae and Z. pseudotritici, two progenitor species of the septoria tritici leaf blotch fungus Z. tritici (synonym: Mycosphaerella graminicola). *Mycologia* **104**: 1397–407.

Tanaka S, Brefort T, Neidig N, Djamei A, Kahnt J, Vermerris W, Koenig S, Feussner K, Feussner I, Kahmann R. **2014**. A secreted *Ustilago maydis* effector promotes virulence by targeting anthocyanin biosynthesis in maize. *eLife* **3**: 1–27.

Thatcher LF, Williams AH, Garg G, Buck S-AG, Singh KB. **2016**. Transcriptome analysis of the fungal pathogen Fusarium oxysporum f. sp. medicaginis during colonisation of resistant and susceptible Medicago truncatula hosts identifies differential pathogenicity profiles and novel candidate effectors. *BMC Genomics* **17**: 860.

Thordal-Christensen H, Zhang Z, Wei Y, Collinge DB. **1997**. Subcellular localization of H2O2 in plants. H2O2 accumulation in papillae and hypersensitive response during the barley-powdery mildew interaction. *Plant Journal* **11**: 1187–1194.

Trapnell C, Hendrickson DG, Sauvageau M, Goff L, Rinn JL, Pachter L. **2013**. Differential analysis of gene regulation at transcript resolution with RNA-seq. *Nature biotechnology* **31**: 46–53.

Tucker SL, Talbot NJ. **2001**. Surface attachment and pre-penetration stage development by plant pathogenic fungi. *Annual Review of Phytopathology* **39**: 385–417.

Turrà D, El Ghalid M, Rossi F, Di Pietro A. **2015**. Fungal pathogen uses sex pheromone receptor for chemotropic sensing of host plant signals. *Nature* **527**: 521–524.

Wawra S, Fesel P, Widmer H, Timm M, Seibel J, Leson L, Kesseler L, Nostadt R, Hilbert M, Langen G, *et al.* 2016. The fungal-specific β-glucan-binding lectin FGB1 alters cell-wall composition and suppresses glucan-triggered immunity in plants. *Nature communications* **7**: 13188.

Wojtaszek P. **1997**. Oxidative burst: an early plant response to pathogen infection. *The Biochemical journal* **322**: 681–692.

Yu SM, Ramkumar G, Lee YH. **2013**. Light quality influences the virulence and physiological responses of Colletotrichum acutatum causing anthracnose in pepper plants. *Journal of Applied Microbiology* **115**: 509–516.

Zhan J, Pettway RE, McDonald BA. **2003**. The global genetic structure of the wheat pathogen Mycosphaerella graminicola is characterized by high nuclear diversity, low mitochondrial diversity, regular recombination, and gene flow. *Fungal Genetics and Biology* **38**: 286–297.

Zhang WJ, Pedersen C, Kwaaitaal M, Gregersen PL, Mørch SM, Hanisch S, Kristensen A, Fuglsang AT, Collinge DB, Thordal-Christensen H. **2012**. Interaction of barley powdery mildew effector candidate CSEP0055 with the defence protein PR17c. *Molecular Plant Pathology* **13**: 1110–1119.

Zurbriggen MD, Carrillo N, Hajirezaei M-R. **2010**. ROS signaling in the hypersensitive response. *Plant Signaling & Behavior* **5**: 393–396.

Zurbriggen MD, Carrillo N, Tognetti VB, Melzer M, Peisker M, Hause B, Hajirezaei MR. **2009**. Chloroplast-generated reactive oxygen species play a major role in localized cell death during the non-host interaction between tobacco and Xanthomonas campestris pv. vesicatoria. *Plant Journal* **60**: 962–973.

Supplementary Information

Supplementary Tables

All supplementary tables are in .xlsx or .gff file format and are deposited on the supplementary USB key.

S1 Table. Detailed overview of *Zymoseptoria* spp. transcriptomes used in this study.

S2 Table. Gene annotation for the *Z. pseudotritici* reference isolate Zp13.

Gene annotation in .gff file format for the Zp13 *de novo* genome assembly based long-read SMRT Sequencing data (Eschenbrenner *et al*., *in prep*).

S3 Table. Gene annotation for the *Z. ardabiliae* reference isolate Za17.

Gene annotation in .gff file format for the Za17 *de novo* genome assembly based long-read SMRT Sequencing data (Möller *et al*., *in prep*).

Table S4. *Zymoseptoria* spp. orthologous genes and effector candidates.

List of 7,309 genes and 147 effector gene candidates that are orthologous in the *Z. tritici* isolates Zt05, Zt09, and Zt10, *Z. pseudotritici* Zp13, and *Z. ardabiliae* Za17. Homology analyses and gene names based on (Grandaubert *et al.*, 2015). Prediction of effector gene candidates by (Stukenbrock & Dutheil, *in press*).

Table S5. List of the 62 shared genes that are up-regulated in *Z. tritici* compared to *Z. pseudotritici* and *Z. ardabiliae*.

List includes names of genes identified to be up-regulated in *Z. tritici* compared to *Z. pseudotritici* Zp13 as well as compared to *Z. ardabiliae* Za17 ("shared"), functional annotation information, and normalized expression values (FPKM) for the *Z. tritici* isolate Zt09 (Haueisen *et al.*, 2017) during wheat infection stages and axenic growth in liquid YMS medium.

Table S6. Summary and analysis of genes that are differentially expressed between the three *Zymoseptoria* species during early wheat infection.

Numbers of differentially expressed genes for the different *Zymoseptoria* species comparison including differentially expressed effector candidate genes, and results for GO and PFAM enrichment analyses. Functional annotation, PFAM, and GO term information from (Grandaubert *et al.*, 2015).

Table S7. List of 57 genes that are up-regulated in *Z. pseudotritici* Zp13 compared to *Z. tritici*.

List includes gene names, functional annotation information, and normalized expression values (FPKM) for the *Z. tritici* isolate Zt09 (Haueisen *et al.*, 2017) during wheat infection stages and axenic growth in liquid YMS medium.

Table S8. List of 136 genes that are up-regulated in *Z. ardabiliae* Za17 compared to *Z. tritici*.

List includes gene names, functional annotation information, and normalized expression values (FPKM) for the *Z. tritici* isolate Zt09 (Haueisen *et al.*, 2017) during wheat infection stages and axenic growth in liquid YMS medium.

Table S9. List of 308 genes that are up-regulated in *Z. tritici* compared to *Z. pseudotritici* Zp13 and *Z. ardabiliae* Za17.

List includes gene names, functional annotation information, and normalized expression values (FPKM) for the *Z. tritici* isolate Zt09 (Haueisen *et al.*, 2017) during wheat infection stages and axenic growth in liquid YMS medium.

Supplementary Figures

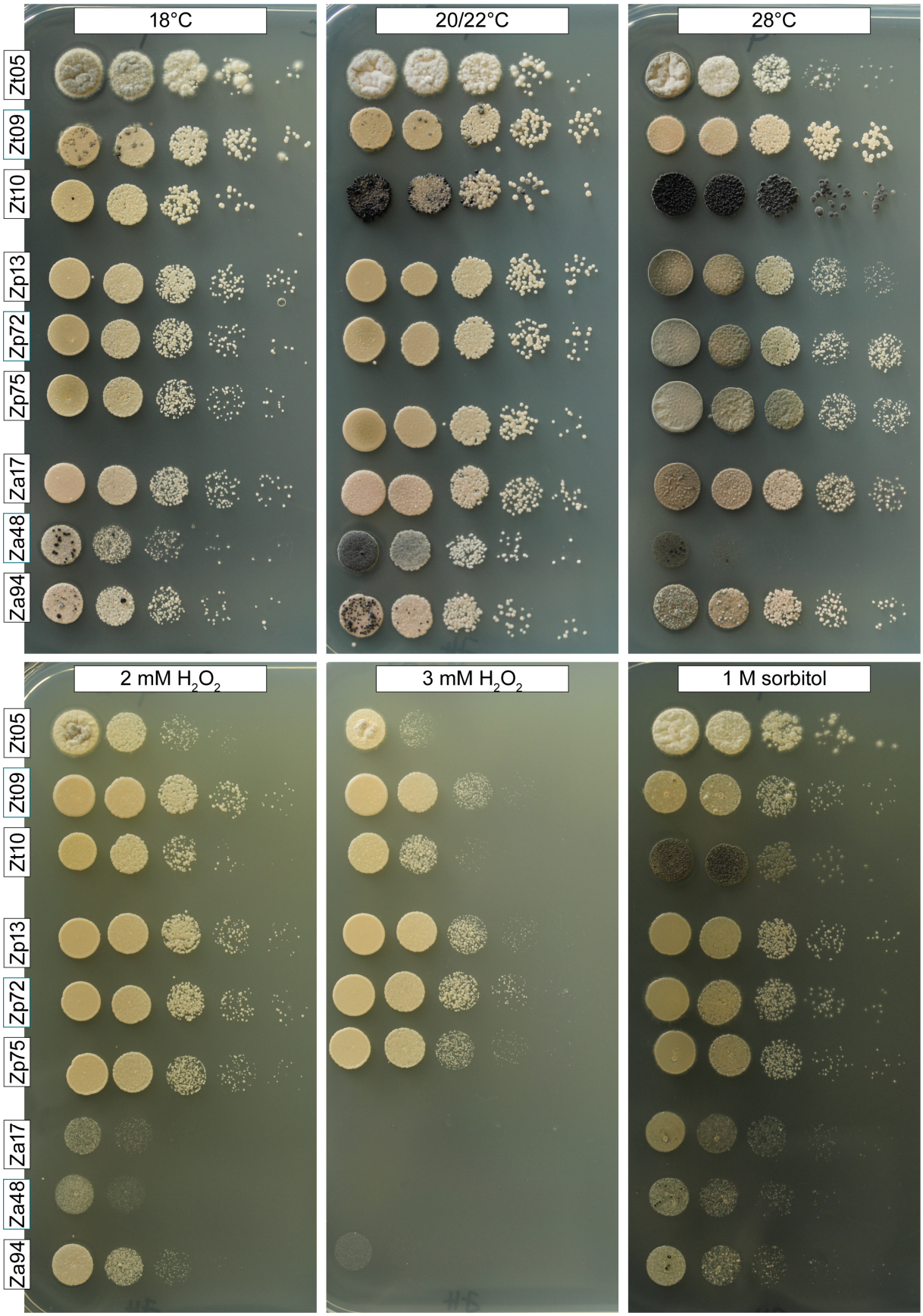

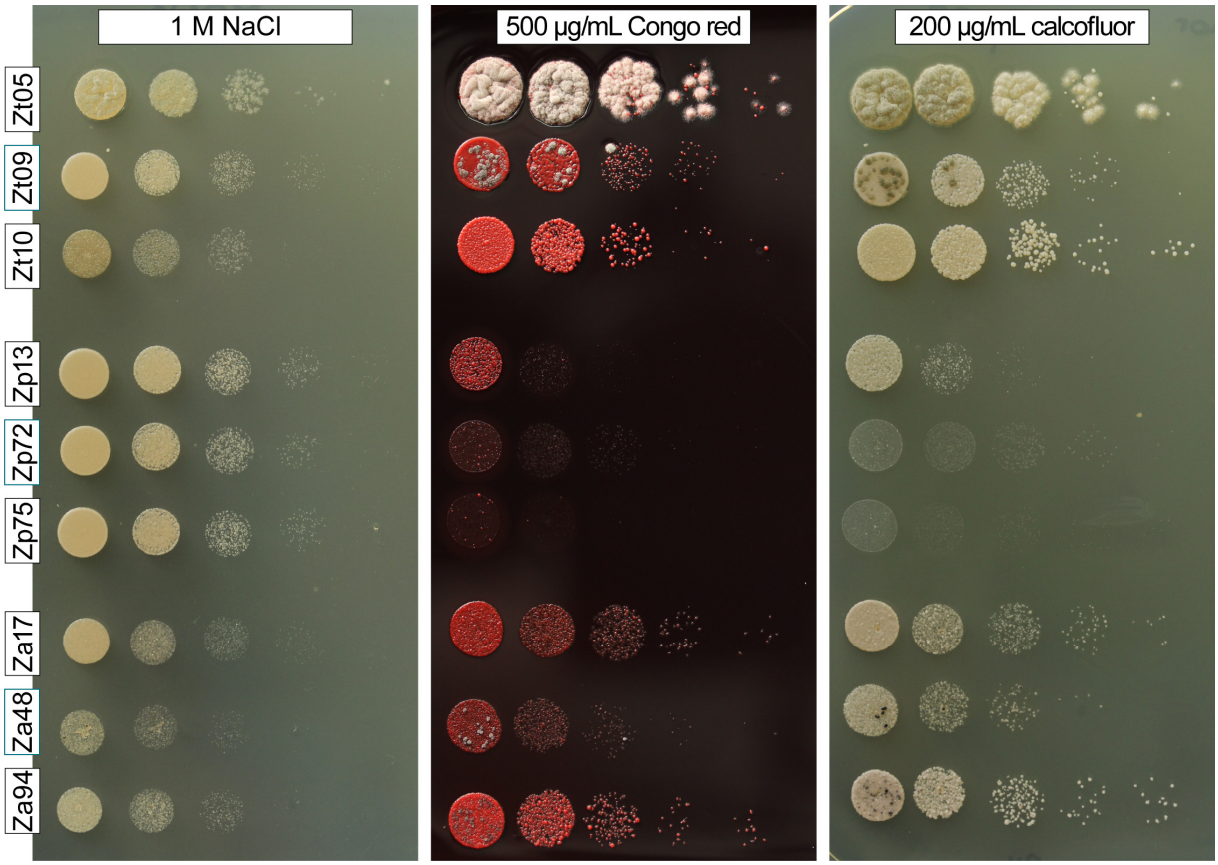

S1 Figure. *In vitro* stress assay demonstrates differences in colony morphology and tolerance towards abiotic stressors between *Z. tritici*, *Z. pseudotritici* and *Z. ardabiliae* isolates. Growth of the nine *Zymoseptoria* spp. isolates Zt05, Zt09, Zt10, Zp13, Zp72, Zp75, Za17, Za48 and Za94 was tested under abiotic stress conditions in comparison to the standard cultivation condition *in vitro* (solid YMS medium at 18°C no light). The following conditions were tested: growing conditions of wheat (20/22°C at 16-h day/8-h night rhythm), heat stress (28°C), oxidative stress (2 and 3 mM H_2O_2), osmotic stress (1 M sorbitol, 1 M NaCl), and cell wall stress (500 µg/ml Congo red, 200 µg/ml calcofluor white). Results for the three *Z. tritici* isolates have been previously published in (Haueisen *et al.*, 2017).

S2 Figure. Different size and shape of *Zymoseptoria* spp. single cells grown in liquid medium. Micrographs of single cells of *Z. tritici* (Zt09), *Z. pseudotritici* (Zp13), and *Z. ardabiliae* (Za17) that were grown in liquid YMS medium for two days at 18°C and 200 rpm. Scale bars ≙ 10 μm.

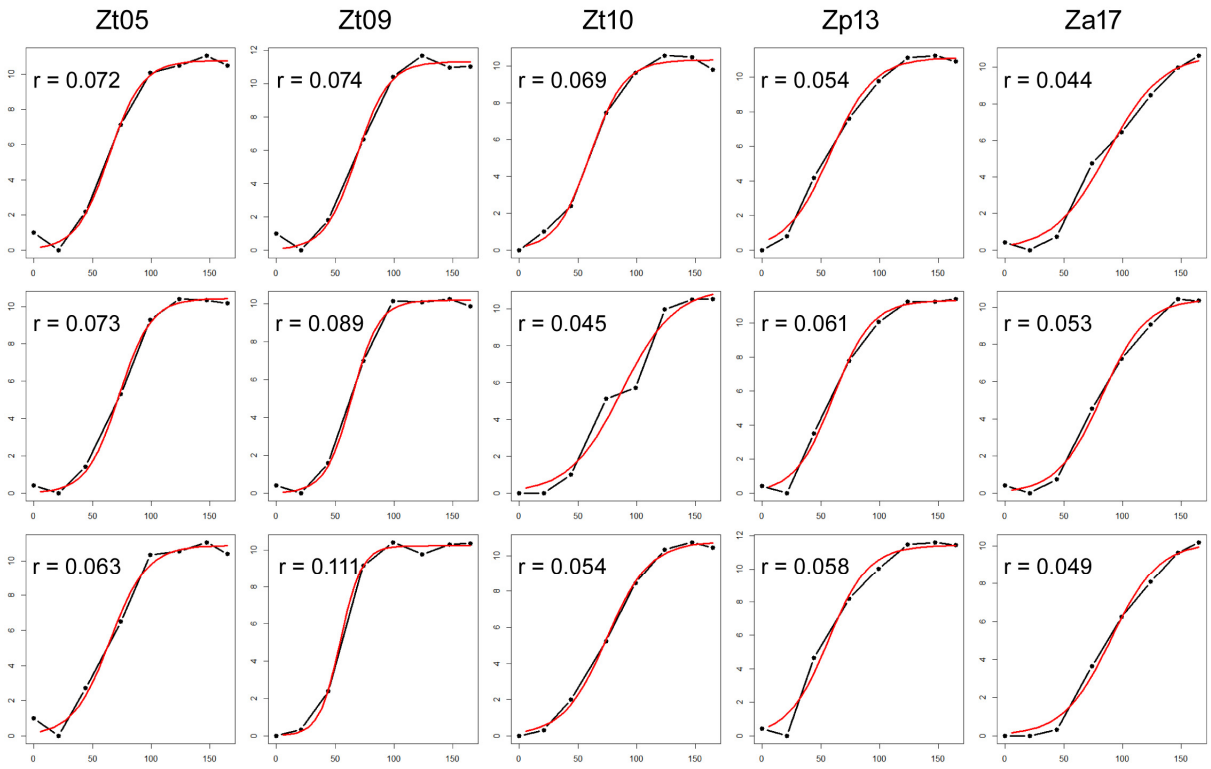

S3 Figure. Growth curves for *Zymoseptoria* spp. grown *in vitro* in liquid YMS cultures. *Z. pseudotritici* Zp13 and *Z. ardabiliae* Za17 grow slower *in vitro* as the *Z. tritici* isolates Zt05 and Zt09. X-axis of plots displays time in hours, y-axis displays transformed cell numbers. Cell concentrations were counted every ~24h for three replicates per isolate. Growth curves were fitted using the R package Growthcurver.

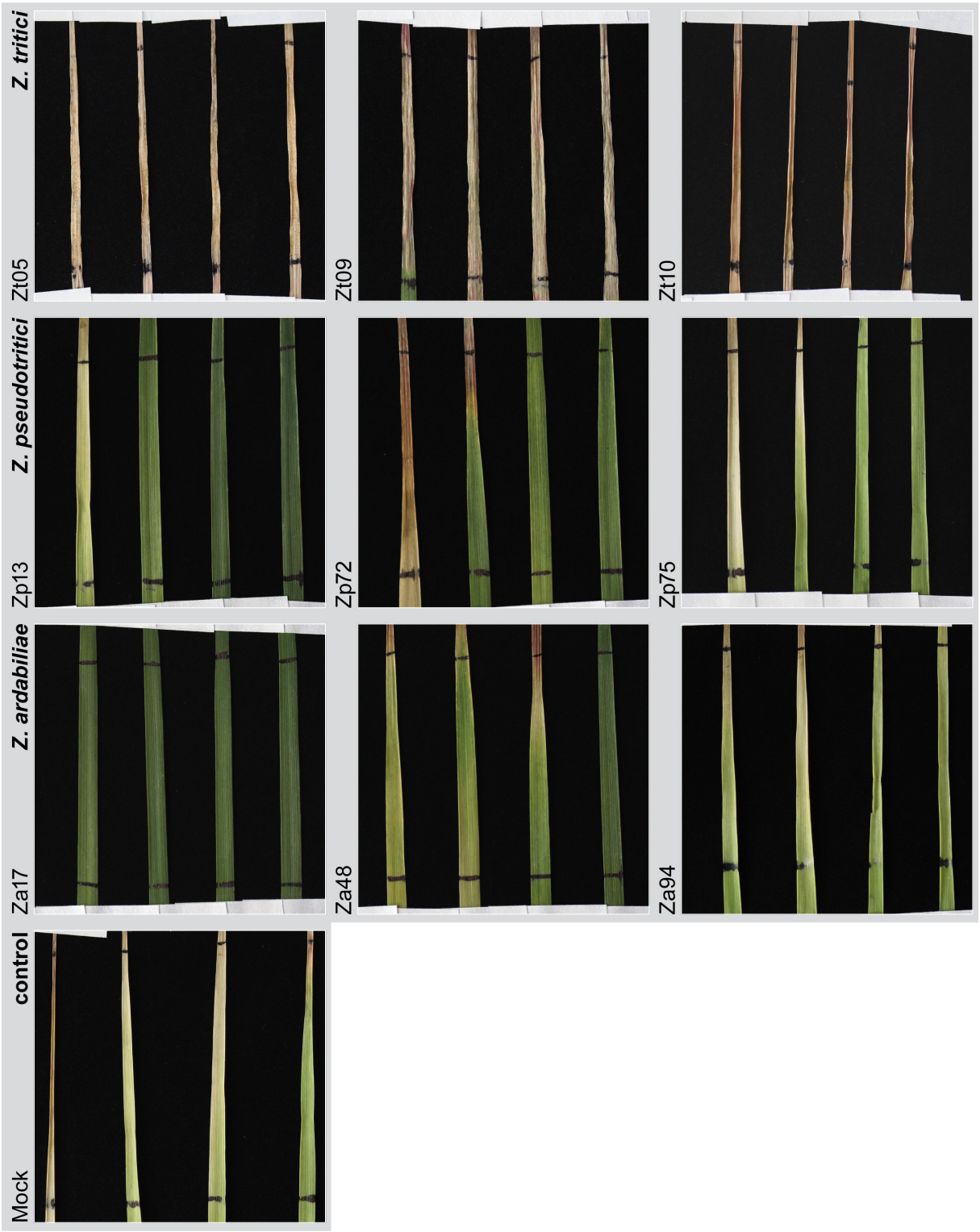

S4 Figure. Disease development on wheat leaves inoculated with isolates of *Zymoseptoria* spp. Photographs of wheat leaves taken 28 days post inoculation with isolates of *Z. tritici* isolates, *Z. pseudotritici* Zp13, and *Z. ardabiliae* Za17 and mock treatment. While *Z. tritici* isolates were virulent and caused disease, as necrosis and pycnidia developed, leaves inoculated with Zp13 and Za17 remained symptomless. Independent of the treatment -inoculation with *Zymoseptoria* spp. or mock- some wheat leaves did show signs of senescence like chlorosis and red coloration of the leaf tip after 28 days.

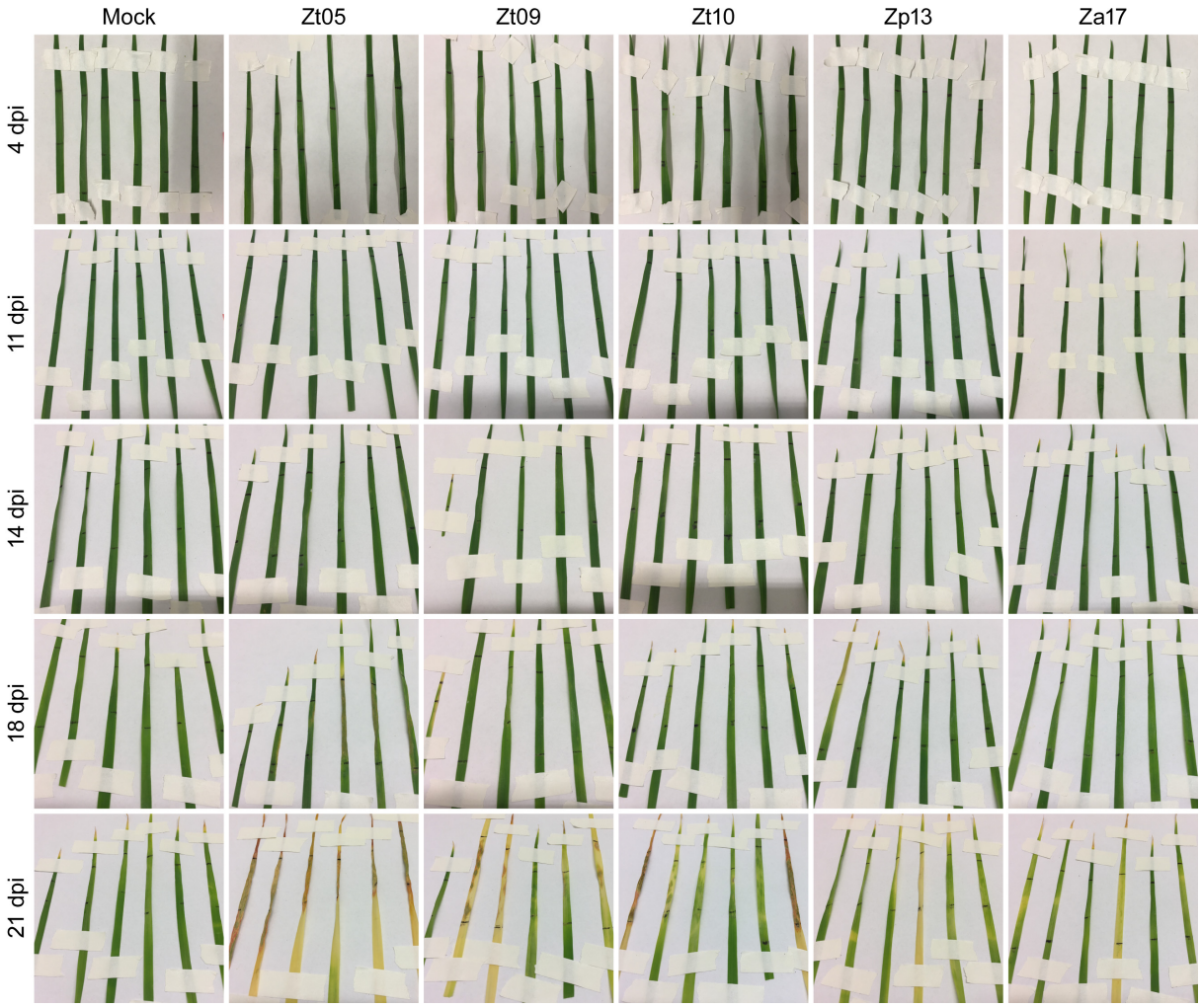

S5 Figure. Symptom development on wheat leaves used for ROS-staining assay. Photographs of *T. aestivum* Obelisk leaves taken at 4, 11, 14, 18 and 21 days post inoculation with the *Zymoseptoria* spp. isolates Zt05, Zt09, Zt10, Zp13, Za17 and mock treatment. Leaves were subsequently subjected to ROS detection staining. Results for the three *Z. tritici* isolates have been previously published in (Haueisen *et al.*, 2017).

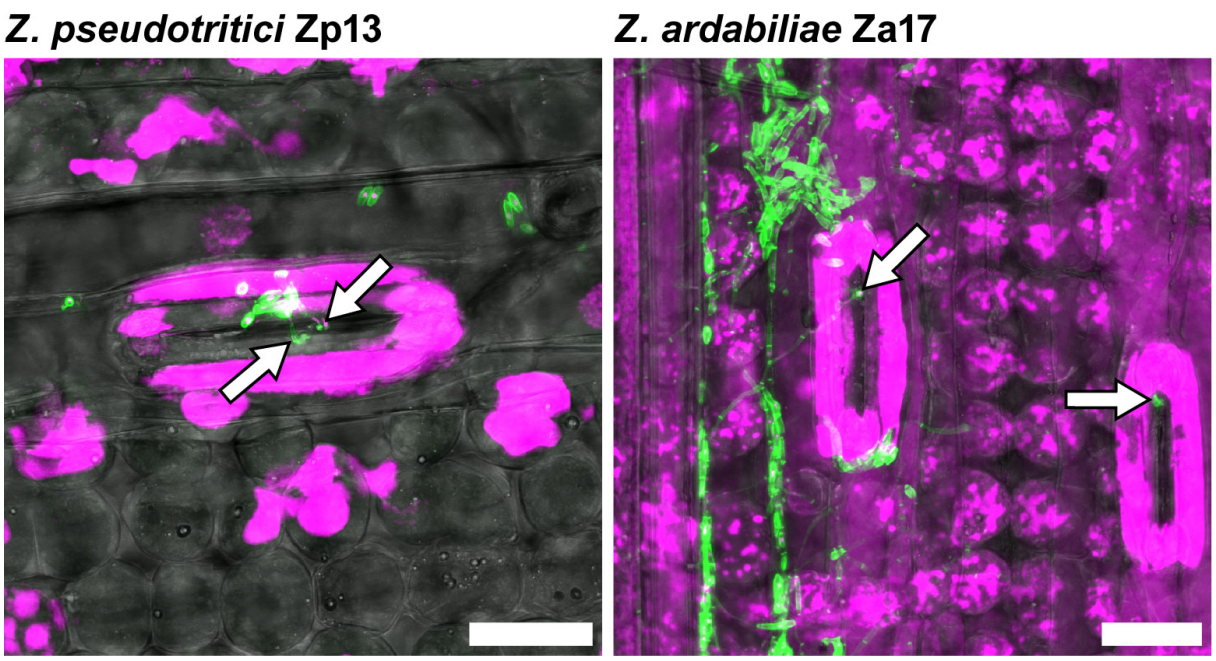

S6 Figure. Infection development of *Z. pseudotritici* and *Z. ardabiliae* on wheat leaves used for RNA-seq. Micrographs showing *Z. pseudotritici* Zp13 and *Z. ardabiliae* Za17 cells on the surface of wheat leaves 10 days post inoculation. Arrows indicate *Zymoseptoria* spp. infection hyphae penetrating wheat stomata. Samples were used for RNA extraction and transcriptome sequencing. Maximum projections of confocal image z-stacks. Nuclei and wheat cells are displayed in *purple*, fungal hyphae and septa in *green*, transmitted image information in *grey*. Scale bars = 30 µm.

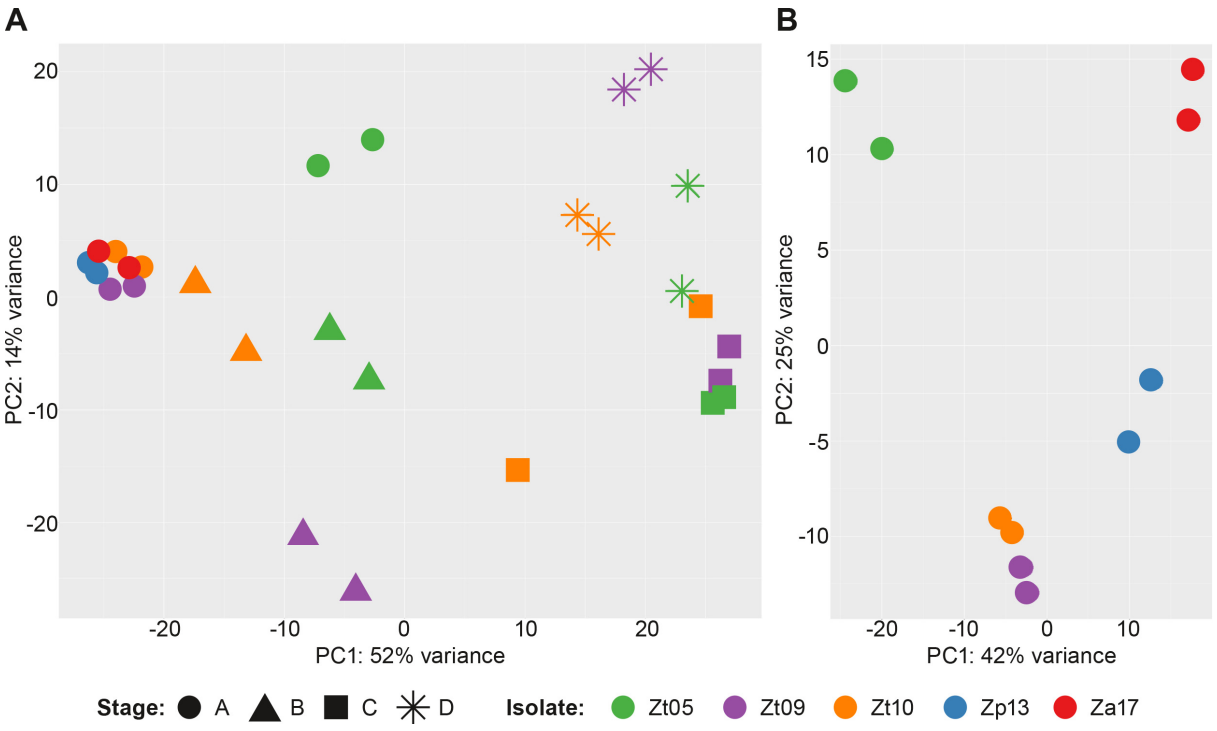

S7 Figure. RNA-seq data principal component analysis plots based on rlog-transformed read counts for genes orthologous in the three *Zymoseptoria* species. (A) Transcriptomes of Zp13 and Za17 during early wheat infection cluster with *Z. tritici* transcriptomes representing infection establishment stage A. PC1 separates datasets from infections stages A and B from stages C and D. **(B)** PC1 separates *Z. tritici* infection stage A datasets from *Z. pseudotritici* Zp13 and *Z. ardabiliae* Za17 transcriptomes representing initial wheat infection. Transcriptome data for the *Z. tritici* isolates Zt05, Zt09, and Zt10 was previously published in (Haueisen *et al.*, 2017).

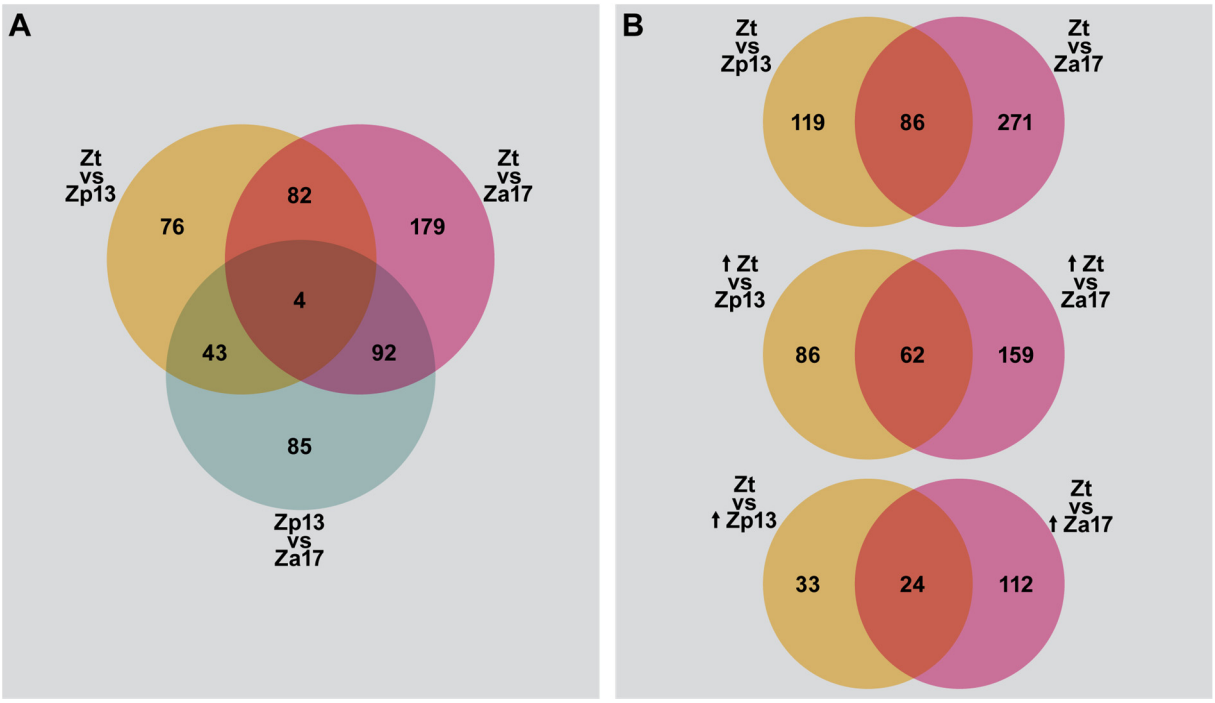

S8 Figure. Venn diagrams showing how differentially expressed genes are shared between the different *Zymoseptoria* spp. comparisons. Differential expression analyses were performed with DESeq2. Differentially expressed genes have $P_{adj} \leq 0.01$ and an absolute $\log_2$ fold change of ≥2. **(A)** 562 orthologous genes are differentially expressed between the three *Zymoseptoria* species; 221 genes are differentially expressed in two species comparisons; 4 genes are differentially expressed in all comparisons. **(B)** 476 genes are differentially expressed between *Z. tritici* and the incompatible *Z. pseudotritici* and *Z. ardabiliae*. Small arrows (↑) indicate the species in which genes are significantly up-regulated. 62 genes are significantly up-regulated in *Z. tritici* compared to both incompatible *Zymoseptoria* species.

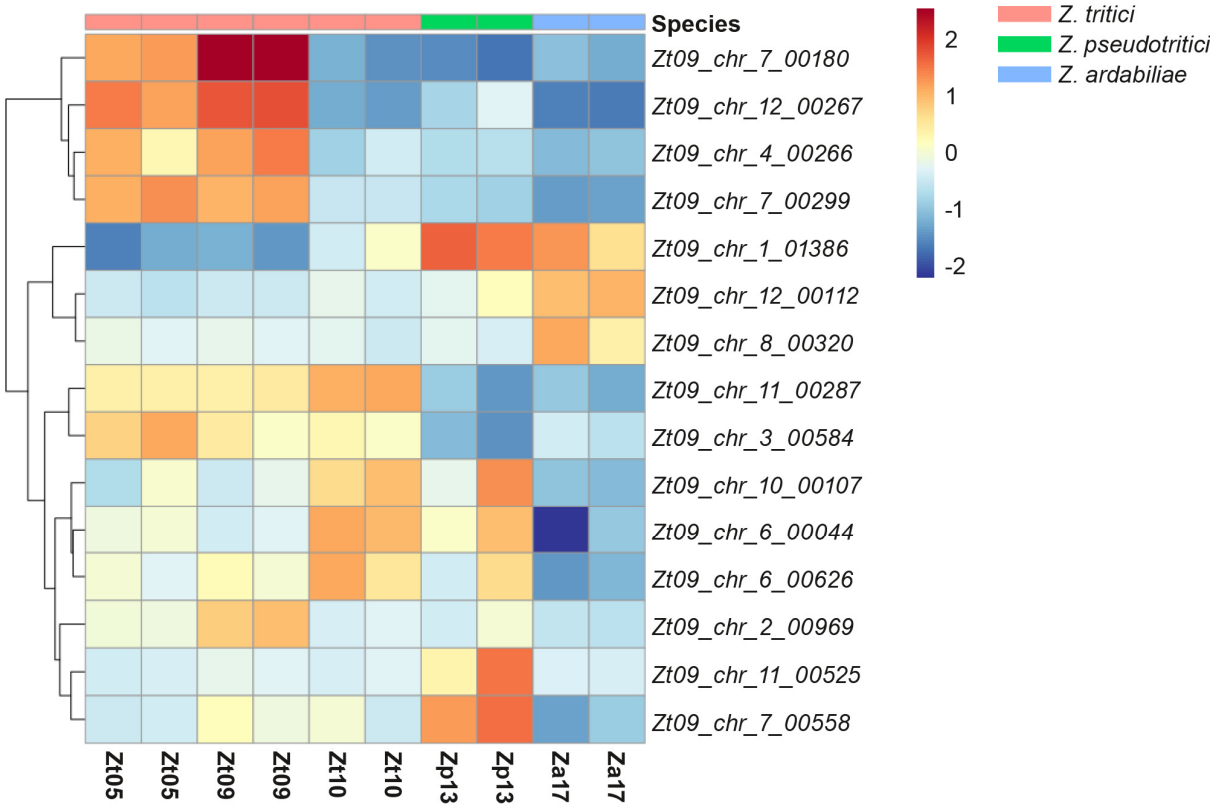

S9 Figure. Expression of ten host-specific effector candidates and five putative avirulence genes. Heatmap displaying how rlog-tranformed read counts differ for the 15 candidate genes across the five *Zymoseptoria* spp. transcriptome datasets used for the comparative transcriptome analyses. Per transcriptome two biological replicates are shown. For four genes in the first cluster, expression of the Iranian *Z. tritici* isolate Zt10 is low and more similar to the incompatible *Z. pseudotritici* Zp13 and *Z. ardabiliae* Za17. Zt10 shows poor biotrophic colonization of wheat mesophyll tissue (Haueisen *et al.*, 2017) what could be a consequence of low expression of putative host-specific and biotrophic effector genes. rlog transformation of raw read counts by DESeq2 R package (Love *et al.*, 2014). Heatmap drawn with R package pheatmap (Kolde, 2015).

Supplementary Animations

All supplementary animations are in .avi file format and are deposited on the supplementary USB key. Animations can be played with standard media players e.g. VLC media player available at http://www.videolan.org/vlc/.

S1 Animation. Directed growth of *Z. pseudotritici* Zp13 hyphae towards wheat stomata 7 dpi. Tomographic animation of confocal image z-stack showing spore germination, filament development, and penetration of wheat stomata by hyphae of *Z. pseudotritici* isolate Zp13 at 7 dpi. Nuclei and wheat cells displayed in *purple* and fungal structures in *green*. Scale bar = 50 µm.

S2 Animation. Directed growth of *Z. ardabiliae* Za17 hyphae towards wheat stomata 17 dpi. Tomographic animation of confocal image z-stack showing spore germination, filament development, and penetration of wheat stomata by hyphae of *Z. ardabiliae* isolate Za17 at 17 dpi. Nuclei and wheat cells displayed in *purple* and fungal structures in *green*. Scale bar = 25 µm.

S3 Animation. *Z. pseudotritici* Zp13 hyphae penetrate wheat stoma 14 dpi. Tomographic animation of confocal image z-stack showing penetration of wheat stoma by two hyphae of *Z. pseudotritici* isolate Zp13 at 14 dpi. Nuclei and wheat cells displayed in *purple* and fungal structures in *green*. Scale bar = 20 µm.

S4 Animation. *Z. ardabiliae* Za94 hyphae penetrate wheat stoma 8 dpi. Tomographic animation of confocal image z-stack showing penetration of wheat stoma by two hyphae of *Z. ardabiliae* isolate Za94 at 8 dpi. Nuclei and wheat cells displayed in *purple* and fungal structures in *green*. Reference transmitted images in *grey*. Scale bar = 25 µm.

S5 Animation. *Z. pseudotritici* Zp72 hypha arrested between guard cells 3 dpi. Tomographic animation of confocal image z-stack showing infecting hypha of *Z. pseudotritici* isolate Zp72 that is arrested between wheat stomatal guard cells at 3 dpi. Nuclei and wheat cells displayed in *purple* and fungal structures in *green*. Scale bar = 25 µm.

S6 Animation. *Z. pseudotritici* Zp72 hypha arrested between guard cells 10 dpi. Tomographic animation of confocal image z-stack showing infecting hypha of *Z. pseudotritici* isolate Zp72 that is arrested at wheat stomatal guard cells at 10 dpi. Nuclei and wheat cells displayed in *purple* and fungal structures in *green*. Reference transmitted images in *grey*. Scale bar = 25 µm.

S7 Animation. *Z. ardabiliae* Za94 hyphae arrested between guard cells 17 dpi. Tomographic animation of confocal image z-stack showing infecting hyphae of *Z. ardabiliae* isolate Za94 that are arrested between wheat stomatal guard cells at 17 dpi. Nuclei and wheat cells displayed in *purple* and fungal structures in *green*. Scale bar = 25 µm.

S8 Animation. *Z. ardabiliae* Za48 hypha arrested in sub-stomatal cavity 8 dpi. Tomographic animation of confocal image z-stack showing infecting hypha of *Z. ardabiliae* isolate Za48 that is arrested in a wheat sub-stomatal cavity at 8 dpi. Nuclei and wheat cells displayed in *purple* and fungal structures in *green*. Reference transmitted images in *grey*. Scale bar = 25 µm.

S9 Animation. *Z. ardabiliae* Za94 hypha arrested in sub-stomatal cavity 10 dpi. Tomographic animation of confocal image z-stack showing infecting hypha of *Z. ardabiliae* isolate Za94 that is arrested in a wheat sub-stomatal cavity at 10 dpi. Nuclei and wheat cells displayed in *purple* and fungal structures in *green*. Reference transmitted images in *grey*. Scale bar = 10 µm.

S10 Animation. *Z. pseudotritici* Zp13 hypha arrested in sub-stomatal cavity 17 dpi. Tomographic animation of confocal image z-stack showing infecting hypha of *Z. pseudotritici* isolate Zp13 that is arrested in a wheat sub-stomatal cavity at 17 dpi. Nuclei and wheat cells displayed in *purple* and fungal structures in *green*. Scale bar = 25 µm.

S11 Animation. *Z. pseudotritici* Zp75 hypha stopped close to mesophyll 10 dpi. Tomographic animation of confocal image z-stack showing infecting hypha of *Z. pseudotritici* isolate Zp75 that grew little further in the sub-stomatal cavity and was arrested close to the mesophyll tissue at 10 dpi. Nuclei and wheat cells displayed in *purple* and fungal structures in *green*. Reference transmitted images in *grey*. Scale bar = 25 µm.

S12 Animation. *Z. ardabiliae* Za17 hypha stopped close to mesophyll 10 dpi. Tomographic animation of confocal image z-stack showing infecting hypha of *Z. ardabiliae* isolate Za17 that grew little further in sub-stomatal cavity and was arrested close to the mesophyll tissue at 10 dpi. Nuclei and wheat cells displayed in *purple* and fungal structures in *green*. Scale bar = 25 µm.

S13 Animation. Deformation of *Z. pseudotritici* Zp13 hyphal tip 12 dpi. Tomographic animation of confocal image z-stack showing bulging of *Z. pseudotritici* Zp13 infecting hypha during stomatal penetration and in the wheat sub-stomatal cavity at 12 dpi; possibly in response to wheat pathogen defense. Nuclei and wheat cells displayed in *purple* and fungal structures in *green*. Reference transmitted images in *grey*. Scale bar = 25 µm.

S14 Animation. Deformation of *Z. ardabiliae* Za17 hyphal tip 10 dpi. Tomographic animation of confocal image z-stack showing bulging of *Z. ardabiliae* Za17 infecting hypha in the wheat sub-stomatal cavity at 10 dpi; possibly in response to wheat pathogen defense. Nuclei and wheat cells displayed in *purple* and fungal structures in *green*. Reference transmitted images in *grey*. Scale bar = 25 µm.

S15 Animation. Deformation of *Z. ardabiliae* Za48 hyphal tips 10 dpi. Tomographic animation of confocal image z-stack showing bulging of *Z. ardabiliae* Za48 infecting hyphae in the wheat sub-stomatal cavity at 10 dpi; possibly in response to wheat pathogen defense. Nuclei and wheat cells displayed in *purple* and fungal structures in *green*. Reference transmitted images in *grey*. Scale bar = 25 µm.

S16 Animation. Deformation of *Z. ardabiliae* Za48 hyphal tip 17 dpi. Tomographic animation of confocal image z-stack showing bulging of *Z. ardabiliae* Za48 infecting hypha in the wheat sub-stomatal cavity at 17 dpi; possibly in response to wheat pathogen defense. Nuclei and wheat cells displayed in *purple* and fungal structures in *green*. Reference transmitted images in *grey*. Scale bar = 25 µm.

Chapter 4

Host infections and plant-associated lifestyles of the *Zymoseptoria tritici* sister species *Z. pseudotritici* and *Z. ardabiliae*

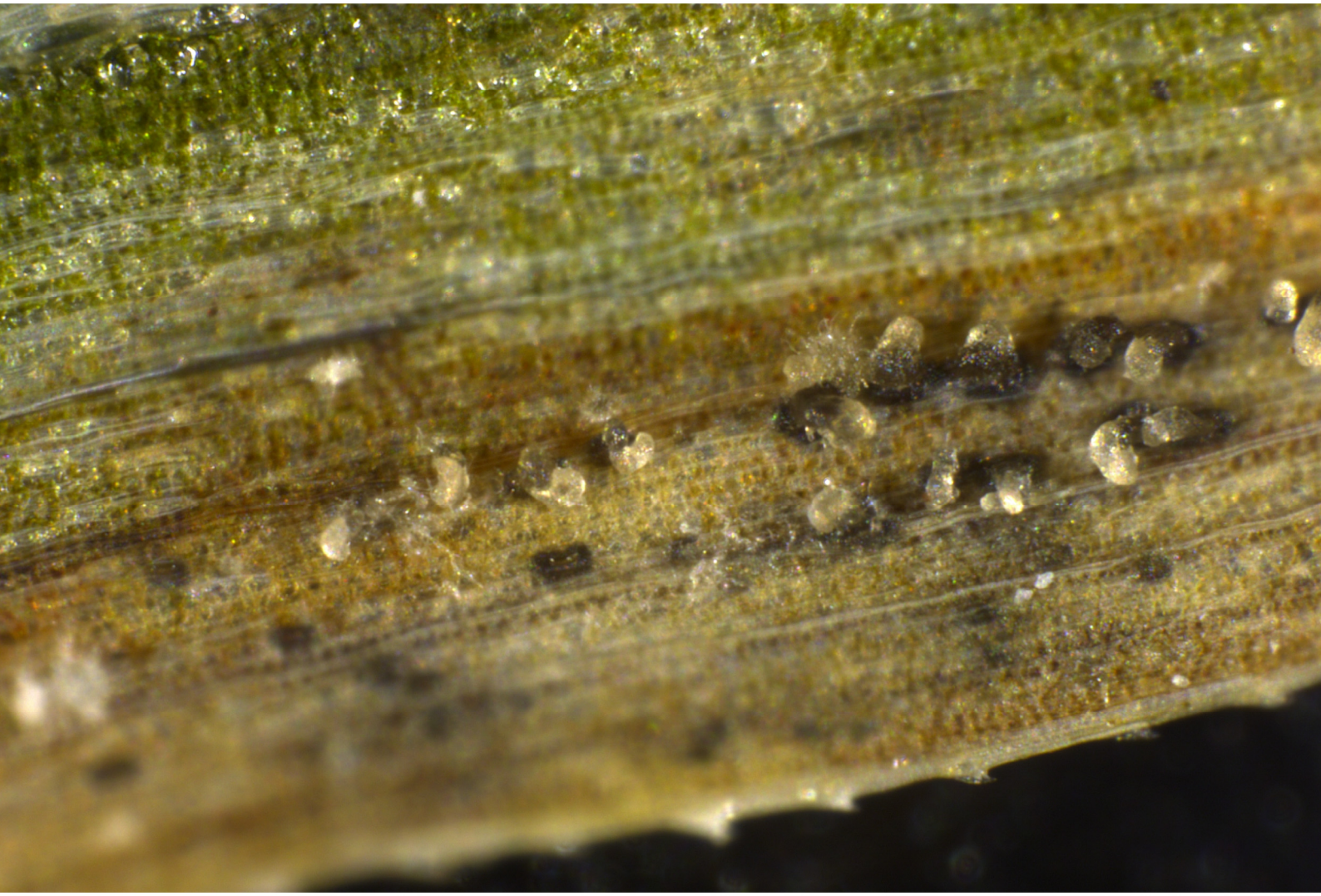

Chapter 4

Host infections and plant-associated lifestyles of the *Zymoseptoria tritici* sister species *Z. pseudotritici* and *Z. ardabiliae*

Research paper manuscript

Authors: Janine Haueisen, Elis Martinelli and Eva H. Stukenbrock

Abstract

Highly virulent and aggressive plant pathogens can arise from lineages diverging from ancestral species that lived as saprotrophs in the soil or associated with plants as endophytes or weak opportunistic pathogens. The goal of this research was to establish host species and to study virulence and host-pathogen interactions of *Zymoseptoria pseudotritici* and *Z. ardabiliae*. Both fungi are close relatives of the highly virulent wheat pathogen *Z. tritici* and were isolated from wild grasses in the Middle East. We conducted large-scale plant infection studies testing 20 host species and genotypes under different growth conditions in *in vivo* and *in vitro* assays, and investigated the influence of abiotic stress and leaf age on the outcome of host-pathogen interactions. We found that *Z. pseudotritici* and *Z. ardabiliae* only reproduce and complete their lifecycle in compromised or weakened host tissue. Our findings suggest that *Z. pseudotritici* and *Z. ardabiliae* have a different plant-associated lifestyle than their sister species and might be weak opportunistic pathogens. This further indicates that *Z. tritici* only acquired traits involved in aggressiveness and induction of host cell death after species divergence 11,000 years ago. *Z. tritici* might have very rapidly evolved from a weak pathogen ancestor with a limited geographical distribution to a highly aggressive and virulent pathogen that has spread worldwide with its host species.

Introduction

Zymoseptoria pseudotritici and *Zymoseptoria ardabiliae* are the closest known relatives of the prominent pathogen *Zymoseptoria tritici* which is the causal agent of septoria tritici leaf blotch on wheat (Stukenbrock *et al.*, 2012). *Z. pseudotritici* and *Z. ardabiliae* have been isolated in natural grasslands in the Ardabil province in Iran. On leaves of the uncultivated grass species *Elymus repens*, *Dactylis glomerata*, and *Lolium perenne*, these fungi produced asexual fruiting bodies in necrotic lesions, the typical symptoms of septoria leaf blotch (Stukenbrock *et al.*, 2007, 2012). However, we still know very little about the biology of *Z. pseudotritici* and *Z. ardabiliae* and how both species interact with their grass hosts.

Based on phylo-geographic and coalescence analyses, divergence of *Z. tritici* from a shared ancestral species occurred only ~11,000 years ago in the Fertile crescent (Banke & McDonald, 2005; Stukenbrock *et al.*, 2007, 2011). As *Z. pseudotritici* and *Z. ardabiliae* are endemic to the Middle East, their natural geographic distribution still overlaps with the center of origin. In contrast, *Z. tritici* has very successfully spread with its host and now occurs in all wheat cultivating agro-ecosystems worldwide (O'Driscoll *et al.*, 2014). Given their recent evolutionary history and adaptation to different hosts and ecosystems, the three *Zymoseptoria* species provide an ideal model system to gain new insight into the biology of fungal pathogens and the factors that facilitate rapid evolution and emergence of plant pathogens. Hence, establishment of an experimental host system for the wild-grass associated sister species *Z. pseudotritici* and *Z. ardabiliae* is of great importance to explore the closely related species as an experimental model system to study the evolution and host specialization of fungal plant pathogens.

In this study, our goal was to find and establish host grass species for *Z. pseudotritici* and *Z. ardabiliae* under laboratory conditions and to study pathogenesis and infections programs. We hypothesized that both fungi would infect wild, un-cultivated grass species following a similar developmental program as *Z. tritici* during infection of wheat leaf tissue (Haueisen *et al.*, 2017). Further, we tested the hypotheses that *Z. pseudotritici* and *Z. ardabiliae* are specialized to host species or genotypes, that successful host infections depend on environmental conditions and that the physiological state of the infected leaf influences plant-*Zymoseptoria* interactions.

To this end, we performed plant infection studies with *Zymoseptoria* spp. isolates including *in vivo* experiments on leaves of 20 plant species and *in vitro* assays on detached leaves of 14 grasses. We also tested the influence of leaf age and light stress on the outcome of *Zymoseptoria* spp. infections. In addition, we generated fluorescent mutants of *Z. tritici*, *Z. pseudotritici*, and *Z. ardabiliae* isolates to be used as tools for future infection studies and *in vivo in planta* microscopy.

Taken together, we found that *Z. pseudotritici* and *Z. ardabiliae* could not infect the tested host species *in vivo* as growth of infecting hyphae was blocked early after infection. However, asexual pycnidia were formed on detached leaves of several species or very rarely and episodically on

grass leaves affected by light stress, senescence, or yet unidentified factors that compromised the tissue. Our results suggest that *Z. pseudotritici* and *Z. ardabiliae* can infect a range of grasses as opportunistic pathogens but that both species are considerably less aggressive than the closely related wheat pathogen *Z. tritici*.

Materials and Methods

Zymoseptoria spp. isolates and bacterial strains

Cells of *Zymoseptoria tritici* Zt05, IPO323, and Zt10, *Z. pseudotritici* Zp13, Zp72, and Zp75, and *Z. ardabiliae* Za17, Za48, and Za94 (S1 Table) were inoculated from glycerol stocks onto YMS agar plates (0.4% [w/v] yeast extract, 0.4% [w/v] malt extract, 0.4% [w/v] sucrose, 2% [w/v] bacto agar) and grown at 18°C for 5 days. Single cells were grown in liquid YMS (200 rpm, 18°C) and harvested by centrifugation (3500 rpm for 10 min).

Plasmids generated in this study were transformed and amplified in *E. coli* TOP10 cells (Invitrogen, Karlsruhe, Germany) (S2 Table). For *Agrobacterium tumefaciens*-mediated transformation (ATMT) of *Zymoseptoria* spp. cells the *A. tumefaciens* strain AGL1 was used. Both bacterial strains were grown on double yeast tryptone (dYT) medium at 37°C (TOP10) or 28°C (AGL1). To maintain AGL1 strain, 50 µg/mL Rifampicin and 100 µg/mL Carbenicillin (both Sigma, Germany) were added to the dYT plates.

Agrobacterium tumefaciens-mediated transformation (ATMT) of *Zymoseptoria* spp.

To obtain fluorescent *Zymoseptoria* strains, we engineered mutants of *Z. tritici* IPO323, Zt05, and Zt10, *Z. pseudotritici* Zp13, and *Z. ardabiliae* Za17 expressing the codon-optimized green fluorescent protein ZtGFP (Kilaru *et al.*, 2015) and the red fluorescent protein mCherry (Schuster *et al.*, 2015) cytoplasmically under control of the constitutive *Aspergillus nidulans gpdA* promotor. For targeted gene integration, we selected non-coding, non-expressed genomic regions in the vicinity of expressed genes (S3 Table) using previously described RNA-seq data (Haueisen *et al.*, 2017). We amplified two DNA fragments approx. 1 kb upstream and downstream of the selected integration sites by PCR that serve as flanking regions and facilitate integration of *Ztgfp*- and *mCherry*-constructs at the target loci via homologous recombination (S3 Table). We further amplified the ORFs of *Ztgfp* and *mCherry* using DNA of pCZtGFP (Kilaru *et al.*, 2015) and pCmCherry (Schuster *et al.*, 2015) as templates, and Geneticin (G418) and Hygromycin resistance cassettes. We assembled the DNA fragments including isolate-specific up- and down-stream flanks, *gpdA* promotor and a combination of *Ztgfp* and the Geneticin resistance cassette or of *mCherry* and the Hygromycin resistance cassette and ligated the constructs into the EcoRV-digested plasmid pES61 using Gibson assembly (Gibson *et al.*, 2009). pES61 is a derivate of the binary vector pNOV-ABCD (Bowler *et al.*, 2010). Electro-competent *A. tumefaciens* AGL1 cells were transformed with the final plasmids (S2 Table) and constructs were introduced into IPO323, Zt05, Zt10, Zp13, and Za17 by ATMT (Zwiers & De Waard, 2001).

Transformed *Zymoseptoria* colonies were visible on YMS plates supplemented with 150 µg/mL Hygromycin (Roth, Germany) or 250 µg/mL Geneticin (Sigma, Germany) two weeks post ATMT. Correct insertions of the *Ztgfp*-Geneticin resistance and *mCherry*-Hygromycin resistance

integration cassettes was confirmed by PCR or by Southern analyses of positive transformants. Lists including all engineered fluorescent *Zymoseptoria* strains, plasmids and primer sequences can be found in S1, S2, and S4 Tables.

Plant infection assays

In order to test virulence of *Zymoseptoria* spp. isolates on different grasses belonging to the Poaceae subfamily Pooideae, we performed 1) infection experiments including 14 grasses and six *Zymoseptoria* spp. isolates in a greenhouse, 2) detached leaf infections assays with the same 14 grasses and six fungal isolates, 3) infection studies on leaves of ten Poaceae and the dicot *Arabidopsis thaliana* in phytochambers with different conditions, and 4) experiments on leaves of wheat and *Dactylis glomerata* of different age. The details are listed below.

1) We conducted a large infection assay including 14 grass species and cultivars (Table 1) (provided by UFA Samen, Switzerland) in a greenhouse (20 – 22°C). Daylight was supplemented by artificial light (16 h/day). Grasses were densely grown in buckets (size: 100 x 17 cm) for 25 days and spray inoculated with cells of *Z. pseudotritici* Zp13, Zp72, and Zp75, and *Z. ardabiliae* Za17, Za48, and Za94 isolates (10^7 cells/mL in 0.1% [v/v] Tween 20 (Roth, Karlsruhe, Germany)) and mock treatment (0.1% Tween 20). Leaves of inoculated plants were manually screened for disease symptoms (chlorosis and necrosis) and pycnidia development five weeks post inoculation.

2) In parallel, we tested infections of the six *Z. pseudotritici* and *Z. ardabiliae* isolates on detached leaves of the 14 grasses (Table 1) as previously described (Stukenbrock *et al.*, 2011). Grasses were grown under greenhouse conditions as described in 1) and leaves were cut after 24 days. We checked the location of stomata on the leaves (adaxial, abaxial, or both) and inoculated leaf areas containing stomata using cotton swabs soaked with fungal cell suspensions (10^7 cells/mL in 0.1% [v/v] Tween 20 (Roth, Karlsruhe, Germany)). Leaves were placed on 1% [w/v] agar plates supplemented with 100 mg/mL benzimidazole and cuts were covered with agar blocks. Plates were sealed and incubated in the greenhouse next to the spray-inoculated plants. Detached inoculated leaves were screened manually after 21 and 27 days and documented using a Leica S8APO equipped with a Leica DFC450 camera.

3) We performed infection experiments in phytochambers with different grasses including *Triticum aestivum* Obelisk, *Hordeum vulgare* Simba, *H. vulgare* Fairytale, *Brachypodium distachyon* Bd21, *Dactylis glomerata* Belunga, *D. glomerata* Loke, *Lolium hybridum* Ibex, *L. perenne* Arvicola, *Arrhenatherum elatius* Arone, *Arabidopsis thaliana* (Col-0 ecotype), and *Festuca arundinaceae* (propagated from seeds collected in Iran in 2011, kindly provided by Bruce McDonald, ETH Zurich). Distinct leaf areas were brush-inoculated with cell suspensions (10^7 cells/mL in 0.1%

[v/v] Tween 20) or control treatment (0.1% Tween 20) and plants were incubated at 100% humidity for 48 hours. Subsequently, plants were grown in phytochambers applying standard (22°C [day]/20°C [night], 70% humidity, 16-h light period with photosynthetically active photon flux density (PPFD) ~ 200 µmol/m²*s) or intense light conditions (22°C [day]/20°C [night], 70% humidity, 16-h light period with PPFD ~ 350 µmol/m²*s).

4) In a final experiment, we aimed to assess the importance of leaf age and senesce on the infection ability of the three *Zymoseptoria* species. To this end, we brush-inoculated second leaves of 504 *T. aestivum* cultivar Obelisk plants after 7, 21, and 35 days (24 leaves per time point and treatment) and of 196 *D. glomerata* Loke plants after 16 and 30 days (14 leaves per time point and treatment) of growth under standard phytochamber conditions. Leaves were harvested and infection symptoms were evaluated manually and using automated image analysis (Stewart *et al.*, 2016) as described in (Habig *et al.*, 2017) at 21 dpi (plant age: 28 days), 24 dpi, and 10 dpi (plant age both: 45 days) for wheat leaves and 38 dpi (plant age: 54 days) and 28 dpi (plant age: 58 days) for *D. glomerata* leaves.

Confocal laser-scanning microscopy

Leaf material was harvested at different time points after inoculation with *Zymoseptoria* spp. isolates in order to analyze host-pathogen interactions and fungal structures by confocal laser-scanning microscopy. Samples were stained with wheat germ agglutinin conjugated to fluorescein isothiocyanate (WGA-FITC) in combination with propidium iodide (PI) and confocal microscopy was conducted using a Leica TCS SP5 (Leica Microsystems, Germany) and a Zeiss LSM880 (Carl Zeiss Microscopy, Germany) as previously described (Haueisen *et al.*, 2017). Plant-*Zymoseptoria* spp. interactions were studied by analyses of large stacks of optical serial sections. Single *Zymoseptoria* cells were grown on solid YMS medium and imaged mounted in 0.2% YMS agar using a Zeiss LSM880 (Carl Zeiss Microscopy, Germany) equipped with a C-Apochromat 63x/1.2 water objective (Carl Zeiss Microscopy, Germany). ZtGFP was excited at 1% of the 488-nm argon laser and fluorescence was detected in the range of 490 to 543 nm. mCherry was excited at 1.8% of the 561 nm laser and signal was detected between 579 to 650 nm. 1% of the 561-nm diode laser was used as light source for reference transmitted images. Micrographs were processed using the software ZEN blue (Carl Zeiss Microscopy, Germany). Images of wildtype cells showing autofluorescence were acquired and processed in the same way.

Zymoseptoria spp. re-isolation and confirmation

To confirm asexual reproduction of *Zymoseptoria* spp. isolates on Obelisk wheat and *D. glomerata* Loke, we treated leaves with pycnidia-like structures as described in (Poppe *et al.*, 2015) to induce maturation and release of pycnidiospores. Leaves were examined for spore production using a

Leica S8APO. Single pycnidiospore-containing cirrhi (spore-mass oozing from mature pycnidia under humid conditions) were picked and spores were propagated in YMS medium. DNA was obtained using a standard phenol-chloroform extraction protocol (Sambrook & Russell, 2001) and used as template for PCR reactions to amplify internal transcribed spacers (ITS) and 5.8S rDNA as described by (White *et al.*, 1990) using the primer combination ITS4/ITS5 and the *β-Tubulin* locus using primers T1/Bt2b (Glass & Donaldson, 1995; O'Donnell & Cigelnik, 1997). PCR products were purified (Wizzard DNA Clean-Up System, Promega) and sequenced. Sequences were curated in SeaView Version 4 (Gouy *et al.*, 2010) and aligned with *Z. tritici*, *Z. pseudotritici*, *Z. ardabiliae*, and *Z. passerinii* reference sequences (Goodwin *et al.*, 2011; Stukenbrock *et al.*, 2012) using MUSCLE (Edgar, 2004). Trees were computed in SeaView 4 by neighbor-joining method, followed by a bootstrap test with 1000 replications.

Results and Discussion

Z. pseudotritici and *Z. ardabiliae* produce pycnidia *in vitro* on detached leaves

The type of plant infection study – *in vivo* on leaves attached to living plants or *in vitro* on detached leaves - was more important for the outcome of *Z. pseudotritici* and *Z. ardabiliae* infections than host species and genotype. We conducted infection assays testing virulence of the isolates Zp13, Zp72, Zp75, Za17, Za48, and Za94 on the leaves of 14 non-cultivated grasses to study the host range of *Z. pseudotritici* and *Z. ardabiliae*. The experiments consisted of an *in vivo* and an *in vitro* approach that were performed in parallel in a greenhouse. *In vivo*, grass leaves were spray-inoculated and remained attached to the plants grown in large pots for five weeks (Fig 1A-B). *In vitro*, cut leaves were inoculated with fungal cells and incubated in a detached leaf assay on water agar plates for 27 days (Fig 1C). Consistent with previous observations (Stukenbrock *et al.*, 2011), *Z. pseudotritici* and *Z. ardabiliae* isolates produced pycnidia, the asexual fruiting bodies of *Zymoseptoria* species, *in vitro* on detached leaves of *Dactylis glomerata*, *Lolium* spp., and *Arrhenatherum elatius* (Fig 1D-F). This indicates a broader host range of *Z. pseudotritici* and *Z. ardabiliae* than of the wheat-specialized *Z. tritici*. However, we observed no pycnidia or disease symptoms like fungal-induced necrotic lesions on *in vivo* leaves of these or the other Poaceae species five weeks post inoculation (Table 1). Hence, under the conditions used in our experiment *Z. pseudotritici* and *Z. ardabiliae* were not able to grow and reproduce in *in vivo* host leaves but could develop pycnidia on detached leaves *in vitro* within three weeks post cutting and inoculation. Detached leaf assays are a common method to study virulence and pathogenesis of plant pathogens (Arraiano *et al.*, 2001; Browne & Cooke, 2004). However, physiology in detached leaves differs substantially from attached leaves as cutting accelerates senescence and eliminates interactions with other plant parts (Smart, 1994). Besides *Zymoseptoria* spp. pycnidia, we observed un-identified microbes colonizing detached leaves (Fig 1G) and possibly growing as saprotrophs feeding on dead plant material. Also, the leaf-associated microbiome that has been demonstrated to play a major role in plant growth and pathogen defense (Vandenkoornhuyse *et al.*, 2015; Ritpitakphong *et al.*, 2016), is altered in detached leaves. Consequently, otherwise resistant hosts were shown to become susceptible in detached leaf assays (Michel *et al.*, 2010) changing the outcome of disease interactions demonstrated in field tests (Amand & Wehner, 1995). We speculate that altered host physiology, in particular accelerated senescence in detached leaves, allowed *Z. pseudotritici* and *Z. ardabiliae* isolates to complete their lifecycle and produce asexual fruiting bodies in otherwise incompatible hosts.

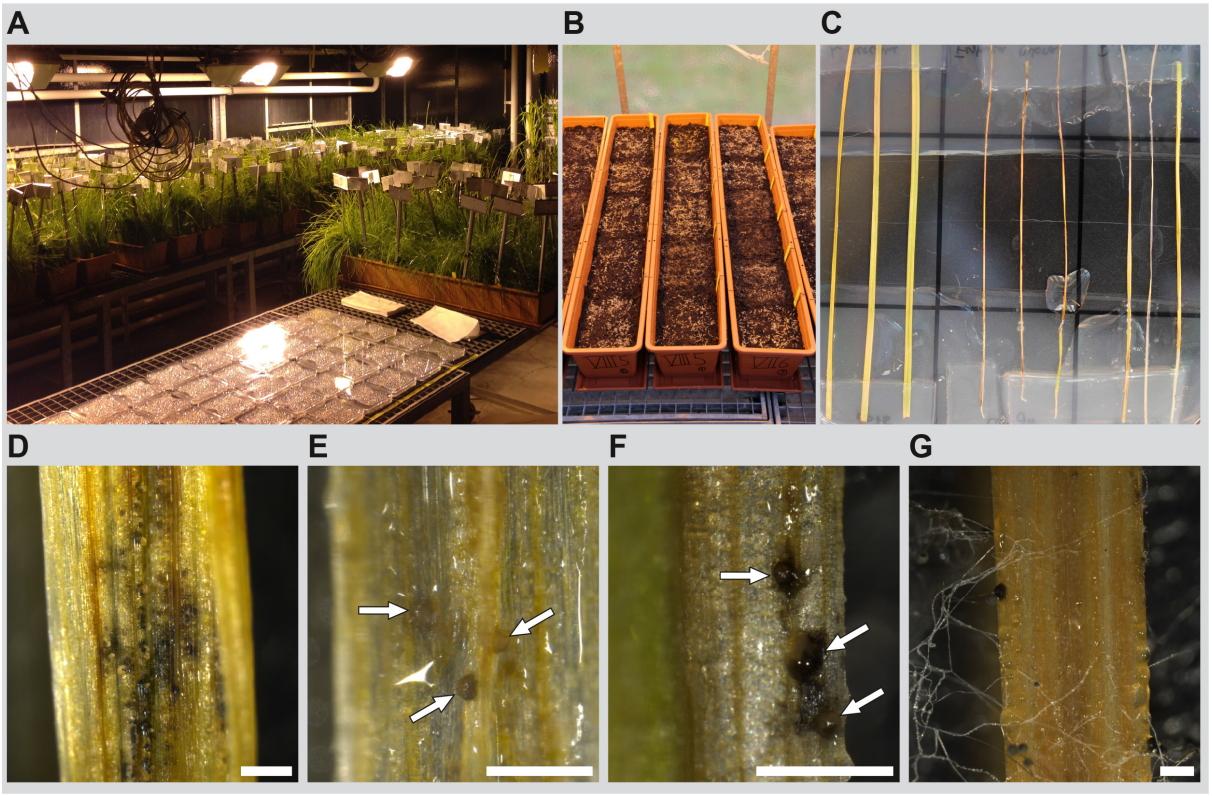

Figure 1. *Z. pseudotritici* and *Z. ardabiliae* isolates produce pycnidia *in vitro* on detached leaves. Photographs showing experimental setup and results of simultaneous plant infection experiments on attached and detached leaves of 14 grasses. **(A)** Grasses were grown in large pots under greenhouse conditions for five weeks post spray inoculation with cells of *Z. pseudotritici* and *Z. ardabiliae* isolates. Likewise, detached leaf assay plates were incubated in the greenhouse. **(B)** Different grasses were cultivated next to each other in one large pot. **(C)** Three detached leaves per grass were inoculated with cells of one *Zymoseptoria* spp. isolate or mock-treated and incubated on water-agar plates for 27 days. **(D-G)** Details of detached leaves 27 dpi. Scale bars = 500 µm. **(D)** Detached leaf of *A. elatius* Arone densely covered with pycnidia of *Z. pseudotritici* Zp75. Pycnidiospores are extruded in cirrhi. **(D)** Pycnidia of *Z. ardabiliae* Za94 covered with pycnidiospores (arrows) on *A. elatius* Arone detached leaf. **(F)** *Z. pseudotritici* Zp75 pycnidia (arrows) within necrotic lesion on *D. glomerata* Loke detached leaf. **(G)** Microbial contamination, putatively by *Aspergillus* sp. on *L. hybridum* Ibex detached leaf.

Table 1. Results of *in vivo* grass infection experiment and *in vitro* detached leaf assay performed simultaneously under greenhouse conditions.

Grass species and cultivars	Zp13		Zp72		Zp75		Za17		Za48		Za94		mock	
	DLA 27 dpi	GH 5 wpi	DLA 27 dpi	GH 5 wpi	DLA 27 dpi	GH 5 wpi	DLA 27 dpi	GH 5 wpi	DLA 27 dpi	GH 5 wpi	DLA 27 dpi	GH 5 wpi	DLA 27 dpi	GH 5 wpi
Alopecurus pratensis Vulpera	–	–	–	–	–	–	–	–	–	–	–	–	–	–
A. pratensis Alopex	–	–	–	–	–	–	–	–	–	–	–	–	–	–
Dactylis glomerata Loke	–	–	–	–	P (2/3)	–	P (2/3)	–	–	–	P (2/3)	–	–	–
D. glomerata Belunga	–	–	–	–	–	–	–	–	–	–	P (1/3)	–	–	–
Lolium hybridum Ibex	P (2/3)	–	P (1/3)	–	–	–	–	–	–	–	–	–	–	–
L. multiflorum Zebra	–	–	–	–	–	–	–	–	–	–	P (2/3)	–	–	–
L. multiflorum Gemini	–	–	–	–	–	–	–	–	–	–	–	–	–	–
L. perenne Arvicola	–	–	–	–	P (1/3)	–	–	–	–	–	P (1/3)	–	–	–
L. perenne Vercade	–	–	–	–	–	–	–	–	–	–	–	–	–	–
Poa pratensis Lato	–	–	–	–	–	–	–	–	–	–	–	–	–	–
Festuca arundinacea Belfine	–	–	–	–	–	–	–	–	–	–	–	–	–	–
F. rubra Reverent	–	–	–	–	–	–	–	–	–	–	–	–	–	–
Agrostis capillaris Highland	–	–	–	–	–	–	–	–	–	–	–	–	–	–
Arrhenatherum elatius Arone	–	–	P (2/3)	–	P (3/3)	–	P (2/3)	–	P (2/3)	–	P (3/3)	–	–	–

Results of combined *in vivo* and *in vitro* grass infection assay for *Z. pseudotritici* isolates Zp13, Zp72, and Zp75 and *Z. ardabiliae* isolates Za17, Za48, and Za94. DLA = *in vitro* detached leaf assay. GH = *in vivo* assay on attached leaves of grasses grown in greenhouse. – = no symptoms observed. dpi = days post inoculation. wpi = weeks post inoculation. P = pycnidia observed on (x/3) leaves.

Pycnidia of *Z. pseudotritici* and *Z. ardabiliae* develop rarely on grass leaves under experimental conditions

We next set out to test whether *Z. pseudotritici* and *Z. ardabiliae* isolates could infect and develop pycnidia on leaves of living plants in *in vivo* infection experiments under controlled conditions. Leaves of *D. glomerata* Loke, *D. glomerata* Belunga, *L. hybridum* Ibex, *L. perenne* Arvicola, and *A. elatius* Arone were brush-inoculated and observed while growing in the phytochamber under standard conditions. We further included plants of *Festuca arundinacea* that were propagated from seeds collected within the natural range of distribution of *Z. pseudotritici* and *Z. ardabiliae* in Iran and additionally tested host capabilities of *Hordeum vulgare* Simba, *H. vulgare* Fairytale, *Brachypodium distachyon* Bd21, and *Arabidopsis thaliana*. Leaves were manually screened for disease symptoms such as necrotic lesions and pycnidia formation and plant-fungal interactions of selected leaf material were investigated in detail by confocal laser-scanning microscopy. Within four to six weeks post inoculation, we observed no typical symptoms of septoria leaf blotch and, with one exception, no pycnidia were formed.

Microscopic analyses demonstrates that host-pathogen interactions were incompatible as infection hyphae developed and penetrated stomata but were arrested between the stomatal guard cells or in the sub-stomatal cavities of the different grasses (Fig 2 A-B and D-E). Interestingly, *Zymoseptoria* spp. cells inoculated on leaves of the dicot *A. thaliana* also developed hyphae that colonized the leaf surface. However, no *A. thaliana* stomata were penetrated even though hyphae grew over guard cells (Fig 2C). This demonstrates that development of *Zymoseptoria* spp. inoculum into filaments is independent of grass leaves and might be triggered by conserved components of plant surfaces, like cutin or epicuticular waxes (Yeats & Rose, 2013), or by starvation in nutrient poor environments. However, the initiation of stomatal penetrations may be induced by specific signals associated with grass stomata as stomatal penetrations by *Zymoseptoria* fungi were only observed on leaves of Poaceae species.

On one of eight *D. glomerata* Loke plants that was inoculated with cells of the *Z. pseudotritici* isolate Zp13, we found pycnidia that were located within necrotic leaf tissue (Fig 2F). Microscopic analyses indicate, however, that the vast majority of *Z. pseudotritici* and *Z. ardabiliae* infections on *D. glomerata* Loke were incompatible as we observed infection hyphae mostly in sub-stomatal cavities (Fig 2E) from where further growth was likely blocked. Taken together, *Z. pseudotritici* and *Z. ardabiliae* isolates were not able to infect the screened plant species in whole plant *in vivo* experiments. Pycnidia developed extremely rarely and the factors that allowed lifecycle completion and reproduction were not recognized in our experiments.

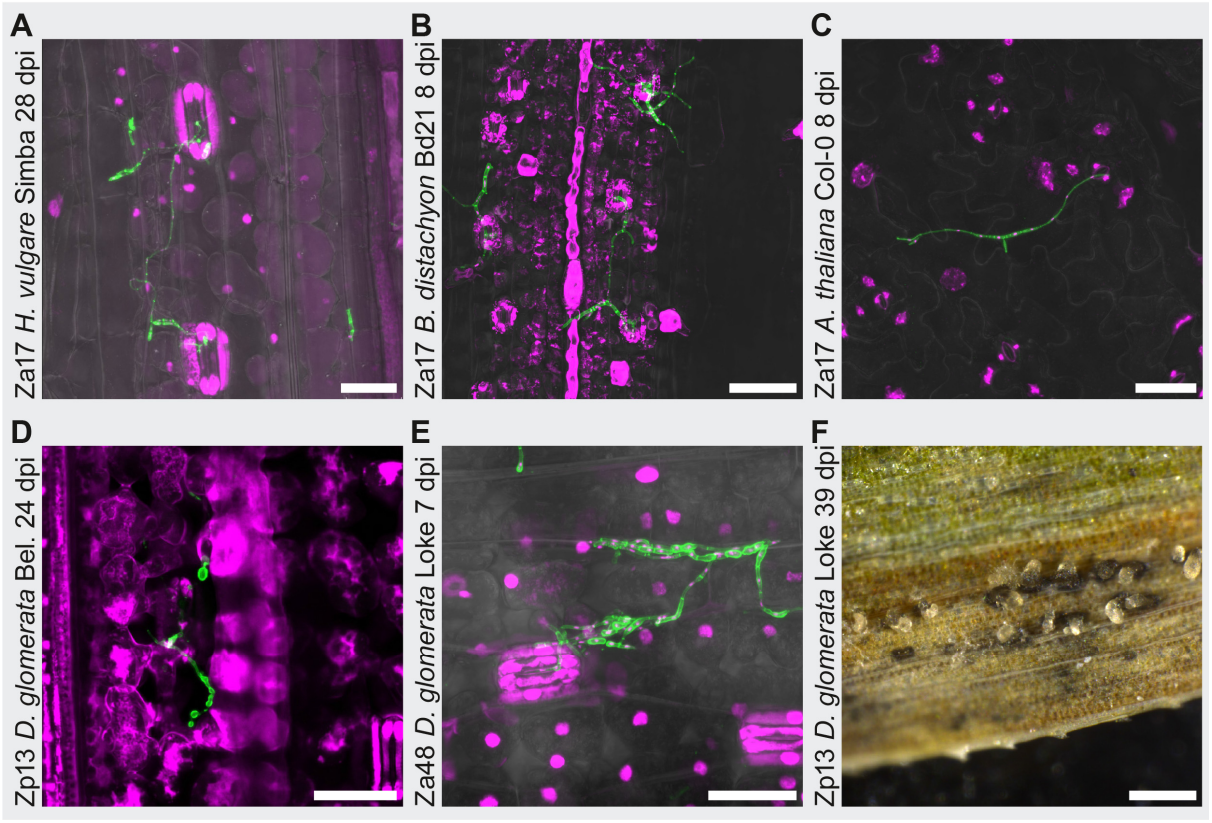

Figure 2. Infections of *Z. pseudotritici* and *Z. ardabiliae* isolates on leaves of different plants are mostly incompatible and rarely result in pycnidia formation. (A-E) Micrographs showing infection structures of *Z. pseudotritici* and *Z. ardabiliae*. Development of infecting hyphae was arrested in sub-stomatal cavities of barley **(A)**, the model grass *B. distachyon* **(B)**, and *D. glomerata* Loke **(E)**. Bulging hyphae of Zp13 inside sub-stomatal cavities of *D. glomerata* Belunga **(D)**. Hypha of Za17 crossing *A. thaliana* stoma **(C)**. Maximum projections of confocal image z-stacks, nuclei and plants cells are displayed in *purple*, fungal hyphae and septa in *green*, transmitted image information in *grey*. Scale bars = 40 µm. **(F)** Rare pycnidia formation of Zp13 on *D. glomerata* Loke at 39 dpi. Scale bar = 200 µm.

Abiotic stress and leaf age matter for the outcome of *Zymoseptoria* infections

Our next step was to investigate factors that possibly contribute to episodic pycnidia formation on otherwise incompatible host grasses. Hence, we tested the influence of light stress and leaf age on the outcome of *Zymoseptoria* infections as compromised host physiology and senescence might facilitate pycnidia development. To this end, we brush-inoculated second leaves of the non-host grass *Triticum aestivum* cultivar Obelisk with cells of *Z. pseudotritici* Zp13, *Z. ardabiliae* Za17, and mock treatment and grew plants under standard and light stress conditions for 28 days post inoculation.

Necrotic leaf area was measured by automated analysis of scanned leaf images and leaves were manually screened for fruiting bodies using a stereo-microscope. Independent of the treatment (fungal cells or mock), leaves of plants grown under light stress conditions showed significantly higher necrosis levels (one-sided Mann-Whitney *U* tests, $P \leq 0.0064$) than plants grown under standard conditions (Fig 3A). We exclude that the observed necrosis is fungal-induced as mock-treated leaves are equally affected (Fig 3A).

Under light stress conditions, pycnidia were found on two and three of 24 wheat leaves for *Z. pseudotritici* Zp13 (Fig 3B) and *Z. ardabiliae* Za17 (Fig 3C), respectively. Initially, increasing photosynthetically active photon flux densities induce higher photosynthetic activity in plants until the absorbed light cannot be utilized in photosynthesis anymore (Demmig-Adams & Adams, 1992). Although plants have developed photoprotection mechanisms to repair and prevent photodamage (Kasahara *et al.*, 2002), excess light leads to increased production of reactive oxygen species (ROS), in particular singlet oxygen (Triantaphylidès & Havaux, 2009). The resulting oxidative stress might have damaged the leaf tissue resulting in the observed increased necrosis levels. We hypothesize that this light-induced erosion of the plant tissue facilitated wheat colonization and reproduction of the non-adapted *Z. pseudotritici* and *Z. ardabiliae*.

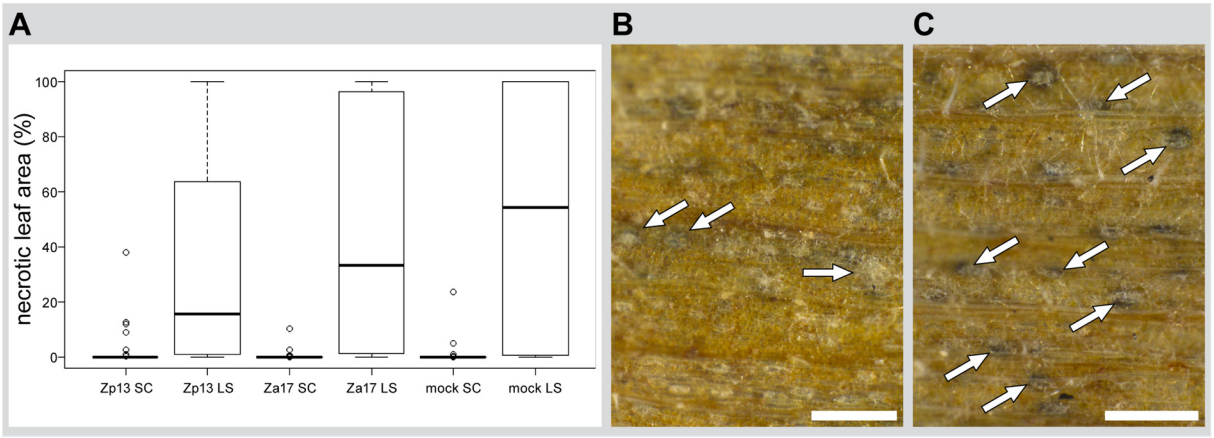

Figure 3. Pycnidia can develop in wheat leaf tissue affected by light stress. (A) Growth of *T. aestivum* Obelisk plants under light stress (LS) conditions leads to significantly higher necrosis levels (one-sided Mann-Whitney *U* tests, $P \leq 0.0064$) as in plants grown under standard conditions (SC) 28 days post inoculation (dpi) and is independent of the applied treatment. SC: 39 plants per treatment tested, LS: 24 plants per treatment tested. **(B-C)** Asexual pycnidia (arrows) of *Z. pseudotritici* Zp13 **(B)** and of *Z. ardabiliae* Za17 **(C)** were found on wheat plants grown under light stress conditions 28 dpi. Scale bars = 200 µm.

To study the influence of leaf age, we performed plant infection assays where we inoculated grass leaves of different ages to test whether *Zymoseptoria* spp. can develop pycnidia on leaves affected by natural senescence. We inoculated second leaves of *T. aestivum* cultivar Obelisk after 7, 21, and 35 days and of *D. glomerata* Loke after 16 and 30 days of growth under standard phytochamber conditions with *Z. tritici* Zt05 and Zt10, *Z. pseudotritici* Zp13 and Zp72, and *Z. ardabiliae* Za17 and Za48. At the time of inoculation, the 35-day old wheat leaves were already fully necrotic.

Leaves were harvested and disease symptoms were analyzed at 21 days post inoculation (dpi) (plant age: 28 days), 24 dpi, and 10 dpi (plant age both: 45 days) for wheat and at 38 dpi (plant age: 54 days) and 28 dpi (plant age: 58 days) for *D. glomerata*. Results for quantitative disease symptoms assessed manually (Fig 4) and by automated analyses of scanned leaf images (S1 Fig) were not consistent. It was demonstrated that automated analysis of leaf images is more precise in assessing quantitative differences in virulence of *Z. tritici* (Stewart & McDonald, 2014) and the method is becoming the standard tool for high-throughput virulence phenotyping (Stewart *et al.*, 2016). However, on senescent leaves, in particular on the older wheat plants, image analysis identified structures that we could not confirm as pycnidia by manual inspection of leaves and leaf images. These false-positive results might be caused by the particular appearance of senescent leaves and suggest that for evaluation of *Zymoseptoria* spp. infections of senescent host tissue manual visual screenings are more suitable.

Independent of fungal inoculation or mock treatment, we observed almost 100% necrosis for all second leaves of plants older than 28 days, likely due to senescence (Fig 4). 28-day old wheat plants (21 dpi) showed high levels of necrosis, mainly on leaves inoculated with *Z. tritici*, and we observed high numbers of pycnidia for Zt05 and Zt10 and some pycnidia for *Z. ardabiliae* Za48 (Fig 4). In contrast, no pycnidia were found on wheat leaves that were inoculated after 21 days of growth and screened at 24 dpi, and very few pycnidia were identified for the isolates Zt05, Zt10, Za17, and Za48 at 10 dpi on leaves of 45-day old plants (Fig 4).

Irrespective of leaf age, pycnidia were observed on *D. glomerata* leaves inoculated with *Z. pseudotritici* Zp72 and *Z. ardabiliae* Za48 (Fig 4).

To confirm our observations and fungal infections, we incubated the respective leaves in petri dishes to induce pycnidia maturation and spore release. We examined these leaves again using a stereo-microscope to re-assess pycnidia and we isolated pycnidiospores from six leaves. Thereby, we confirmed pycnidia formation for *Z. tritici* isolates Zt05 and Zt10 on leaves of 28-day old wheat plants 21 dpi (Fig 5A), but not on 45-day old plants 10 dpi (Fig 5D). Structures observed on wheat leaves inoculated with *Z. ardabiliae* Za17 and Za48 could not be confirmed as *Zymoseptoria* fruiting bodies (Fig 5F). Likely, the pycnidia-like structures were formed by contaminating organisms as we observed strong colonization by putatively saprotrophic microbes on the respective leaves after incubation (Fig 5 E and G). However, Zp72 and Za48 pycnidia on *D. glomerata* leaves could be confirmed (Fig 5 B and C). We re-isolated pycnidiospores of both

isolates from *D. glomerata* and of Zt05 from wheat leaves (28-day old plants) and confirmed the *Zymoseptoria* species by sequencing of ITS and *β-Tubulin* (S2 Fig).

Our findings demonstrate that leaf age and senescence-related changes in host physiology play important roles for the outcome of *Z. tritici* infections. *Z. tritici* is specialized to wheat and was described as a hemibiotrophic pathogen. Infections are characterized by a long symptomless phase that is followed by rapid host cell death and necrotrophic colonization (Ponomarenko *et al.*, 2011; Goodwin *et al.*, 2011). Our results suggest that for successful infections and lifecycle completion, *Z. tritici* strongly depends on the interaction with living host tissue for a long initial phase as no pycnidia were developed on wheat leaves that were affected by natural senescence at the time of inoculation or shortly afterwards.

In this experiment, asexual fruiting bodies of *Z. pseudotritici* and *Z. ardabiliae* isolates developed on *D. glomerata* leaves but not on wheat. However, pycnidia were found only on a small number of leaves and developed episodically and independent of host leaf age. Based on these observations, we cannot draw further conclusions about pathogenesis of both species. However, for none of the three *Zymoseptoria* species we observed growth on dead wheat tissue by confocal microscopy analyses of leaves affected by natural senescence. This suggests that *Zymoseptoria* species depend on interactions with living host cells during initial infection stages and can only grow and feed from dead host tissue after a lifestyle switch as described for the root endophyte *Piriformospora indica* (Zuccaro *et al.*, 2011) or *Colletotrichum* species (O'Connell *et al.*, 2012; Hacquard *et al.*, 2016).

To detect rare pycnidia formation and estimate quantitative virulence if pycnidia only develop episodically, both methods for screening *Zymoseptoria* symptoms - manual visual evaluation and automated analyses of leaf images - produce some false-positive results likely caused by the particular appearance of senescent leaves and pycnidia-like structures of contaminating microbes. For future experiments involving senescent host tissue, we propose to combine both methods and confirmation of infecting species by re-isolation to minimize false-positive pycnidia identification.

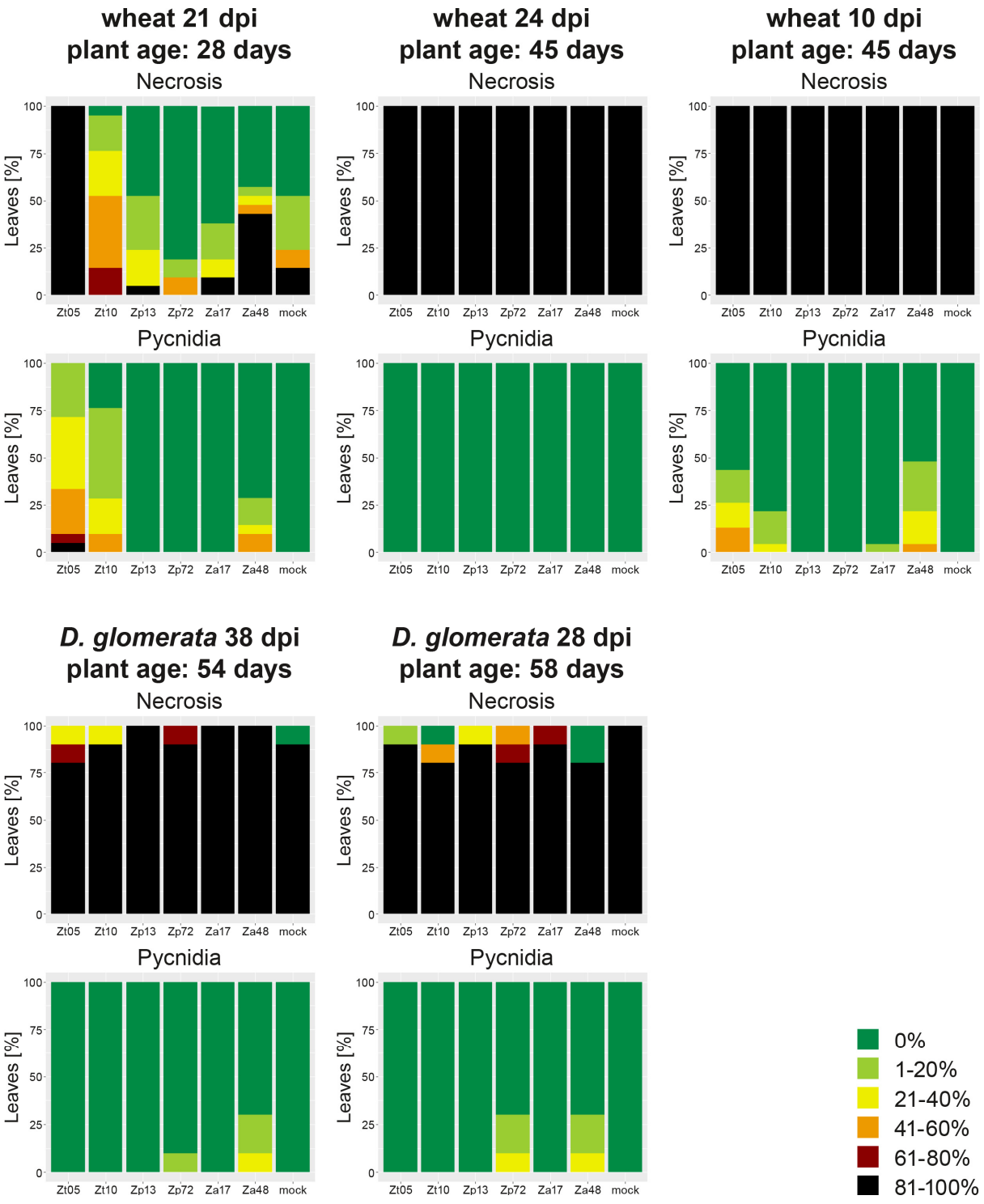

Figure 4. Necrosis and pycnidia coverage of *T. aestivum* Obelisk and *D. glomerata* Loke leaves inoculated with *Zymoseptoria* spp. at different plant ages identified by manual visual evaluation. Quantitative differences in necrosis and pycnidia coverage of inoculated leaf areas were manually assessed based on six categories: 0 (without visible symptoms), 1 (1-20 %), 2 (21-40 %), 3 (41-60 %), 4 (61-80 %), 5 (81-100 %). 21 wheat and 10 *D. glomerata* leaves were screened per treatment (fungal inoculation or mock) and leaf age. Leaves of plants older than 28 days were largely necrotic, independent of fungal inoculation or mock treatment. Pycnidia and

pycnidia-like structures were observed for *Z. tritici* isolates on wheat leaves as well as for *Z. pseudotritici* Zp72 and *Z. ardabiliae* Za17 and Za48 on necrotic wheat and *D. glomerata* leaves.

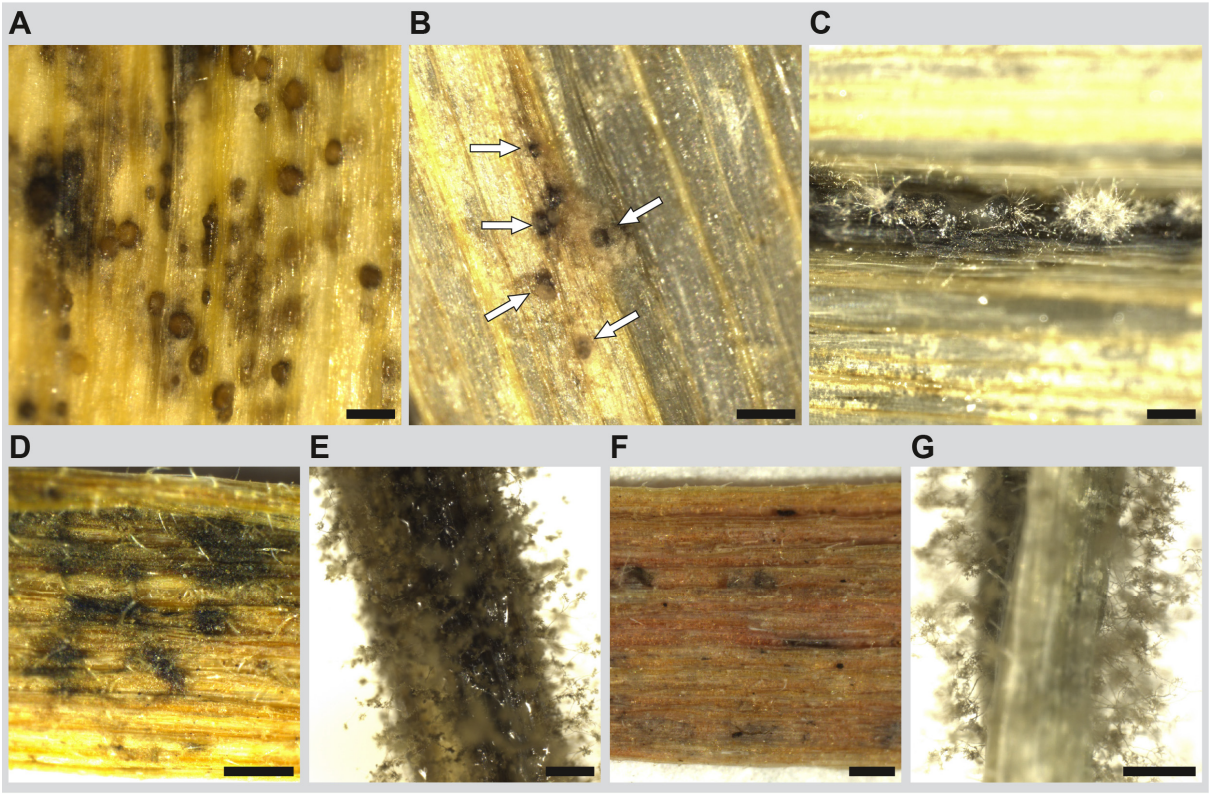

Figure 5. Asexual reproduction of *Zymoseptoria* spp. depends on host species and host physiology. Pycnidia of *Zymoseptoria* spp. isolates on wheat and *D. glomerata* leaves and pycnidia-like structures of contaminating microbial organisms. **(A)** Asexual fruiting bodies of *Z. tritici* Zt05 on leaf of 28-day old wheat plant. **(B)** Pycnidia releasing pycnidiospores (arrows) of *Z. pseudotritici* Zp72 on leaf of 54-day old *D. glomerata* plant. **(C)** Pycnidiospores on top of *Z. ardabiliae* Za48 pycnidia that develop filaments on leaf of 58-day old *D. glomerata* plant. **(D-G)** Pycnidia-like structures and filamentous growth of contaminating microorganisms on leaves of 45-day old wheat plants **(D-E)** and 28-day old wheat plants **(F-G)**. Scale bars = 200 µm.

Fluorescent *Zymoseptoria* spp. strains as tools to investigate plant-associated lifestyles

Fluorescence microscopy and genetically modified fluorescent strains are highly valuable tools to study fungal biology and plant-fungal interactions (Lorang *et al.*, 2001; Rath *et al.*, 2014; Minker *et al.*, 2016). Expression of different fluorescent proteins and additional markers such as antibiotic resistances allows detection and easy selection, and facilitates a wide range of experimental approaches that not only allow to study plant-fungal but also fungal-fungal interactions *in vitro* as well as *in planta*.

In order to generate versatile tools for further studies of the plant-associated lifestyles of *Zymoseptoria* species, we engineered mutants of the *Z. tritici* isolates IPO323, Zt05, Zt10, *Z. pseudotritici* Zp13, and *Z. ardabiliae* Za17 that cytoplasmically express the green fluorescent protein ZtGFP (Kilaru *et al.*, 2015) and are resistant to the antibiotic Geneticin or that express the red fluorescent protein mCherry (Schuster *et al.*, 2015) in combination with resistance to Hygromycin.

Fungal cells were transformed by *Agrobacterium*-mediated transformation (Zwiers & De Waard, 2001) and the respective genes were integrated at non-coding genomic loci (S3 Table) in order to avoid disruption of coding sequences and minimize interference. Correct integrations of the constructs were confirmed by PCR screens and Southern analyses (S1 Table). Translation of ZtGFP and mCherry in the transformed *Zymoseptoria* strains was confirmed by confocal microscopy of single cells grown in axenic culture. The *Ztgfp*-carrying mutant strains showed strong green fluorescence in the range of 490 – 543 nm upon excitation with a 488-nm argon laser (Fig 6 A and C). The *mCherry*-carrying strains showed bright red fluorescence in the range of 579 – 650 nm upon excitation with a 561-nm diode laser (Fig 6 B and D). As previously reported (Kilaru *et al.*, 2015; Schuster *et al.*, 2015), wildtype *Zymoseptoria* spp. cells showed almost no autofluorescence upon excitation at 488 nm and 561 nm (Fig 6).

Bright fluorescence of the generated *Zymoseptoria* spp. mutants will allow us to conduct *in vivo in planta* microscopy of plant-fungal interactions as well as of plant tissues infected with *Zymoseptoria* strain mixtures. Successful infections of host-adapted biotrophic pathogens have been shown to facilitate opportunistic co-infections of non-adapted pathogens as plant immunity is already suppressed (McMullan *et al.*, 2015). Preliminary results indicate that *Z. tritici* infections induce higher susceptibility of wheat as quantitative colonization of a non-adapted bacterial plant pathogen is strongly increased in co-infections (Heike Seybold, unpublished). We plan to perform wheat infection experiments by co-inoculating *Z. tritici* and *Z. pseudotritici* or *Z. ardabiliae* strains to test if the non-adapted *Zymoseptoria* spp. grow and reproduce when the wheat tissue is compromised by infections caused by the adapted pathogen *Z. tritici*. The different antibiotic resistances will allow us to re-isolate and separate the mixed strains from infected leaves to quantify their rates of colonization and reproduction inside host tissue.

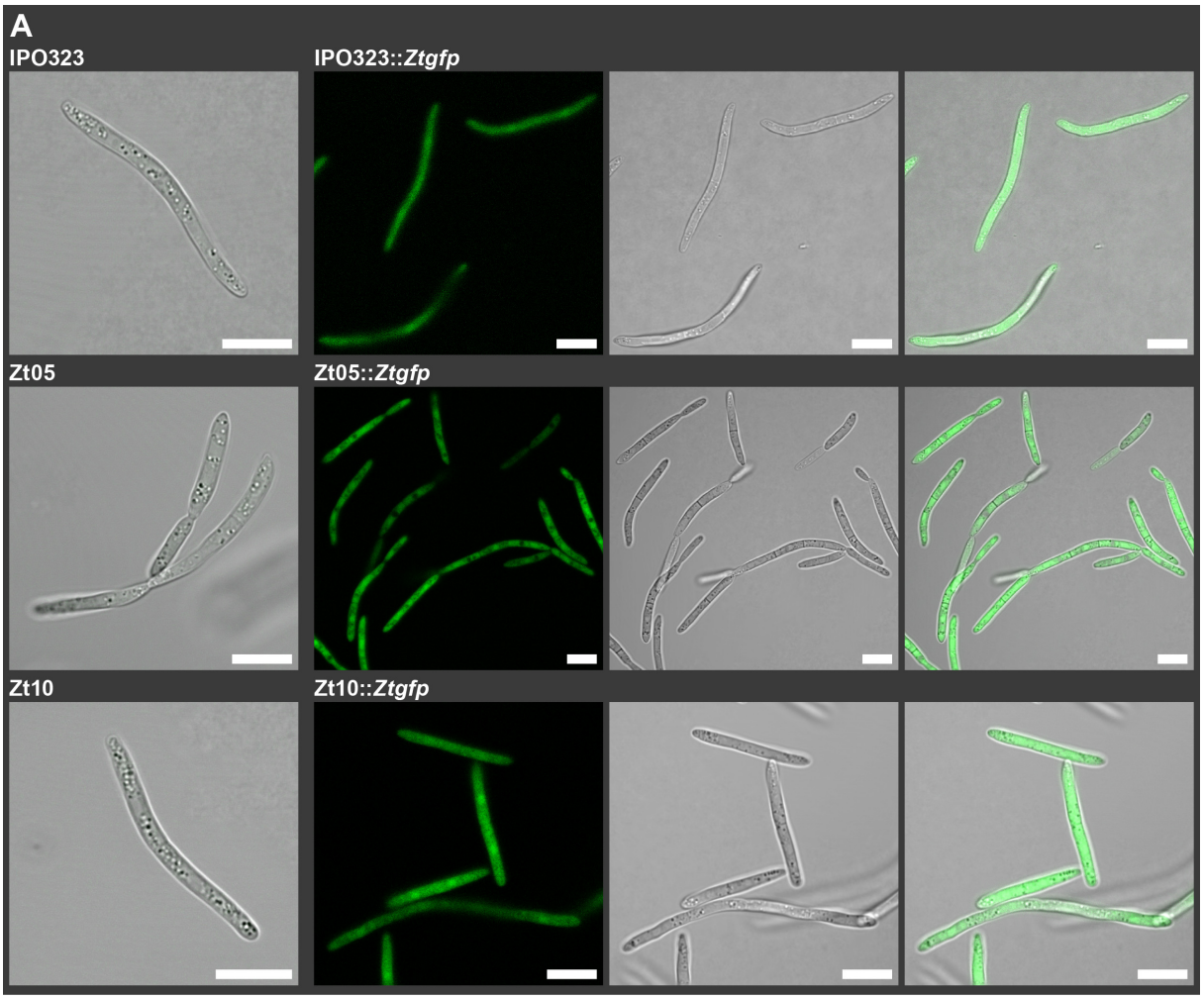
A
IPO323
IPO323::Ztgfp
Zt05
Zt05::Ztgfp
Zt10
Zt10::Ztgfp

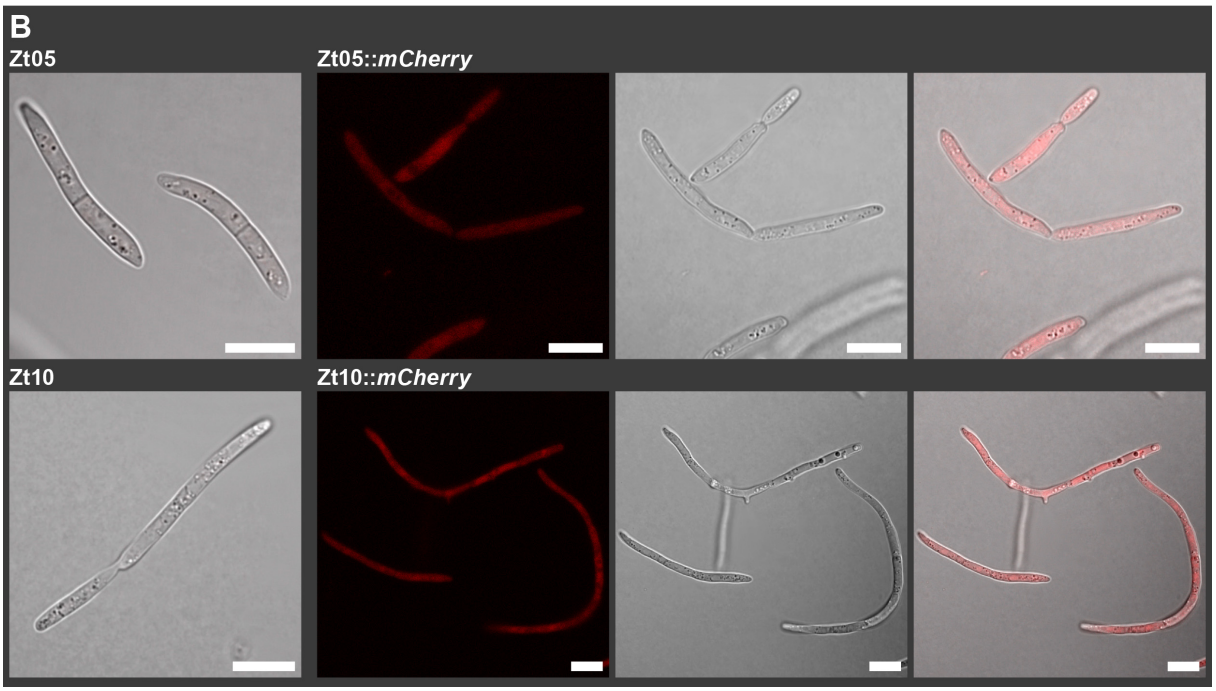
B
Zt05
Zt05::mCherry
Zt10
Zt10::mCherry

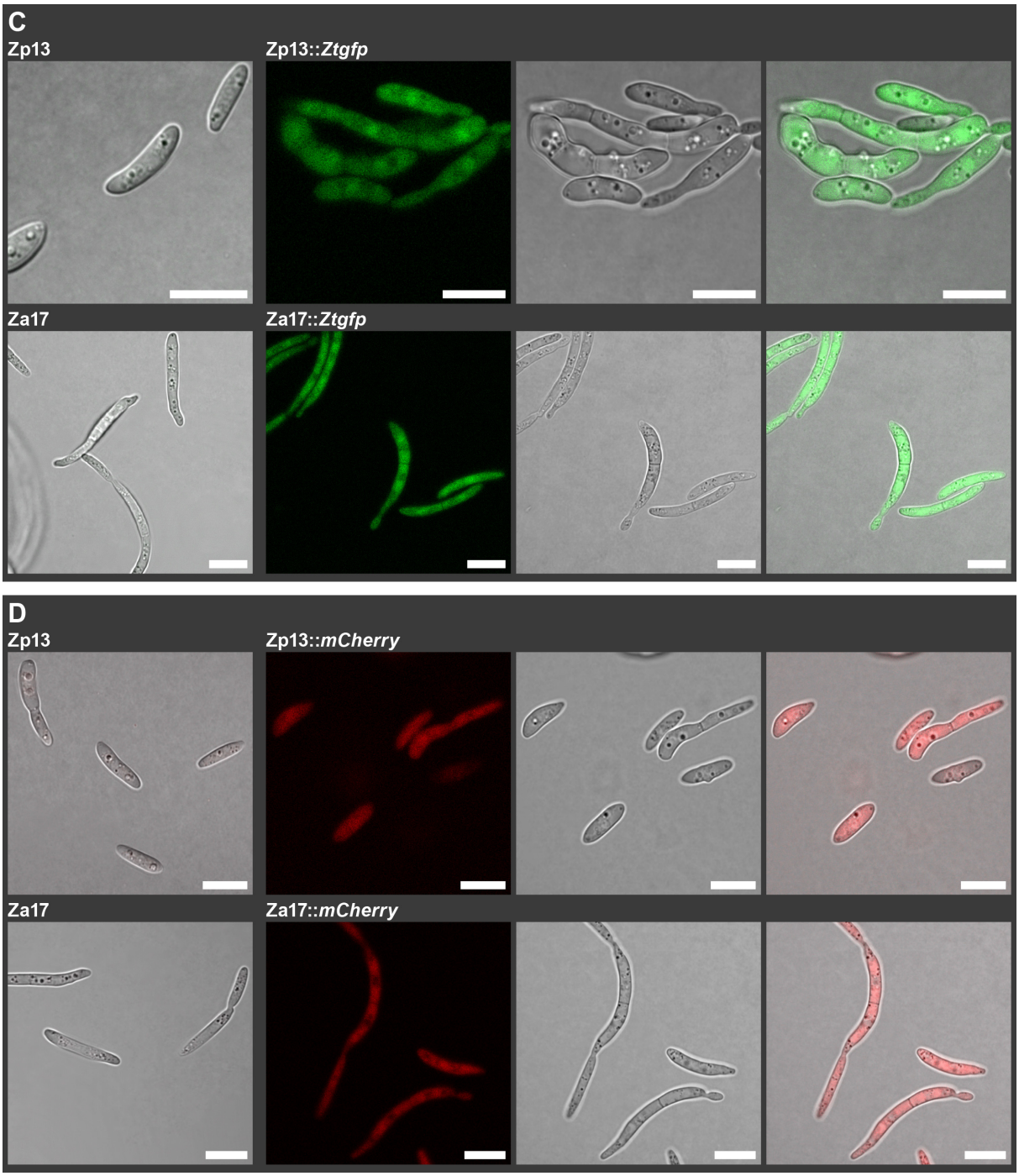

Figure 6. Cytoplasmic expression of ZtGFP and mCherry in modified *Zymoseptoria* spp. strains. Micrographs showing green and red fluorescence of *Zymoseptoria* spp. strains, respective reference transmitted images, and overlays of fluorescence and transmitted images. Wildtype cells (only overlays shown) show almost no autofluorescence. Transformed *Zymoseptoria* spp. cells emit strong green or red fluorescence upon excitation with 488 nm (ZtGFP) or 561 nm (mCherry). All images were acquired and processed identically. Scale bars = 10 µm. **(A)** Cytoplasmic ZtGFP in *Z. tritici* isolates IPO323, Zt05, and Zt10. **(B)** Cytoplasmic mCherry in *Z. tritici* isolates Zt05 and Zt10. **(C)** Cytoplasmic ZtGFP in *Z. pseudotritici* Zp13 and *Z. ardabiliae* Za17. **(D)** Cytoplasmic mCherry in *Z. pseudotritici* Zp13 and *Z. ardabiliae* Za17.

Conclusions

With the experiments performed so far, we have not been successful in identifying and establishing host species for *Z. pseudotritici* and *Z. ardabiliae* under laboratory conditions. Nevertheless, we have gained insight in the plant-associated lifestyles of both species which we propose to be different from the lifestyle of the closely related wheat pathogen *Z. tritici*. Based on the observation of episodic pycnidia formation and lifecycle completion on compromised, detached grass leaves, we suggest that *Z. pseudotritici* and *Z. ardabiliae* are weak pathogens that rely on opportunistic infections. Opportunistic pathogens are able to rapidly occupy and colonize new niches but also depend on the availability of those niches to complete their lifecycle. Opportunistic fungal pathogens hold long-lived environmental stages that are mostly associated with soil and saprotrophic growth, and only become pathogenic when compatible ecological niches, e.g. immunocompromised hosts, are available (Druzhinina *et al.*, 2011; Fisher *et al.*, 2012; Kozubowski & Heitman, 2012; Bignell, 2014). Ascospores, the primal source of inoculum for *Z. tritici*, are found in the soil on wheat stubble and debris (Scott *et al.*, 1988) but further, in-depth knowledge about putative environmental, soil-associated stages of the *Zymoseptoria* species is lacking. However, in our experiments *Z. pseudotritici* and *Z. ardabiliae* rarely infected host plants and only developed pycnidia on leaves that were compromised by advanced leaf age, accelerated senescence, or abiotic stress. This indicates an opportunistic pathogen lifestyle that strongly depends on the availability of a particular ecological niche which in this case is likely defined by host grass physiology.

Zymoseptoria species depend on host tissue for mating and sexual recombination (Habig et al., *in prep*). We speculate that limited host niche availability in the natural habitat of *Z. pseudotritici* and *Z. ardabiliae* contributes to strong population bottlenecks and subsequently to the lower intraspecific genetic diversity in populations of both species (Stukenbrock *et al.*, 2011) as compared to the genetically highly variable *Z. tritici* (Linde *et al.*, 2002; Zhan *et al.*, 2003; McDonald *et al.*, 2016). Further, weak pathogenicity limits the production of pycnidiospores and sexual ascospores which are in particular important for long-distance dispersal (Shaw & Royle, 1989). We propose that this plays an important role for the limited geographical distribution of *Z. pseudotritici* and *Z. ardabiliae* as both species are reported to be endemic in the Middle East (Stukenbrock *et al.*, 2012). We hypothesize that the shared ancestral species had a similar plant-associated lifestyle as the putatively opportunistic pathogens *Z. pseudotritici* and *Z. ardabiliae*. In this case, speciation and host-specialization of *Z. tritici* must have involved rapid gain of traits related to aggressiveness and killing of host tissue.

To be able to fully explore the potential of the closely related *Zymoseptoria* species as a model for speciation and host specialization of plant pathogens, an important future challenge will be to identify the factors that create compatible host niches for *Z. pseudotritici* and *Z. ardabiliae*.

In collaboration with Iranian colleagues, we will collect additional *Z. pseudotritici* and *Z. ardabiliae* isolates and local grass species to increase pathogen and host diversity in future experiments and to investigate the role of environmental stages. We plan to conduct additional controlled infection studies on compromised grass species by specifically applying abiotic stresses, by inducing plant senescence by hormone treatment, and by using immuno-deficient mutants of the model grass *B. distachyon*. Further, we will take advantage of the generated fluorescent *Zymoseptoria* strains and study infections of strain mixtures, e.g. by *in vivo in planta* confocal microscopy. To gain insight in the genomic traits underlying the possibly different plant-associated lifestyles, we will perform comparative genome analyses including *Z. tritici*, *Z. pseudotritici* and *Z. ardabiliae* and mine their genomes for plant infection-related traits like effectors, hydrolytic enzymes and genes involved in secondary metabolite production.

Acknowledgement

We are grateful to Alina Nommensen and Ben Auxier for providing assistance with plasmid generation and transformations, and thank Mareike Möller and Christoph J. Eschenbrenner for help with plant infection experiments.

Funding statement

This work was supported by intramural funding of the Max Planck Society and a personal grant from the State of Schleswig-Holstein to Eva H. Stukenbrock. The funders had no role in study design, data collection and analyses, decision to publish, or preparation of the manuscript.

References

Amand PCS, Wehner TC. **1995**. Greenhouse, Detached-leaf, and Field Testing Methods to Determine Cucumber Resistance to Gummy Stem Blight. *J. Amer. Soc. Hort. Sci* **120**: 673–680.

Arraiano LS, Brading PA., Brown JKM. **2001**. A detached seedling leaf technique to study resistance to Mycosphaerella graminicola (anamorph Septoria tritici) in wheat. *Plant Pathology* **50**: 339–346.

Banke S, McDonald BA. **2005**. Migration patterns among global populations of the pathogenic fungus Mycosphaerella graminicola. *Molecular ecology* **14**: 1881–96.

Bignell E. **2014**. Aspergillus fumigatus : Saprotroph to Pathogen II . Aspergillus fumigatus : A Three-Step Transition from Saprotroph to Pathogen. *Human Fungal Pathogens, 2nd edition*.

Bowler J, Scott E, Tailor R, Scalliet G, Ray J, Csukai M. **2010**. New capabilities for Mycosphaerella graminicola research. *Molecular Plant Pathology* **11**: 691–704.

Browne RA., Cooke BM. **2004**. Development and Evaluation of an in vitro Detached Leaf Assay forc Pre-Screening Resistance to Fusarium Head Blight in Wheat. *European Journal of Plant Pathology* **110**: 91–102.

Demmig-Adams B, Adams WW. **1992**. Responses of plants to high light stress. *Annu. Rev. Plant Physiol. Plant Mol. Biol.* **43**: 599–626.

Druzhinina IS, Seidl-Seiboth V, Herrera-Estrella A, Horwitz BA, Kenerley CM, Monte E, Mukherjee PK, Zeilinger S, Grigoriev I V., Kubicek CP. **2011**. Trichoderma: The genomics of opportunistic success. *Nature Reviews Microbiology* **9**: 749–759.

Edgar RC. **2004**. MUSCLE: Multiple sequence alignment with high accuracy and high throughput. *Nucleic Acids Research* **32**: 1792–1797.

Fisher MC, Henk DA., Briggs CJ, Brownstein JS, Madoff LC, McCraw SL, Gurr SJ. **2012**. Emerging fungal threats to animal, plant and ecosystem health. *Nature* **484**: 186–194.

Gibson DG, Young L, Chuang RY, Venter JC, Hutchison CA, Smith HO. **2009**. Enzymatic assembly of DNA molecules up to several hundred kilobases. *Nature Methods* **6**: 343–345.

Glass NL, Donaldson GC. **1995**. Development of primer sets designed for use with the PCR to amplify conserved genes from filamentous ascomycetes. *Applied and Environmental Microbiology* **61**: 1323–1330.

Goodwin SB, M'barek S Ben, Dhillon B, Wittenberg AHJ, Crane CF, Hane JK, Foster AJ, Van der Lee T a J, Grimwood J, Aerts A, *et al.* 2011. Finished genome of the fungal wheat pathogen Mycosphaerella graminicola reveals dispensome structure, chromosome plasticity, and stealth pathogenesis. *PLoS genetics* **7**: e1002070.

Gouy M, Guindon S, Gascuel O. 2010. Sea view version 4: A multiplatform graphical user interface for sequence alignment and phylogenetic tree building. *Molecular Biology and Evolution* **27**: 221–224.

Habig M, Quade J, Stukenbrock EH. 2017. Forward genetics approach reveals host-genotype dependent importance of accessory chromosomes in the fungal wheat pathogen Zymoseptoria tritici. *mBio* **8**: 1–16.

Hacquard S, Kracher B, Hiruma K, Münch PC, Garrido-Oter R, Thon MR, Weimann A, Damm U, Dallery J-F, Hainaut M, *et al.* 2016. Survival trade-offs in plant roots during colonization by closely related beneficial and pathogenic fungi. *Nature Communications* **7**: 11362.

Haueisen J, Möller M, Eschenbrenner CJ, Grandaubert J, Seybold H, Adamiak H, Stukenbrock EH. 2017. Extremely flexible infection programs in a fungal plant pathogen. *bioRxiv*. doi: 10.1101/229997

Kasahara M, Kagawa T, Olkawa K, Suetsugu N, Miyao M, Wada M. 2002. Chloroplast avoidance movement reduces photodamage in plants. *Nature* **420**: 829–832.

Kilaru S, Schuster M, Studholme D, Soanes D, Lin C, Talbot NJ, Steinberg G. 2015. A codon-optimized green fluorescent protein for live cell imaging in Zymoseptoria tritici. *Fungal Genetics and Biology* **79**: 125–131.

Kozubowski L, Heitman J. 2012. Profiling a killer, the development of Cryptococcus neoformans. *FEMS microbiology reviews* **36**: 78–94.

Linde CC, Zhan J, McDonald BA. 2002. Population Structure of Mycosphaerella graminicola: From Lesions to Continents. *Phytopathology* **92**: 946–55.

Lorang JM, Tuori RP, Martinez JP, L ST, S RR, A RJ, J WT, B JK, J RR, Dickman MB, *et al.* 2001. Green Fluorescent Protein Is Lighting Up Fungal Biology. *Applied and environmental microbiology* **67**: 1987–1994.

McDonald MC, McGinness L, Hane JK, Williams AH, Milgate A, Solomon PS. 2016. Utilizing Gene Tree Variation to Identify Candidate Effector Genes in Zymoseptoria tritici. *G3 (Bethesda, Md.)* **6**: 779–91.

McMullan M, Gardiner A, Bailey K, Kemen E, Ward BJ, Cevik V, Robert-Seilaniantz A, Schultz-Larsen T, Balmuth A, Holub E, *et al.* 2015. Evidence for suppression of immunity as a driver for genomic introgressions and host range expansion in races of Albugo candida, a generalist parasite. *eLife* **4**: 1–24.

Michel AP, Mian MAR, Davila-Olivas NH, Cañas LA. 2010. Detached leaf and whole plant assays for soybean aphid resistance: differential responses among resistance sources and biotypes. *Journal of Economic Entomology* **103**: 949–957.

Minker KR, Biedrzycki ML, Kolagunda A, Rhein S, Perina FJ, Jacobs SS, Moore M, Jamann TM, Yang Q, Nelson R, *et al.* 2016. Semiautomated confocal imaging of fungal pathogenesis on plants: Microscopic analysis of macroscopic specimens. *Microscopy Research and Technique* **0**: 1–12.

O'Connell RJ, Thon MR, Hacquard S, Amyotte SG, Kleemann J, Torres MF, Damm U, Buiate EA, Epstein L, Alkan N, *et al.* 2012. Lifestyle transitions in plant pathogenic Colletotrichum fungi deciphered by genome and transcriptome analyses. *Nature genetics* **44**: 1060–5.

O'Donnell K, Cigelnik E. 1997. Two Divergent Intragenomic rDNA ITS2 Types within a Monophyletic Lineage of the FungusFusariumAre Nonorthologous. *Molecular Phylogenetics and Evolution* **7**: 103–116.

O'Driscoll A, Kildea S, Doohan F, Spink J, Mullins E. 2014. The wheat-Septoria conflict: a new front opening up? *Trends in plant science* **19**: 602–10.

Ponomarenko A, Goodwin SB, Kema GHJ. 2011. Septoria tritici blotch (STB) of wheat. *Plant Health Instructor*: 1–7.

Poppe S, Dorsheimer L, Happel P, Stukenbrock EH. 2015. Rapidly Evolving Genes Are Key Players in Host Specialization and Virulence of the Fungal Wheat Pathogen Zymoseptoria tritici (Mycosphaerella graminicola). *PLOS Pathogens* **11**: e1005055.

Rath M, Grolig F, Haueisen J, Imhof S. 2014. Combining microtomy and confocal laser scanning microscopy for structural analyses of plant-fungus associations. *Mycorrhiza* **24**: 293–300.

Ritpitakphong U, Falquet L, Vimoltust A, Berger A, Etraux J-PM, L 'haridon F. 2016. The microbiome of the leaf surface of Arabidopsis protects against a fungal pathogen. *New Phytologist*.

Sambrook J, Russell D. 2001. *Molecular cloning: a laboratory manual.* Cold Spring Harbor, N. Y: Cold Spring Harbor Laboratory.

Schuster M, Kilaru S, Guo M, Sommerauer M, Lin C, Steinberg G. **2015**. Red fluorescent proteins for imaging Zymoseptoria tritici during invasion of wheat. *Fungal Genetics and Biology* **79**: 132–140.

Scott PR, Sanderson FR, Benedikz PW. **1988**. Occurrence of Mycosphaerella graminicola, teleomorph of Septoria tritici, on wheat debris in the UK. *Plant Pathology* **37**: 285–290.

Shaw MW, Royle DJ. **1989**. Airborne Inoculum as a Major Source of Septoria-Tritici (Mycosphaerella-Graminicola) Infections in Winter-Wheat Crops in the Uk. *Plant Pathology* **38**: 35–43.

Smart CM. **1994**. Gene expression during leaf senescence. *New Phytologist* **126**: 419–448.

Stewart EL, Hagerty CH, Mikaberidze A, Mundt CC, Zhong Z, McDonald BA. **2016**. An Improved Method for Measuring Quantitative Resistance to the Wheat Pathogen Zymoseptoria tritici Using High-Throughput Automated Image Analysis. *Phytopathology* **106**: 782–788.

Stewart EL, McDonald BA. **2014**. Measuring quantitative virulence in the wheat pathogen Zymoseptoria tritici using high-throughput automated image analysis. *Phytopathology* **104**: 985–92.

Stukenbrock EH, Banke S, Javan-Nikkhah M, McDonald BA. **2007**. Origin and domestication of the fungal wheat pathogen Mycosphaerella graminicola via sympatric speciation. *Molecular biology and evolution* **24**: 398–411.

Stukenbrock EH, Bataillon T, Dutheil JY, Hansen TT, Li R, Zala M, McDonald BA, Wang J, Schierup MH. **2011**. The making of a new pathogen: insights from comparative population genomics of the domesticated wheat pathogen Mycosphaerella graminicola and its wild sister species. *Genome research* **21**: 2157–66.

Stukenbrock EH, Quaedvlieg W, Javan-Nikhah M, Zala M, Crous PW, McDonald BA. **2012**. Zymoseptoria ardabiliae and Z. pseudotritici, two progenitor species of the septoria tritici leaf blotch fungus Z. tritici (synonym: Mycosphaerella graminicola). *Mycologia* **104**: 1397–407.

Triantaphylidès C, Havaux M. **2009**. Singlet oxygen in plants: production, detoxification and signaling. *Trends in Plant Science* **14**: 219–228.

Vandenkoornhuyse P, Quaiser A, Duhamel M, Le Van A, Dufresne A. **2015**. The importance of the microbiome of the plant holobiont. *New Phytologist* **206**: 1196–1206.

White TJ, Bruns T, Lee S, Taylor J. **1990**. AMPLIFICATION AND DIRECT SEQUENCING OF FUNGAL RIBOSOMAL RNA GENES FOR PHYLOGENETICS. In: PCR Protocols. 315–322.

Yeats TH, Rose JKC. **2013**. The Formation and Function of Plant Cuticles. *Plant Physiology* **163**: 5–20.

Zhan J, Pettway RE, McDonald BA. **2003**. The global genetic structure of the wheat pathogen Mycosphaerella graminicola is characterized by high nuclear diversity, low mitochondrial diversity, regular recombination, and gene flow. *Fungal Genetics and Biology* **38**: 286–297.

Zuccaro A, Lahrmann U, Güldener U, Langen G, Pfiffi S, Biedenkopf D, Wong P, Samans B, Grimm C, Basiewicz M, *et al.* 2011. Endophytic life strategies decoded by genome and transcriptome analyses of the mutualistic root symbiont Piriformospora indica. *PLoS Pathogens* **7**.

Zwiers LH, De Waard MA. **2001**. Efficient Agrobacterium tumefaciens-mediated gene disruption in the phytopathogen Mycosphaerella graminicola. *Current Genetics* **39**: 388–393.

Supplementary Information

Supplementary Tables

All supplementary tables are in .xlsx file format and are deposited on the supplementary USB key.

S1 Table. All *Zymoseptoria* spp. isolates and mutants used and generated in this study.

S2 Table. List of all plasmids used and generated in this study.

S3 Table. Non-coding genomic loci in *Zymoseptoria* spp. used for targeted integrations.

S4 Table. List of all primers used in this study.

Supplementary Figures

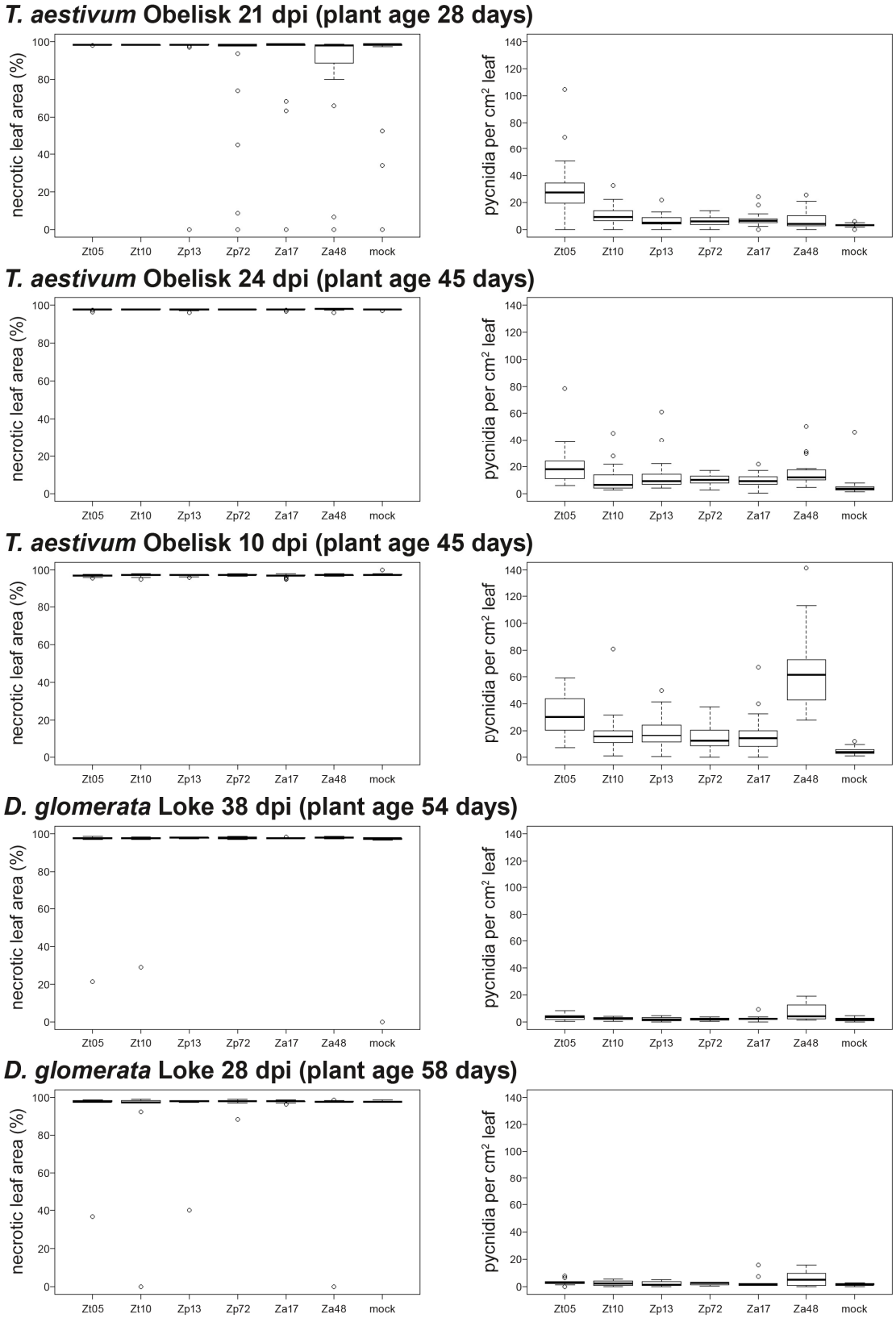

S1 Figure. Necrosis and pycnidia on leaves inoculated with *Zymoseptoria* spp. at different plant ages identified by automated image analyses. Image analyses identified higher necrosis levels than manual visual screening and false-positive pycnidia on senescent leaves. 21 wheat and 10 *D. glomerata* leaves were screened per treatment (fungal inoculation or mock) and leaf age.

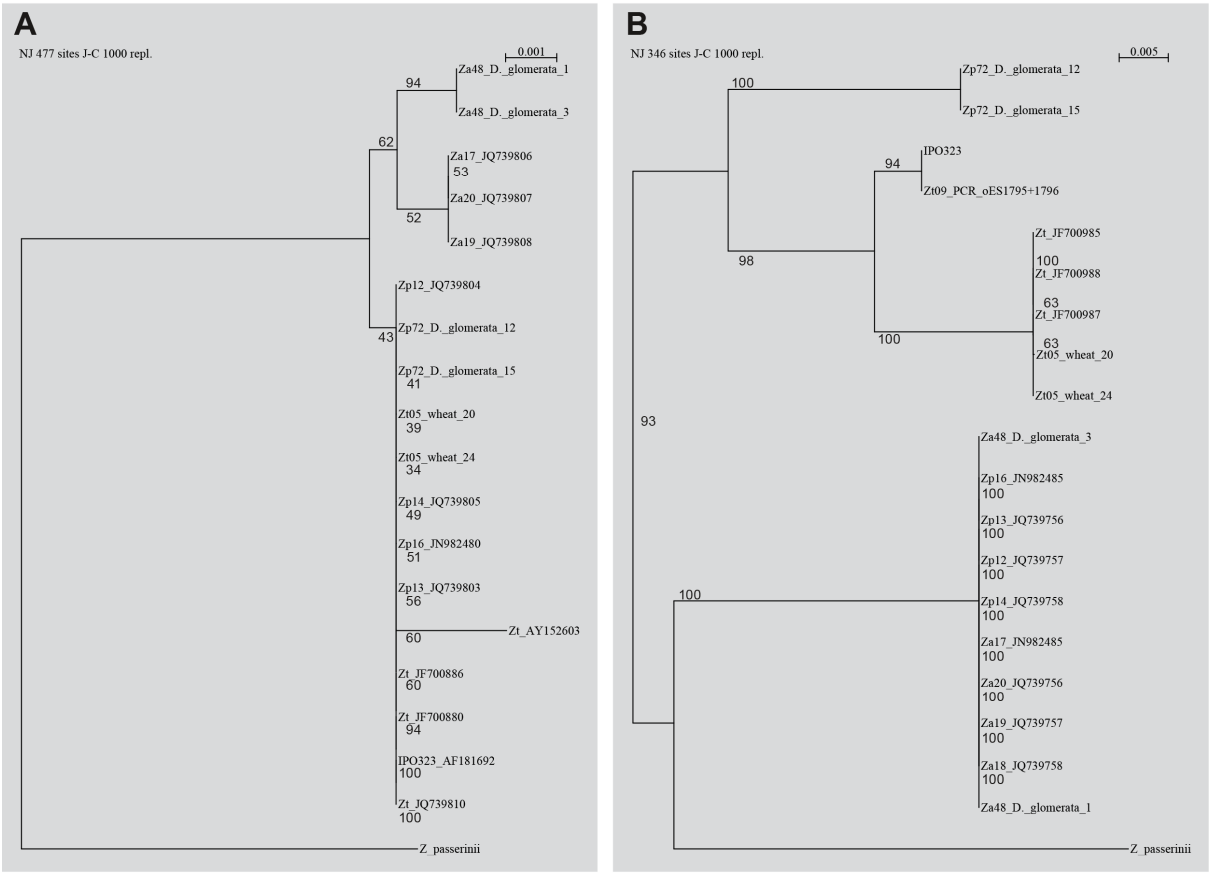

S2 Figure. Neighbor-joining trees from ITS and *β-Tubulin* sequence alignments of *Zymoseptoria* species. (A) ITS and **(B)** *β-Tubulin* sequences amplified from DNA of pycnidiospores, re-isolated from *D. glomerata* leaves inoculated with *Z. pseudotritici* Zp72 and *Z. ardabiliae* Za48, and from wheat leaves inoculated with the *Z. tritici* isolate Zt05, confirm that spores were produced by the respective *Zymoseptoria* species. Bootstrap support values from 1000 replications are indicated at the nodes. *Z. passerinii* serves as outgroup.

General Conclusions and Perspectives

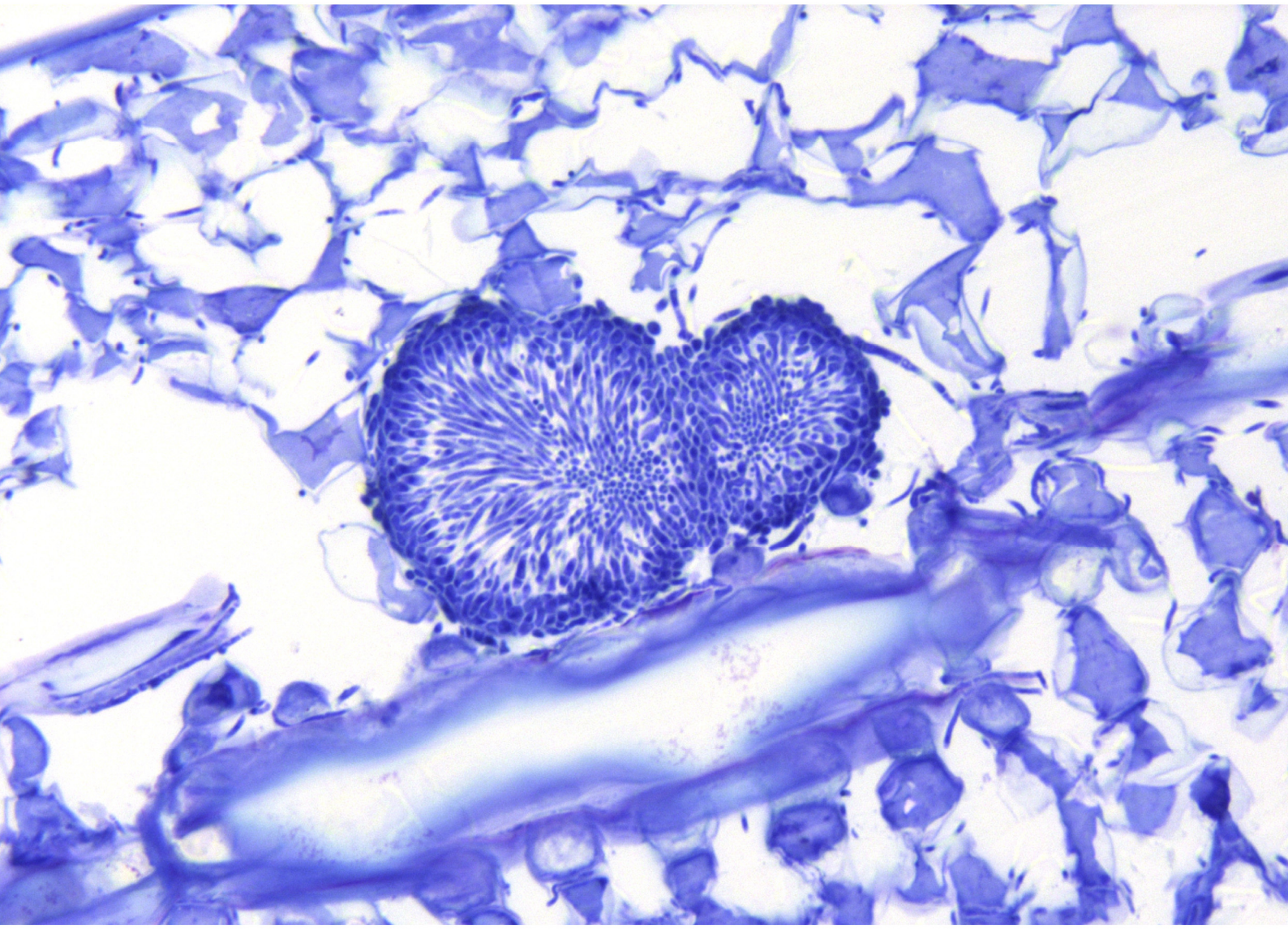

General Conclusions and Perspectives

The aim of this work has been to shed light on the infection biology and host specialization of closely related fungal plant pathogen species that are adapted to different hosts and different ecosystems. To this end, we investigated the infection phenotypes of the highly specialized, world-wide distributed wheat pathogen *Zymoseptoria tritici* and its sister species *Zymoseptoria pseudotritici* and *Zymoseptoria ardabiliae* that infect wild grasses in the Middle East.

Three isolates of *Z. tritici* that differ significantly in their genomic composition are equally virulent on a susceptible wheat cultivar. However, infection development and transcriptional programs are highly variable in these three isolates during colonization and reproduction on leaves of this host genotype. We demonstrated that individuals of a host-specialized plant pathogen have highly differentiated infection programs that are characterized by flexible infection strategies and functional redundancy. A narrow host-range and strong host adaptation did not result in a highly conserved infection program. Isolates share a core infection program but isolate-specific morphological and transcriptional traits strongly define and shape infection programs.

In other pathogens that, like *Z. tritici*, maintain high levels of genetic diversity, e.g. by frequent sexual recombination, host interactions might be similarly variable. Virulence factors such as effectors, secondary metabolites, and plant cell wall degrading enzymes might play an important role in host infections of some pathogen individuals while they are less important for others. The diversity of infection phenotypes in pathogen populations needs to be acknowledged to understand host-pathogen interactions and pathogen evolution and should be considered for the development of sustainable crops and crop protection strategies.

Studying infections of additional genetically distinct *Z. tritici* isolates and infections on more host genotypes will allow to further explore the spectrum of phenotypic diversity and to understand how genomic variation of pathogens influences infection phenotypes.

Diverse infection phenotypes of *Z. tritici* are also important in the context of co-infections. In natural infections, necrotic leaf lesions are composed of several pathogen genotypes (Linde *et al.*, 2002). It will be highly relevant to study intraspecific interactions within lesions, e.g. by using the differentially fluorescent strains, to test whether different infection phenotypes complement or antagonize each other and lead to changes in pathogen virulence and fitness.

Interactions between *Z. tritici* individuals are an important aspect of the wheat-associated microbiota, however, it will be essential to study how different *Z. tritici* strains affect other wheat-colonizing microbes. Strategies for interspecific *Z. tritici*-microbe interactions might be similarly diverse and can shape the wheat microbiome in different ways causing fundamental impacts on plant health (Vandenkoornhuyse *et al.*, 2015).

The *Z. tritici* sister species *Z. pseudotritici* and *Z. ardabiliae* cannot infect wheat. Infecting hyphae cause a plant defense response and are blocked in wheat sub-stomatal cavities. However, during early wheat interactions infection development and gene expression profiles of the three species are conserved to a large extent. We propose that a small number of developmental and transcriptional key traits are involved in facilitating host specialization and determining host specificity in the closely related pathogens. For instance, faster growth and higher phenotypic diversity of *Z. tritici* compared to the sister species might reflect adaptations to a fast developing annual host and to the diversity of wheat cultivars and wheat growing agroecosystems worldwide. Even though cultivated wheat, ancestral wheat species, and wild grasses have a very different ecology, the niche for growth and reproduction of *Zymoseptoria* pathogens in their leaves is considerably conserved, e.g. in terms of morphological infection programs, nutrient composition and availability, and reproduction and dispersal strategies. Hence, for pathogen species that diverged less recently and infect more distantly related host species, we expect more traits to be different because of divergent host adaptation.

Function and contribution to host specialization of the identified candidate genes will be further elucidated by generation and phenotyping of *Zymoseptoria* spp. mutants. We will study how gene deletions of host-specific effector candidates and over or constitutive expression of putative avirulence genes influences virulence and infection phenotypes of *Z. tritici* isolates on wheat. In *Z. pseudotritici* and *Z. ardabiliae* isolates, it will be interesting to modify the expression of the effector candidates that were only up-regulated in *Z. tritici* and to knock out putative avirulence factors to test the effect on wheat infections of both species.

Here, we have conducted comparative analyses of the expression of orthologous *Zymoseptoria* genes. However, we expect that species-specific genes and genomic traits also play important roles in host infection and host adaptation. It would be ideal to study the transcriptomes of several *Zymoseptoria* spp. isolates during all stages of compatible host infections and scan their stage-specific gene expression profiles for common and species-specific patterns. A first step to identify such genomic traits will be comparative analyses of the *Zymoseptoria* spp. genomes focusing on plant infection-related traits such as effectors, carbohydrate-active enzymes, and secondary metabolite genes.

A current limitation of the *Zymoseptoria* spp. model system is the lack of a stable experimental host system for the wild grass-associated species. So far, we have not succeeded to identify and establish host grasses that would allow high-throughput virulence screenings, as for *Z. tritici* on wheat. Nevertheless, we have shed light on the plant-associated lifestyles of *Z. pseudotritici* and *Z. ardabiliae*. Our findings suggest that both fungi are weak opportunistic pathogens that depend on the availability of compatible niches to grow and reproduce in grass leaves. We demonstrate that changes, and in particular impairment of the physiological state of the host tissue, triggered

by leaf senescence and abiotic stress, lead to the emergence of compatible host niches for *Z. pseudotritici* and *Z. ardabiliae*. We speculate that the common ancestor of the three *Zymoseptoria* species had a similar opportunistic plant-associated lifestyle. In this case, speciation and host specialization of *Z. tritici* involved transitioning from a weak opportunistic pathogen to a highly virulent, host-specialized species and must have been facilitated by a rapid development of traits related to aggressiveness, virulence, and killing of host cells.

To be able to gain more insight into the infection biology and lifestyle of the wild grass-associated species, it is fundamental to study and identify the factors that create compatible host niches.

Infection studies, whereby grass leaf tissue becomes compromised in a controlled way, e.g. by specific application of abiotic stress, by induction of host senescence applying hormone treatments, or by using functionally characterized immuno-deficient mutants of model plants, will allow to elucidate the host factors that facilitate infections of *Z. pseudotritici* and *Z. ardabiliae*. Mixed infections with *Z. tritici* isolates on wheat leaves, preferably using the differentially labelled strains, will provide first insight to what extent other grass-associated microbes contribute to the generation of a compatible host niche for *Z. pseudotritici* and *Z. ardabiliae*.

Collaborations with Iranian colleagues will allow us to include additional *Z. pseudotritici* and *Z. ardabiliae* isolates and grass genotypes originating from the Middle East in future experiments. New *Zymoseptoria* collections in the Middle East will also allow to investigate potential soil-associated, environmental stages that have been described in other opportunistic pathogen species and that are very important to survive outside the host (Fisher *et al.*, 2012).

Gaining more insight into the biology of the wild relatives of pathogens will support the identification of microorganisms that could serve as the “raw material” for future pathogens and will help to develop strategies to prevent and fight the emergence of new pathogenic strains.

References General Introduction & Conclusions and Perspectives

Banke S, McDonald BA. **2005**. Migration patterns among global populations of the pathogenic fungus Mycosphaerella graminicola. *Molecular ecology* **14**: 1881–96.

Becker M, Becker Y, Green K, Scott B. **2016**. The endophytic symbiont Epichloe festucae establishes an epiphyllous net on the surface of Lolium perenne leaves by development of an expressorium, an appressorium-like leaf exit structure. *New Phytologist* **211**: 240–254.

Bradshaw RE, Guo Y, Sim A, Kabir MS, Chettri P, Ozturk IK, Hunziker L, Ganley RL, Cox MP. **2015**. Genome-wide gene expression dynamics of the fungal pathogen *Dothistroma septosporum* throughout its infection cycle of the gymnosperm host *Pinus radiata*. *Molecular Plant Pathology*

Croll D, Lendenmann MH, Stewart E, McDonald BA. **2015**. The impact of recombination hotspots on genome evolution of a fungal plant pathogen. *Genetics* **201**: 1213–1228.

Dagdas YF, Beihaj K, Maqbool A, Chaparro-Garcia A, Pandey P, Petre B, Tabassum N, Cruz-Mireles N, Hughes RK, Sklenar J, *et al.* 2016. An effector of the irish potato famine pathogen antagonizes a host autophagy cargo receptor. *eLife* **5**: 1–19.

van der Does HC, Rep M. **2017**. Adaptation to the Host Environment by Plant-Pathogenic Fungi. *Annual Review of Phytopathology* **55**: 427–450.

Farman M, Peterson G, Chen L, Starnes J, Valent B, Bachi P, Murdock L, Hershmann D, Pedley K, Fernandes JM, *et al.* 2017. The Lolium Pathotype of Magnaporthe oryzae Recovered from a Single Blasted Wheat Plant in the United States. *Plant Disease* **101**: 684–692.

Fisher MC, Henk DA ., Briggs CJ, Brownstein JS, Madoff LC, McCraw SL, Gurr SJ. **2012**. Emerging fungal threats to animal, plant and ecosystem health. *Nature* **484**: 186–194.

Grandaubert J, Dutheil JY, Stukenbrock EH. **2017**. The genomic rate of adaptation in the fungal wheat pathogen Zymoseptoria tritici. *bioRxiv*. doi: 10.1101/176727

Hartmann FE, Sánchez-Vallet A, McDonald BA, Croll D. **2017**. A fungal wheat pathogen evolved host specialization by extensive chromosomal rearrangements. *The ISME Journal*: 1189–1204.

Haueisen J, Stukenbrock EH. **2016**. Life cycle specialization of filamentous pathogens - colonization and reproduction in plant tissues. *Current Opinion in Microbiology* **32**: 31–37.

Hemetsberger C, Herrberger C, Zechmann B, Hillmer M, Doehlemann G. **2012**. The Ustilago maydis effector Pep1 suppresses plant immunity by inhibition of host peroxidase activity. *PLoS Pathogens* **8**.

Inoué S. **2006**. Foundations of confocal scanned imaging in light microscopy. *Handbook of Biological Confocal Microscopy: Third Edition*: 1–19.

Khang CH, Berruyer R, Giraldo MC, Kankanala P, Park S-Y, Czymmek K, Kang S, Valent B. **2010**. Translocation of Magnaporthe oryzae effectors into rice cells and their subsequent cell-to-cell movement. *The Plant cell* **22**: 1388–1403.

Linde CC, Zhan J, McDonald BA. **2002**. Population Structure of Mycosphaerella graminicola: From Lesions to Continents. *Phytopathology* **92**: 946–55.

Manning VA, Ciuffetti LM. **2005**. Localization of Ptr ToxA Produced by Pyrenophora tritici-repentis Reveals Protein Import into Wheat Mesophyll Cells. *The Plant cell* **17**: 3203–3212.

Marcel S, Sawers R, Oakeley E, Angliker H, Paszkowski U. **2010**. Tissue-Adapted Invasion Strategies of the Rice Blast Fungus Magnaporthe oryzae. *The Plant Cell* **22**: 3177–3187.

McDonald BA, Stukenbrock EH. **2016**. Rapid emergence of pathogens in agro-ecosystems : global threats to agricultural sustainability and food security. *Philosophical Transactions of the Royal Society B: Biological Sciences* **371**: 20160026.

Menardo F, Praz C, Wyder S, Bourras S. A, McNally KE, Parlange F, Riba A, Roffler S, Schaefer L, Shimizu KK, *et al.* 2016. Hybridization of powdery mildew strains gives raise to pathogens on novel agricultural crop species. *Nature genetics* **48**: 1–24.

Minker KR, Biedrzycki ML, Kolagunda A, Rhein S, Perina FJ, Jacobs SS, Moore M, Jamann TM, Yang Q, Nelson R, *et al.* 2016. Semiautomated confocal imaging of fungal pathogenesis on plants: Microscopic analysis of macroscopic specimens. *Microscopy Research and Technique* **0**: 1–12.

Möller M, Stukenbrock EH. **2017**. Evolution and genome architecture in fungal plant pathogens. *Nature Reviews Microbiology* **15**: 756–771.

O'Connell RJ, Thon MR, Hacquard S, Amyotte SG, Kleemann J, Torres MF, Damm U, Buiate E a, Epstein L, Alkan N, *et al.* 2012. Lifestyle transitions in plant pathogenic Colletotrichum fungi deciphered by genome and transcriptome analyses. *Nature genetics* **44**: 1060–5.

O'Driscoll A, Kildea S, Doohan F, Spink J, Mullins E. **2014**. The wheat-Septoria conflict: a new front opening up? *Trends in plant science* **19**: 602–10.

Poppe S, Dorsheimer L, Happel P, Stukenbrock EH. **2015**. Rapidly Evolving Genes Are Key Players in Host Specialization and Virulence of the Fungal Wheat Pathogen Zymoseptoria tritici (Mycosphaerella graminicola). *PLOS Pathogens* **11**: e1005055.

Rath M, Grolig F, Haueisen J, Imhof S. **2014**. Combining microtomy and confocal laser scanning microscopy for structural analyses of plant-fungus associations. *Mycorrhiza* **24**: 293–300.

Restrepo S, Tabima JF, Mideros MF, Grünwald NJ, Matute DR. **2014**. Speciation in Fungal and Oomycete Plant Pathogens. *Annual Review of Phytopathology* **52**: 289–316.

Sørensen CK, Justesen AF, Hovmøller MS. **2012**. 3-D imaging of temporal and spatial development of Puccinia striiformis haustoria in wheat. *Mycologia* **104**: 1381–1389.

Stukenbrock EH, Banke S, Javan-Nikkhah M, McDonald BA. **2007**. Origin and domestication of the fungal wheat pathogen Mycosphaerella graminicola via sympatric speciation. *Molecular biology and evolution* **24**: 398–411.

Stukenbrock EH, Bataillon T, Dutheil JY, Hansen TT, Li R, Zala M, McDonald BA, Wang J, Schierup MH. **2011**. The making of a new pathogen: insights from comparative population genomics of the domesticated wheat pathogen Mycosphaerella graminicola and its wild sister species. *Genome research* **21**: 2157–66.

Stukenbrock EH, Christiansen FB, Hansen TT, Dutheil JY, Schierup MH. **2012a**. Fusion of two divergent fungal individuals led to the recent emergence of a unique widespread pathogen species. *Proceedings of the National Academy of Sciences of the United States of America* **109**: 1–6.

Stukenbrock E, Dutheil JY. In press. Comparison of fine-scale recombination maps in fungal plant pathogens reveals dynamic recombination landscapes and intragenic hotspots. *Genetics*.

Stukenbrock EH, Jørgensen FG, Zala M, Hansen TT, McDonald BA, Schierup MH. **2010**. Whole-genome and chromosome evolution associated with host adaptation and speciation of the wheat pathogen Mycosphaerella graminicola. *PLoS genetics* **6**: e1001189.

Stukenbrock EH, Quaedvlieg W, Javan-Nikhah M, Zala M, Crous PW, McDonald B a. **2012b**. Zymoseptoria ardabiliae and Z. pseudotritici, two progenitor species of the septoria tritici leaf blotch fungus Z. tritici (synonym: Mycosphaerella graminicola). *Mycologia* **104**: 1397–407.

Vandenkoornhuyse P, Quaiser A, Duhamel M, Le Van A, Dufresne A. **2015**. The importance of the microbiome of the plant holobiont. *New Phytologist* **206**: 1196–1206.

Wawra S, Fesel P, Widmer H, Timm M, Seibel J, Leson L, Kesseler L, Nostadt R, Hilbert M, Langen G, *et al.* 2016. The fungal-specific β-glucan-binding lectin FGB1 alters cell-wall composition and suppresses glucan-triggered immunity in plants. *Nature communications* **7**: 13188.

White JG, Amos WB, Fordham M. **1987**. An Evaluation of Confocal Versus Conventional Imaging of Biological Structures by Fluorescence Light Microscopy. *Cell* **105**: 41–48.

Zuccaro A, Lahrmann U, Güldener U, Langen G, Pfiffi S, Biedenkopf D, Wong P, Samans B, Grimm C, Basiewicz M, *et al.* 2011. Endophytic life strategies decoded by genome and transcriptome analyses of the mutualistic root symbiont Piriformospora indica. *PLoS Pathogens* **7**.

Zwiers LH, De Waard MA. **2001**. Efficient Agrobacterium tumefaciens-mediated gene disruption in the phytopathogen Mycosphaerella graminicola. *Current Genetics* **39**: 388–393.

Acknowledgements

Finishing a PhD thesis at the end of a (in my case) five year long journey is a fantastic feeling that makes me realize how much I enjoyed this experience and how much it allowed me to learn and to grow as a person and as a scientist.
Clearly, none of this would have been possible without my supervisor Eva Stukenbrock. I was so proud when I started working with you at the MPI in Marburg and became a member of the "Fungal Biodiversity" group. Not for a second, I want to miss having moved to Kiel with you and the team. I felt and I feel very privileged for the opportunity you gave me with this PhD project. I contributed my background and experience and I was allowed and also challenged to acquire a complete new set of skills. I must thank you for the freedom and independence, and your patience and constant encouragement – in particular when it comes to writing. I finally agree – it becomes easier eventually and sometimes even fun. Last but not least, you are my role model for women in science. I admire your commitment to improve work-family-life balance and to create a healthy working environment for young scientists.

The chapters of this thesis clearly are the results of a concerted effort that would not have been possible without a fantastic team and many people who provided help and advice. I want to thank Heike, Elis, Christoph, and Jonathan for your great support and your important contributions to the manuscripts.

I am grateful to Michael, Klaas, Stephan, Andrea and all current and past members of the Stukenbrock lab for their camaraderie, their support and feedback, for lively lunch and coffee breaks, and a very friendly and welcoming atmosphere in the lab and in the office.

Further, I would like to thank Julien Dutheil for supporting the transcriptome analyses, Petra Happel for great help with *in vitro* assays and for teaching me how to work with our fungi, Michael Freitag and Ronny Kellner for insightful comments to the manuscripts of chapters 1 and 2, Ben Auxier and Alina Nommensen for help with plasmid generations and fungal transformations, and Magnus Rath for advice and support with microscopy.

I am grateful that Alga Zuccaro, who already was a member of my thesis advisory committee in Marburg, agreed to become the second referee of my thesis. I want to thank her and Margret Sauter for their time and interest in my PhD research.

Mareike, ich möchte dir für so vieles danken, aber ganz besonders für deine Freundschaft. Ich kann mir niemanden vorstellen, mit dem ich lieber die viele Zeit im Labor und im Büro – the Happy Office – verbringen würde, als mit dir. Ich kann mir nicht vorstellen, wie es sein wird, wenn wir irgendwann mal nicht mehr in der gleichen Gruppe arbeiten. Ich bewundere dein Wissen, deine Beharrlichkeit und wie effizient und pragmatisch du an Probleme herangehst. Unsere Diskussionen und deine kritische Meinung sind mir sehr wichtig und haben die Kapitel dieser Arbeit maßgeblich beeinflusst und verbessert. Natürlich möchte ich dir auch für deinen Anteil an den Manuskripten und die vielen Experimente, die wir gemeinsam gemacht haben, herzlich danken. Ich wünsche mir, dass wir auch in Zukunft so viel Spaß zusammen haben und dabei richtig coole Forschung machen.

An meine Familie

Vielen Dank an Opa Norbert, Oma Christa, und Margit und Reinhard, von denen ich mich trotz der immer größer werdenden geographischen Distanz - erst in Marburg und später in Kiel – immer unterstützt gefühlt habe. Ich weiß, dass ihr oft an mich gedacht und mir immer die Daumen gedrückt habt.

Mutti und Vati, ihr habt die Höhen miterlebt und in den Tiefen mit gelitten, aber immer daran geglaubt, dass ich meine Ziele erreichen werde. Ich bin euch sehr dankbar, dass ihr mir immer alle Freiheit gelassen habt meinen eigenen Weg zu gehen. Auf eure Unterstützung kann ich mich immer hundertprozentig verlassen und ich weiß, dass ihr sofort alles stehen und liegen lasst, wenn ich euch brauche. Ich habe euch lieb und ich freue mich darauf, dass wir uns im kommenden Jahr wieder häufiger sehen werden.

An meinen lieben Mann Holger: Leute, die uns kennen, sagen, dass ich ohne dich absolut aufgeschmissen wäre. Sie haben ja alle sowas von Recht. Und ich meine damit bei Weitem nicht nur dein riesiges Talent wunderschöne Abbildungen zu gestalten und die unendliche Geduld und Mühe, mit der du mir dabei hilfst meine Vorstellungen in die Realität umzusetzen. Du hat alles in Bewegung gesetzt und große Veränderungen in Kauf genommen, damit wir gemeinsam in Kiel leben können. Wenn es dir irgendwie möglich war, hast du für mich alle Hürden aus dem Weg geräumt und warst in den vergangenen Monaten mein Schutzschild gegen alles. Es klingt so abgedroschen, aber du warst wirklich immer für mich da. Du hast mich an jedem einzelnen Tag unterstützt. Ich liebe dich und bin dir so dankbar.

Declaration of Author's Contribution

This thesis comprises four chapters in form of published and unpublished manuscripts. Specific contributions for the chapter are detailed below.

Chapter 1: Life cycle specialization of filamentous pathogens – colonization and reproduction in plant tissues

Janine Haueisen and Eva H. Stukenbrock

Chapter 1 was published in Current Opinion in Microbiology in 2016.

Haueisen J, Stukenbrock EH. **2016**. Life cycle specialization of filamentous pathogens - colonization and reproduction in plant tissues. *Current Opinion in Microbiology* **32**: 31–37.

Conceptualization, manuscript writing and editing: JH, EHS.

Chapter 2: Extremely flexible infection programs in a fungal plant pathogen

Janine Haueisen, Mareike Möller, Christoph J. Eschenbrenner, Jonathan Grandaubert, Heike Seybold, Holger Adamiak and Eva H. Stukenbrock

Chapter 2 was published as preprint on bioRxiv (doi: 10.1101/229997). Currently, submitted and under peer review.

Conceptualization: JH, EHS. Wheat infection experiments and *in vitro* stress assay: JH. *In planta* ROS assay: JH, HS. Karyotyping and synteny analyses: JH, MM. Confocal microscopy analyses and data visualization: JH, HA. Genome sequencing and *de novo* genome assemblies: MM, CJH. Transcriptome sequencing, data curation and comparative transcriptome analyses: JH. Gene and TE annotations, software for enrichment analyses: JG. Preparation and writing of manuscript: JH, EHS. Editing of original manuscript: JH, EHS, MM, and HS.

Chapter 3: Few key factors determine incompatible and compatible host-pathogen interactions in closely related grass infecting fungi

Janine Haueisen, Mareike Möller, Heike Seybold and Eva H. Stukenbrock

Conceptualization: JH, EHS. Wheat infection experiments and *in vitro* stress assay: JH. I*n vitro* growth assay: JH, MM. ROS staining: JH, HS. RNA extraction, transcriptome sequencing data curation and analyses: JH. Confocal microscopy analyses and data visualization: JH. Preparation and writing of manuscript: JH. Editing of original manuscript: JH, EHS.

Chapter 4: Host infections and plant-associated lifestyles of the *Zymoseptoria tritici* sister species *Z. pseudotritici* and *Z. ardabiliae*

Janine Haueisen, Elis Martinelli and Eva H. Stukenbrock

Conceptualization: JH. Infection assays to test influence of leaf age: JH, EM. All other *in vivo* and *in vitro* plant infection experiments including strain re-isolation and sequencing: JH. Confocal microscopy analyses and data visualization: JH. Plasmid generation and transformation of fungal strains: JH. Preparation and writing of manuscript: JH. Editing of original manuscript: JH, EHS.

Affidavit

I hereby declare that this dissertation

- concerning content and design is the product of my own work under guidance of my supervisor Prof. Dr. Eva H. Stukenbrock. I used no other tools or sources but the cited ones. Contributions of other authors are listed in detail in the 'Declaration of author's contribution' section of this thesis.
- has been conducted and prepared following the Rules of Good Scientific Practice of the German Research Foundation.
- has not been submitted elsewhere partially or wholly as part of a doctoral degree to another examining body, and no other materials are published or submitted for publication than indicated in the thesis.

Janine Haueisen
Kiel, 18.12.17